



THE UNIVERSITY *of* EDINBURGH

This thesis has been submitted in fulfilment of the requirements for a postgraduate degree (e.g. PhD, MPhil, DClinPsychol) at the University of Edinburgh. Please note the following terms and conditions of use:

- This work is protected by copyright and other intellectual property rights, which are retained by the thesis author, unless otherwise stated.
- A copy can be downloaded for personal non-commercial research or study, without prior permission or charge.
- This thesis cannot be reproduced or quoted extensively from without first obtaining permission in writing from the author.
- The content must not be changed in any way or sold commercially in any format or medium without the formal permission of the author.
- When referring to this work, full bibliographic details including the author, title, awarding institution and date of the thesis must be given.

Molecular characterisation and functional analysis of eEF1B subunits in mammals

Miriam Botelho Duarte Portela

A thesis submitted for the degree of Doctor of Philosophy
The University of Edinburgh
2009

To my parents

Declaration

I declare that this thesis has been composed by myself and that all the work described has been performed by myself unless where clearly stated in the text. All sources of information other than this study have been acknowledged. This work has not been submitted for any other degree or professional qualification.

Miriam Botelho Duarte Portela

Acknowledgements

Doing this PhD would not have been possible without the support, guidance and friendship of a long list of people. I am indebted to all of them for their help. First I would like to thank my supervisor Cathy Abbott for giving me this opportunity to work on this project, her patient guidance and support. And many thanks to my second supervisor Kathy Evans for her advice and support. I would also like to thank David Porteous and Ian Jackson from my committee for their advice and suggestions, and Nick Hastie for his advice and encouragement on my future career.

I would like to thank David Melton for allowing me to use some of his lab material, Ann-Marie and Laura for help with the FACS, Abby and Heather for microscope training, Oliver for help with immunocytochemistry, Song for a couple of antibodies and, Scott Badder, Abby, Sheila and Barbie for cell lines. I would also like to mention Martin Hooper for his caring support, Jim Selfridge for support and technical advice, the BRF staff, and everyone in the Medical Genetics section and Sir Alastair Currie Laboratories who has helped me in any way or form. I would also like to acknowledge the Fundação para a Ciência e Tecnologia for funding, the Institute of genetics for the travel grant which allowed me to travel to the Translation Control meeting at Cold Spring Harbour and big thanks to Michael, Gabriele and Karen for the great time I spent there.

Thank to all the past and present members of the Abbott group and all the undergraduate students in particular Antonia, Iain, Tom, Chris and Kasia for all the laughs. I wish all the best of luck to Cheryl who is taking over my project. Big thanks to Justyna and Mariam for our holiday together, good luck for your PhDs and hope we will be able to stay in touch. To all the other MMC students a massive thanks for help keeping my level of sanity, in particular Antonia, David, Gareth, Helen, John, Manu and Nick (note the alphabetical order). A special thanks to Lowri for all the fun times, trips to the cinema, trips to the pub, holidays together, and for helping me keep things in perspective.

To everyone away from the lab who provided a much needed form of escape from my studies a big thanks. To Lee, Frances, Alex and the rest of the pub quiz team for the Sundays' entertainment. To Andreia, little Fabio, Luiz, Nuno and

Ze for their love and care that allowed me to feel closer to home. To all my friends from my undergrad time at the University of Hertfordshire and Cambridge, in particular Thulasi for her encouragement, support and willingness to read my thesis. To Andrew for support, encouragement and putting up with me in this final stage of writing. With no particular order, to my all-time friends Filipa, Gisela, Marilia, Marisa e Ze a huge THANK YOU for their love and encouragement!

Finally, to my parents who I dedicate this thesis for always believing in me, encouraging me to follow my dreams, for their whole-hearted love and for helping in whatever way they could – “Obrigada”.

Table of contents

Title page	i
Dedication	ii
Declaration	iii
Acknowledgments	iv
Table of contents	vi
List of figures	xi
List of tables	xv
List of abbreviations	xvi
Abstract	xxvii
Chapter 1 – Introduction	1
1.1 Protein synthesis	1
1.2 Eukaryotic translation elongation factor 1 A	4
1.3 Eukaryotic translation elongation factor 1 B	5
1.3.1 eEF1B α	6
1.3.2 eEF1B δ	7
1.3.3 eEF1B γ	8
1.4 Eukaryotic translation elongation factor 1 B structure and regulation	9
1.4.1 Models of eEF1B complex quaternary structure and GEF rates	9
1.4.2 Regulation of eEF1B subunits	12
1.5 eEF1B and cancer	16
1.5.1 eEF1B α	16
1.5.2 eEF1B δ	17
1.5.3 eEF1B γ	29
1.6 eEF1B and other functions	23
1.6.1 eEF1B and DNA repair/cellular stress	23
1.6.2 eEF1B and cell cycle	26
1.6.3 eEF1B and the cytoskeleton	27

1.6.4	eEF1B and translation fidelity	30
1.7	RNAi	31
1.8	Aims	34
Chapter 2 – Materials and methods		35
2.1	Bioinformatics	35
2.1.1	Identification of related sequences	35
2.1.2	Alignment of similar sequences	36
2.1.3	Genomic DNA and mRNA characteristics	36
2.1.4	Protein characteristics	38
2.1.5	Protein structure	40
2.1.6	Protein-protein interactions	41
2.1.7	Perl scripts	42
2.2	Materials	43
2.2.1	Solutions and buffers	43
2.2.2	Cell lines	44
2.2.3	Animals	44
2.2.4	Antibodies	45
2.2.5	Slides	46
2.2.6	DNA primers	47
2.2.7	DNA	48
2.2.8	siRNAs	49
2.3	Cell culture	50
2.3.1	Cell culture maintenance	50
2.3.2	Cell count	50
2.3.3	Cryostat preservation of cell lines	50
2.3.4	RNAi	50
2.3.5	Transfection by Lipofectamine	51
2.3.6	Transfection by Nucleofection	51
2.4	Protein-related methods	52

2.4.1	Antibodies production	52
2.4.2	Cell lysates	53
2.4.3	Western blot	54
2.4.4	Immunocytochemistry	57
2.4.5	Immunohistochemistry	58
2.5	Molecular biology methods	59
2.5.1	PCR sample preparation	59
2.5.2	PCR reactions	60
2.5.3	Sequencing PCR products and plasmids	61
2.5.4	Purification of PCR products	64
2.5.5	DNA electrophoresis	65
2.5.6	Culture of bacteria	66
2.5.7	Cloning techniques	68
2.5.8	Cell culture assays	71
Chapter 3 – <i>in silico</i> characterisation of eEF1B subunits		73
3.1	Introduction	73
3.2	Results	74
3.2.1	Related eEF1B subunits sequences	74
3.2.2	eEF1B δ has an extra exon and more transcript variants	77
3.2.3	Expression at mRNA level	81
3.2.4	Regulation at the transcription level	82
3.2.5	Comparison between subunits	87
3.2.6	Protein homologues	90
3.2.7	Similar proteins and domains	96
3.2.8	Secondary structure and other structural features	98
3.2.9	3D structure prediction and folding	104
3.2.10	eEF1B post-translational modifications	107
3.2.11	Protein-protein interactions	113
3.3	Discussion	119

3.3.1	eEF1B and related sequences	119
3.3.2	eEF1B δ alternative splicing and expression	120
3.3.3	Similarities and differences between subunits	121
3.3.4	Putative non-canonical functions	125
Chapter 4 – Expression of the eEF1B subunits		127
4.1	Introduction	127
4.2	Results	128
4.2.1	eEF1B α and eEF1B γ are ubiquitously expressed in mouse tissues at mRNA level	128
4.2.2	eEF1B δ has multiple mRNA transcripts some of which show tissue-specificity	132
4.2.3	Peptide design and antibody production	134
4.2.4	eEF1B protein expression in adult mouse tissues and cell lines	138
4.2.5	eEF1B protein expression during mouse development	145
4.2.6	Immunohistochemical analysis of eEF1B subunits in a variety of mouse and human tissues	150
4.2.7	eEF1B expression in wild-type and wasted mice brain	172
4.2.8	Cytoplasmic and nuclear expression in tissues	177
4.2.9	eEF1B sub-cellular localisation	179
4.2.10	eEF1B expression during cell cycle	183
4.3	Discussion	187
4.3.1	Expression levels and multiple variants in translation	187
4.3.2	Correlation of expression between eEF1 factors and implications for eEF1B function	190
4.3.3	Nuclear and cell cycle dependent translation	192
Chapter 5 – eEF1B function		195
5.1	Introduction	195
5.2	Results	196
5.2.1	RNAi used to knockdown successfully eEF1B subunits at mRNA	196

level	
5.2.2 siRNA mediated knockdown of eEF1B subunits at protein level	199
5.2.3 Optimisation of eEF1B subunits siRNA mediated knockdown	203
5.2.4 Knockdown of either eEF1B α or eEF1B δ reduce expression of eEF1B γ	207
5.2.5 No apparent phenotypic abnormalities demonstrated by immunofluorescence microscopy	212
5.2.6 Significant reduction of cell growth in cells with eEF1B down-regulation	217
5.2.7 Increased G0/G1 phase and reduced S- and G2/M phase cells with eEF1B knock down expression	220
5.2.8 siRNA mediated knockdown of eEF1B enhances apoptosis	224
5.2.9 Correlation between eEF1B protein level with cell proliferation, cell cycle and apoptosis	230
5.2.10 Overexpression of eEF1B subunits induces proliferation and cell viability	233
5.3 Discussion	238
Chapter 6 – General discussion	247
6.1 Future studies	250
6.2 Conclusion	255
References	256
Appendices	Cd

List of figures

1.1	Diagram of translation elongation in mammals	4
1.2	Diagram of the eEF1B [®] gene structure showing three different 5' UTR that arose by alternative splicing	7
1.3	eEF1B complex quaternary structure models	11
1.4	Phosphorylation sites of eEF1B subunits	15
3.1	Chromosomal location of the genes encoding each eEF1B subunit and pseudogenes	75
3.2	<i>eEF1Bδ</i> gene structure model extrapolated from mouse ESTs	79
3.3	Mouse and human gene structure of each eEF1B subunit	80
3.4	Putative promoter region and regulatory sites prediction for human <i>eEF1Bα</i>	83
3.5	Putative promoter region and regulatory sites prediction for human <i>eEF1Bδ</i>	84
3.6	Putative promoter region and regulatory sites prediction for human <i>eEF1Bγ</i>	86
3.7	Multiple protein sequence alignment of eEF1B α and eEF1B δ C-termini from 4 different mammalian species.	88
3.8	Multiple protein sequence alignment of mouse eEF1B δ isoforms a and b and putative isoforms c, d and e	89
3.9	Multiple eEF1B α protein sequence alignment from 10 different eukaryotic species	91
3.10	Multiple sequence alignment of eEF1B δ isoform b from 9 different eukaryotic species	92
3.11	Multiple sequence alignment of eEF1B δ isoform a N-terminus from 9 different eukaryotic species	93
3.12	Multiple eEF1B γ protein sequence alignment from 10 different eukaryotic species.	95
3.13	eEF1B subunit domain prediction, amino acid sequence variation and known functional residues.	97
3.14	eEF1B α structural features and secondary structure prediction	99
3.15	eEF1B δ isoform a N-terminus structural features and secondary structure prediction.	100
3.16	eEF1B δ isoform b structural features and secondary structure prediction.	102

3.17	eEF1B γ structural features and secondary structure prediction	103
3.18	Human eEF1B α and eEF1B δ C-terminal 3-D protein structure model	105
3.19	Diagram of the post translational modifications predicted for human eEF1B α	109
3.20	Diagram of the post translational modifications predicted for human eEF1B δ N-terminus isoform a	110
3.21	Diagram of the post translational modifications predicted for human eEF1B δ isoform b	111
3.22	Diagram of the post translational modifications predicted for human eEF1B γ	112
3.23	eEF1B α protein-protein interactions network	114
3.24	eEF1B δ protein-protein interactions network	115
3.25	eEF1B γ protein-protein interactions network	117
3.26	eEF1 subunits minimal protein-protein interactions network	118
4.1	eEF1B α and eEF1B γ mRNA expression in normal mouse tissues	129
4.2	<i>Eef1bα</i> and <i>Eef1bγ</i> quantitative mRNA expression in normal mouse tissues	131
4.3	<i>Eef1bδ</i> mRNA expression in normal mouse tissues	133
4.4	Protein characteristics and features and peptide sequence for each eEF1B subunit	135
4.5	Antibody specificity for the peptide it was raised against measured by ELISA	137
4.6	Immunoblot of eEF1B α expression in a mouse tissue panel	139
4.7	Immunoblot of eEF1B δ expression in a mouse tissue panel	141
4.8	Immunoblot of eEF1B γ expression in a mouse tissue panel	142
4.9	Immunoblot of eEF1B subunits expression in a variety of cell lines.	144
4.10	Immunoblot of eEF1B subunits expression during various mouse developmental stages	146
4.11	Immunohistochemical analysis of eEF1B subunits protein distribution in embryonic and post-natal day 1 mice	148
4.12	Immunohistochemical analysis of eEF1B subunits protein distribution in mouse and human liver	151
4.13	Immunohistochemical analysis of eEF1B subunits protein distribution in mouse and human lung	153
4.14	Immunohistochemical analysis of eEF1B subunits protein distribution	155

	in mouse and human spleen	
4.15	Immunohistochemical analysis of eEF1B subunits protein distribution in mouse and human kidney	157
4.16	Immunohistochemical analysis of eEF1B subunits protein distribution in mouse and human pancreas	160
4.17	Immunohistochemical analysis of eEF1B subunits protein distribution in mouse and human skeletal muscle	161
4.18	Immunohistochemical analysis of eEF1B subunits protein distribution in mouse and human cardiac muscle.	163
4.19	Immunohistochemical analysis of eEF1B subunits protein distribution in mouse and human brain	165
4.20	Immunohistochemical analysis of eEF1B subunits protein distribution in mouse spinal cord	167
4.21	Immunohistochemical analysis of eEF1B subunits protein distribution in mouse colon	169
4.22	Immunohistochemical analysis of eEF1B subunits protein distribution in mice testis and ovary	170
4.23	Immunoblot of eEF1B subunits protein expression in wasted and wild-type mice	173
4.24	Immunohistochemical analysis of eEF1B subunits protein distribution in wasted and wild-type hippocampus	174
4.25	Immunohistochemical analysis of eEF1B subunits protein distribution in wasted and wild-type cerebellum	175
4.26	Immunoblot of eEF1B subunits protein expression in nuclear and cytoplasmic fractions from mice and human of brain and liver tissues	178
4.27	eEF1B subunits show cytoplasmic staining in double immunofluorescence on HeLa cells	180
4.28	Perinuclear co-localisation of eEF1B subunits in HeLa cells	181
4.29	eEF1B protein levels during cell cycle	184
4.30	Cytoplasmic staining present for all the eEF1B subunits through out cell cycle	186
5.1	eEF1B subunits knockdown of mRNA level by sequence specific siRNAs	197
5.2	eEF1B subunits protein knockdown by sequence specific siRNAs	200
5.3	eEF1B subunits knockdown using different siRNA concentrations	204
5.4	Immunoblot of a time course transient transfection of siRNAs	206

	targeting eEF1B subunits	
5.5	The expression of eEF1B subunits when a particular subunit has been knockeddown changes post-transcriptionally	208
5.6	Efficient knockdown of eEF1B subunits in HCT116, DLD1 and HepG2 cells	210
5.7	No obvious phenotypic abnormalities observed by immunofluorescence microscopy after transfection with siRNAs targeting eEF1B α in HeLa cells	213
5.8	Alpha-tubulin appears to be disrupted in some cells observed by immunofluorescence microscopy after transfection with siRNAs targeting eEF1B δ in HeLa cells	214
5.9	No obvious phenotypic abnormalities observed by immunofluorescence microscopy after transfection with siRNAs targeting eEF1B γ in HeLa cells	216
5.10	Lower cellular growth is observed when any of the eEF1B subunit protein level is decreased by siRNAs in HCT116, DLD1 and HepG2 cells	218
5.11	Knockdown of eEF1B subunits leads to G0/G1 cell cycle arrest with decreased S-phase and G2/M phase in HeLa cells	221
5.12	Cell cycle distribution of HCT116, DLD1 and HepG2 cells transfected with siRNAs targeting eEF1B subunits	222
5.13	Transfection of siRNA targeting eEF1B subunits leads to increased apoptosis compared to non-targeting siRNAs in HeLa cells	225
5.14	Transfection of siRNA targeting eEF1B subunits leads to increased apoptosis compared to non-targeting siRNAs in HCT116, DLD1 and HepG2 cells	226
5.15	RNAi mediated knockdown of eEF1B in DLD1 cells leads to increase of Caspase-3/7 cleavage by fluorescence based assay but not Caspase-3 by Western Blot	228
5.16	Time course of eEF1B knockdown impact on proliferation, cell cycle distribution and apoptosis ratio	231
5.17	Overexpression of eEF1B subunits tagged with V5 in HeLa cells	234
5.18	Overexpression of eEF1B subunits increases proliferation, in cells in G0/G1 phase and reduces apoptosis compared with V5 plasmid only	235

List of tables

1.1	Nomenclature of elongation factor 1 B multimer in animals	6
1.2	Summary table of the different tumours and cancer cells in which overexpression of eEF1B subunits have been associated to	23
2.1	The variants of BLAST searches according to different the query sequence and database type of sequence	35
2.2	Post-translational modification prediction tools used	39
2.3	Recipes of all the solutions and buffers used for the methods described in this chapter	43
2.4	List of cell lines, species, cell type, source and media in which each cell line was grown	44
2.5	List of antibodies used and conditions under which they were used for Western blotting, immunocytochemistry and immunohistochemistry	45
2.6	List of primers names, targets and primer sequences used for RT-qPCR, cloning, and isoform amplification	46
2.7	All the plasmids used for cloning of C-terminal V5 tagged eEF1B subunits, vectors, source and antibiotic resistance	48
2.8	List of siRNA names that were used in this project as well as reference name, targets, sequences and source	48
2.9	List of restriction enzymes specific for each eEF1B subunit and respective buffers	69
2.10	Percentage of identity between the human eEF1B subunits	87
5.1	Relationship between protein expression, proliferation, cell cycle distribution and apoptosis for each eEF1B subunit knocked down in each cell line	225
5.2	Relationship between protein expression, proliferation, cell cycle distribution and apoptosis for each eEF1B subunit knocked down and up-regulated in HeLa cells	235

List of abbreviations

Proteins

eEF1A	Eukaryotic translation elongation factor 1A
eEF1B	Eukaryotic translation elongation factor 1B complex
eEF1B α	Eukaryotic translation elongation factor 1B alpha subunit
eEF1B δ	Eukaryotic translation elongation factor 1B delta subunit
eEF1B γ	Eukaryotic translation elongation factor 1B gamma subunit
GAPDH	glyceraldehyde-3-phosphate dehydrogenase

Protein UNIPROT IDs

1433E	14-3-3 protein epsilon
1433F	14-3-3 protein eta
1433G	14-3-3 protein gamma
1433Z	14-3-3 protein zeta/delta
1B42	HLA class I histocompatibility antigen, B-42 alpha chain
2A5B	Serine/threonine-protein phosphatase 2A 56 kDa regulatory subunit beta isoform
2ABB	Serine/threonine-protein phosphatase 2A 55 kDa regulatory subunit B beta isoform
41	Protein 4.1
AAKB1	5'-AMP-activated protein kinase subunit beta-1
ABCC9	ATP-binding cassette transporter sub-family C member 9
ABRA	Actin-binding Rho-activating protein
ACON	Aconitate hydratase, mitochondrial
ACTB	Actin, cytoplasmic 1
ANXA1	Annexin A1
ANXA2	Annexin A2
ANXA6	Annexin A6
ARC1A	Actin-related protein 2/3 complex subunit 1A
ARCH	Protein archease
ARF1	ADP-ribosylation factor 1
ARHG4	Rho guanine nucleotide exchange factor 4
ARI2	Protein ariadne-2 homolog
ARP6	Actin-related protein 6
ARRB2	Beta-arrestin-2
ASCC2	Activating signal cointegrator 1 complex subunit 2
AT2C1	Calcium-transporting ATPase type 2C member 1
ATG5	Autophagy protein 5
ATPA	ATP synthase subunit alpha, mitochondrial
BCAR3	Breast cancer anti-estrogen resistance protein 3
C1QBP	Complement component 1 Q subcomponent-binding protein, mitochondrial
CA174	UPF0688 protein C1orf174
CALM	Calmodulin
CBX8	Chromobox protein homolog 8
CC106	Coiled-coil domain-containing protein 106

CD2B2	CD2 antigen cytoplasmic tail-binding protein 2
CD4	T-cell surface glycoprotein CD4
CD48	CD48 antigen
CDC2	Cell division control protein 2 homolog
CDC42	Cell division control protein 42 homolog
CENPE	Centromere-associated protein E
CG020	UPF0363 protein C7orf20
CH60	60 kDa heat shock protein, mitochondrial
CHFR	E3 ubiquitin-protein ligase CHFR
CK5P2	CDK5 regulatory subunit-associated protein 2
CL004	Uncharacterized protein C12orf4
COG6	Conserved oligomeric Golgi complex subunit 6
COPB2	Coatomer subunit beta'
COT1	COUP transcription factor 1
CP014	Uncharacterized protein C16orf14
CPSF5	Cleavage and polyadenylation specificity factor subunit 5
CRCM	Colorectal mutant cancer protein
CREL1	Cysteine-rich with EGF-like domain protein 1
CRNL1	Crooked neck-like protein 1
CSK21	Casein kinase II subunit alpha
CSK22	Casein kinase II subunit alpha'
CSTF2	Cleavage stimulation factor 64 kDa subunit
CTBP1	C-terminal-binding protein 1
CTBP2	C-terminal-binding protein 2
CTNB1	Catenin beta-1
CUL1	Cullin-1
CUL2	Cullin-2
CUL3	Cullin-3
CUL4A	Cullin-4A
CUL4B	Cullin-4B
CUL5	Cullin-5
CXL13	C-X-C motif chemokine 13
DCP1A	mRNA-decapping enzyme 1A
DCP1B	mRNA-decapping enzyme 1B
DCPS	Scavenger mRNA-decapping enzyme DcpS
DDB1	DNA damage-binding protein 1
DDX3X	ATP-dependent RNA helicase DDX3X
DDX3Y	ATP-dependent RNA helicase DDX3Y
DDX5	Probable ATP-dependent RNA helicase DDX5
DHR11	Dehydrogenase/reductase SDR family member 11
DHRS2	Dehydrogenase/reductase SDR family member 2
DHX15	Putative pre-mRNA-splicing factor ATP-dependent RNA helicase DHX15
DKC1	H/ACA ribonucleoprotein complex subunit 4
DLRB2	Dynein light chain roadblock-type 2
DNJC2	DnaJ homolog subfamily C member 2
DPYL1	Dihydropyrimidinase-related protein 1
DRD3	D(3) dopamine receptor

DSPP	Dentin sialophosphoprotein
ECH1	Delta(3,5)-Delta(2,4)-dienoyl-CoA isomerase
EF1A1	Elongation factor 1-alpha 1
EF1A2	Elongation factor 1-alpha 2
EF1B	Elongation factor 1-beta
EF1D	Elongation factor 1-delta
EF1G	Elongation factor 1-gamma
EF2	Elongation factor 2
EFG1	Elongation factor G 1, mitochondrial
EFNA1	Ephrin-A1
EID2B	EP300-interacting inhibitor of differentiation 2B
EIF1B	Eukaryotic translation initiation factor 1b
EIF2A	Eukaryotic translation initiation factor 2A
EIF3B	Eukaryotic translation initiation factor 3 subunit B
EIF3C	Eukaryotic translation initiation factor 3 subunit C
EIF3D	Eukaryotic translation initiation factor 3 subunit D
EIF3E	Eukaryotic translation initiation factor 3 subunit E
EIF3I	Eukaryotic translation initiation factor 3 subunit I
EIF3K	Eukaryotic translation initiation factor 3 subunit K
EIF3M	Eukaryotic translation initiation factor 3 subunit M
ELAV2	ELAV-like protein 2
ELF3	ETS-related transcription factor Elf-3
ENOA	Alpha-enolase
ENOX1	Ecto-NOX disulfide-thiol exchanger 1
ERG19	Diphosphomevalonate decarboxylase
EST2	Carboxylesterase 2
EXOC8	Exocyst complex component 8
F10C1	Protein FRA10AC1
FBXW7	F-box/WD repeat-containing protein 7
FEN1	Flap endonuclease 1
FOS	Proto-oncogene protein c-fos
FOXG1	Forkhead box protein G1
FPPS	Farnesyl pyrophosphate synthetase
G3P	Glyceraldehyde-3-phosphate dehydrogenase
GA45G	Growth arrest and DNA-damage-inducible protein GADD45 gamma
GAS1	Growth arrest-specific protein 1
GBLP	Guanine nucleotide-binding protein subunit beta-2-like 1
GCN1L	Translational activator GCN1
GDIA	Rab GDP dissociation inhibitor alpha
GFPT2	Glucosamine--fructose-6-phosphate aminotransferase [isomerizing] 2
GLYM	Serine hydroxymethyltransferase, mitochondrial
GNAI2	Guanine nucleotide-binding protein G
GOSR2	Golgi SNAP receptor complex member 2
GRB2	Growth factor receptor-bound protein 2
GRP78	78 kDa glucose-regulated protein
GSTO1	Glutathione S-transferase omega-1
GTR8	Solute carrier family 2, facilitated glucose transporter member 8

H2AX	Histone H2A.x
H2B1C	Histone H2B type 1-C/E/F/G/I
H2B2E	Histone H2B type 2-E
H4	Histone H4
HDAC5	Histone deacetylase 5
HECW2	E3 ubiquitin-protein ligase HECW2
HEXA	Beta-hexosaminidase subunit alpha
HEXDC	Hexosaminidase domain-containing protein
HLTF	Helicase-like transcription factor
HMOX2	Heme oxygenase 2
HNRH1	Heterogeneous nuclear ribonucleoprotein H
HNRH3	Heterogeneous nuclear ribonucleoprotein H3
HNRL1	Heterogeneous nuclear ribonucleoprotein U-like protein 1
HNRPD	Heterogeneous nuclear ribonucleoprotein D0
HNRPU	Heterogeneous nuclear ribonucleoprotein U
HS90A	Heat shock protein HSP 90-alpha
HS90B	Heat shock protein HSP 90-beta
HSP7C	Heat shock cognate 71 kDa protein
HXA7	Homeobox protein Hox-A7
IDHC	Isocitrate dehydrogenase [NADP] cytoplasmic
IF4A1	Eukaryotic initiation factor 4A-I
IF4A2	Eukaryotic initiation factor 4A-II
IF4E	Eukaryotic translation initiation factor 4E
IF5A1	Eukaryotic translation initiation factor 5A-1
IF6	Eukaryotic translation initiation factor 6
IKKE	Inhibitor of nuclear factor kappa-B kinase subunit epsilon
ILF2	Interleukin enhancer-binding factor 2
IMB1	Importin subunit beta-1
IMDH1	Inosine-5'-monophosphate dehydrogenase 1
IPO4	Importin-4
IPO7	Importin-7
IQGA1	Ras GTPase-activating-like protein IQGAP1
IRAK4	Interleukin-1 receptor-associated kinase 4
K6PL	6-phosphofructokinase, liver type
K6PP	6-phosphofructokinase type C
KAD2	Adenylate kinase 2, mitochondrial
KAP2	cAMP-dependent protein kinase type II-alpha regulatory subunit
KELL	Kell blood group glycoprotein
KPCA	Protein kinase C alpha type
KPYM	Pyruvate kinase isozymes M1/M2
KRA57	Keratin-associated protein 5-7
KS6A1	Ribosomal protein S6 kinase alpha-1
KTN1	Kinectin
LCK	Proto-oncogene tyrosine-protein kinase LCK
LEU1	Leukemia-associated protein 1
LPPRC	Leucine-rich PPR motif-containing protein, mitochondrial
LRP1B	Low-density lipoprotein receptor-related protein 1B

LSM3	U6 snRNA-associated Sm-like protein LSm3
LZTS1	Leucine zipper putative tumor suppressor 1
M3K8	Mitogen-activated protein kinase kinase kinase 8
MAOM	NAD-dependent malic enzyme, mitochondrial
MATR3	Matrin-3
MCM4	DNA replication licensing factor MCM4
MCM5	DNA replication licensing factor MCM5
MDHM	Malate dehydrogenase, mitochondrial
MED31	Mediator of RNA polymerase II transcription subunit 31
MK01	Mitogen-activated protein kinase 1
MTR1A	Melatonin receptor type 1A
MYC	Myc proto-oncogene protein
MYL6	Myosin light polypeptide 6
MYO5A	Myosin-Va
NADK	NAD kinase
NCK2	Cytoplasmic protein NCK2
NDRG1	Protein NDRG1
NEDD8	NEDD8
NEMO	NF-kappa-B essential modulator
NEP	Neprilysin
NEP1	Probable ribosome biogenesis protein NEP1
NFX1	Transcriptional repressor NF-X1
NIPS1	Protein NipSnap homolog 1
NPM	Nucleophosmin
NUCL	Nucleolin
NUP85	Nucleoporin NUP85
ODO1	2-oxoglutarate dehydrogenase E1 component, mitochondrial
OGFD2	2-oxoglutarate and iron-dependent oxygenase domain-containing protein 2
PCNA	Proliferating cell nuclear antigen
PDCD5	Programmed cell death protein 5
PGRC1	Membrane-associated progesterone receptor component 1
PHAR3	Phosphatase and actin regulator 3
PHB	Prohibitin
PHS	Pterin-4-alpha-carbinolamine dehydratase
PIAS1	E3 SUMO-protein ligase PIAS1
PIAS2	E3 SUMO-protein ligase PIAS2
PKHA4	Pleckstrin homology domain-containing family A member 4
PP2AA	Serine/threonine-protein phosphatase 2A catalytic subunit alpha isoform
PP2BB	Serine/threonine-protein phosphatase 2B catalytic subunit beta isoform
PP4R1	Serine/threonine-protein phosphatase 4 regulatory subunit 1
PPIH	Peptidyl-prolyl cis-trans isomerase H
PRPF3	U4/U6 small nuclear ribonucleoprotein Prp3
PRS7	26S protease regulatory subunit 7
PRS8	26S protease regulatory subunit 8
PSD11	26S proteasome non-ATPase regulatory subunit 11
PSMD1	26S proteasome non-ATPase regulatory subunit 1
PTN4	Tyrosine-protein phosphatase non-receptor type 4

PTPRS	Receptor-type tyrosine-protein phosphatase S
PYR1	CAD protein [Includes: Glutamine-dependent carbamoyl-phosphate synthase
Q15136	Protein kinase A-alpha
Q53FG3	Interleukin enhancer binding factor 2 variant
Q59EG8	Proteasome 26S non-ATPase subunit 2 variant
Q5H9B5	TIMP metalloproteinase inhibitor 1
Q5JYX0	Cell division cycle 42
Q5STK0	Ral guanine nucleotide dissociation stimulator-like 2
Q6FID1	MRPL42 protein
Q6IPH7	RPL14 protein
Q6LEE2	4a-carbinolamine dehydratase
Q6NUQ0	WD repeat domain 33
Q6PJ22	FLJ13052 protein
Q7Z4W5	RNA helicase
Q86XT7	ABCC9 protein
Q8N4N7	PTPRS protein
Q92942	RalGDS-like
Q96I38	EEF1D protein
Q96J99	HTB
Q9H2P2	HT029
Q9HB23	Lysyl-tRNA synthetase
QK1	Protein quaking
QORX	Putative quinone oxidoreductase
RAB6A	Ras-related protein Rab-6A
RAD52	DNA repair protein RAD52 homolog
RAN	GTP-binding nuclear protein Ran
RB11B	Ras-related protein Rab-11B
RB22A	Ras-related protein Rab-22A
RB27A	Ras-related protein Rab-27A
RBM22	Pre-mRNA-splicing factor RBM22
RBM7	RNA-binding protein 7
RD23A	UV excision repair protein RAD23 homolog A
RECO5	ATP-dependent DNA helicase Q5
RGL2	Ral guanine nucleotide dissociation stimulator-like 2
RIPK3	Receptor-interacting serine/threonine-protein kinase 3
RL10A	60S ribosomal protein L10a
RL11	60S ribosomal protein L11
RL12	60S ribosomal protein L12
RL13	60S ribosomal protein L13
RL14	60S ribosomal protein L14
RL15	60S ribosomal protein L15
RL17	60S ribosomal protein L17
RL18	60S ribosomal protein L18
RL21	60S ribosomal protein L21
RL22	60S ribosomal protein L22
RL23	60S ribosomal protein L23
RL24	60S ribosomal protein L24

RL26	60S ribosomal protein L26
RL27	60S ribosomal protein L27
RL29	60S ribosomal protein L29
RL30	60S ribosomal protein L30
RL31	60S ribosomal protein L31
RL35A	60S ribosomal protein L35a
RL4	60S ribosomal protein L4
RL5	60S ribosomal protein L5
RL6	60S ribosomal protein L6
RL7	60S ribosomal protein L7
RL7A	60S ribosomal protein L7a
RL8	60S ribosomal protein L8
RL9	60S ribosomal protein L9
RLA0	60S acidic ribosomal protein P0
RLA1	60S acidic ribosomal protein P1
RO52	52 kDa Ro protein
ROA1	Heterogeneous nuclear ribonucleoprotein A1
ROA2	Heterogeneous nuclear ribonucleoproteins A2/B1
RPB3	DNA-directed RNA polymerase II subunit RPB3
RRBP1	Ribosome-binding protein 1
RRMJ1	Putative ribosomal RNA methyltransferase 1
RS10	40S ribosomal protein S10
RS11	40S ribosomal protein S11
RS12	40S ribosomal protein S12
RS13	40S ribosomal protein S13
RS14	40S ribosomal protein S14
RS15A	40S ribosomal protein S15a
RS16	40S ribosomal protein S16
RS18	40S ribosomal protein S18
RS19	40S ribosomal protein S19
RS2	40S ribosomal protein S2
RS20	40S ribosomal protein S20
RS23	40S ribosomal protein S23
RS24	40S ribosomal protein S24
RS26	40S ribosomal protein S26
RS28	40S ribosomal protein S28
RS3	40S ribosomal protein S3
RS3A	40S ribosomal protein S3a
RS4X	40S ribosomal protein S4, X isoform
RS6	40S ribosomal protein S6
RS7	40S ribosomal protein S7
RS8	40S ribosomal protein S8
RS9	40S ribosomal protein S9
RSSA	40S ribosomal protein SA
SAHH	Adenosylhomocysteinase
SAT1	Diamine acetyltransferase 1
SEN15	tRNA-splicing endonuclease subunit Sen15

SF3B3	Splicing factor 3B subunit 3
SFPQ	Splicing factor, proline- and glutamine-rich
SKIL	Ski-like protein
SKP1	S-phase kinase-associated protein 1
SMD2	Small nuclear ribonucleoprotein Sm D2
SMUF2	E3 ubiquitin-protein ligase SMURF2
SNAPN	SNARE-associated protein Snapin
SNW1	SNW domain-containing protein 1
SOMA	Somatotropin
SPSB1	SPRY domain-containing SOCS box protein 1
SPTA2	Spectrin alpha chain, brain
SRR	Serine racemase
SSRP1	FACT complex subunit SSRP1
STK3	Serine/threonine-protein kinase 3
SUMO2	Small ubiquitin-related modifier 2
SUMO3	Small ubiquitin-related modifier 3
SYAC	Alanyl-tRNA synthetase, cytoplasmic
SYCC	Cysteinyl-tRNA synthetase, cytoplasmic
SYDC	Aspartyl-tRNA synthetase, cytoplasmic
SYEP	Bifunctional aminoacyl-tRNA synthetase
SYFB	Phenylalanyl-tRNA synthetase beta chain
SYG	Glycyl-tRNA synthetase
SYHC	Histidyl-tRNA synthetase, cytoplasmic
SYK	Lysyl-tRNA synthetase
SYLC	Leucyl-tRNA synthetase, cytoplasmic
YSYM	Seryl-tRNA synthetase, mitochondrial
SYTC	Threonyl-tRNA synthetase, cytoplasmic
SYVC	Valyl-tRNA synthetase
SYVM	Valyl-tRNA synthetase, mitochondrial
SYWC	Tryptophanyl-tRNA synthetase, cytoplasmic
TAB2	Mitogen-activated protein kinase kinase kinase 7-interacting protein 2
TAF1A	TATA box-binding protein-associated factor RNA polymerase I subunit A
TAF2	Transcription initiation factor TFIID subunit 2
TAF5	Transcription initiation factor TFIID subunit 5
TAF6	Transcription initiation factor TFIID subunit 6
TAF8	Transcription initiation factor TFIID subunit 8
TBA1A	Tubulin alpha-1A chain
TBB1	Tubulin beta-1 chain
TBB3	Tubulin beta-3 chain
TBB4	Tubulin beta-4 chain
TBB5	Tubulin beta chain
TCPH	T-complex protein 1 subunit eta
TCPO	T-complex protein 1 subunit theta
TCTP	Translationally-controlled tumor protein
TENX	Tenascin-X
TF65	Transcription factor p65
TIMP1	Metalloproteinase inhibitor 1

TM16A	Transmembrane protein 223
TNPO1	Transportin-1
TRAF6	TNF receptor-associated factor 6
TRAP1	Heat shock protein 75 kDa, mitochondrial
TRI55	Tripartite motif-containing protein 55
TRI63	E3 ubiquitin-protein ligase TRIM63
TRIB3	Tribbles homolog 3
TSP3	Thrombospondin-3
UAP56	Spliceosome RNA helicase BAT1
UBC12	Ubiquitin-like modifier-activating enzyme 1
UBE1	NEDD8-conjugating enzyme Ubc12
UBIP1	Upstream-binding protein 1
UBIQ	Ubiquitin
UBP8	Ubiquitin carboxyl-terminal hydrolase 8
UBR5	E3 ubiquitin-protein ligase UBR5
ULA1	NEDD8-activating enzyme E1 regulatory subunit
ULK2	Serine/threonine-protein kinase ULK2
VATA	V-type proton ATPase catalytic subunit A
VATB1	V-type proton ATPase subunit B, kidney isoform
VATE1	V-type proton ATPase subunit E 1
VDAC1	Voltage-dependent anion-selective channel protein 1
VDAC2	Voltage-dependent anion-selective channel protein 2
VDAC3	Voltage-dependent anion-selective channel protein 3
VHL	Von Hippel-Lindau disease tumor suppressor
VIME	Vimentin
VPS39	Vam6/Vps39-like protein
WDR33	WD repeat-containing protein 33
XPF	DNA repair endonuclease XPF
YBOX1	Nuclease-sensitive element-binding protein 1
ZN703	Zinc finger protein 703
ZNF24	Zinc finger protein 24
ZPR1	Zinc finger protein ZPR1

Amino acids

A	Alanine
C	Cysteine
D	Aspartic acid
E	Glutamic acid
F	Phenylalanine
G	Glycine
H	Histidine
I	Isoleucine
K	Lysine
L	Leucine
M	Methionine

N	Asparagine
P	Proline
Q	Glutamine
R	Arginine
S	Serine
T	Threonine
U	Valine
W	Tryptophan
Y	Tyrosine

Nucleotides

A	Adenine
T	Cytosine
C	Guanine
G	Thymidine

Units

°C	Degrees centigrade
A	Ampere
Bp	Nucleic acid base pair
Da	Daltons
G	Gram
K	Kilo ($\times 10^3$)
L	Litre
M	Metre
M	Molar (moles per litre)
M	Mili ($\times 10^{-3}$)
Mol	Moles
N	Nano ($\times 10^{-9}$)
rpm	Revolutions per minute
U	Micro ($\times 10^{-6}$)
V	Volt
W	Watt

Other abbreviations

AMPS	2-Acrylamido-2-Methylpropane Sulphonic Acid
ATRA	All-trans-retinoic acid
BSA	Bovine serum albumin
cDNA	Complementary DNA
CO ²	Carbon dioxide
DAPI	4',6-diamidino-2-phenylindole
dH ₂ O	Distilled water

D-MEM	Dulbecco's Modified Eagle's Medium
DMSO	Dimethyl sulfoxide
DNA	Deoxyribonucleic acid
dNTPs	Deoxynucleosides
DTT	Dithiothreitol
GAP	GTPase activating protein
GDP	Guanosine diphosphate
GEF	guanine nucleotide exchange factor
GTP	Guanosine triphosphate
HCl	Hydrochloric acid
ICC	Immunocytochemistry
IHC	Immunohistochemistry
Mw	Molecular weight
N/A	Not applicable
NP-40	Nonyl phenoxypolyethoxyethanol
OPD	o-phenylenediamine dihydrochloride
PBS	Phosphate buffered saline
PCR	Polymerase chain reaction
PTI-1	Prostate tumour inducing protein
RIPA	Radioimmunoprecipitation
RNA	Ribonucleic acid
RNAi	RNA interference
SDS	Sodium dodecyl sulphate
SNP	Single nucleotide polymorphisms
TBS	Tris buffered saline
TEMED	Tetramethylethylenediamine
TIAR	T-cell-restricted intracellular antigen-1 like protein
WB	Western blotting

Abstract

During the elongation of the polypeptide chain in eukaryotic protein synthesis, GTP-bound eukaryotic translation elongation factor 1A recruits the aminoacyl tRNA to the A-site of the ribosome. The GDP-GTP recycling is catalysed by the elongation factor 1B complex (eEF1B) which in higher eukaryotes consists of three different subunits: alpha, delta and gamma. Previous studies on eEF1B focused mainly on biochemical analysis and reports of overexpression in tumours and correlation to decreased survival rate but not a lot is known about its biology. The aim of this PhD is to characterise the eEF1B subunits at the molecular level in view of their potential involvement in tumourigenesis using a variety of bioinformatic and laboratory techniques.

All three subunits were found to be ubiquitously expressed at mRNA and protein levels in all mouse tissues analysed. In addition, eEF1B δ has several transcript variants in mice derived from alternative splicing and multiple isoforms, including a brain and testis specific heavier isoform and a muscle-specific form in addition to other forms. The characteristics of each eEF1B subunit were catalogued by further bioinformatic analysis.

eEF1B α was not detectable at early mouse developmental stages, eEF1B δ showed stronger expression at pre-natal and early post-natal stages than adult stage whereas eEF1B γ is ubiquitously expressed at similar levels throughout mouse development. In adult mice and human tissues, eEF1B subunits appeared to be expressed in different cell types and cell sub-populations. Surprisingly, cytoplasmic and some nuclear expression was observed *in vivo*. This nuclear expression pattern could not be observed in cell lines and it was not related to the cell cycle stage *in vitro*. The expression of eEF1B subunits did not change during the cell cycle except eEF1B δ which was highly expressed in S-phase arrested cells.

Knockdown by siRNAs of eEF1B subunits leads to decreased proliferation, increased number of cells in G0/G1 phase and increase in apoptosis in HeLa, HCT116, DLD1 and HepG2 cells. In contrast, overexpression in HeLa cells with a V5-tagged constructs lead to increased proliferation, increased number of cells in the G2/M phase and increased viability. Knockdown of eEF1B α and eEF1B δ leads to

a reduction in eEF1B γ levels; it is therefore possible that the phenotype shown by the knockdown of each subunit individually might be due to the reduced levels of eEF1B γ . However, overexpression of each subunit did not affect the protein levels of the other subunits.

The presence of multiple forms, the complex expression pattern and distribution of each eEF1B subunit in mouse and human tissues, and the knockdown and overexpression effect on cells suggests that the eEF1B complex might have different quaternary forms throughout development and in different cell types, possibly a more intricate role in translation, potential non-canonical functions any of which may be implicated in the potential role of eEF1B subunits in tumourgenesis.

Chapter 1 – Introduction

1.1 Protein synthesis

The central dogma first suggested by Francis Crick describes the flow of biological information in that DNA can be replicated and transcribed into mRNA, which in turn will serve as a template for the synthesis of proteins. The information from proteins cannot be transferred back to nucleic acid and proteins have a vital function in cells. These facts make the process by which proteins are synthesised an essential mechanism. Protein synthesis, also called translation, is conventionally divided into three stages. Firstly, all the components required to start translation are assembled and the first amino acid is taken to the ribosome, followed by elongation of the peptide chain until the complete peptide is released.

Initiation

For protein synthesis to take place, the ribosome subunits have to be assembled onto the mRNA around the start codon AUG. Ribosomes are comprised of two subunits: the large (60S in eukaryotes) and the small subunit (40S in eukaryotes) and contain binding sites for the transfer RNA (tRNA). Each tRNA, composed of around 75 base pairs, contains an amino acid that will be recruited to the ribosome and incorporated into the peptide chain as well as an anti-codon triplet, specific to that particular amino acid, which is complementary and has the ability to bind to the correspondent mRNA codon (amino-acyl tRNA).

In the initiation stage the initiator tRNA, which contains the amino acid methionine (iMet), is recruited to the peptidyl-site (P-site) of the ribosome and the translational machinery binds to the start codon (Ghosh and Ghosh, 1972). In eukaryotes multiple protein factors are involved in this highly regulated process with many being essential for translation initiation. eIF2 bound to GTP assists the

recruitment and binding of the methionyl tRNA to the 40S ribosomal subunit. On the other hand, the eIF4 complex is composed of multiple factors that are essential for binding of the mRNA to the ribosomes. eIF4A, which has RNA helicase activity, together with eIF4B is thought to unwind the RNA secondary structures. Along with the cap-binding protein eIF4E and the interaction of eIF3, the scaffolding protein eIF4G directs the ribosomal machinery to the mRNA 5' terminal cap structure. Once positioned on the mRNA the ribosome scans through the mRNA and upon recognition of a start codon in a favourable context, usually near a 'Kozak' sequence (Kozak and Shatkin, 1978), eIF5B catalyse the joining of the ribosomal subunits and translation starts.

However in some cases, the ribosomal machinery is assembled near or at the start codon, with no need for scanning. These internal ribosome entry sites (IRES) were first described in viral RNAs, but are now also known to exist in eukaryotes (Sonenberg and Meervitch, 1990). Cap-dependent protein synthesis in animal cells is inhibited by heat shock, serum deprivation, metaphase arrest, and infection with certain viruses (Mathews et al., 2007).

Besides mRNA specific regulation by, for example, IRES or miRNAs, translation initiation can also be regulated globally by acting on eIF2, eIF4E and eIF4G (reviewed at Gebauer and Hentze, 2004). eIF2 is involved in the met-tRNA binding to the ribosome, and can be activated by the guanine nucleotide exchange factor (GEF) eIF2B complex and inactivated by the GTPase activating protein (GAP) eIF5. Moreover, eIF4E binding to eIF4G can be blocked by phosphorylation of eIF4E binding proteins (4E-BPs) (Proud, 2002).

Elongation

Once the met-tRNA is on the P-site of the ribosome, another tRNA with a anti-codon complementary to the second codon of the mRNA is recruited to the

aminoacyl-site (A-site) of the ribosome. The amino acid on the P-site forms a covalent bond with the amino acid on the A-site elongating a peptide chain catalysed by peptidyl transferase activity of the ribosomal RNA (rRNA)(Grove and Johnson, 1974). The tRNA on the P-site moves to the exit-site (E-site), the ribosome moves one codon downstream and the tRNA on the A-site with the peptide chain moves onto the P-site. That allows another tRNA to be recruited to the available A-site and the peptide chain continues to grow during the elongation phase (Figure 1.1).

Similar to initiation, several protein factors are also involved in elongation. Eukaryotic translation elongation factor 1A (eEF1A) bound to GTP recruits the amino-acyl-tRNA to the A-site of the ribosome, elongation factor 1 B complex (eEF1B) acts as eEF1A guanine nucleotide exchange factor (GEF), the ribosome acts as GTPase activating protein (GAP) (Campuzano and Modolell, 1980) but translationally controlled tumour protein (TCTP) can also possibly act as eEF1A GAP (Cans et al., 2003), and elongation factor 2 (eEF2) is responsible for the translocation. At the elongation phase, tRNA discrimination and selection is regulated in order to maintain translational fidelity (reviewed in Zaher and Green, 2009).

Termination

The peptide chain elongation continues until a stop codon is reached. When a stop codon is reached, instead of a tRNA binding to the ribosome A-site, a termination release factor binds to it (eRF1 and eRF3) and facilitates the release of the completed polypeptide chain. Missing or misinterpretation of a stop codon can lead to translation beyond the end of the coding sequence resulting in non-functional protein or possibly even one that is toxic to the cell. Regulation of the nonsense mediated decay (NMD) by release factors (eRF1 and eRF3) and poly A binding protein (PABP), amongst other proteins, is essential for the wellbeing of the cell (mammalian NMD reviewed in Silva and Romao, 2009).

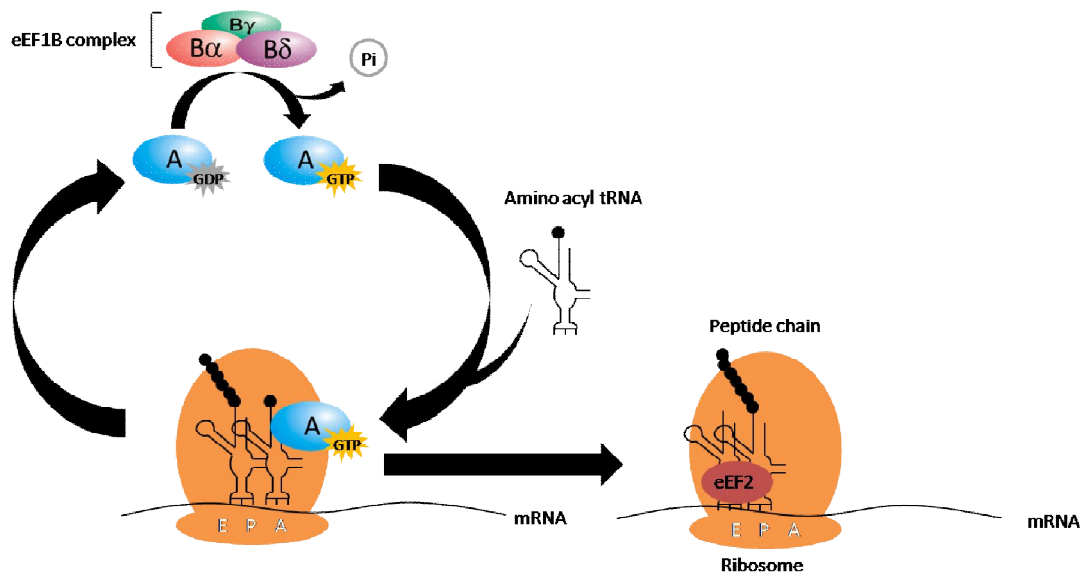


Figure 1.1 Diagram of translation elongation in mammals. A – eEF1A, B α – eEF1B α , B δ – eEF1B δ , B γ – eEF1B γ .

1.2 Eukaryotic translation elongation factor 1 A

Eukaryotic translation elongation factor 1A, formerly known as eEF1 α and equivalent to the bacterial elongation factor transfer unstable (EF-Tu), is responsible for the recruitment of the charged amino acylated tRNAs to the ribosomal A-site when activated upon GTP binding. GTP is hydrolysed to GDP, and eEF1A:GDP is recycled to eEF1A:GTP by eEF1B forming a translation elongation heavy complex (eEF1H). In lower eukaryotes such as *Saccharomyces cerevisiae*, there are at least two genes which encode for two eEF1A identical proteins, TEF1 and TEF2, whereas in higher eukaryotes, eEF1A exists as two tissue specific variants, eEF1A1 and eEF1A2.

During early development eEF1A1 is ubiquitously expressed, however during early postnatal developmental a switch occurs in mice and rats where eEF1A1 levels in skeletal muscle, cardiac muscle and neurons drop to undetectable levels and eEF1A2 expression increases in those tissues thus becoming the major form (Chambers et al., 1998, Newbery et al., 2007). eEF1A1 and eEF1A2 are mutually exclusively expressed except in certain tumour cells and cell lines where

eEF1A2 is overexpressed (Tomlinson et al., 2005, Anand et al., 2002). Mice homozygous for the wasted mutation (*wst*), which lack eEF1A2 amongst other genes, develop a motor neuron degeneration disease phenotype which coincides with the variant expression switch (Chambers et al., 1998). The wasted spontaneous autosomal recessive mutation in mice is characterised by vacuolar degeneration of motor neurons, weight loss due to loss of muscle bulk, tremors and spleen and thymus atrophy leading to death by about 28 days. The deletion of a 15.8 kilobase region which includes the eEF1A2 promoter and first non-coding exon as well as several other genes, causes loss of eEF1A2 which is in turn fully responsible for the wasted phenotype (Chambers et al., 1998, Newbery et al., 2007).

Besides its role in translation, eEF1A1 has multiple non-canonical roles in cytoskeleton remodelling, apoptosis, stress response and protein degradation, that will be discussed briefly later (reviewed in Lamberti et al., 2004).

1.3 Eukaryotic translation elongation factor 1 B

Eukaryotic translation elongation factor 1B complex is responsible for the guanine exchange activity of eEF1A. In lower eukaryotes, the complex is formed by two subunits, alpha and gamma, whereas in higher eukaryotes it has an additional subunit, delta. Both eEF1B α and eEF1B δ have guanine nucleotide exchange activity (GEF) whereas eEF1B γ has no known role in translation. Throughout the last few decades since this complex was first purified, the nomenclature of the subunits has constantly changed. Bearing in mind that at some point both eEF1B α and eEF1B δ were called beta, and for the sake of keeping this thesis as easy to follow as possible, only one universal nomenclature, as was suggested by Le Sourd et al., will be used (Le Sourd et al., 2006a). This table shows the various names by which eEF1B subunits were known (Table 1.1).

Table 1.1 Nomenclature of elongation factor 1 B multimer in human

Nomenclature Committee of the International Union of Biochemistry (NC-IUB) nomenclature (1988)	International Union of Biochemistry and Molecular Biology (IUBMB) nomenclature (1996)	Merrick's nomenclature (2001)	Le Sourd's nomenclature (2006)	Locus symbol	Molecular Weight (kDa)
eEF-1 β	eEF1 β	eEF1B α		EEF1B	28-30
eEF-1 δ	eEF1 δ	eEF1B β	eEF1B δ	EEF1D	33-36
eEF-1 γ	eEF1B γ			EEF1G	47-50

1.3.1 eEF1B α

eEF1B α was first sequenced and mapped to human chromosome 2 in 1991 by two independent groups. The sequences differed in their 5' untranslated region (UTR) but encoded an identical protein (Sanders et al., 1991, von der Kammer et al., 1991) (Figure 1.2). Three other related sequences were mapped on chromosome 15 (eEF1B1), 5 (eEF1B3) and X chromosome (eEF1B4). eEF1B3 locus was reported to be a brain and muscle specific transcript that arose from a pseudogene while eEF1B1 was suggested to be a recent retrotransposition event (Chambers et al., 2001).

eEF1B α is equivalent to the bacterial elongation factor transfer stable (EF-Ts). The catalytic site of eEF1B α is on the C terminus, which is responsible for binding to eEF1A and for GEF activity. eEF1B α binding to eEF1A confers a conformational change which favours the GDP to be released so that the less abundant GTP can bind specifically to eEF1A (Andersen et al., 2001). eEF1B α protein purified from rat and rabbit liver highly stimulates the exchange of GDP to GTP on eEF1A, tRNA binding to the ribosome and phenylalanine synthesis rate (Bec et al., 1994, Sheu and Traugh, 1997).

eEF1B α in yeast *Saccharomyces cerevisiae* is essential for normal survival (Hiraga et al., 1993) and interestingly, over expression of eEF1A in yeast overcomes

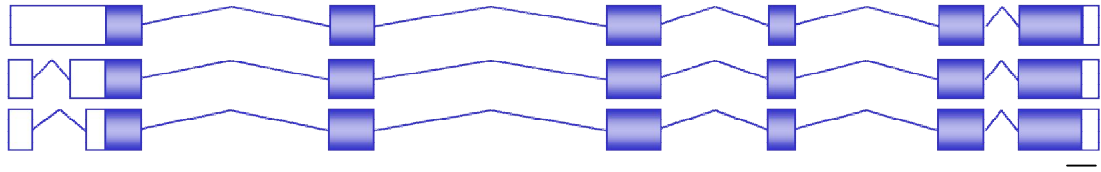


Figure 1.2 – Diagram of the eEF1B α gene structure showing three different 5' UTR that arose by alternative splicing. *Black bar at the bottom right indicates 100bp.*

the eEF1B α knockout lethal phenotype but the rescued yeast still possess growth defects and reduced translation fidelity (Kinzy and Woolford, 1995). The absence of the eEF1B α GEF activity in the C terminus but not the N terminus is responsible for the lethal phenotype and the human eEF1B α sequence rescues the yeast eEF1B α knockout lethal phenotype, indicating a highly conserved function (Carr-Schmid et al., 1999b).

1.3.2 eEF1B δ

The delta subunit of eEF1B complex was first sequenced, mapped to human chromosome 8 and found to have a leucine zipper motif in the predicted amino acid sequence 53 to 97 in 1993 by Sanders and colleagues (Sanders et al., 1993).

The C-terminus of eEF1B δ is almost identical to eEF1B α , and eEF1B δ from rat and rabbit liver also possesses GEF activity as seen for eEF1B α but with a much shorter half-life. Furthermore, in both rat and rabbit liver a portion of the purified eEF1B δ travels as a high molecular weight aggregate, above 1000kDa. The short half-life coincides with the formation of the eEF1B δ aggregates, indicating that they might be inactive (Bec et al., 1994, Sheu and Traugh, 1997).

Although it has an almost identical C-terminus to eEF1B α , overexpression of human eEF1B δ , which is not present in yeast, does not rescue the yeast eEF1B α knockout lethal phenotype (Carr-Schmid et al., 1999b).

1.3.3 eEF1B γ

Human eEF1B γ was first sequenced and mapped to chromosome 11 in 1992 (Kumabe et al., 1992). It is known to have a conserved glutathione S-transferase (GST) domain, enzymes which catalyse a variety of substrates and play a role in cellular stress, but its ability to possess GST activity is controversial and will be discussed later (Koonin et al., 1994). In yeast *S. cerevisiae*, two genes encode proteins homologues to eEF1B γ , TEF-3 and TEF-4, which are not essential for growth and their knockout does not alter translation rate (Kinzy et al., 1994).

Although eEF1B γ as a monomer does not affect the GEF rate, when in complex with eEF1B α but not with eEF1B δ , it leads to an increased GEF rate by probably changing the conformation of the eEF1A:eEF1B α :eEF1B γ complex (Bec et al., 1994). Together with the fact that eEF1B γ has affinity with the cytoskeleton and membranes, has lead to the suggestion that it serves as an anchor for the eEF1B complex (Bec et al., 1994). Moreover, eEF1B γ was found to exist as a higher form complex, possibly a trimer, in rat liver (Bec et al., 1994).

1.4 Eukaryotic translation elongation factor 1 B structure and regulation

1.4.1 Models of eEF1B complex quaternary structure and GEF rates

Purified eEF1A from rat and rabbit liver alone led to a steady but very low eEF1A:GDP exchange rate (Bec et al., 1994, Motorin Yu et al., 1988, Venema et al., 1991b), phenylalanine synthesis rate (Sheu and Traugh, 1997) and efficient binding of tRNAs to ribosome which indicates a remote possibility of another eEF1A GEF with lower activity existing, however this is most likely due to the presence of a small portion of eEF1B complex in the purified fraction. eEF1B complexed with eEF1A gives rise to a greater eEF1A GEF rate and tRNA ribosome binding activity compared with other complex forms (Bec et al., 1994, Venema et al., 1991b, Motorin et al., 1991).

Interestingly, no interaction was ever found between eEF1B α and eEF1B δ in several species by purification of the complex, co-immunoprecipitation or even yeast two-hybrid (Bec et al., 1994, Ong et al., 2006, Mansilla et al., 2002). Yeast eEF1A was found to interact moderately with human eEF1B α and strongly with eEF1B δ (Carr-Schmid et al., 1999b).

Amino acid tRNA synthetases catalyse the aminoacylation process which involves linking an amino acid to a phosphate of ATP, forming aminoacyl-adenylate and subsequently linking to the 2' or 3' terminal hydroxyl groups of the tRNA, forming the aminoacyl-tRNA. This 'charged' aminoacyl-tRNA can then be delivered to the ribosome by eEF1A. Valyl-tRNA synthetase (VARS) is the only tRNA synthetase that, when purified in both rat and rabbit, completely co-purifies with the eEF1B complex (Motorin Yu et al., 1988, Bec et al., 1994, Venema et al., 1991b). The exception is one study which reported the purification of valyl-tRNA synthetase as monomers in rat liver (Godar and Yang, 1988). VARS:eEF1B shows a complex of 700 and 760kDa in rat liver and *Xenopus* oocytes respectively, and VARS:eEF1H complexes ranging from 700kDa in brine shrimp up to 800kDa in rat and rabbit tissues (Venema et al., 1991b, Bec et al., 1994, Motorin et al., 1991, Brandsma et al., 1995, Minella et al., 1998). Only a portion of the eEF1B complex is predicted to be bound to valyl-tRNA synthetase in *Xenopus* and rabbit liver (Bec et

al., 1989, Minella et al., 1998, Venema et al., 1991b). VARS:eEF1B is predicted to give a small but clear GEF rate increase and lead to an increase in tRNA ribosome binding compared with eEF1B complex alone (Bec et al., 1994, Motorin et al., 1991, Peters et al., 1995).

In vertebrates, no other tRNA synthetase is known to co-purify with eEF1B, and valyl-tRNA synthetase does not co-purify with any other tRNA synthetase (Bec et al., 1989). However, in *S. cerevisiae*, valyl-tRNA synthetase does not bind to the eEF1B complex (Brandsma et al., 1995). Valyl-tRNA synthetase N-terminus extension with a GST domain, which is specific to vertebrates, was found to bind to the eEF1B δ subunit but not to any other subunit in rabbit liver cells (Bec et al., 1994). Interestingly, other tRNA synthetases have been found to interact with eEF1B α and eEF1B γ subunits by yeast two-hybrid, including leucyl and histidyl-tRNA synthetases (Sang Lee et al., 2002). Furthermore, in higher eukaryotes, nine aminoacyl-tRNA synthetases and three auxiliary proteins (p18, p38 and p43) form the multisynthetase complex (Kerjan et al., 1994), a poorly characterised complex which has no known function. The auxiliary protein, p18, shares an N-terminal domain with eEF1B α and eEF1B γ and it has been suggested it should be renamed eukaryotic translation elongation factor 1 epsilon (eEF1B ϵ) (Quevillon and Mirande, 1996). However, there is no confirmation of interaction between p18 and any of the eEF1B subunits. Interestingly, as well as p18 most tRNA synthetases and the auxiliary protein p36 share a domain with eEF1B α and eEF1B γ . Furthermore, eEF1A has the ability to bind deacylated tRNAs that belong to the multisynthetase complex and stimulate aminoacylation in rabbit (Petrushenko et al., 1997). eEF1A can also stimulate VARS aminoacylation, most likely through the interaction of eEF1B with VARS since eEF1A does not interact physically with VARS (Negrutskii et al., 1999).

Several quaternary models have been proposed throughout the last few years which, besides differing in the actual number of subunits that compose the complex, also differ in the interaction sites (N- or C-terminus) between the different subunits (Bec et al., 1994, Janssen et al., 1994, Sheu and Traugh, 1999, Mansilla et al., 2002). A summary diagram of all the eEF1B, eEF1H and eEF1H:VARS structure models is given in figure 1.3.

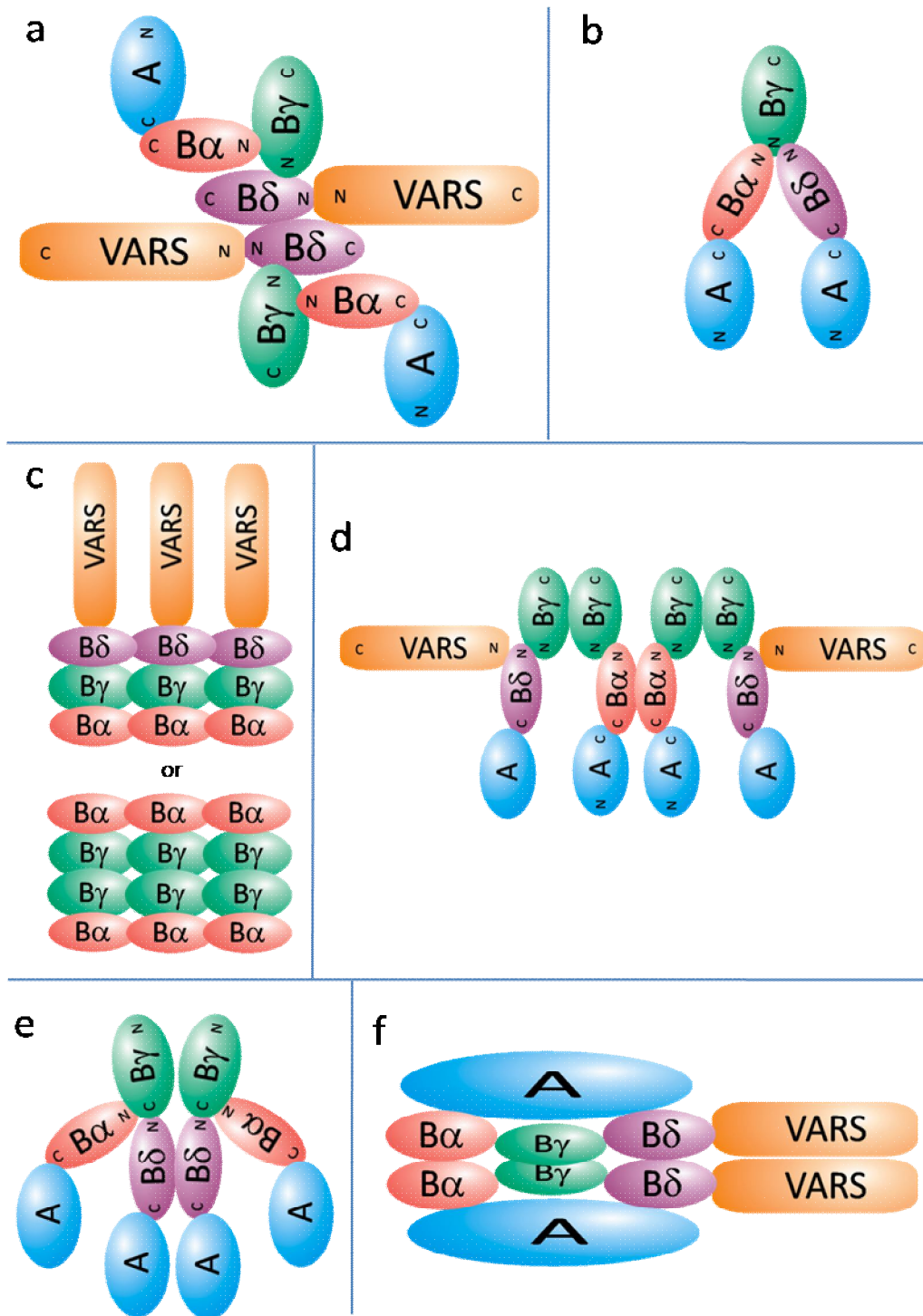


Figure 1.3 eEF1B complex quaternary structure models: (a) Bec et. al. 1994, (b) Janssen et. al. 1994, (c) Minella et. al. 1998, (d) Sheu and Traugh 1999, (e) Mansila et. al. 2002, and (f) Jiang et. al. 2005. A – eEF1A; B α – eEF1B α ; B δ – eEF1B δ ; B γ – eEF1B γ ; VARS – Valyl tRNA synthetase

1.4.2 Regulation of eEF1B subunits

There are multiple reports on the ability of eEF1B subunits to be phosphorylated by certain stimuli. Phorbol 12-myristate 13-acetate (PMA) which mimics induced growth hormone release factor by activating protein kinase C (PKC) (Chuang et al., 1998) was found to phosphorylate eEF1A, eEF1B α , eEF1B δ and VARS, and to lead to an increase in phenylalanine synthesis in rabbit reticulocytes (Venema et al., 1991b). The same phosphorylation sites were phosphorylated *in vitro* by PKC, but only phosphorylation of eEF1B α and eEF1B δ led to increased elongation rates and tRNA binding to the ribosome upon growth hormone stimulation (Venema et al., 1991a, Peters et al., 1995). More recently, eEF1B γ was found to interact with the dopamine D3 receptor (D3R) and form clusters on the plasma membrane, but not with D2R or D4R (Cho et al., 2003). eEF1B α was phosphorylated in response to stimulation by D3R and depletion of PKC abolished eEF1B α phosphorylation. Furthermore, activation of PKC resulted in D3R and eEF1B α phosphorylation but activation of D3R did not activate PKC. This indicates that eEF1B α is phosphorylated by D3R activation by eEF1B γ interaction in a PKC level dependent manner (Cho et al., 2003).

eEF1A, eEF1B α and eEF1B δ are phosphorylated by multipotential S6K as a result of insulin stimulation (Chang and Traugh, 1997). In the presence of little or no eEF1A, phosphorylation of purified eEF1B α and eEF1B δ by S6K leads to an increase in phenylalanine synthesis and tRNA binding to the ribosomes by more than 2 fold compared with serum-deprived mouse 3T3 cells (Chang and Traugh, 1997). All phosphorylation sites on both eEF1B α and eEF1B δ are the same for insulin- and S6K-induced phosphorylation (Chang and Traugh, 1998). Phosphorylation of eEF1B α and eEF1B δ were stimulated by PMA to a similar extent as that found with insulin, and the phosphorylation sites were found to be identical. eEF1B α , eEF1B γ and eEF1A1 were identified, by microarray study and confirmed by real time PCR, as being regulated in a serum and rapamycin-dependent way by tuberous sclerosis

1 and 2, TSC1 and TSC2 (Bilanges et al., 2007). Moreover, all human eEF1B genes have 5' terminal oligopyrimidine track (5' TOP) upstream, a stretch of pyrimidine residues that act as cis-acting modulators of translation efficiency and were thought to be regulated by S6K1. However TSC1/2 and mTOR affect translation via phosphorylation of S6K1 independently from the 5' TOP status (Iadevaia et al., 2008).

Both eEF1B δ and eEF1B γ in *Xenopus* oocytes are major maturation promoting factor (or cell division cycle p38 cdc2) substrates (Mulner-Lorillon et al., 1994, Asselin et al., 1984). eEF1B γ was found to be phosphorylated by p38 cdc2 in mature oocytes but not in prophase-arrested oocytes (Mulner-Lorillon et al., 1992). This phosphorylation resulted in decreased rate of incorporation (synthesis) of valine and increased synthesis of serine and phenylalanine (Monnier et al., 2001a) but did not alter the guanine exchange rate (Mulner-Lorillon et al., 1992, Mulner-Lorillon et al., 1989). Monnier suggested that p38 cdc2 inactivated eEF1B:VARS leaving more freely available eEF1B for protein synthesis (Monnier et al., 2001a). Activation of p38 cdc2 is involved in the progression into mitosis and exit of mitosis involves its inactivation (discussed later) (Doree, 1990).

Brine shrimp eEF1B α along with *Xenopus* and rabbit eEF1B α and eEF1B δ are phosphorylated by casein kinase II (CKII) (Chen and Traugh, 1995, Palen et al., 1994, Janssen et al., 1988, Belle et al., 1989). CKII phosphorylation of eEF1B δ was only seen in the presence of GDP whereas eEF1B α phosphorylation was stimulated by GDP, lysine and arginine (Palen et al., 1994). No change was observed in the phenylalanine synthesis rate upon CKII phosphorylation of rabbit recombinant eEF1B α or eEF1B δ proteins (Chen and Traugh, 1995). However, in the brine shrimp phosphorylation by CKII of eEF1B α leads to an increase in eEF1A:GDP of about 50% (Janssen et al., 1988). Furthermore, CKII is phosphorylated and activated by p34 cdc2 in a cell cycle dependent manner upon stimulation by growth factors (Homma and Homma, 2005). CKII knockout in yeast and mouse is lethal (Buchou et

al., 2003) and besides its involvement in the cell cycle, CKII also phosphorylates a wide range of targets upon stress and DNA damage (Ahmed et al., 2002, Keller et al., 2001).

eEF1B δ is known to be phosphorylated by herpes simplex virus (HSV-1) UL-13 kinase (Kawaguchi et al., 1998), cytomegalovirus (CMV) UL-97 kinase (Kawaguchi et al., 1999) and Epstein-Barr virus (EBV) BGLF4 kinase (Kato et al., 2001) upon viral infection. The eEF1B δ phosphorylation site was identified as being the same site that is phosphorylated by cdc2, suggesting that viral kinases might mimic cdc2 in infected cells (Kawaguchi et al., 2003). eEF1B δ is also known to interact with a transactivator of HSV-1, infected cell protein 0 (ICP0). Co-immunoprecipitation of ICP0 and eEF1B δ results in a decrease in the rate of incorporation of methionine compared to precipitation of eEF1B δ alone (Kawaguchi et al., 1997). It is also known that eEF1B δ interaction with HIV-1 Tat mRNA highly reduces methionine incorporation rate but not that of viral protein synthesis (Xiao et al., 1998). Regulation of eEF1B subunits might play an important role in mitotic translation and translation during viral infection.

In addition to all of the regulation of eEF1B by phosphorylation described above, eEF1B γ was also found to be phosphorylated following addition of the chemotherapy drug Paclitaxel (taxol) which stabilizes microtubules and causes G2/M arrest-induced apoptosis via c-Jun N-terminal kinase (JNK) activation and B-cell lymphoma protein 2 (Bcl-2) phosphorylation (Prado et al., 2007). Yeast eEF1B α dephosphorylation by Ppz1 phosphatase enhances translation fidelity *in vitro* (Aksenova et al., 2007). In addition, all eEF1B subunits were found to be up-regulated by Myc overexpression in human and chicken tumour cells (Boon et al., 2001, Neiman et al., 2001). However, in non-transformed rat and mouse cells, no change was observed in eEF1B subunits when comparing Myc overexpressing cells to Myc null cells (Watson et al., 2002) suggesting that up-regulation might be a due to the transformed cancer cell rather than a direct effect of myc overexpression. The eEF1B subunits link to tumourigenesis will be further discussed. Figure 1.4 shows a summary diagram of all phosphorylation sites in eEF1B subunits.

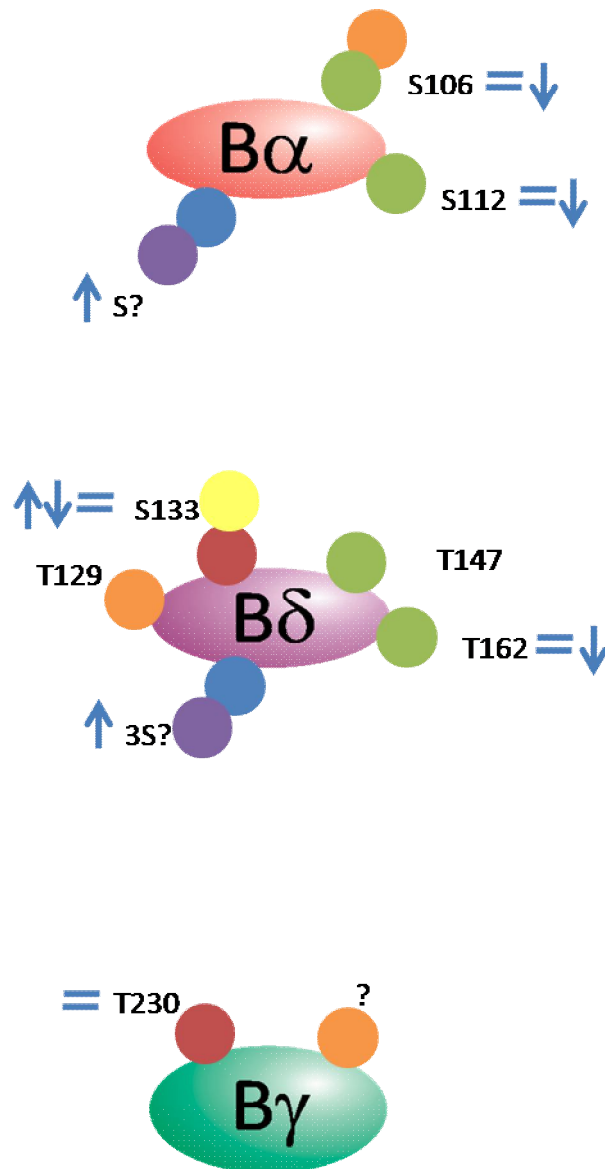


Figure 1.3 Phosphorylation sites of eEF1B subunits and their influence in the translation elongation rate by measuring a particular amino acid synthesis and guanine exchange rate indicated by arrows or equal signs where no change was detected.

Yellow circle: viral; Blue circle: PKC; Red circle: p38 cdc2; Green circle: CKII; Purple circle: S6K; Orange circle: others. B α – eEF1B α ; B δ – eEF1B δ ; B γ – eEF1B γ ; S – Serine; T – Threonine

1.5 eEF1B and cancer

A common mechanism of cancer involves aberrant transcription and translation leading to up and down regulation of proteins. Failure to reduce protein synthesis can lead to an increased rate of translational errors, increased synthesis of oncogenic proteins and consequent transformation of cells (Mathews et al., 2007). The initiation factors known to be highly regulated and alter translation rate have been extensively studied for their involvement in transformation and tumourigenesis (reviewed in Clemens, 2004).

The elongation rate is known to be regulated by serum or insulin stimulation (eEF1B α , eEF1B δ and eEF2)(Proud and Denton, 1997), heat shock (eEF1A1) (Theodorakis et al., 1988), and might even be cell-cycle dependent (eEF1B δ and eEF1B γ)(Cormier et al., 2003). Plus, an increase in translation elongation rate of the protein synthesis has been previous linked to increased protein translation errors (Carr-Schmid et al., 1999a). On the one hand, the oncogene prostate tumour inducing protein-1 (PTI-1), a eEF1A1 truncated form which has 5'UTR homologous to 23S rRNA (Shen et al., 1995), has been reported to reduce translational fidelity leading to tumourigenesis (Gopalkrishnan et al., 1999). eEF1A1 has also been suggested to be a regulator of apoptosis and susceptible to chemical and radiation-induced transformation (reviewed in Lamberti et al., 2004). On the other hand, eEF1A2 is overexpressed in ovarian, breast and pancreatic tumours (Anand et al., 2002, Tomlinson et al., 2007, Tomlinson et al., 2005, Cao et al., 2009).

1.5.1 eEF1B α

eEF1B α mRNA has been found to be overexpressed more than 20 fold in a number of transformed cells compared with non-transformed cells (Sanders et al., 1992) and 2 to 3 fold in breast cancer cell lines compared with non-transformed cell lines (Al-Maghrebi et al., 2005), but protein levels were not looked into. So far, only

one study mentions eEF1B α protein overexpression in relation to highly metastatic prostate cancer cells (PC3M-LN4) compared with low metastatic cells (PC3M) (Everley et al., 2004).

1.5.2 eEF1B δ

eEF1B δ has been reported to be overexpressed in a large range of tumour and cancer cells compared with non-cancerous cells. It showed a 2 fold increase in human primary ductal carcinoma cells, breast carcinoma cells (T-47), and breast adenocarcinoma cells (MCF-7 and MDA-MB-361) compared with non-transformed cell lines (Joseph et al., 2004). eEF1B δ was also shown by Northern blot to be overexpressed in all the mammary and ovarian cancer cell lines tested compared with non-transformed cells (Jacob et al., 1996). As well as eEF1B α , eEF1B δ protein was also found to be overexpressed in highly metastatic prostate cancer cells (PC3M-LN4) compared with low metastatic cells (PC3M) (Everley et al., 2004). The relationship between eEF1B δ and overexpression of several oncogenes was studied further. eEF1B δ mRNA expression levels did not change with overexpression of oncogenes c-erbB, tumour growth factor α , viral-src, viral-myc nor viral-FBJ murine osteosarcoma (v-Fos) (Kolettas et al., 1998). However, the expression levels were reduced by 3 to 5 fold by overexpression of viral-ras in human keratinocytes but not in human diploid fibroblasts, with no obvious reason for this effect and specificity (Kolettas et al., 1998).

eEF1B δ mRNA was found to be overexpressed in 73% of 52 patients with both benign and malignant oesophageal tumours (Ogawa et al., 2004). The eEF1B δ overexpression was found to a greater extent in cancerous tissues compared with non-cancerous. Furthermore, eEF1B δ overexpression significantly correlated with the presence of lymph node metastases, advanced stage cancer and poor prognosis (Ogawa et al., 2004). eEF1B δ was identified as being overexpressed in all 10 gastric

carcinoma tissues compared with adjacent normal tissues (Zeng et al., 2007). Zeng and colleagues suggested that eEF1B δ expression could be used as a biomarker for gastric cancer (Zeng et al., 2007).

In hepatocellular carcinoma, eEF1B δ has been reported to be overexpressed more than 2 fold and by almost 5 fold in hepatitis B virus associated hepatocellular carcinoma compared to adjacent normal liver tissues (Shuda et al., 2000, Blanc et al., 2005). It has also been identified as a colon tumour antigen recognised by the humoral immune system (Scanlan et al., 1998) and found to be up-regulated in protein expression profiles of colon tumours compared with adjacent tissues (Roblick et al., 2004).

In a study which investigated chromosomal copy number aberrations in medulloblastoma, a gain of the 8p chromosomal region was associated with worse overall survival rate in 71 tumour samples. Overexpression of *myc*, encoded by a gene in the same amplified region, could not be entirely responsible for the worse survival rate. However, amplification and mRNA overexpression of eEF1B δ and two ribosomal proteins were found to be statistically significantly associated with the worst survival rate (De Bortoli et al., 2006). De Bortoli and colleagues also found that eEF1B δ mRNA up-regulation was associated with worst survival in most medulloblastomas even when chromosome 8p was not amplified, but the protein level was not investigated. However, in a different study, eEF1B δ protein was also found to be up-regulated in medulloblastomas compared with adjacent normal tissues (Peyrl et al., 2003). In six lung adenoma cell lines, eEF1B δ was also found to have increased genomic copy number and to be up-regulated at the mRNA level but not at the protein level compared with normal bronchial epithelial cell lines (Li et al., 2006). However, in non-small cell lung cancer, eEF1B δ protein is up-regulated up to 4 fold compared to normal bronchial epithelial cells (Liu et al., 2004). Moreover, eEF1B δ protein overexpression is correlated with high metastatic status compared with less invasive squamous lung cancer cell lines (Keenan et al., 2009).

eEF1B δ is known to interact with the FBJ osteosarcoma oncogene (Fos) in mice (Miyamoto-Sato et al., 2005), to interact with human translationally controlled tumour protein (TCTP, (Langdon et al., 2004), and has been implicated in chemical, radiation-induced transformation and drug resistance (discussed below). A 2D-electrophoresis model was used to identify proteins associated with the development of chemo resistance in malignant melanoma, where eEF1B δ was found to be overexpressed in comparison with non-resistant melanoma (Sinha et al., 2000). Furthermore, the eEF1B δ protein level but not the mRNA level as well as that of eEF1A and eEF1B γ decreased by more than 50% upon treatment with all-trans-retinoic acid (ATRA) which induces growth inhibition, differentiation and apoptosis in cancer cells and is often used to treat acute promyelocytic leukaemia (APL) (Harris et al., 2004).

Joseph et al. suggested that cell transformation and tumourigenesis induced by cadmium is in part due to eEF1B δ overexpression since eEF1B δ is up regulated in BALB/c NIH-3T3 cells transformed with cadmium and the oncogenic potential was reversed by transfection with eEF1B δ antisense oligonucleotides (Joseph et al., 2002). Subsequently, Joseph et al showed that overexpression of the delta subunit of eEF1B by transfection was oncogenic in NIH3T3 cells as evidenced by the appearance of transformed foci exhibiting anchorage-independent growth and the potential for the cells to grow as tumours in nude mice. In 2002, another independent study over-expressed eEF1B δ in non-transformed NIH3T3 cells, which resulted in the transformation of cells and this effect was able to be reversed by transfecting cells with eEF1B δ antisense oligonucleotides (Lei et al., 2002). Although no study focused on changes in protein synthesis and hence it is unknown if the protein synthesis was elevated in those cancer samples, both of these studies suggest that eEF1B δ has oncogenic potential by itself.

1.5.3 eEF1B γ

eEF1B γ mRNA was found to be up-regulated 2 to 3 fold in breast cancer cell lines compared with non transformed cell lines (Al-Maghrebi et al., 2005, Joseph et al., 2004), but the protein levels were not examined. eEF1B γ , as well as eEF1B α and eEF1B δ , showed overexpression at the protein level in highly metastatic prostate cancer cells (PC3M-LN4) compared with low metastatic cells (PC3M) (Everley et al., 2004).

In lung adenoma cell lines, eEF1B γ was found to have increased genomic copy number, and overexpressed at the mRNA and protein level compared with normal bronchial epithelial cell lines (Li et al., 2006). Only four genes were found to have increased genomic copy number and overexpressed at both mRNA and protein levels, which included eEF1A2, and were further studied. However, eEF1B γ was not further examined although their data suggested that it fulfilled the criteria. It is likely that eEF1B γ was misidentified since although eEF1B γ was the only gene that showed increased copy number and overexpression at mRNA level according to supplementary data, it was not included in the main findings table (Li et al., 2006).

Furthermore, eEF1B γ mRNA was found to be overexpressed in 22 of 30 (73%) gastric carcinomas compared with adjacent normal mucosa. No correlation was found between overexpression and grading of the tumour or invasiveness but there is a trend towards correlation with vascular permeation (Mimori et al., 1995). However, it was also found to be overexpressed 2-fold in 5 of 36 (14%) oesophageal carcinoma compared with adjacent tissue and the overexpression was highly correlated with the presence of several lymph node metastases and grade of the tumour (Mimori et al., 1996). In hepatocellular carcinoma, on the other hand, eEF1B γ has been reported to be overexpressed 1.5 to 2 fold in carcinoma compared to adjacent normal liver tissues (Shuda et al., 2000).

eEF1B γ has been reported to be overexpressed 2 fold or more in 86% of 29 colorectal carcinomas compared with adjacent normal tissues (Chi et al., 1992) and in 56% of colorectal carcinomas compared with corresponding normal-appearing distant tissue from patients without familial adenomatous polyposis (Ender et al., 1993). Moreover, eEF1B γ was observed to be overexpressed in colorectal carcinoma Dukes Stage B, C and D tumours in 17 of 27 patients (63%) when compared with adjacent normal tissues. No overexpression was detected in the two patients with Dukes Stage A (Mathur et al., 1998). At the mRNA level, eEF1B γ was found to be overexpressed in 7 out of 9 pancreatic adenocarcinoma tissues compared with normal adjacent pancreatic tissues (Lew et al., 1992). The mechanisms by which eEF1B γ is overexpressed have been studied by Frazier and colleagues. They found no gene amplification or rearrangement in colorectal carcinomas and pancreatic adenocarcinomas, so the overexpression mechanism remains unknown (Frazier et al., 1998). A mutation was identified, L158 -> S, but only in one colorectal tumour. This mutation was not identified in any of the other tumours and hence was considered to have a low frequency which does not match the frequency of overexpression (Frazier et al., 1998).

eEF1B γ , as described earlier, gets phosphorylated upon the addition of chemotherapy drug Paclitaxel (taxol) (Prado et al., 2007) as well as showing greater than 50% reduction in the protein level but not mRNA level upon treatment with the chemotherapy drug all-trans-retinoic acid (ATRA) (Harris et al., 2004).

The oncogenic status and cancer progression stage seem to be correlated with increased levels of eEF1B subunits, in particular eEF1B δ and eEF1B γ , which may be due to their role in translation or their potential oncogenicity. Summary table of the different tumours and cancer cells in which overexpression of eEF1B subunits have been associated to on table 1.2.

Table 1.2 Summary table of overexpression of eEF1B subunits in different tumours and cancer cells, and overexpression associated to highly metastatic cells with respective references

Overexpression	eEF1B α	eEF1B δ	eEF1B γ
Breast cancer cells compared to non-transformed cells	Al-Maghrebie et al., 2005	Joseph et al., 2004; Jacob et al., 1996	Al-Maghrebie et al., 2005
Prostate cancer cells compared to non-transformed cells	Everley et al., 2004	Everley et al., 2004	Everley et al., 2004
Skin cancer cells compared to non-transformed cells		Sinha et al., 2000	
Ovarian cancer cells compared to non-transformed cells		Jacob et al., 1996	
Gastric carcinoma compared to normal adjacent tissues		Ogawa et al., 2004; Zeng et al., 2007	Minori et al., 1995; Minori et al., 1996
Liver carcinoma compared to normal adjacent tissues		Shuda et al., 2000; Blanc et al., 2005	Shuda et al., 2000
Colon carcinoma compared to normal adjacent tissues		Scanlan et al., 1998; Roblick et al., 2004	Ohl et al., 1992; Ender et al., 1993; Mathur et al., 1998
Pancreas carcinoma compared to normal adjacent tissues			Lew et al., 1992
Brain carcinoma compared to normal adjacent tissues		De Bortoli et al., 2006; Peyrl et al., 2003	Joseph et al., 2004; Jacob et al., 1996
Lung carcinoma compared to normal adjacent tissues		Li et al., 2006; Liu et al., 2004; Keenan et al., 2009	Li et al., 2006
Associated to radiation induced tumourigenesis		Joseph et al., 2002	
Associated to highly metastatic tumours/cells	Everley et al., 2004	Everley et al., 2004; Ogawa et al., 2004; De Bortoli et al., 2006; Keenan et al., 2009	Everley et al., 2004; Minori et al., 1995; Minori et al., 1996

1.6 eEF1B and other functions

1.6.1 eEF1B and DNA repair/cellular stress

All eEF1B subunits have been reported to be regulated upon treatment with radiation, have DNA and RNA binding properties and change expression during DNA damage or stress under specific conditions, suggesting a possible involvement in oxidative stress mechanisms (Malone and Ullrich, 2007, Olarewaju et al., 2004, Shenton and Grant, 2003, Matsuoka et al., 2007). eEF1B subunits display DNA binding activity to damaged DNA on treatment with chromium- and the chemotherapy drug transplatin but not in response to the chemotherapy drug cisplatin, suggesting that the eEF1B complex can bind specifically to different DNA damage conformations in ovarian carcinoma cells (Wang et al., 1997). eEF1B δ has the ability to bind to the HIV-1 Tat mRNA although the biological significance of this interaction is unknown (Xiao et al., 1998). Furthermore, the T-cell-restricted intracellular antigen-1 like RNA-binding protein TIAR, which is thought to inhibit protein synthesis by promoting formation of stress granules (Mazan-Mamczarz et al., 2006), selectively binds to the 3'UTR of eEF1B α but not eEF1B δ or eEF1B γ in human cells, suppressing the translation of eEF1B α in response to low levels of short-wavelength UV (UVC) irradiation (Mazan-Mamczarz et al., 2006). Moreover, eEF1B α was found to be down regulated after exposure of human mammary epithelial cells to ionizing gamma radiation that induces double strand DNA breaks or base oxidations (Malone and Ullrich, 2007).

In slime mold, hyperosmotic stress induces cell volume reduction and induces ubiquitination of cellular proteins and leads to differences in membrane and cytoskeletal fractions but not in protein levels (Zischka et al., 1999). Both eEF1A and eEF1B α are up-regulated upon hyperosmotic stress in the cytoskeletal fraction compared with the membrane fraction (Zischka et al., 1999). They suggested that association of eEF1A and eEF1B α with the cytoskeletal fraction reduces translation since this becomes rate-limiting based on reduced rate of incorporation of

methionine when eEF1A is associated with actin (Edmonds et al., 1998, Liu et al., 1996) although they did not test this hypothesis. In yeast cells, eEF1B α was found to be regulated in response to cadmium in yeast cells where both thiol redox systems, glutathione and thioredoxin are involved (Vido et al., 2001). eEF1B α knockout in yeast cells which overexpress eEF1A show a even greater resistance to CdSO₄ and H₂O₂ but not overexpression of eEF1A alone (Olarewaju et al., 2004). eEF1B α was further identified to be down-regulated immediately after exposure to H₂O₂ in *S. cerevisiae* cells (Godon et al., 1998). Moreover, S-thiolation also leads to a down-regulation of the eEF1B α protein in response to oxidative stress (Shenton and Grant, 2003). A similar down-regulation at both mRNA and protein levels is seen following heat shock in rice (Lin et al., 2005).

Compared with eEF1B α , eEF1B δ showed an opposite response to ionizing radiation, reaching the highest peak of expression 8h after radiation (Jung et al., 1994a) just before G2 arrest (Jung et al., 1994b). As previously described, eEF1B δ is overexpressed in cadmium-induced transformation (Joseph et al., 2002). In addition, mouse eEF1B δ is phosphorylated in response to DNA damage on consensus sites recognized by ATM and ATR (Matsuoka et al., 2007), which may indicate a possible DNA damage response mechanism.

In yeast, loss of eEF1B γ (TEF3) or eEF1B γ homologue (TEF4) gives a greater stress resistance to cadmium and H₂O₂ (Olarewaju et al., 2004). TEF4 also regulates methionine sulfoxide reductase A (MsrA) by binding to its promoter and enhancing the MsrA activity which protects cells against oxidative stress (Hanbauer 2003). In slime mold, overexpression of eEF1B γ causes resistance to the antidepressant drug clomipramine, suggesting involvement in the detoxification *in vivo* of toxins (Billaut-Mulot et al., 1997). Since eEF1B γ has a GST like domain, several studies have focused on determining if it actually has the ability to catalyse reactions important for detoxification. GST activity was detected in the purified eEF1B complex and in the monomeric eEF1B γ recombinant protein in rice but to a much

lower extent (50 fold less) than GST (Kobayashi et al., 2001). In addition, silk worm eEF1B γ was found to be able to bind to glutathione (Kamiie et al., 2002) and in *Trypanosome cruzi*, overexpression of eEF1B γ causes increased resistance to clomopramine, a lipophilic compound that is detoxified by GSTs (Billaut-Mulot et al., 1997). Furthermore, eEF1A, eEF1B α and eEF1B γ from trypanosome were found to be part of the trypanothione S-transferase complex, have GST activity only as a complex not as monomers and were bound directly to the GST complex by eEF1B γ (Vickers and Fairlamb, 2004, Vickers et al., 2004). However, Jeppesen *et al.* solved the N-terminus GST-like domain structure of yeast eEF1B γ , also assayed for GST activity but no GST activity was detected *in vitro* (Jeppesen et al., 2003). No studies have reported to investigate GST activity in eEF1B γ in higher eukaryotes.

Besides eEF1B subunits, eEF1A has also been shown to be involved in cellular stress response. eEF1A together with heat shock RNA-1 (HSR-1) is essential for heat shock transcription factor 1 (HSF1) activation and consequence induction of heat shock proteins during heat shock (Shamovsky et al., 2006). eEF1A2 interaction with Prdx1 increases resistance against oxidative stress by hydrogen peroxidase treatment (Chang and Wang, 2007). eEF1A1 knockdown increased resistance to hydrogen peroxidase treatment (Borradaile et al., 2006).

1.6.2 eEF1B and the cell cycle

As described above, eEF1B δ up-regulation coincides with G2/M cell arrest under exposure to ionising radiation, suggesting that eEF1B δ might be involved in cell cycle dependent response to DNA damage (Jung et al., 1994a). Furthermore, in sea urchin early embryonic cell cycles the eEF1B δ protein level does not change, although a fraction of eEF1B δ changes location (Boulben et al., 2003). At the S-phase and just before nuclear membrane breakdown, a pool of eEF1B δ was shown as a ring around the nucleus and during mitosis as two large spheres around the spindle pole which could influence the availability of eEF1B δ for translation.

Proteolysis plays an important role in the regulation of meiotic and mitotic cell cycles during early oocyte maturation (G2/M transition) and metaphase. The 26S proteasome is involved in the ubiquitin dependent proteolytic process. eEF1B γ was present in a fraction of the 26S proteasome purified upon *Xenopus* oocytes maturation. In addition all eEF1B subunits co-immunoprecipitated with the matured *Xenopus* oocytes 26S proteasome, and eEF1B δ and eEF1B γ with the 20S proteasome (Tokumoto et al., 2003). Furthermore, eEF1B γ gets phosphorylated by cdc2 only when it is associated with 26S proteasome in a cell-cycle dependent manner (Tokumoto et al., 2003).

As mentioned earlier, eEF1B subunits are regulated by kinases which are involved or directly regulated in the cell cycle. Phosphorylation of eEF1B δ and eEF1B γ by p38cdc2 and of eEF1B α and eEF1B δ by CKII coincide with highly reduced cap-dependent protein synthesis during mitosis (Monnier et al., 2001b) and increased translation of cap-independent IRES-containing mRNAs (Qin and Sarnow, 2004), 5'TOP genes (Hamilton et al., 2006) and with viral infection (Kawaguchi et al., 2003).

1.6.3 eEF1B and the cytoskeleton

Minella and colleagues studied the sub-cellular localisation of eEF1B subunits in human cell lines and determined that eEF1B subunits only co-localised to the endoplasmic reticulum (Minella et al., 1996a). However several studies have found eEF1B subunits to interact with and even suggested a possible role for eEF1B in cytoskeleton remodelling.

eEF1B α has been identified as a major physical interactor with unpolymerised actin (Furukawa et al., 2001). It was shown that in slime mold eEF1B α expression is diffused through the cytosol with a fraction concentrated in the cortical cytoskeleton. Monomeric eEF1B α stimulates actin assembly but not in a concentration dependent manner, whereas the wheat eEF1B α :eEF1B γ complex stimulates actin assembly in a concentration dependent manner. Hence, eEF1B α may promote the nucleation phase of the actin assembly reaction. However, in yeast *S. cerevisiae*, only cells overexpressing eEF1A, and not eEF1B α , show altered actin localisation, larger and rounder cells and increased number of unbedded cells (Munshi et al., 2001), which might indicate that eEF1B α may not, at least as a monomer, affect the assembly of actin in yeast. Interestingly, eEF1A is involved in actin remodelling in yeast (Gross and Kinzy, 2005, Munshi et al., 2001). In human cell lines, it has been suggested that eEF1A2 is involved in Akt and PI3K-dependent cytoskeleton remodelling during tumourigenesis (Amiri et al., 2007).

When purifying tubulin, eEF1B α and eEF1B γ are often associated with tubulin in brine shrimp (Janssen and Moller, 1988). eEF1B γ co-precipitates with tubulin, as does eEF1B α to a lesser extent (Janssen and Moller, 1988). They suggested that the binding of tubulin to eEF1B γ is competitive with eEF1B α binding and hence the interaction region must be the same or overlapping. Furthermore, they estimated that 5% of the eEF1B α :eEF1B γ complex was found to be present in the membrane fraction where no eEF1A was present. The authors suggested that

eEF1B γ may help to anchor eEF1B α to the membrane and microtubules in brine shrimp.

During the cell cycle in sea urchins, eEF1B δ does not co-localise with microtubules at interphase, however at metaphase, anaphase and telophase eEF1B δ is expressed around the astral microtubules but not the spindle microtubules (Boulben et al., 2003). In addition, upon treatment with taxol (paclitaxel), which stabilizes microtubules against depolymerisation, and nocodazol, which depolymerise microtubules, the expression pattern of eEF1B δ was completely disrupted. This indicates that eEF1B δ localisation in the cell is dependent on microtubule dynamic structures. As described earlier, treatment with taxol phosphorylates human eEF1B γ but the expression level and pattern was not investigated (Prado et al., 2007). Kinectin, a microtubule-dependent membrane anchor for several targets including kinesin, has been found to bind eEF1B δ and anchor eEF1B complex to the endoplasmatic reticulum (ER) *in vivo* and *in vitro* (Ong et al., 2003). Overexpression of kinectin and treatment with nocodazol once again disrupted the eEF1B δ expression pattern in human cells but not the ER structure (Ong et al., 2003). eEF1B α and eEF1B γ did not interact with kinectin by yeast-2-hybrid or co-immunoprecipitation with endogenous and exogenous protein (Ong et al., 2006). However, knockdown of the kinectin isoform that interacts with eEF1B δ reduced all eEF1B subunits protein levels by around 40% and the ER-like staining of the subunits was reduced near the cell periphery while microtubules and ER were not disrupted (Ong et al., 2006). Cells lacking this particular kinectin isoform also showed increased cytosolic protein synthesis and reduced membrane protein synthesis (Ong et al., 2006). These results demonstrate a direct link between cytoskeleton dynamics and protein synthesis, at least in part due to eEF1B complex disruption via eEF1B δ .

eEF1B α and eEF1B γ were also found to co-immunoprecipitate and co-localise with endogenous cytoskeleton keratin intermediate filaments in

keratinocytes from newborn mice (Kim et al., 2007). The N-terminus (185-223) of eEF1B γ interacts with K6-K17 in human epithelial cells. Transient knockdown of eEF1B γ reduced protein synthesis rate, monitored by the incorporation of labelled methionine and cysteine, and increased 80S ribosomal peak, indicating an increase in freely available ribosomes and a defect in translation initiation (Kim et al., 2007). This phenotype is similar to the knockout of actin-regulating proteins in yeast including eEF1A mutants (Gross and Kinzy, 2007). A similar effect was observed when the interaction of eEF1B γ and keratin was disrupted (Kim et al., 2007). It was suggested by the authors that binding of eEF1B α via eEF1B γ and eEF1A to the cytoskeleton while eEF1A is still in excess, it decreases eEF1B α availability of for the cytosolic protein synthesis and becoming rate limiting and causing translation initiation block (Kim et al., 2007).

In summary, kinectin binding seems to be specific to eEF1B δ and the disruption in the other subunits indicates that kinectin anchors the eEF1B complex via eEF1B δ to the ER, whereas the eEF1B complex is anchored to keratin by eEF1B γ , although eEF1B δ was not investigated. These two particular studies provide evidence of specific binding of eEF1B subunits to particular cytoskeleton filaments and also evidence for the involvement of not just eEF1B γ but also eEF1B δ in stabilising the complex structure. In several studies interaction between eEF1A and eEF1B subunits with cytoskeletal proteins seems to decrease cytosolic protein synthesis, implying a much greater role of the cytoskeleton regulation in protein synthesis. Furthermore, during hyperosmotic stress which induces cytoskeleton reorganisation in slime mold, both eEF1A and eEF1B α were found to be overexpressed in the cytoskeletal fraction compared with the membrane fraction (Zischka et al., 1999). Based on previous studies of eEF1A and its interaction with the cytoskeleton, the authors also suggest that upon hyperosmotic stress, eEF1A and eEF1B α bind to the cytoskeleton and become rate-limiting. This might provide a link between cellular stress, cytoskeleton regulation and protein synthesis.

1.6.4 eEF1B and translation fidelity

Yeast *S. cerevisiae* eEF1B α knockout is lethal, but the lethal phenotype can be overcome by overexpression of eEF1A, resulting in slow growth and reduced translational fidelity (Hiraga et al., 1993, Kinzy and Woolford, 1995). Mutations in the eEF1B α GEF domain lead to a decreased translation rate and increased translation non-sense suppression in all three nonsense codons (Carr-Schmid et al., 1999b). Further investigation identified mutations that affected translation rate but not necessarily fidelity (Andersen et al., 2000). Overexpression of eEF1B α overcomes the protein phosphatase Ppz1 overexpression slow growth phenotype by interacting with Ppz1 (de Nadal et al., 2001). Furthermore, Ppz1 phosphatase, as described earlier, dephosphorylates eEF1B α at S86, corresponding to human residue S106, and increases translation fidelity *in vitro* (Aksenova et al., 2007).

Individually, in yeast, overexpression of eEF1A and eEF1B α does not affect fidelity, however when co-expressed they increase fidelity (Munshi et al., 2001). Overexpression of eEF1B γ does not alter GEF rate (Carr-Schmid et al., 1999b) but causes loss of non-sense suppression hence reduced fidelity (Benko et al., 2000).

Regulation of several translation factors, including eEF1A, also cause changes in translation fidelity (Munshi et al., 2001, Carr-Schmid et al., 1999a, Sandbaken and Culbertson, 1988, Liebman et al., 1995).

1.7 RNAi

Just over ten years ago, Andrew Fire and Craig Mello showed how gene expression could be regulated in the worm *Caenorhabditis elegans* by double stranded RNA molecules that had the ability to silence the gene in a sequence specific way (Fire et al., 1998). This RNA interference (RNAi) was later found to be conserved amongst eukaryotes, and is thought to have evolved as a protection mechanism against viral infections. The RNAi machinery is now used as a valuable tool in molecular biology and medicine in silencing gene expression.

RNAi can be triggered by long double stranded RNA, plasmid-based short hairpin RNAs (shRNAs) and microRNAs (miRNAs). The endonuclease Dicer cleaves RNA molecules into small interfering RNAs (siRNAs) of around 21 nucleotides (Bernstein et al., 2001). The RNA-induced silencing complex (RISC) unwinds the duplex siRNAs into single-stranded molecules. This in turn guides RISC to the complementary RNA sequence where RISC cleaves the target RNA at a specific site leading to RNA degradation (Boutla et al., 2001).

Tuschl and colleagues chemically synthesised 21 nucleotide siRNAs that were able to trigger RNAi (Tuschl et al., 1999). Antisense oligonucleotides had been used before to silence genes in the same manner as siRNAs. Antisense oligonucleotides are single stranded DNA molecules, which induce cleavage by activation of RNaseH in the nucleus, whereas RNAi induce cleavage of the target RNA molecule in the cytoplasm (Tuschl et al., 1999). It is thought that the use of an endogenous system by RNAi accounts for the much higher efficiency compared with antisense oligonucleotides (Grunweller et al., 2003).

The degradation of the target RNA usually begins immediately after the siRNA delivery to the cell (Zamore et al., 2000). The decrease in the protein level depends on the target protein half-life and generally inhibition of the protein can be seen by approximately 48h after transfection (Morris, 2008). However, siRNA effects

are transient, usually lasting for about five to seven days since the siRNAs degrade over time and become attenuated by cell division (Morris, 2008). Off-target effects can be reduced by the use of lower concentrations of siRNA and by careful design of the siRNA: by generally designing an siRNA that is specific to the target and not to any other molecule and by paying particular attention to the design of the seed region, nucleotides 2 to 8, of the siRNA complementary to a region of the target RNA that differs from other RNA molecules (Birmingham et al., 2006).

Plasmid expressed short hairpin RNAs (shRNAs) can be used instead of chemically synthesised siRNAs to extend gene silencing. Furthermore, a resistance gene in the plasmid can be used to select cells with the construct. Moreover, an inducible system, such as tetracycline or an adapted Cre-lox system, can give specific temporal control over the silencing of the gene. Plasmid based shRNAs can be used to create stable cell lines or even transgenic animals.

Endogenous miRNAs, however, function slightly different from the other RNA silencing molecules. The miRNA precursors (pre-miRNAs) are present usually in noncoding RNAs or in introns that are excised by Drosha, processed by Dicer, used as guide to the target RNA by RISC, binds to partially identical RNA targets, usually around the 3'UTR, and causes gene silencing by inhibiting translation, and accelerating mRNA deadenylation and decay (Wu et al., 2006, Giraldez et al., 2006). Each miRNA is able to silence several RNA targets and it is thought that they regulate about 30% of mammalian genes. They have been implicated in many diseases such as cancer, diabetes and cardiac diseases (reviewed in Perron and Provost, 2009).

In most cases the majority, but not all, of the target RNA molecules are cleaved, hence RNAi is said to be a knockdown and not a knockout. The advantage of using shRNA transgenic animals is that they might better reflect the outcome of a drug therapy targeting the gene and obtaining only a partial, rather than a complete

knockout. However, shRNA transgenic animals may not reflect the phenotype of knockout animals since reduced levels of protein might lead to different compensation mechanisms compared with total loss of protein.

Applications of RNAi

The RNAi mechanism can be used to investigate a particular gene function by silencing the product of the gene. To minimise potential off-target effects careful design of the siRNA is essential, as well as the use of controls such as by siRNA targeting a known gene, a non-targeting siRNA, to determine the lowest effective concentration of siRNA, and the use of multiple siRNAs targeting the same gene. It can also be used for screening in large-scale studies using siRNA libraries. With the evidence of the potential of RNAi demonstrated in basic science applications, RNAi can also be used as a therapeutic drug for viral infections (reviewed in Martinez, 2009; Haasnoot and Berkhout, 2009), cancer (reviewed in Canaani, 2009; Lage, 2009) and other diseases (reviewed in Moschos et al. 2008; Lee and Chiang, 2008). Although siRNA and shRNA delivery in cells can be carried out by transfection, *in vivo* these methods are often toxic. Currently in mammals, siRNA or shRNA therapy are delivered directly to the diseased tissue by injection or ingestion or inhalation, and non-viral methods such as lipids are becoming more popular where the big challenge is to deliver to a specific cell type.

1.8 Aims

The large majority of studies that mentioned eEF1B subunits were large-scale studies which provide relatively little specific information. Only a few studies actually address structure and possible function of eEF1B subunits and most of these were performed in yeast, *Xenopus* oocytes, sea urchin and brine shrimp. Taken together, little is known about the characteristics, expression and function of eEF1B subunits, particularly in mammals.

The aim of this project is to characterise eEF1B subunits at the molecular level in view of their potential involvement in tumourigenesis using a variety of bioinformatic tools and laboratory based techniques. These are used to study expression at mRNA and protein levels as well as to evaluate the biological changes that result from down and up-regulation of eEF1B subunits by siRNA-mediated knockdown and overexpression of each eEF1B subunit.

2. Materials and methods

2.1 Bioinformatics

In silico prediction and analysis of eEF1B subunits characteristics involved a variety of webtools and software as well as the design of two Perl scripts.

2.1.1 Identification of related sequences

Database similarity searching allows us to determine which of the hundreds of thousands of sequences present in the database are potentially related to a particular sequence of interest. This is achieved by aligning a query sequence to each subject sequence in the database. The Basic Local Alignment Search Tool (BLAST) (Altschul et al., 1990) is a popular method of ascertaining sequence similarity, by searching a query sequence supplied by the user against a database; results are reported as ranked hit list. BLAST searches were carried out with the eEF1B subunits' DNA, mRNA or protein sequences against GenBank databases (Benson et al., 2009), the universal protein database (UNIPROT) (UniProt Consortium, 2009) and the protein structure databank (PDB) (Berman et al., 2000). These searches were restricted to organisms, reference or non-reference sequences, as well as DNA, ESTs, mRNA and protein sequences. Several variants of BLAST were used, each distinguished by the type of sequence of the query and database sequence (Table 2.1).

Table 2.1 The variants of BLAST searches according to different the query sequence and database type of sequence.

Program	Query sequence	Database
BLASTn	Nucleotide	nucleotide
BLASTx	nucleotide (translated)	protein
BLASTp	Protein	protein
tBLASTn	Protein	nucleotide
tBLASTx	Nucleotide (six frames translated)	Nucleotide (six frames translated)
PSI-BLAST	Protein	protein patterns

2.1.2 Alignment of similar sequences

Sequence alignment is useful to check for sufficient similarity such that the sequences can be considered to share a common evolutionary history or share a domain that might indicate similar function. Sequences can be aligned along the entire sequence length (global) or aligned in sub-sequences (local) which is useful for identification of similar parts of a sequence such as domains and exons/introns. DiAlign (Morgenstern, 2004) and Spidey (Wheelan et al., 2001) was used to perform local multiple sequence alignments, whereas ClustalW (Thompson et al., 1994) and Muscle (Edgar, 2004) were used to compare multiple sequences along the full length. All of these tools required sequences in FASTA format as the input. FASTA format contains a definition line which starts with a "greater than" sign (>) and is usually followed by the sequence name and description. The sequence itself starts on the next line. Default values were used for producing all the sequence alignments. The Jemboss Alignment Editor (Carver and Mullan, 2005) was used for visualisation, editing of sequences alignments and obtaining identity information.

2.1.3 Genomic DNA and mRNA characteristics

In order to predict if genes encoding eEF1B subunits only transcribe one transcript variant, the gene structure and alternative splices were predicted by GeneScan (Burge and Karlin, 1998), GeneID (Blanco and Abril, 2009), GeneSplicer (Pertea et al., 2001) and Alternative Splice Site Predictor (ASSP) (Wang and Marin, 2006). Since none of the tools predicted a different gene structure from the one already known for each of the eEF1B subunits and there was evidence for more transcript variants, a script in Perl was designed to predict the eEF1B δ gene structure (section 2.1.7). Furthermore, the location of single nucleotide polymorphisms (SNPs) shown on Ensembl (Hubbard et al., 2009) and UCSC genome (Kuhn et al., 2009) browsers was identified to reduce future problems that might arise from polymorphisms.

2.1.3.1 Promoter and transcription factors

The promoter region and the regulatory elements that bind to it is important in regulating the gene expression. The promoters of the genes encoding eEF1B subunits were predicted by using FirstEF (Davuluri, 2003), Ensembl own promoter prediction (Hubbard et al., 2009) and El Dourado which is part of MatInspector (Cartharius et al., 2005). It was also complemented with the prediction of CpG islands using the EMBOSS CpG tool (Rice et al., 2000). Once the putative promoter region was identified, it was used as the input sequence for P-Match search (Chekmenev et al., 2005) against the transcription factors database, TRANSFAC (Matys et al., 2006). The P-Match retrieves the most likely transcription factors to bind to a particular region based on the transcription factor binding pattern and frequency of that pattern in the human genome.

2.1.3.2 Other regulatory motifs

Other regulatory elements present in the mRNA are also important, such as those in UTRs. UTRScan (Mignone et al., 2005) was used to compare eEF1B subunit UTR sequences against a database of UTR regulatory elements sites. RegRNA (Huang et al., 2006), as well as searching for UTR regulatory elements, was also used to predict upstream open reading frames and 5' TOP sequences. Although RegRNA also predicts miRNA binding sites, microCOSM from miRBASE (Griffiths-Jones et al., 2008) was used to retrieve all putative miRNA binding sites since its prediction is based on a comprehensive miRNA database. The poly A signal was predicted by Poly (A) signal miner (Liu et al., 2005) which compares the input sequence with more than 2000 known poly A signals.

2.1.3.3 Expression data

Small mRNA tags, expressed sequence tags (ESTs) and serial analysis of gene expression (SAGE) tags can be retrieved to determine which tissue they were extracted from and hence build up a knowledge of gene expression at the mRNA level. The GenBank gene expression profile (Benson et al., 2009) and the Cancer Genome Anatomy Project (CGAP) (Hess, 2003) were searched for eEF1B subunit ESTs and SAGE derived sequences' tissue source. However, these databases can only be searched by the gene name and do not distinguish between transcript variants. For this reason, a script in Perl was designed to analyse the ESTs expression in an exon specific manner (section 2.1.7).

2.1.4 Protein characteristics

Protein amino acid properties such as charge, accessibility, conservation, hydropathy, ability to form low-complexity regions, disordered regions and particular secondary structures were catalogued for each eEF1B subunit. If the protein sequence was not available, the mRNA sequence was translated into protein sequence by ExPASy Translate tool (Gasteiger et al., 2003). Residues chemical properties and hydropathy were plotted using EMBOSS PepInfo (Rice et al., 2000). Low complexity and disordered regions were predicted by SEG (Ryden and Hunt, 1993) and DisEMBL (Linding et al., 2003) respectively. And the ability to form disulphide bonds was predicted by Predict Protein DiSulFind (Ceroni et al., 2006). To predict the ability to be directed to a particular organelle SignalP 3.0 (Emanuelsson et al., 2007) prediction was carried out.

2.1.4.1 Domains

Assigning sequences to protein families is a very valuable way of predicting protein function. Database searches can also be used to find specific protein families or domains through the use of profiles. Protein profiles are built from common patterns observed in multiple sequence alignments of related sequences. Position-specific iterated BLAST (PSI-BLAST) (section 2.1.1) was used to search for profiles similar to eEF1B subunits. Many proteins are built up from domains in a modular architecture. eEF1B subunits were also compared to a protein family database, Pfam database (Finn et al., 2008), and to an integrated resource of protein families and domains, InterPro (Hunter et al., 2009).

2.1.4.2 Post-translational modifications and other motifs

Motifs are any conserved element of a sequence alignment, which is likely to be a structural/functional region. Putative motif sequences were identified by comparing the eEF1B subunit sequences against Mini-Motif Miner (MnM) (Rajasekaran et al., 2009), Human Protein Reference Database (HPRD) (Keshava Prasad et al., 2009), PROSITE (Hulo et al., 2006), ELM Functional Sites in Proteins database (Puntervoll et al., 2003). To identify possible post-translational modifications motifs, several specific tools were used and these are shown in table 2.2.

Table 2.2 Post-translational modification prediction tools used.

Tool name	Post-translational modification predicted	Reference
NetPhos	Phosphorylation sites	(Blom et al., 1999)
NetPhosK	Kinase specific phosphorylation sites	(Blom et al., 2004)
DisPhos	Phosphorylation sites based on disordered regions	(Iakoucheva et al., 2004)
NetGlycate	Glycation	(Johansen et al., 2006)
NetNGlyc	N-glycosylation	(Blom et al., 2004)
NetOGlyc	N-Acetylgalactosamine O-glycosylation	(Julenius et al., 2005)
Sulfinator	Sulfation	(Monigatti et al., 2002)
SUMOsp 2.0	Sumoylation	(Ren et al., 2009)
NetAcet	Acetylation	(Kiemer et al., 2005)
NetCGlyc	C-mannosylation glycosylation	(Julenius, 2007)

In order to obtain information on all phosphorylation sites experimentally determined by large-scale studies a search at the PhosphoSitePlus (Hornbeck et al., 2004) database was carried out.

2.1.5 Protein structure

There are four main levels of protein structure. The amino acid sequence is generally referred to as the primary structure. The secondary structure occurs when the sequence of amino acids is linked by hydrogen bonds, forming mainly alpha helices, beta strands and loops or coils. The secondary helical, strand and loop structures interact with each other to assemble into a compact globular structure called the tertiary structure or fold. Proteins composed of more than one peptide chain, their organisation and interconnections is called the quaternary structure.

2.1.5.1 Secondary structure

There are several methods available for predicting the ability of a sequence to form alpha-helices and beta-strands. Jpred (Cuff et al., 1998), PHD Predict Protein (Rost et al., 2004) and PSIPRED (McGuffin et al., 2000) were used to predict the eEF1B subunit secondary structures by using the default values. Jpred receives the amino acid sequence as an input, and predicts the secondary structure based on two neural networks systems, a form of learning method, and filtered by PSI-BLAST. PHD Predict Protein uses three neural networks also filtered by PSI-BLAST whilst PSI-PRED incorporates a four-level system of neural networks to increase prediction accuracy of the secondary structure prediction based also on output obtained from PSI-BLAST. Furthermore, the tool COILS (Lupas et al., 1991) was used to predict coiled regions by comparing the input sequence with a database of known parallel two-stranded coiled-coils.

Transmembrane helices in integral membrane proteins are composed of stretches of predominantly hydrophobic residues separated by polar connecting loops and were predicted by PHDhtm Predict Protein (Rost et al., 2004) and by TM Pred (Hofmann and Stoffel, 1993).

2.1.5.2 3D structure

The protein data bank (PDB) (Berman et al., 2000) is the primary resource for protein structural data, containing three-dimensional structures of proteins, nucleic acids and carbohydrates. The data have been derived experimentally from X-ray crystallography and nuclear magnetic resonance (NMR) studies. PDB was searched by a BLAST search to identify known eEF1Bsubunit 3D structures. In order to search for proteins with similar structures compared to eEF1B subunits, the prediction-based threading tool PredictProtein Agape (Rost et al., 2004) was used. Modeller (Eswar et al., 2008) can also be used to predict proteins with similar structures, however besides this, it can also be used to build a structural model in 3D by comparison with a protein with known structure. Modeller was used to produce a 3D structure model for the C-terminus of eEF1B δ based on its similarity to the C-terminus of eEF1B α using the default settings. Furthermore, ProFunc (Jensen et al., 2003) was used to predict protein binding and interaction clefts for both eEF1B α and eEF1B δ C-termini.

2.1.6 Protein-protein interactions

Proteins can interact with other proteins forming pathways and these interactions are stored in specific databases. APID2NET (Hernandez-Toro et al., 2007) and CytoScape (Cline et al., 2007) integrate several of these databases. All the protein-protein interaction information for each eEF1B subunit was combined and visualised using CytoScape. BINGO CytoScape plugin (Maere et al., 2005) was used

to retrieve the Gene Ontology classifications (Ashburner et al., 2000) of all the interactors and compared them to the gene classification frequencies in the human genome.

2.1.7 Perl scripts

The multiple local alignment tool Spidey (Wheelan et al., 2001) used to align ESTs to the genomic DNA gave a complex output. The Spidey output was used as the input for the Perl script. The script then searched for the ESTs accession numbers and the corresponding genomic sequence location to which each exon was identical (appendix 1.1). In this case, ESTs were searched for the presence of each of the eEF1B δ exons. The output was in a text table format which could be imported by Microsoft Excel. Once in table format, the number of ESTs sequences that is derived from particular exons were counted.

Another Perl script was designed to further explore the ESTs expression data displayed in the GenBank EST profile. Firstly, all the GenBank profiles from each EST were collected and used as input for the Perl script (appendix 1.2). They were then simplified into an output table that distinguished sequence length, sex, developmental stage, mouse strain, tissue and the EST nucleotide sequence. The table was then imported into Microsoft Excel and the ESTs could be grouped by feature and counted.

2.2 Materials

2.2.1 Solutions and buffers

The buffers and solutions recipes are listed in table 2.3. Unless stated otherwise all chemicals were obtained from Sigma-Aldrich. Suppliers names and addresses can be found on appendix 2.

Table 2.3 Recipes of all the solutions and buffers used for the methods described in this chapter.

Radioimmunoprecipitation assay (RIPA) buffer	50mM Tris-HCL (pH 7.5), 150mM Sodium chloride, 1% NP-40, 0.5% Sodium deoxycholate, 0.1% SDS. Stored at 4 °C before the addition and at -20 °C after addition of 1 tablet of complete protease inhibitors cocktail (Roche)
TE buffer	10ml 1M Tris-HCL (pH 7.5), 2ml 500mM EDTA and up to 1l with dH ₂ O. Stored at room temperature.
Primers storing buffer	5% TE buffer, 5% DMSO, 5% glycerol and up to 5ml dH ₂ O
10x Tris Buffered saline (TBS)	40g Sodium chloride, 100ml 1M Tris (pH 7.5) and up to 500ml dH ₂ O. Stored at room temperature
Phosphate Buffer Saline (PBS)	1 PBS tablet (Sigma) dissolved in 100ml of dH ₂ O and autoclaved.
PBS-tween-20 (PBS-T)	As above and 0.1% (v/v) Tween-20 (Sigma)
2x Laemmli loading buffer	60nM Tris HCl (pH 6.8), 2% SDS, 0.1% bromophenol blue, 10% glycerol
10x Laemmli running buffer	250mM Tris HCl (pH 8.3), 1.9M Glycine and 10% SDS
Transfer buffer	200ml of 1x Laemmli loading buffer, 200ml of methanol up to 1l dH ₂ O
TBE (Tris Borate-EDTA)	108g Tris, 55g Boric acid and 9.3g of Na ₄ EDTA in 1l of dH ₂ O 90mM Tris-Borate and 2mM of EDTA (pH 8.0)
Lithium carbonate	5g (67.7mM) lithium carbonate per 1l dH ₂ O
LB (Luria-Bertani) medium	1.0% tryptone, 0.5% yeast extract, 1.0% NaCl (pH 7.0). Medium was autoclaved.
LB agar plates	Prepared has above with additional 15g/l agar before autoclaving
Peroxidase blocking solution	2ml 30% H ₂ O ₂ , 10% Sodium azide and up to 400ml dH ₂ O
Lysis buffer	10 mM HEPES, 1.5 mM MgCl ₂ , 10 mM KCl, 0.5 mM DTT, 0.5% NP40 and adjust pH 7.5. Stored at 4 °C before the addition and at -20 °C after addition of 1 tablet of protease inhibitors cocktail
Nuclear lysis buffer	15 mM HEPES pH 7.9, 1.5 mM MgCl ₂ , 0.2 mM EDTA, 0.5 mM DTT, 25% glycerol (v/v), 400mM NaCl and adjust pH 7.9. Stored at -20 °C after addition of 1 tablet of protease inhibitors cocktail.
Stripping buffer	100mM β-mercaptoethanol, 2% SDS and 62.5 mM tris-HCl pH 6.7
10x DNA sample loading buffer	20g Sucrose, 100mg of Orange G and up to 50ml dH ₂ O
propidium iodide staining solution	3.8mM sodium citrate, 50ug/ml propidium iodide in PBS 10ug/ml RNaseA
SOC media	20g Bacto-tryptone, 5g Bacto-yeast extract, 0.5g NaCl, 2.5mL 1M KCl and up to 1l in dH ₂ O and adjust pH to 7.0. Autoclave to sterilise and add 20ml 1M glucose.

2. MATERIALS AND METHODS

CCMB80 buffer	10 mM KOAc pH 7.0, 80 mM CaCl ₂ .2H ₂ O, 20 mM MnCl ₂ .4H ₂ O, 10 mM MgCl ₂ .6H ₂ O, 10% glycerol and adjust pH to 6.4. Filter the solution and store at 4 °C.
Saturated ammonium sulphate	4.1M of ammonium sulphate
ELISA coating buffer	15mM Na ₂ CO ₃ , 35mM NaHCO ₃ , 3.0mM NaN ₃ and adjust pH to 9.6.
ELISA wash buffer	0.14M NaCl, 1.5mM KH ₂ PO ₄ , 8.0mM Na ₂ HPO ₃ , 2.68M KCl, 0.05% (v/v) Tween 20 and adjust pH to 7.4.
o-phenylenediamine dihydrochloride (OPD) substrate	1 tablet of OPD to 25ml OPD buffer and 10µl 30% H ₂ O ₂ .
OPD buffer	25mM citric acid, 0.1M Na ₂ HPO ₄ and adjust 5.0.

2.2.2 Cell lines

Several cell lines were used in this study. Table 2.4 shows the list of all cell lines used.

Table 2.4 List of cell lines, species, cell type, source and media in which each cell line was grown. Species refers to the species in which the cell line originated from.

Cell line	Species	Cell type	Source	Medium
HEK293	Human	Transformed embryonic kidney cells	Sheila Christie ¹	EMEM + 10% FBS
NIH3T3	Mouse	Embryonic fibroblast	ATCC ²	DMEM + 10% FBS
SHSY5Y	Human	Neuroblastoma	Barbara Stevenson ¹	1:1 DMEM and Ham's F12 medium + 10% FBS
HeLa	Human	Cervical cancer epithelial	ATCC ²	DMEM + 10% FBS
DLD1	Human	Colon carcinoma epithelial	Scott Bader ²	DMEM + 10% FBS
HCT116	Human	Colon carcinoma epithelial	ATCC ²	McCoy's 5A Medium + 10% FBS
HepG2	Human	Liver carcinoma epithelial	Barbara Stevenson ¹	DMEM + 10% FBS
NSC-34	Mouse	Motor neuron neuroblastoma hybrid		DMEM + 10% FBS
Rat2	Rat	Fibroblast	ATCC ²	DMEM + 10% FBS
Cos7	Monkey	Kidney fibroblast	Sheila Christie ¹	DMEM + 10% FBS
A549	Human	Lung carcinoma epithelial	Abby Wilson ¹	n.a. – given as pellet
Lan5	Human	Neuroblastoma	Barbara Stevenson ¹	n.a. – given as pellet

1 - Medical Genetics, Molecular Medicine Centre, University of Edinburgh

2 - LGC Standards, Teddington, TW11 0LY

3 - Sir Alastair Currie Cancer Research UK Laboratories, Molecular Medicine Centre, University of Edinburgh

2.2.3 Animals

All mice were maintained in the small animal Biomedical Research Facility at the Western General Hospital.

2.2.4 Antibodies

Details of the various antibodies used in this project including the conditions under which they were used can be found in table 2.5.

Table 2.5 List of antibodies used and conditions under which they were used for Western blotting (WB), immunocytochemistry (ICC) and immunohistochemistry (IHC). Species refers to the species in which the antibody was raised. All antibody dilutions are for typical experiments and may vary depending on the nature of the experiment.

Name	Specificity	Species	Source	Dilution (WB)	Dilution (ICC)	Dilution (IHC)
eEF1B	eEF1B α	Rabbit	Custom	1:2000	1:50	1:20
eEF1D1	eEF1B δ isoform a	Rabbit	Custom	Didn't work	-	-
eEF1D2	eEF1B δ all isoforms	Rabbit	Custom	Didn't work	-	-
eEF1G	eEF1B γ	Rabbit	Custom	1:1500	1:50	1:20
eEF1B2	eEF1B α	Rabbit	Abcam	1:3000	1:100	1:200
EEF1B2	eEF1B α – polyclonal	Rabbit	Proteintech group	1:2000	1:100	1:100
eEF1D	eEF1B δ	Rabbit	Bethyl	1:4000	1:500	1:400
EEF1D	eEF1B δ – polyclonal	Rabbit	Proteintech group	1:3000	1:500	1:400
EEF1G	eEF1B γ	Mouse	Abnova	1:2000	1:100	1:100
	eEF1B γ	Mouse	Bethyl	1:3000	1:100	1:200
eEF1A1-3	eEF1A1	Sheep	Helen Newbery ¹	1:200	-	-
eEF1A2-3	eEF1A2	Sheep	Helen Newbery ¹	1:200	-	-
Tubulin	Tubulin	Mouse	Sigma	1:5000	1:3000	-
Tubulin	Tubulin	Rabbit	Sigma ²	-	1:1000	-
Actin	β -actin	Rabbit	Sigma	1:5000	1:500	-
V5	V5 tag	Mouse	Invitrogen	1:5000	1:300	-
PCNA	PCNA	Mouse	Santa Cruz ²	-	1:100	-
Nuclear marker	Lamin A + C	Rabbit	Abcam	Didn't work	-	-
Active caspase-3	Active-caspase-3	Rabbit	Abcam ²	4 ^o C (overnight)	-	-
Caspase-3	Caspase-3	Rabbit	Sigma	Didn't work	-	-
NeuN	Neuronal nuclei	Mouse	Chemicon	-	-	1:500
GAPDH	GAPDH	Mouse	Chemicon	1:30000	-	-
HRP Rabbit-anti-mouse	Mouse Ig	Rabbit	Dako cytation	1:1000	-	-
HRP Goat-anti-rabbit	Rabbit Ig	Goat	Dako cytation	1:1000	-	-
HRP Rabbit-anti-	Goat/sheep Ig	Rabbit	Dako	1:500	-	-

2. MATERIALS AND METHODS

goat			cytomation			
HRP Donkey-anti rabbit 594 (red)	Rabbit Ig	Donkey	Alexa Flour (Invitrogen)	-	1:1000	-
HRP Donkey-anti mouse 488 (green)	Mouse Ig	Donkey	Alexa Flour (Invitrogen)	-	1:700	-
HRP Goat-anti-mouse 594 (red)	Mouse Ig	Goat	Alexa Flour (Invitrogen)	-	1:900	-
HRP Goat-anti-rabbit 488 (green)	Rabbit Ig	Goat	Alexa Flour (Invitrogen)	-	1:700	-

1 – Medical Genetics, Molecular Medicine Centre, University of Edinburgh

2 – Given by Liang Song, Sir Alastair Currie CRUK labs, Molecular Medicine Centre, University of Edinburgh

2.2.5 Slides

For the human tissue slides paraffin embedded adult human normal multi-tissue panel – major organs (Biochain) were used. The details of all the human samples used are shown in table 2.6.

Table 2.6 List of tissues, patient sex, age and pathological diagnosis of the human samples used

Tissue	Sex	Age (years)	Pathological diagnosis
Heart	Male	28	Normal
Brain	Male	73	Normal
Kidney	Male	26	Normal
Liver	Male	30	Normal
Lung	Male	26	Normal
Pancreas	Male	66	Normal
Spleen	Male	30	Normal
Skeletal muscle	Female	46	Normal

All of the mouse tissues slides were cut using a microtoe (Leitz 1512) or by Dawn Lyster or Bob Morris from the University of Edinburgh histology facilities at the Western General Hospital.

2.2.6 DNA primers

A list of oligonucleotide primers used in this project can be seen in table 2.6. Primers were supplied by Sigma or Invitrogen. Primer design was assisted by use of Primer3 webtool (Rozen and Skaletsky, 2000) and the predicted specificity of primers was investigated using BLASTn (Altschul et al., 1990). Primers were stored in primer storage solution (section 2.2.1) at a concentration of 100 μ M at -20 °C. The primers were further diluted 1:40 (2.5 μ M) and used as a working dilution unless otherwise specified.

Table 2.7 List of primers names, targets and primer sequences used for RT-qPCR, cloning, and isoform amplification.

Name	Species	Target	Sequence 5' to 3'
EEF1B2_HsF	Human	eEF1B α	CATGGGTTTCGGAGACCTGAAA
B_RTqPCRf	Mouse and human	eEF1B α	GATTACCTGGCGGACAAGAG
BfullLenF	Human	eEF1B α	AGCTCCCGTTCAGCCTTC
BattbFwd	Human	eEF1B α	GTACAAAAAGCAGGCTTCGAAGGAGAT AGAACCATGGGGTTTCGGAGACCTGAAA
EEF1B2_HsR	Human	eEF1B α	CTGCTTCAACAAGATCTAA
B_RTqPCRr	Mouse and human	eEF1B α	TACCAACGTAGGCATGACA
BfullLenR	Human	eEF1B α	TTAAATCTTGTTAAAGCAG
BattbRev	Human	eEF1B α	GTACAAGAAAGCTGGGCCTA TTAGATCTTGTTGAAAGCAGC
GfullLenF	Mouse and human	eEF1B γ	CACCATGGCGGCTGGGACCCTG
G_Hs_Fb	Human	eEF1B γ	GCTCTCATCGCTGCTCAGTA
G_RTqPCRf	Mouse and human	eEF1B γ	AGGGTGATGATGGATTCTGTG
EEF1G_MmF	Mouse	eEF1B γ	GGCATTATGCACCACAACAA
GattbFwd	Human	eEF1B γ	GTACAAAAAGCAGGCTTCGAAGGAGAT AGAACCATGGGCGGCTGGGACCCTGTAC
GfullLenR	Mouse and human	eEF1B γ	ATGTTCACTGAAGATCTTGCC
G_Hs_Ra	Human	eEF1B γ	ACTGGCCATCTTCTCACAC
G_RTqPCRr	Mouse and human	eEF1B γ	AGTGGCCTGTTGTTGTGGT
EEF1G_MmR	Mouse	eEF1B γ	AGGTGCAGGAGCTAGGCGA
GattbRev	Human	eEF1B γ	GTACAAGAAAGCTGGGCCTA TCACTTGAAGATCTTGCCCTG
Dex3MmF	Mouse	eEF1B δ	CCTCTTGTGCACTGGAGACC
Dex3HsF	Human	eEF1B δ	ACTTTTCGACCAGGCAGAGA
Dex4MmF	Mouse	eEF1B δ	GCGCATGAGAAGATCTGGTT
Dex4HsF	Human	eEF1B δ	GACGACGCAGAAAGGAGATT
Dex5MmF	Mouse	eEF1B δ	TGCAAGAGCCAGAGAGAACA
Dex5HsF	Human	eEF1B δ	ATTGCGAGGCCAGAGAGAA
Dex6MmF	Mouse	eEF1B δ	GACCTGGTGGAGACCACAGT
Dex6HsF	Human	eEF1B δ	GCCAGTCTGGAAGTGGAGAA
Dex7MmF	Mouse	eEF1B δ	AGCAGGCCATTTCCAAGTT
Dex7HsF	Human	eEF1B δ	CTGAACGTGCTGGAGAAGAG
DattbFwd	Human	eEF1B δ	GTACAAAAAGCAGGCTTCGAAGGAGAT AGAACCATGGGCTACAACTTCTAGCA
Dex3MmR	Mouse	eEF1B δ	CTCTGCCTCCTCAGTGTCT

2. MATERIALS AND METHODS

Dex3HsR	Human	eEF1B δ	GGAGGACTTGTTGACCCAGA
Dex4MmR	Mouse	eEF1B δ	GCCCGTTCATCTGCTCATAG
Dex4HsR	Human	eEF1B δ	GAATCTCCTTCTGCGTCGT
Dex5MmR	Mouse	eEF1B δ	CTTGCAATGTCTCGGAGGAT
Dex5HsR	Human	eEF1B δ	TTCTCTCTGGCTCTCGCAAT
Dex6MmR	Mouse	eEF1B δ	CGAAGGTTCTGGTTCTCCA
Dex6HsR	Human	eEF1B δ	CACTTCCAGACTGGCAATCC
Dex7MmR	Mouse	eEF1B δ	GCTCGGGGAGTAGGTGAAGT
Dex7HsR	Human	eEF1B δ	GAGCTCTTCCAGCACGTT
Dex8MmR	Mouse	eEF1B δ	GGGCAGCCTCCTTATCTTCT
Dex8HsR	Human	eEF1B δ	CATTGTCACTGCCAAACAGG
Dex9MmR	Mouse	eEF1B δ	CCCCTTTGTCATCCTCCAC
Dex9HsR	Human	eEF1B δ	CAAGTCTGTCCCCACCTTGT
Dex10MmR	Mouse	eEF1B δ	TTGTTGAAAGCTGCGATGTC
Dex10HsR	Human	eEF1B δ	GCTGCGATATCGACACTCTG
DattbRev	Human	eEF1B δ	GTACAAGAAAGCTGGGTCTTA TCAGATCTTGTTGAAAGCTGC
GAPDHFwd	Mouse and human	GAPDH	CATCACCATCTTCCAGGAGC
GAPDHRev	Mouse and human	GAPDH	ATGACCTTGCCACAGCCTT
18srRNAF	Mouse and human	18S rRNA	CATGCGCGTTCTTAGTTGGT
18srRNAR	Mouse and human	18S rRNA	GAACGCCACTTGCCCTCTA
B2MFwd	Mouse	β -2-m	AATGCTGAAGAACGGGAAAA
B2MRev	Mouse	β -2-m	CAGTCTCAGTGGGGGTGAAT
bActinF	Mouse and human	β -actin	GTCCACCTTCCAGCAGATGT
bActinR	Mouse and human	β -actin	TCTGCGCAAGTTAGGTTTTG
M13Fwd	Plasmids	M13	GTA AACGACGGCCAG
M13Rev	Plasmids	M13	CAGGAAACAGCTATGAC

2.2.7 DNA

Plasmids used for cloning are described in table 2.8.

Table 2.8 All the plasmids used for cloning of C-terminal V5 tagged eEF1B subunits, vectors, source and antibiotic resistance

Name	Insert	Vector	Notes/source	Antibiotic
pDONR221	n.a.	pDONR221	Invitrogen	Kanamycin
pcDNA-DEST40	C-terminal V5 tag	pcDNA-DEST40	Invitrogen	Ampicillin
3611581	Human eEF1B α	pOTB7	GeneService (IMAGE clone)	Chloramphenicol
5299844	Human eEF1B α	pBluescriptR	GeneService (IMAGE clone)	Chloramphenicol
5470872	Human eEF1B α	pOTB7	GeneService (IMAGE clone)	Ampicillin
3349601	Human eEF1B δ iso a	pOTB7	GeneService (IMAGE clone)	Chloramphenicol
4129368	Human eEF1B δ iso a	pOTB7	GeneService (IMAGE clone)	Chloramphenicol
2961609	Human eEF1B δ iso b	pOTB7	GeneService (IMAGE clone)	Chloramphenicol
5442454	Human eEF1B δ iso b	pOTB7	GeneService (IMAGE clone)	Chloramphenicol
2961341	Human eEF1B δ iso c	pOTB7	GeneService (IMAGE clone)	Chloramphenicol
2821006	Human eEF1B γ	pOTB7	GeneService (IMAGE clone)	Chloramphenicol
3611581	Human eEF1B γ	pOTB7	GeneService (IMAGE clone)	Chloramphenicol

2.2.8 siRNAs

List of siRNAs used for RNAi experiments in this study are shown in table 2.9.

Table 2.9 List of siRNA names that were used in this project as well as reference name, targets, sequences and source

Name	Reference name	Target	Sequence 5' to 3'	Source
eEF1B α siRNA a	10885	eEF1B α exon 3	GGAAGUGGAGCUACAGAUAtt	Ambion
eEF1B α siRNA b	10977	eEF1B α span exon 3 and 4	GGAAAGUGAAGAAGCAAAGtt	Ambion
eEF1B α siRNA c	s194388	eEF1B α exon 4	GGAAGAACGUCUJUGCACAAtt	Ambion
eEF1B δ siRNA a	42605	eEF1B δ exon 4	GUUCAAAUAUGACGACGCAtt	Ambion
eEF1B δ siRNA b	s4485	eEF1B δ exon 8	GGCAGUACGCGGAGAAGAAtt	Ambion
eEF1B δ siRNA c	146798	eEF1B δ exon 10	GCCUGAGUGUGUGUACGUGtt	Ambion
eEF1B γ siRNA a	9851	eEF1B γ exon 3	GGGUGAUGAUGGAUUCUGUtt	Ambion
eEF1B γ siRNA b	9939	eEF1B γ span exon 5 and 6	GGUUCUAGAGCCUUCUUUctt	Ambion
eEF1B γ siRNA c	s4489	eEF1B γ span exon 6 and 7	GUUUGAUGCUGCCUAGUUUtt	Ambion
β -actin siRNA	Actin positive control	β -actin	Not provided	Invitrogen
Non-targeting siRNA	Negative control 1	Non-targeting	Not provided	Ambion
Non-targeting siRNA 2	Negative control 2	Non-targeting	Not provided	Ambion
Non-targeting siRNA 3	Negative control 3	Non-targeting	Not provided	Ambion

2.3 Cell culture

2.3.1 Cell culture maintenance

Cell lines were grown in Cell Start T25 or T75 flasks (Greiner Bio-One) with 25ml or 50ml of media respectively, using the media shown in table 2.4, at 37 °C, 5% CO₂ in a Galaxy S incubator (Scientific Laboratory Supplies). To passage the cells, the media was aspirated, the cells were washed in PBS and incubated in a 1:1 mix of trypsin:versene (Invitrogen) for 2-5 minutes, before media was added. The cells suspension was centrifuged at 1000 rpm for 5 minutes, the supernatant was aspirated and the pelleted cells were resuspended in 5ml of new media and split usually 1 in 10 into a new flask of the same size or 1 in 5 into a bigger flask. The cells were split approximately every 3 to 7 days and once they reached passage number 15 the cells were discarded.

2.3.2 Cell count

Cells were counted by first being washed in PBS and trypsinised as described above. Then, after the addition of the media, 100µl was mixed into 9.9ml of isotone and the cells were counted using a Coulter Counter Z (Beckman coulter).

2.3.3 Cryostat preservation of cell lines

In order to store cells in liquid nitrogen, cells in a T75 flask were trypsinised and centrifuged as described in section 2.3.1. The cells were then resuspended in 10mls of 90%FBS and 10%DMSO and transferred into about 10 cryopreservation vials of 1ml each. The samples are then frozen at -70 °C overnight and finally transferred to liquid nitrogen.

2.3.4 RNAi

The SDS tool, available on <http://i.cs.hku.hk/~sirna/software/sirna.php>, shows several siRNA design tools output and the consensus sequences. The SDS tool consistently showed a siRNA consensus sequence for all the eEF1B subunits

that were pre-designed siRNA from Ambion. Hence, two Silencer siRNAs and one Silencer Select were obtained for each eEF1B subunits (table 2.8). Each of the siRNAs was resuspended to a concentration of 100 μ M and stored at -70 °C. Furthermore, a positive siRNA targeting β -actin and a non-targeting negative siRNA control were used. The sequences of these were not supplied by the manufacturer.

2.3.5 Transfection by lipofectamine

In order to exogenously express protein in culture cells and transfect siRNAs, cells that were about 70-80% confluent were washed in PBS, trypsinised and counted as described before (2.3.1), and the appropriate number was resuspended in OptiMEM (Invitrogen) and then transfected with plasmids or siRNAs using Lipofectamine 2000 (Invitrogen), according to manufacturer's instructions. After 5 to 6 hours, the cells media was replaced by their normal growth media. Cells with no siRNA or plasmid or cells not subjected to transfection were used as controls.

2.3.6 Transfection by nucleofection

The nucleofector system (Amaxa Biosystems) was used to transfect siRNAs into HeLa cells. In order to transfect, cells were grown until about 70-80% confluency, trypsinised and counted as described before (2.3.1). For each well on a 6-well plate, 0.5x10⁶ HeLa cells were pelleted, resuspended in the appropriate volume of siRNAs and 100 μ l of nucleofector solution R (Amaxa Biosystems). Cells were then subjected to nucleofection using the I-13 program and according to the manufacturer's instructions. In brief, 500 μ l of medium was added immediately after the cell suspension and this was transferred to a well which already contained 1ml of medium. Cells with no siRNA or cells with no solution and not subjected to nucleofection were used as controls.

2.4 Protein-related methods

2.4.1 Antibody production

Peptides were designed against eEF1B α , eEF1B δ isoform a, eEF1B δ all isoforms and eEF1B γ . The peptides were designed taking into consideration SNPs, hydrophobicity, protein secondary structure, antigenicity, conservation in mammals and similarity between subunits. Peptides were conjugated with KLH cysteine by Cancer Research UK antibody resources and the KLH conjugated peptide was injected into a rabbit at Easter Bush, Edinburgh. The serum was purified as described below before being used in assays.

2.4.1.1 Antibody purification

The serum was subjected to ammonium sulphate precipitation and affinity purification. In order to purify by ammonium sulphate, the serum was centrifuged 3000g for 30 minutes and 0.5 (v/v) of saturated ammonium sulphate (table 2.3) was added to the supernatant and stirred overnight at 4 °C. The serum was then subjected to the same procedure again however the supernatant was discarded and the pellet was resuspended in 0.3-0.5 (v/v) of starting volume PBS. The serum was then subjected to dialysis overnight with several changes of PBS. To further purify, the serum was subjected to affinity purification by using SulfoLink kit (Pierce) and according to the manufacturer's instructions.

2.4.1.2 Antibody titration by ELISA

Peptide titration curves were performed to ensure the antibodies were specific to the peptide against which they were raised. Different concentrations of peptides ranging from 0.01 μ g/ml to 10 μ g/ml in 200 μ l of coating buffer (table 2.3) were incubated in Maxisorp plates (Nunc) overnight at 4 °C. Some wells were not coated with the peptides (only with the coating buffer) to act as negative controls.

The plates were then washed three times with ELISA wash buffer (table 2.3), blocked in wash buffer with 1% BSA for 1 hour and washed again three times. They were then incubated for 1 hour with different dilutions of serum from 1 in 100 to 1 in 50 000 in wash buffer and washed for three times. The plates were then incubated in 200 μ l of o-phenylenediamine dihydrochloride (OPD) substrate (table 2.3) for 15 minutes and absorbance readings were taken at 450nm. The procedure was performed at room temperature unless stated otherwise.

2.4.2 Cell lysates

2.4.2.1 Production of cell lysates

In order to produce cell lysates, cells were grown until they were 70 to 90% confluent. The media was aspirated off and the cells were washed once with PBS. A small amount of cold RIPA was added to the cells just enough to cover the well bottom (30 μ l in 24 well plate), and the cells were incubated at 4 °C for about 10 minutes. The cells that were still adjacent to the wells were displaced by using a cell scraper. The crude lysates were transferred to a micro-centrifuge tube and centrifuged at 13,000 rpm for 30 minutes at 4 °C and the pellet was discarded. The supernatant (lysates) were stored at -20 °C. In order to produce tissue lysates, tissues were washed in PBS and homogenised in a sucrose solution (0.32M or 109.5g per liter of distilled water) with complete protease inhibitors cocktail (Roche) and stored at -20 °C.

2.4.2.2 Sub-cellular fractionation

Mouse whole brain and liver were firstly washed in PBS and then were homogenised in 500 μ l of lysis buffer (table 2.3). They were then centrifuged at 16,000g for 10 minutes at 4 °C. The supernatant (cytoplasm) was transferred to another tube and stored at -70 °C. The pellet was resuspended in 300 μ l nuclear lysis

buffer (table 2.3), further homogenised, incubated on ice for 30 minutes and centrifuged at 20,000g for 10 minutes at 4 °C. The supernatant (nuclear protein fraction) was transferred to another microcentrifuge tube and stored at -70 °C.

2.4.2.3 Measuring protein concentration in cell lysates

The concentration of total protein in lysates was measured by BioRad DC protein assay according to the manufactures' description. A serial dilution of BSA from 0 to 2.0mg/ml in lysis buffer was used to establish the standard curve. Usually, 1µl of lysates was added to a 96-well plate in triplicate and diluted 1:5 with lysis buffer. Then, 20µl of reagent S was added to 1ml of reagent A' and mixed. Of this solution, 25µl were added to 5µl of protein sample on the 96 well plate and the plate was swirled. Finally, 200µl of reagent B were added to each well. The plate was incubated at room temperature for 15 minutes and absorbance readings were taken at 750nm. The absorbance value for each BSA protein standard was plotted against the protein concentration and a standard curve was generated. This curve was then used to determine the concentrations of the protein lysates.

2.4.3 Western blot

2.4.3.1 Sample preparation

Lysates (section 2.4.2) were prepared for Western blotting by mixing 1:1 with protein sample buffer (table 2.3) and 1:10 with 1M DTT. In order to denature the proteins and disrupt protein-protein interactions, samples were then heated at 100 °C for 5 minutes. To some samples, β-mercaptoethanol was added for further disruption of protein-protein interactions.

2.4.3.2 SDS-Polyacrylamide gel electrophoresis

Separating gels (11%) were produced as follows (enough for 2 gels):

2. MATERIALS AND METHODS

30% acrylamide	5.0 ml
1.5M Tris pH 8.8	4 ml
dH ₂ O	6.08 ml
20% SDS	80 µl
TEMED	10 µl
25% 2-Acrylamido-2-Methylpropane Sulphonic Acid (AMPS)	40 µl

The gel solution was mixed and then poured between two BioRad glass plates, leaving 1-2 cm at the top which was initially filled with dH₂O. After 30 minutes, when the separating gel was set, the water was removed and replaced with 4% stacking gel solution prepared as follows.

30% acrylamide	1.45 ml
0.5M Tris-HCl pH 6.8	2.5 ml
dH ₂ O	5.95 ml
20% SDS	50 µl
TEMED	5 µl
25% AMPS	50 µl

A comb of either 10 or 15 wells (BioRad) was added to the top and the gel allowed to set for another 30 minutes. When the gels were set, they were placed into a Mini TransBlot Cell (BioRad) which was filled up with 1x Laemmli running buffer (table 2.3). The combs were removed and the samples prepared as described above were then loaded into the gel along with a protein size marker (Fullrange rainbow – BioRad). Gels were then run at 110V for about 90 minutes to separate the proteins in the samples by molecular weight. Gels were removed and soaked in transfer buffer as well as two 6cm by 8cm pieces of 1.7mm card (Whatman) and two sponges per gel. For each gel, a 6cm by 8cm piece of Hybond-P PVDF membrane (Amersham) was cut, soaked in methanol and then soaked in transfer buffer. A sponge, one piece of card, followed by the gel, the membrane, another piece of card

and a sponge were assembled on the transfer cell and put into a tank filled with transfer buffer (table 2.3). It was then run at 60A overnight at 4 °C in order to transfer the protein, including the marker, from the gel to the membrane. The membrane was then removed, washed and blocked with a membrane blocking buffer (usually 5% powdered milk in PBS-T – table 2.3) for about one hour at room temperature.

2.4.3.3 Western blotting

After blocking, membranes were transferred to an appropriate dish and incubated with a primary antibody in blocking buffer at a particular dilution and conditions shown in table 2.5. The membrane was then washed for 1, 2, 5 and 10 minutes with wash buffer (usually PSB-T – table 2.3). The membrane was then incubated with HRP conjugated secondary antibody diluted as shown in table 2.5 in blocking buffer for one hour at room temperature. The membrane was washed as before with an extra wash with PBS only (no Tween). The proteins were visualised by using enhanced chemiluminescence (ECL) detection kit (Amersham).

2.4.3.4 Densitometry

In order to quantitatively analyse Western blot results, the shortest exposure in which bands were visible in the films were scanned into a computer and the signal intensity of the bands was measured using the program ImageJ (Abramoff et al., 2004).

2.4.3.5 Re-probing of membranes

In order to re-probe a membrane with an additional antibody, the membranes were incubated for 30 minutes at 4 °C with stripping buffer (table 2.3)

with gentle shaking. The membrane was then washed three times with wash buffer, blocked and stained with the new antibody as described before (table 2.5).

2.4.3.6 Pre-absorption of antibodies

To test if an antibody binds to the peptide against which it was raised, blocking buffer with the antibody at a concentration at which it was normally used together with 100ng/ml of the peptide it was originally raised against were incubated overnight at 4 °C while mixing at 30 rpm on a rotary wheel.

2.4.4 Immunocytochemistry

In order to visualise the expression pattern of proteins within individual cells, immunocytochemistry was used. The cells must be fixed before the procedure to cease cellular processes and to expose epitopes for antibody binding. Media was removed from cells, the cover slips were washed with PBS and cold 1:1 methanol:acetone was added to the well just enough to cover the bottom of the well. The plate was incubated at -20 °C for about 30 minutes to fix the cells. Cover slips were then washed three times with room temperature PBS with 0.1% Triton X100 and 3% BSA and incubated at room temperature for one hour to block and permeabilise. Coverslips were then incubated with appropriately diluted antibody in PBS with 1% Triton X100 and 3% BSA for 1 hour using just enough liquid to cover the cells. Cells were incubated with two antibodies in case of double-immunostaining. Coverslips were then washed three times with PBS and 0.1% Triton X100 and incubated for a further 30 minutes with appropriately diluted fluorescent secondary antibody in PBS 1% Triton X100 and 3% BSA. The plates were wrapped in foil to keep out of the light. Coverslips were then washed in PBS with 0.1% Triton X100 three times and mounted onto glass slides using Vectashield mounting solution containing 4',6-diamidino-2-phenylindole (DAPI). Acetone was added to the side of the coverslips in order to seal the coverslips to the glass slides. Coverslips were then stored at 4 °C in the dark and visualised on a Zeiss Axioskop 2

fluorescent microscope using Smart Capture 2 software. Cells not incubated with the primary antibody were used as negative controls.

2.4.5 Immunohistochemistry

In order to visualise the expression pattern of proteins within tissues, immunohistochemistry was used. Paraffin embedded sections of human and mouse tissues were deparaffinised with xylene and rehydrated in 75% and absolute ethanol. Slides were then washed in dH₂O and PBS and loaded into a Sequenzer. The tissues were blocked in peroxidise blocking solution (table 2.3) for 5 minutes. Slides were then washed and blocked in goat serum diluted 1:5 with PBS for 10 minutes. Primary antibody was added at the dilutions and conditions described in table 2.5. The slides were then incubated and visualised using ChemMate DAKO EnVision Detection Kit (DAKO) according to the manufacturer's instructions. In brief, the slides were then washed in PBS and three drops of ChemMate DAKO Envision/HRP Rabbit/Mouse secondary antibody (DAKO Cytomation) were added to each slide and incubated for a further 30 minutes. The slides were washed with PBS, removed from the sequenzer and 0.5ml of DAB working solution was added to each slide and incubated for 2 minutes. Finally, the slides were washed in dH₂O, counterstained in haematoxylin, stained with lithium carbonate and dehydrated in absolute ethanol and 75% ethanol, cleared in xylene and mounted in pertex. The entire procedure was performed at room temperature. Sections were viewed by light microscopy on Olympus BX51 using DP software (Olympus).

2.5 Molecular biology methods

2.5.1 PCR sample preparation

2.5.1.1 RNA extraction

In order to extract RNA from cells, the cells were washed, trypsinised and pelleted as described on section 2.3.1. Supernatant was removed and the pellets were stored at -70 °C until use. RNA was extracted from cells using the RNeasy Mini Kit (Qiagen) according to the manufacturer's instructions, whereas to extract RNA from tissues, tissues were washed with PBS, homogenised and RNA was extracted using the RNeasy Midi Kit (Qiagen) according to the manufacturer's instructions.

2.5.1.2 Measuring RNA concentration

In order to determine the concentration of RNA samples, a nanodrop was used. The device was set to measure absorbance reading of 260nm and calibrate with the buffer on which the RNA was dissolved. The RNA concentration ($\mu\text{g/ml}$) was calculated by multiplying the OD260 reading by a factor of 40 considering that an OD260 of 1 corresponds to 40 $\mu\text{g/ml}$ of single stranded RNA.

2.5.1.3 cDNA synthesis

The First Strand cDNA Synthesis kit (Roche) was used to produce cDNA from RNA as follows. The following reaction was performed:

2 μl 10x reaction buffer
4 μl 25mM Magnesium chloride
2 μl dNTPs mix
1 μl Oligo-dT primers
1 μl Random primers

1 μ l RNase inhibitor
0.8 μ l AMV reverse transcriptase
1-5 μ l RNA
Up to 20 μ l dH₂O

Reactions were subjected to the following incubations:

10 minutes at room temperature
42 °C for 60 minutes
95 °C for 5 minutes
4 °C for 5 minutes

Negative controls were processed in the same way, except lacking AMV reverse transcriptase. The reactions were then stored at -20 °C.

2.5.2 PCR reactions

Different PCR methods were used to amplify a specific segment of DNA.

2.5.2.1 RT-PCR with *taq* polymerase

The following PCR reaction was used for the majority of applications. Each PCR reaction was set up using the following:

10x PCR reaction buffer (Sigma)	2.5 μ l
25mM magnesium chloride (range from 10 up to 100mM)	
10mM dNTPs	2.0 μ l
1 μ M of each primer	2.5 μ l
Template cDNA or plasmid	1 μ l
Taq polymerase (Sigma)	0.5 μ l
dH ₂ O	up to 25 μ l

The reactions were then processed on a thermal cycler using the following program:

Step 1	Initial denaturation	1x	92 °C	3 minutes
Step 2	Denaturation	28x	92 °C	30 seconds
	Annealing		50-60 °C	30 seconds
	Extension		72 °C	30-90 seconds
Step 3	Final extension	1x	72 °C	10 minutes
			4 °C	until needed

The length of the extension step varied depending on the predicted length of the PCR product (1 minute per kilobase). And the annealing temperature varied depending on the stringency and melting temperature of the primers.

A sample with no reverse transcriptase, hence with just RNA, was used as minus control to determine DNA contamination in the RNA.

2.5.2.2 PCR with Phusion polymerase

In order to amplify a PCR product with a high-fidelity DNA polymerase, the Phusion PCR master mix was used (NEB) according to the manufacturer's instructions. PCR programme was as follows:

Step number	cycles	temperature	time
Step 1	1x	98 °C	30 seconds
Step 2	24x	98 °C	10 seconds
		57 °C	30 seconds
		72 °C	1 minute
Step 3	1x	72 °C	10 minutes
		4 °C	until needed

2.5.2.3 RT-qPCR

A standard curve method of analysis was used. For each tissue sample, a standard curve was created by a serial dilution (1:10, 1:100, 1:1000, 1:10000, 1:100000). Primers for the eEF1B subunits, β -2-microglobulin, 18S rRNA and β -actin (table 2.6) were designed to amplify a product of between 100 and 120bp with no secondary structure and expected to have low primer dimer formation to minimise the effects on product amplification. Only the results that showed a coefficient higher than 0.99 or PCR efficiency between 95 and 105% were used. eEF1B subunits results were normalised against the reference genes. No cDNA, no PCR solution and just dH₂O were used as controls to determine PCR reagent and RNA contamination. Samples were always in triplicate. The mean was taken from the normalised expression ratios for each sample of identical tissues. A melting curve was carried out to confirm specificity of the primers where a sharp peak indicates a single product.

PCR reaction was set up using the following:

2x Supermix	10 μ l
0.8 μ M primers	2 μ l
cDNA diluted in dH ₂ O	6 μ l

The PCR cycling programmed used is shown bellow.

Step number	cycles	temperature	time
Step 1	1x	95 °C	8.5 minutes
Step 2	40x	95 °C	30 seconds
		62 °C	30 seconds
		72 °C	30 seconds – data collection
Step 3	1x	95 °C	1 minute
Step 4	1x	60 °C	1 minute
Step 5	80x	60 °C	10 seconds – data collection

(increase 0.5 °C per cycle to produce the melting curve)

2.5.2.4 BigDye pre-sequencing PCR

In order to sequence a PCR product or a plasmid construct, the BigDye Terminator Ready Reaction Mix v3.1 system (Applied Biosystems) was used. Each reaction was set up as follows where each PCR reaction makes use of only one primer:

5x BigDye sequencing buffer	1.5 μ l
2.5x BigDye mix	1.0 μ l
template (purified PCR product or plasmid DNA)	3 μ l
primer (forward or reverse)	1.5 μ l
dH ₂ O	3 μ l

The following PCR program was used:

Step 1	1x	96 °C	1 minute
Step 2	24x	96 °C	30 seconds
		50 °C	15 seconds
		60 °C	4 minutes
Step 3		4 °C	until needed

2.5.2.5 Colony PCR

In order to screen several bacterial colonies for the presence of a particular insert. A single bacterial colony was picked, grown in LB and put in a PCR plate well with 30 μ l dH₂O. It was incubated at 99 °C for 2 minutes to disrupt the bacterial wall. The colony PCR was prepared as follows:

10x PCR Buffer (Sigma)	2.5 μ l
10mM dNTPs	1.0 μ l
5 μ M each primer	2.5 μ l
Bacterial DNA	1.0 μ l
5u/ul Taq polymerase	0.5 μ l
Up to 15 μ l with dH ₂ O	

The reactions were then subjected to the following PCR program:

Step 1	1x:	95 °C	2minutes
Step 2	30x:	95 °C	30 seconds
		50 °C	30 seconds
		72 °C	2 minutes
Step 3	1x:	72 °C	10 minutes
		4 °C	until needed

2.5.3 Sequencing PCR products and plasmids

After each pre-sequencing PCR reaction was performed, to each product of this PCR reaction was added 2.5µl of 125nM EDTA and 30µl absolute ethanol. The plate was flicked and then incubated at room temperature for 10-15 minutes. Tubes were centrifuged at 3,000rpm in a plate centrifuge for 30 minutes at 4 °C. The plates were placed upside down on absorbent paper and spun briefly to a maximum of 1,000 rpm to remove the ethanol. Then 35µl of 70% ethanol was added to each well and the plate was centrifuged at 3,000rpm for a further 15 minutes. The ethanol was removed as described before and the wells were left to air dry for 10 minutes at room temperature before storing at -20 °C. The sequencing was carried out by either Agnes Gallacher or Alison Condie (Medical Research Council Human Genetics Unit or Wellcome Trust Clinical Research Facility). The sequences were visualised using the program BioEdit (Hall, 1999) and were compared to known DNA sequences by using BLASTn (Altschul et al., 1990), FASTA (Pearson, 1990), CLUSTALw (Thompson et al., 1994) and Muscle tools (Edgar, 2004).

2.5.4 Purification of PCR products

In some circumstances such as prior to a ligation, recombination reaction and pre-sequencing PCR reaction, PCR products need to be purified in order to remove other elements of the PCR reaction mix. This was done using a QIAquick

PCR purification kit (Qiagen) according to the manufacturer's instructions. In the case of the pre-sequencing PCR reaction, PCR products were cleaned by ExoSapit (Applied Biosystem) by adding 1 μ l of ExoSapit per 5 μ l of PCR product and incubating at 37 °C for 15 minutes followed by incubation at 80 °C for 15 minutes.

2.5.5 DNA electrophoresis

2.5.5.1 Making and running of agarose gels

Agarose gels were prepared by adding 1 to 2% agarose powder to 0.5x TBE buffer. This was heated until the powder was dissolved in a microwave. The solution was allowed to cool down and 1:100 SYBR Safe DNA gel stain (Invitrogen) was added and mixed. The agarose was then poured into a tray, combs were added and the gel was allowed to set. Meanwhile, the DNA samples were prepared by mixing 1:1 with DNA loading buffer (table 2.3). The gel was then placed in an electrophoresis tank which was filled with 0.5x TBE buffer, the combs were removed and the DNA samples were loaded into the wells along with a 1kb DNA ladder (Invitrogen) as a molecular weight marker. Depending on the size of the DNA product to be viewed, the gel was run for between 20 minutes up to 120 minutes at 80-120V. Gels were then viewed under GelDoc and photographed.

2.5.5.2 Isolation of DNA fragments from agarose gels

Agarose gels can also be used in order to separate DNA of a certain size from a sample. In order to do this, the sample was run on a gel made using low-melting point agarose, but otherwise as described above. After the gel was run, the DNA was visualised on a UV box and the band of interest excised using a sterile scalpel. This gel fragment was then processed using a QIAquick Gel Extraction Kit (Qiagen), according to the manufacturer's instructions, in order to isolate the DNA contained within it.

2.5.6 Culture of bacteria transformed with plasmid constructs

2.5.6.1 Competent bacteria cells production

In order to produce chemically competent bacteria, TOP10 cells (Invitrogen) were grown streaked on a plate and incubated overnight at 23 °C. A single clone was isolated and grown in LB at 23 °C. 15% glycerol was added to a portion of the LB solution and stored at -70 °C in cryotubes. TOP10 cells in LB (1ml) were added to 250ml of LB and incubated at 20 °C to an absorbance at 600nm of about 0.3 which takes approximately between 14 and 18 hours. The bacterial suspension was centrifuged at 3,000rpm at 4 °C for 10 minutes and the pellet resuspended in 80ml of ice cold CCMB80 buffer. After being incubated on ice for 20 minutes, the cell solution was centrifuged as before and resuspended in 10ml of CCMB80 buffer. More ice-cold buffer was added to the solution until the absorbance reading at 600nm was between 1.0 and 1.5. The bacterial cells were subjected to another incubation on ice for 20 minutes, aliquoted in vials and stored at -70 °C for future use.

2.5.6.2 Transformation of bacteria with plasmid constructs

1µl of plasmid construct was transformed into chemically competent TOP10 cells as follows: cells were thawed on ice, the plasmid DNA was added to them and the mixture was incubated on ice for 15 minutes. Cells were then heat-shocked by incubation at 42 °C for 30-40 seconds, before cooling down on ice for a further 2 minutes. 200µl of LB or SOC media was then added to the cells and they were incubated at 37 °C with 200rpm for about 2 hours in an Innova 4300 incubator shaker (New Brunswick Scientific). After the incubation, 30-70µl of the bacterial culture was spread across an LB agar with 50µg/ml ampicillin (Sigma) or 100µg/ml kanamycin (Sigma) or 20µg/ml chloramphenicol (Sigma) using a sterile scraper. Plates were sealed and incubated until colonies were visible (typically 16 to 24 hours after) at 37 °C with 5% CO₂ in a Plus II incubator (Gallencamp).

2.5.6.3 Bacterial culture and selection

Cultures of bacteria, transformed as described above, can be set up by selecting a single colony of the LB agar/antibody plate and then allowed to grow in LB/antibody media at 37 °C shaking at 200rpm.

2.5.6.4 Measuring DNA concentration

In order to determine the concentration of a plasmid construct or other DNA solution, a nanodrop was used. The device was set to measure absorbance reading of 260nm and calibrated with either dH₂O or TE buffer depending on which buffer the DNA was dissolved in. The DNA concentration ($\mu\text{g}/\mu\text{l}$) was calculated by multiplying the OD₂₆₀ reading by a factor of 0.05.

2.5.6.5 Plasmid preparation

Small cultures of 1-5 ml media were centrifuged at 13,000rpm for 1 minute in a desktop centrifuge in order to pellet the bacteria. The supernatant was then discarded and the plasmids harvested from the pellet using a Spin Miniprep kit (Qiagen) according to the manufacturer's instructions. Alternatively, 200ml cultures were centrifuged using an Avanti J-20I centrifuge (Beckman Coulter) at 5000rpm 4 °C for 10 minutes. The bacterial pellet was processed using a Plasmid Maxiprep kit (Qiagen), according to the manufacturer's instructions. After purification, plasmid DNA was suspended in TE (pH 7.5) or dH₂O and stored at either -20 °C.

2.5.6.6 Precipitation of DNA

In order to precipitate the plasmids to obtain a higher concentration prior to transfection, 0.1x (v/v) 3M sodium acetate and 2x (v/v) of 100% ethanol was added to the DNA samples and incubated for 30 minutes at -20 °C. The samples were spun at maximum speed for 10 minutes at 4 °C. The supernatant was then removed, the

pellet was resuspended in 70% ethanol, centrifuged as previously and the pellet allowed to air dry for 10 minutes. Finally the pellet was resuspended in a smaller volume of H₂O or TE.

2.5.7 Cloning techniques

2.5.7.1 Generation of C-terminally V5 tagged human eEF1B subunit constructs

In order to create C-terminal V5 tagged eEF1B α , eEF1B δ and eEF1B γ constructs, the Gateway cloning system (Invitrogen) was used. Several human cDNA IMAGE clones (Geneservice) for each eEF1B subunit were obtained (table 2.7), grown on LB with selective antibiotic, and then multiple bacterial clones were isolated, sequenced using the M13 forward and reverse primers as described above and the ones that matched the eEF1B subunits sequence were grown in LB with selective antibiotic and bacterial glycerol stocks were stored at -70 °C. In order to generate the V5 tagged constructs, the eEF1B cDNA sequence had to be inserted into an entry vector pDONR221 (Invitrogen) by bacteriophage (BP) recombination enzyme mix reaction containing bacteriophage lambda recombination proteins that catalyze the in vitro recombination of PCR (see below), followed by the entry vector recombination to the destination vector which in this case was pcDNA-DEST40 (Invitrogen) for expression as a C-terminal V5 tagged protein by bacteriophage lambda recombination (LR) proteins.

2.5.7.1.1 BP recombination reaction

The series of recombinations to take place are based on the ability of attB sites to drive site-specific recombination. Hence, primers were designed to contain part of the eEF1B subunits sequence, the attB site and several base pairs complementary to the entry plasmid to facilitate recombination. A few base pairs before the start codon, including the Kozak sequence, were included in the forward

primer since they facilitate the translation of the protein. The list of the primers used is shown in table 2.6. A PCR reaction with these specific primers and using the IMAGE clones as templates was performed by Phusion polymerase as described on section 2.5.1.2. The PCR product was run on an agarose gel to confirm the size and purified using the PCR purification kit as described on section 2.5.3. Once purified, the BP reaction was carried out between the purified PCR reaction and the pDORN221 vector following the manufacturer's instructions and used to transform competent TOP10 cells (section 2.5.6.1). Clones were isolated, subjected to miniprep (section 2.5.6.5), digested using restriction enzymes (section 2.5.7.2.1) to confirm the presence and size of the insert and the positive clones were then sequenced.

2.5.7.1.2 LP recombination reaction

Once a positive clone was identified for each of the eEF1B subunits, the LR recombination reaction was carried out between the plasmid DNA obtained from the miniprep and pcDNA-DEST40 according to the manufacturer's instructions and used to transform competent TOP10 cells. Once again, bacterial clones were isolated, subjected to digestion by restriction enzymes and sequenced.

2.5.7.2 Cloning of transcript variants

2.5.7.2.1 Restriction enzyme digests

In order to digest DNA at selective sites, specific restriction enzymes obtained from NEB were used. The DNA to be digested was made up in a buffer appropriate for the enzyme and the enzyme was added. The reaction was then incubated at 37 °C for 1-18 hours. A list of enzymes used, along with their corresponding buffers is shown in table 2.9. These products could then be run on an agarose gel and the pattern of the digested bands visualised.

Table 2.9 List of restriction enzymes specific for each eEF1B subunit and respective buffers

eEF1B subunit	Restriction enzyme	Buffer
eEF1B γ	BamHI	Buffer 3 (NEB)
	XbaI	Buffer 4 (NEB)
eEF1B δ	PstI	Buffer 3 (NEB)
	BfaI	Buffer 4 (NEB)
	EcoRV	Buffer 3 (NEB)
eEF1B α	HindIII	Buffer 2 (NEB)

2.5.7.2.2 Ligation reaction

In order to ligate DNA inserts containing restriction sites into plasmids, both the insert and plasmid were first restriction digested. A 10 μ l ligation reaction was then set up containing 1 μ l T4 ligase (Invitrogen), vector and insert in T4 ligase buffer (Invitrogen). Approximately 2 μ l of vector was used, along with insert in a 1:3 molar ratio with it. Reactions were incubated at 24 °C for 1 hour and then transformed into TOP10 cells (section 2.5.6.1).

2.5.8 Cell culture assays

2.5.8.1 Cell cycle arrest

HeLa cells were incubated with 1 μ M aphidicolin (Sigma), which inhibits DNA replication blocking cell cycle at the S-phase, for 24 hours. The media was then replaced with new media and samples were taken every 2 hours to be analysed by Western blot and flow cytometry.

2.5.8.2 Cell cycle analysis by flow cytometry

In order to determine the ratio of cells in a particular cell cycle stage, cells were resuspended and incubated in 500 μ l propidium iodide staining solution (table 2.3) for 20 minutes before being analysed using a Coulter EPICS XL flow cytometer (Beckman Coulter). Upon addition of the propidium iodide staining solution, the

tube was wrapped in foil to protect from light. A dot-plot was drawn of forward light scatter (FLS) against side scatter (SSC), which are influenced by size and refractive index, and all cells were gated for further analysis except dead cells and cell debris by using the EXPO ADC analysis software. A FL3 histogram with a linear x axis was used to visualise the DNA content of the cells. No compensation was required since only one fluorochrome was used. The flow rate was set to low to be more accurate and FL3 histogram was obtained from 10,000 events data. Multicycle AV software (Phoenix Flow systems) was used to analyse the output. As controls, unsynchronised cells and cells treated with 1 μ M staurosporine (Sigma), known to induce reduction of cell growth leading to apoptosis, for 24h were used as controls.

2.5.8.3 Reduction of cellular metabolites by Alamar blue

In order to measure changes metabolic breakdown which is in most cases comparable to the cell proliferation, Alamar blue (AbDserotec) was which is sensitive, quick and not toxic to the cells. Alamar blue, which acts as a redox indicator, was used in an assay according to manufacturer's instructions and the signal was read by fluorometry (Biotech synergy HT Plate Reader - Fisher Scientific). The fluorescence readings were taken at excitation of 560nm and emission of 590nm. In brief, the cells were incubated with 1:10 Alamar blue solution and incubated as normal and the signal read up to 6 hours after when the colour changes from blue to pink. This colour change is due to the blue oxidised form of resazurin being reduced to the pink resorufin form by mitochondrial respiration which is indicating of cell metabolites being converted into adenosine triphosphate (ATP) (Abe et al., 2002). A blank control, non-treated cells and mock transfected cells were used as controls.

2.5.8.4 Apoptosis analysis

2.5.8.4.1 By flow cytometry

Annexin-V-Fluos kit (Roche) was used to determine the ratio of apoptotic cells detected by flow cytometry, according to the manufacturer's instructions. Annexin V stains cells just before loss of membrane integrity which used together with live/dead dye propidium iodide can distinguish early from late apoptotic cells. Since the signal from the annexin V bleeds into the propidium iodide signal the fluorescence was adjusted and compensated. A dotplot of FL2 vs FL1 was drawn and data was obtained from 10,000 events. As a control, non stained cells, cells only stained with annexin V or only with propidium iodide and cells treated with 1-3 μ M staurosporine for 24h were used as controls.

2.5.8.4.2 By fluorometry

Fluorometric analysis was also used to detect caspase 3 and 7 activation by the use of the Apo-One homogenous caspase3/7 assay (Promega). The fluorescence readings were taken at excitation of 560nm and emission of 590nm. This procedure was performed according to the manufacturer's instructions. A blank control, non-treated cells, mock transfected cells and cells treated with 1 μ M staurosporine were used as controls.

Chapter 3 – *in silico* characterisation of eEF1B subunits

3.1 Introduction

The composition of the eEF1B complex and the involvement of the complex in protein synthesis as the factor responsible for eEF1A:GDP/eEF1A:GTP recycling during elongation was well established in various eukaryotic species almost two decades ago. Since those purification studies were performed, only a few more studies have addressed the possible characteristics or features of the eEF1B subunits and their regulation, with most of them being conducted in yeast and *Xenopus* oocytes. The large majority of studies that mentioned eEF1B subunits were investigations into overexpressed genes or proteins in tumour samples. In order to understand the biology, it is important to catalogue features and characteristics of the eEF1B subunits in mammals.

The GenBank database was searched to identify the genomic location of the genes encoding the eEF1B subunits as well as to identify known transcripts and proteins and their respective sizes. In addition, the presence of isoforms and related sequences such as pseudogenes was checked since these might complicate future analysis. The degree of homology between subunits at the mRNA and protein level as well as across species was determined. Several expression databases were screened for changes in expression levels of eEF1B subunits in tumours. Protein characteristics such as antigenicity, hydrophobicity, surface accessibility and protein secondary structure were predicted using webtools. In addition, domains, motifs, patterns, transmembranes, peptide signals and post-translational modifications such as putative kinases phosphorylation sites were predicted.

3.2 Results

3.2.1 Related eEF1B subunit sequences

Before doing any in depth bioinformatic and molecular analysis, it is essential to determine if there are any related sequences, as pseudogenes and paralogues (such as the two variants of eEF1A) might complicate further analysis. In order to search for related sequences, the nucleotide sequences of mouse and human eEF1B subunits were obtained from GenBank, at both gene and mRNA levels, and a BLAST search was carried out against the genomic GenBank database. Since most amino acids can be derived from multiple codons, eEF1B subunit protein sequences were also searched against the same database using tBLASTn (Chapter 2 for more details). This type of BLAST search first reverse translates the amino acid sequence into all its possible codon sequences and then searches the nucleotide databases for matching or similar sequences.

All BLAST searches identified the actual gene-coding sequence as the most statistical significant match (100% identity), as expected. No additional genomic locations were found to be similar to the eEF1B subunit gene-coding genes suggesting that each eEF1B subunit is encoded by only one gene and that no duplicated pseudogenes exist. However, several genomic locations were identified as being similar to the mRNA and, if translated *in silico*, showed a similar protein sequence suggesting potential pseudogenes. Figure 3.1 shows the chromosomal location of the gene-coding genes and the pseudogenes in both human and mouse karyotypes. To analyse these pseudogenes further, their sequence was examined for the presence of introns, insertions, deletions, base pairs variations, frame shifts and poly-A tail signal. Each pseudogene sequence was translated *in silico* and the predicted protein sequence was compared to the reference protein sequence by alignment using ClustalW. Furthermore, the pseudogene sequences were compared with ESTs and non-redundant mRNA databases from GenBank to look for mRNA expression using BLASTn as well as comparing the predicted protein sequences of

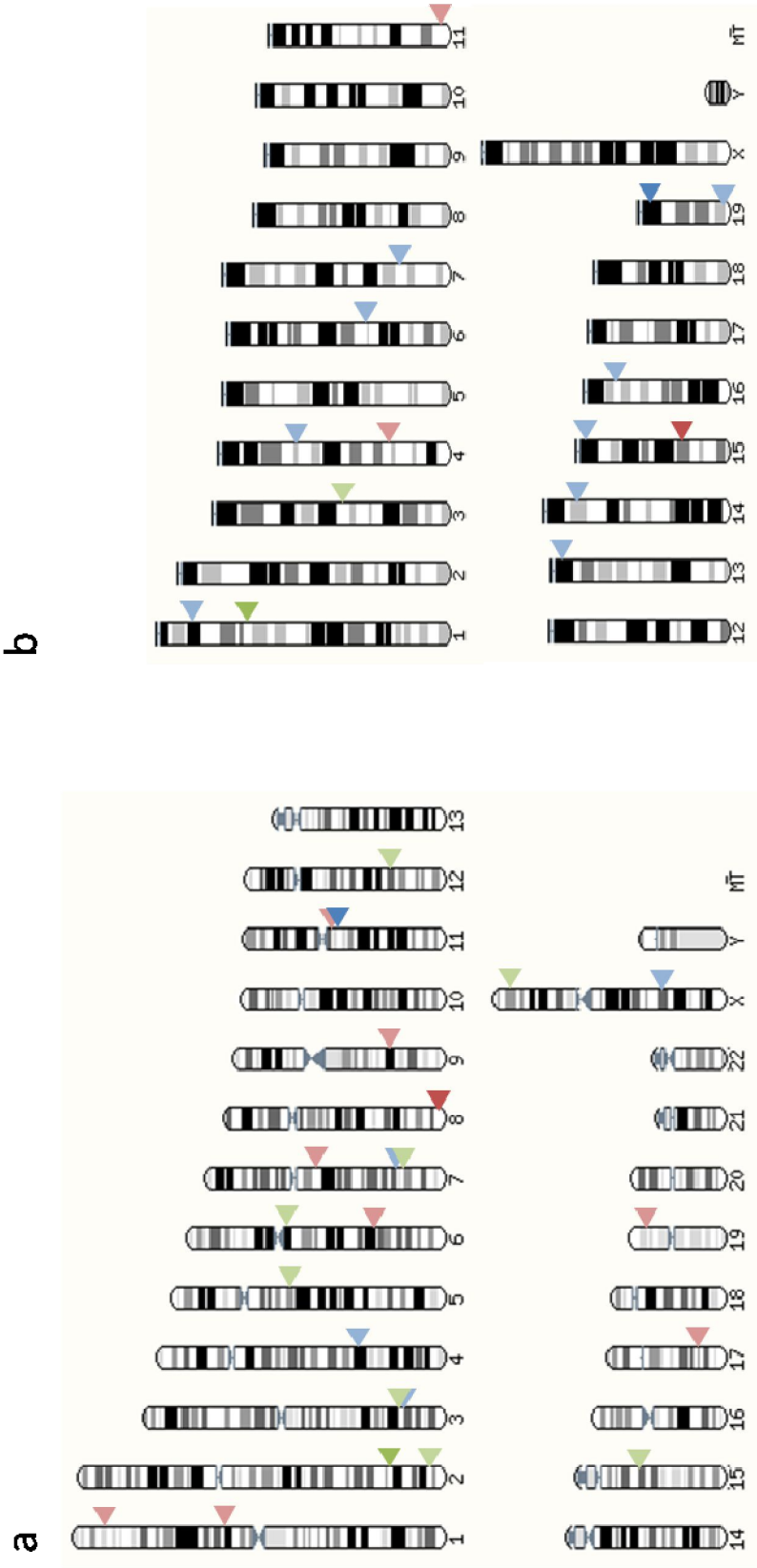


Figure 3.1 Chromosomal location of the genes encoding each eEF1B subunit and pseudogenes. Location in the **(a)** human karyotype and **(b)** mouse karyotype. Image based on karyotype image from Ensembl. Genes and pseudogenes are represented by triangles.

◀ eEF1B α ,
 ◀ eEF1B β ,
 ◀ eEF1B γ ,
 ◀ eEF1B δ pseudogene;
 ◀ eEF1B δ pseudogene;
 ◀ eEF1B δ pseudogene;
 ◀ eEF1B δ pseudogene. Figure adapted from Ensembl.

3. *IN SILICO* CHARACTERISATION OF EEF1B SUBUNITS

the pseudogenes with non-redundant GenBank protein sequence database to identify possible protein expression.

In humans, eight different locations of eEF1B α related sequences were identified on chromosomes 2, 3, 5, 6, 7, 12, 15 and X, whereas, in mice only one pseudogene in chromosome 3 was identified. All of these sequences have some amino acid differences compared with the eEF1B α protein sequence, the majority were intronless and had in-frame stop codons, and one had an inversion. (Appendix 3.1).

The search for eEF1B δ related sequences also retrieved eight different locations on human chromosomes 1, 6, 7, 9, 11, 13, 17 and 19 and three on mouse chromosomes 4, 11 and 15. All of these sequences have some amino acid differences compared with the eEF1B δ protein sequence, and the majority had frame-shifts and were intronless. In addition, several pseudogenes had truncated N- and C-termini (Appendix 3.2).

In humans, the BLAST search for eEF1B γ retrieved four different locations on human chromosomes 3, 4, 7 and X and nine on mouse chromosomes 1, 4, 7, 13, 14, 15, 16, 17 and 19. All of the pseudogenes have a few amino acid differences compared with the eEF1B γ reference protein sequence, just over half have poly-A tail signals, the majority have frame-shifts and in-frame stop codons, and all have a different or absent N-terminus (Appendix 3.3).

None of the eEF1B subunit related sequences showed evidence of expression at either mRNA or protein level. Hence these results suggest that none of the pseudogenes are expressed and functional.

3.2.2 eEF1B δ has an extra exon and more transcript variants

Although each of the eEF1B subunits is encoded by only one gene and no expressed pseudogene has been identified, the existence of transcript variants may also complicate future studies. It is known that eEF1B α in humans has three different spliced variants that only vary on their 5' UTR but that all three transcript variants encode for an identical protein and that eEF1B δ has two isoforms derived from alternative splicing, giving rise to two isoforms with one isoform lacking part of the N-terminus (Chapter 1). Hence, I attempted to address whether there are any other transcript variants that give rise to different previously unknown isoforms.

To answer this question, the mRNA and protein sequences of each eEF1B subunit were submitted to BLASTn search against the expressed sequence tags (ESTs) GenBank database and to BLASTp search against the non-redundant protein GenBank database respectively (Chapter 2 for more details).

Both types of BLAST searches for eEF1B α and eEF1B γ only retrieved the sequences previously known to exist. In contrast, BLAST searches using the eEF1B δ sequence identified several ESTs and non-redundant proteins with different DNA and amino acid sequences. In humans, a BLASTn search with the eEF1B δ mRNA sequence identified several ESTs with a 72bp central deletion. By comparing the deleted sequence with the gene structure information on the genomic human GenBank database for eEF1B δ it was found to be exon 5. A search against the non-redundant protein database also retrieved a protein lacking 24 amino acids (accession number: AAH00678) which was found to correspond to the missing exon 5. In mouse, besides several ESTs with exon 5 missing and the correspondent non-redundant protein BAB30841, there were a couple of ESTs with a further 57bp between exons 5 and 6 which translated into 19 extra amino acids. A non-redundant protein was found to be identical to the mouse eEF1B δ protein sequence with that same extra 19 amino acids (AAH13059).

To investigate further the possible existence of an additional exon leading to transcript variants, several gene structure prediction tools were used (see Chapter 2). All failed to identify the transcript variant without exon 5 and the extra exon

3. *IN SILICO* CHARACTERISATION OF eEF1B SUBUNITS

between exon 5 and 6. For that reason, all mouse eEF1B δ ESTs sequences were retrieved from GenBank (over 55,000) and filtered for 99% similarity to the genomic sequence to exclude poor quality ESTs. The NCBI Spidey tool was used to further align the remaining ESTs (over 3,400) to the eEF1B δ gene sequence. A Perl script was designed to retrieve the ESTs gene structure in a table format (Chapter 2 for more details). All the transcript variants retrieved from high quality ESTs were mapped and this suggested a proposed gene structure with an extra exon (exon 5b) (Figure 3.2).

Is this extra exon only present in mouse tissues? How conserved is the gene structure between human and mouse? Are exons and introns sizes similar between the two species and between the GEF coding exons of eEF1B α and eEF1B δ ?

The sequences of the genes coding for each eEF1B subunit were compared between human and mouse by the multiple sequence alignment tool MUSCLE. The gene structures and the conserved base pairs are represented in figure 3.3. The gene structure between both species is very similar. The human and mouse gene structures of each subunit are shown in Figure 3.3. The DNA sequence encoding the C-terminal GEF domain of eEF1B α and eEF1B δ , from human or mouse, is not particularly conserved (20%) however the eEF1B α mRNA sequence of the GEF coding exons compared with the eEF1B δ nevertheless showed 61% identity. The relatively low sequence identity between both GEF coding region of eEF1B α and eEF1B δ is mainly because although the gene structure and exon sequence is similar, the length of the introns varies considerably.

The region of mouse exon 5b is not conserved in humans and, correspondingly, this extra exon seems not to be present in humans. Another difference between the human and the mouse eEF1B δ gene structure is the presence of a much longer 3' UTR in the mouse sequence, which might affect the mRNA stability.

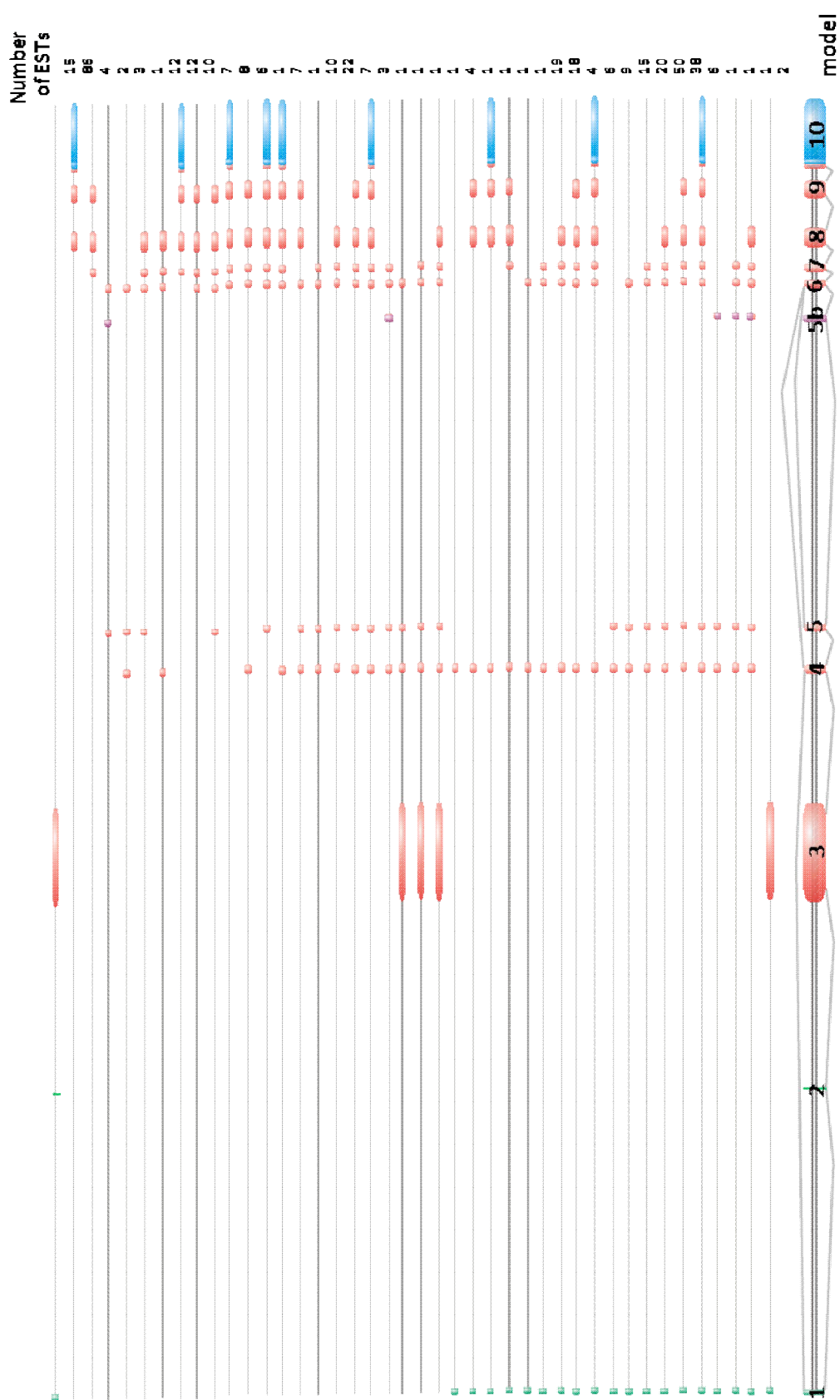


Figure 3.2 eEF1B δ gene structure model extrapolated from mouse ESTs. An exon seems to be present between exons 5 and 6 (exon 5b) in a number of ESTs. Different splice variants can be inferred from the ESTs data. Exons are represented by rectangles: green are 5'UTR exons, red are coding exons, blue are 3'UTR exons and purple the extra exon 5b.

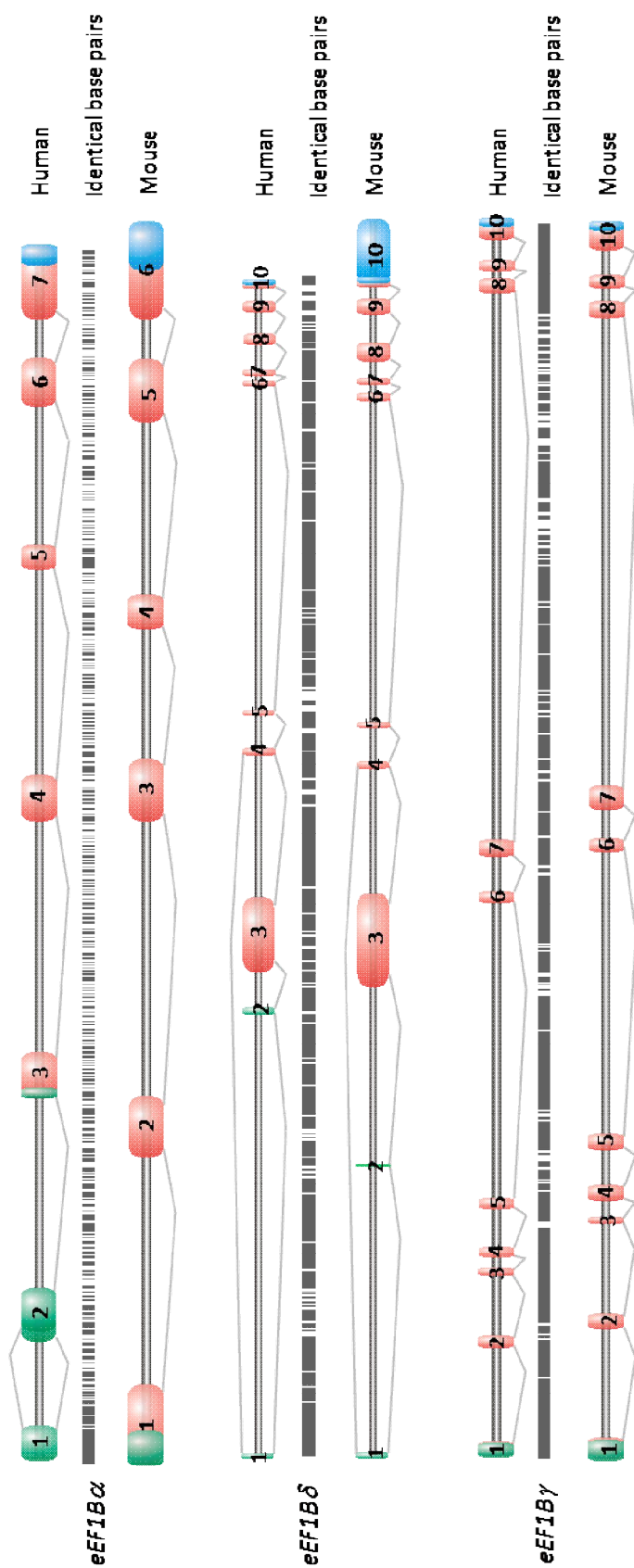


Figure 3.3 Mouse and human gene structure of each eEF1B subunit and identical base pairs between both species. Exons are represented by numbered rectangles: green are 5'UTR exons, red are coding exons, and blue are 3'UTR exons. Identical base pairs between human and mouse gene sequences are shown in black (not to scale).

3.2.3 Expression at mRNA level

ESTs and SAGE profiles can be clustered by the tissue source from which they originate, giving an idea of where any gene is expressed. Data from the EST profiles from NCBI and SAGE data from CGAP were therefore analysed for the expression of eEF1B subunits (Chapter 2 for more details). In addition, the SAGE data from CGAP also gives information on expression in different forms of cancer.

eEF1B α was found to be widely expressed, with kidney and colon showing a lower levels of expression as judged by the number of total ESTs. eEF1B α mRNA was found to be up-regulated in brain, eye, thyroid, stomach, kidney, colon, peritoneum and muscle cancerous tissues when compared to non-cancerous tissues. The data available for eEF1B δ in CGAP was obtained from only a few ESTs and is far from comprehensive, but the data from NCBI showed wide spread expression. eEF1B γ was also found to be widely expressed and to be more highly expressed in brain, eye, thyroid, lung, kidney, colon, peritoneum, prostate and bone marrow cancer compared to non cancerous tissues.

Since there was evidence of multiple transcript variants for eEF1B δ and to further explore the ESTs expression data available in the GenBank database on eEF1B δ , all the GenBank data from each EST was collected and another Perl script was designed to, once again, simplify the output into a table format that lists sequence length, sex, developmental stage, mouse strain, tissue and the actual sequence (for more details see chapter 2). No difference in gene structure was found between males and females, or between different mice strains or developmental stages but particular exons seemed to be more highly expressed in particular tissues than others. ESTs containing exons 2 and 3, corresponding to transcript variant a (isoform a), were all from mouse normal brain, eye, testis tissues and mammary carcinoma while all the ESTs missing exons 2 and 3 were from a variety of tissues.

No apparent correlation was found between eEF1B subunits or eEF1A1 and eEF1A2. Carefull interpretation of these results is required since ESTs and SAGE data in CGAP database were not experimentally validated and hence only reflect a crude measure of ESTs expression in normal versus cancer tissues.

3.2.4 Regulation at the transcription level

The presence of multiple transcript variants of both eEF1B α and eEF1B δ , and the tissue restricted expression of a putative transcript variant are indicative of gene expression regulation. To gain insight into how a gene is regulated it is important first to predict the location of the promoter region and then to search for potential regulatory elements preferably in regions conserved between mouse and human. Several databases and prediction tools were used to define the location of the promoter region (Chapter 2). This putative promoter sequence was then analysed against the transcription factors database TRANSFAC at a highly restrictive threshold to reduce false positives (chapter 2 for more details).

All the promoter and CpG island predictions for eEF1B α overlapped with the non-coding exons 1 and 2 and extended up to 508bp upstream of the gene. One promoter prediction tool, FirstEF, failed to predict a promoter region. Several transcription factors binding sites were predicted with maximum score and these are known to be involved in cell cycle and cell growth (ATF, STAT and CREB), immune response (NF κ B, c-Rel, XBP-1 and IRF-1) and stress (ATF, NF-E2, XBP-1 and NRF-2) (Figure 3.4).

Two promoter prediction tools predicted an eEF1B δ promoter overlapping the first non-coding exon with over 200bp to either side to the exon. Ensembl and the CpG island prediction tool predicted a much longer promoter from -485bp downstream up to +1324bp upstream of the gene. Several transcription factors binding sites were predicted with maximum score and these are known to be involved in cell cycle and cell growth (ATF, CREB, STAT, E47, Pbx1b and YY1), immune response (NF κ B, XBP-1, E47, Olf-1, Pbx1b and c-Rel), stress (AhR:Arnt, ATF, NF-E2, XBP-1 and NRF-2) and muscle specific (E47 and YY1) (Figure 3.5).

All the promoter prediction tools for eEF1B γ predicted a long promoter overlapping with the first and second non-coding exons and extending up to 2487bp upstream of the gene. One promoter prediction tool, FirstEF, failed to

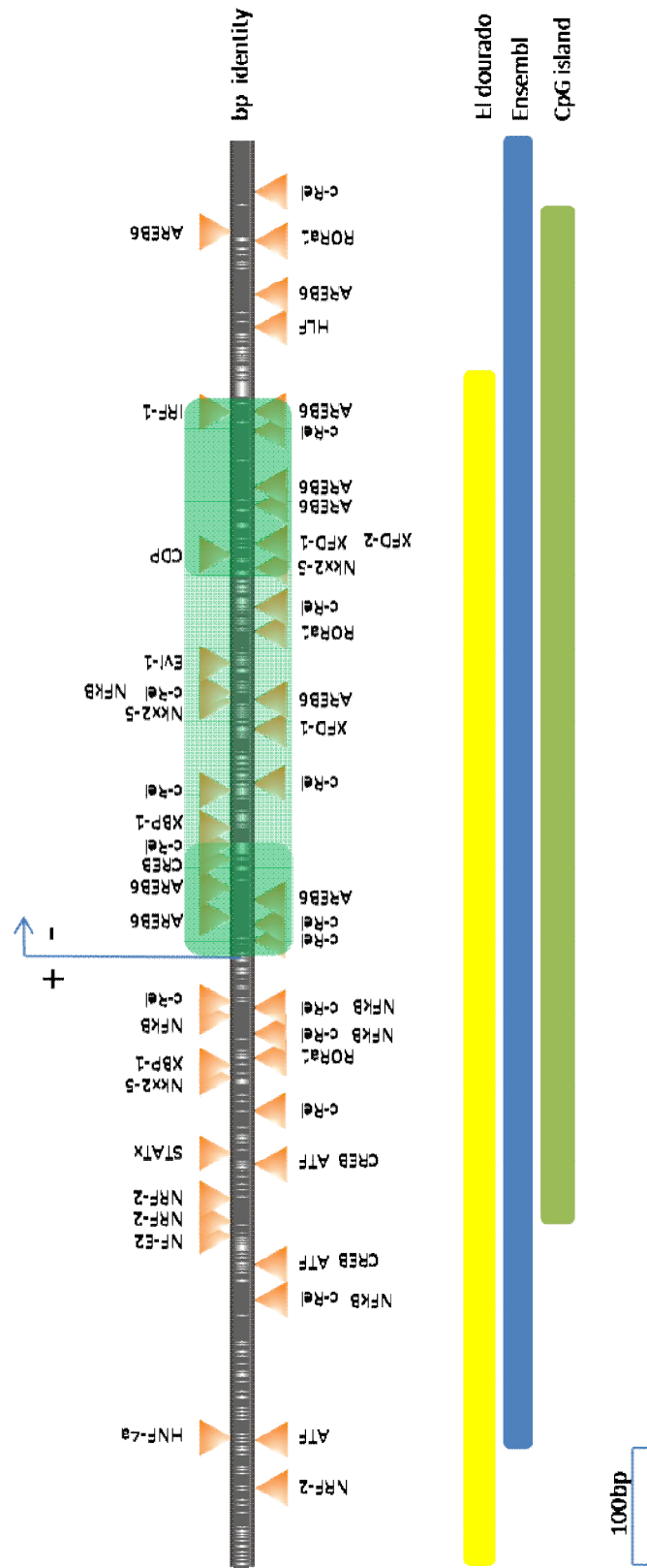


Figure 3.4 Putative promoter region and regulatory sites prediction for human eEF1B α . The databases and prediction tools listed were used to identify a putative promoter region, indicated by different colours. Regulatory sites and respective transcription factors represented were predicted as top scores by P-match weight based search on the TRANSFAC database. Identical base pairs between human and mouse sequences are shown in black. The first exon is shaded green and the arrow indicates the beginning of the gene.

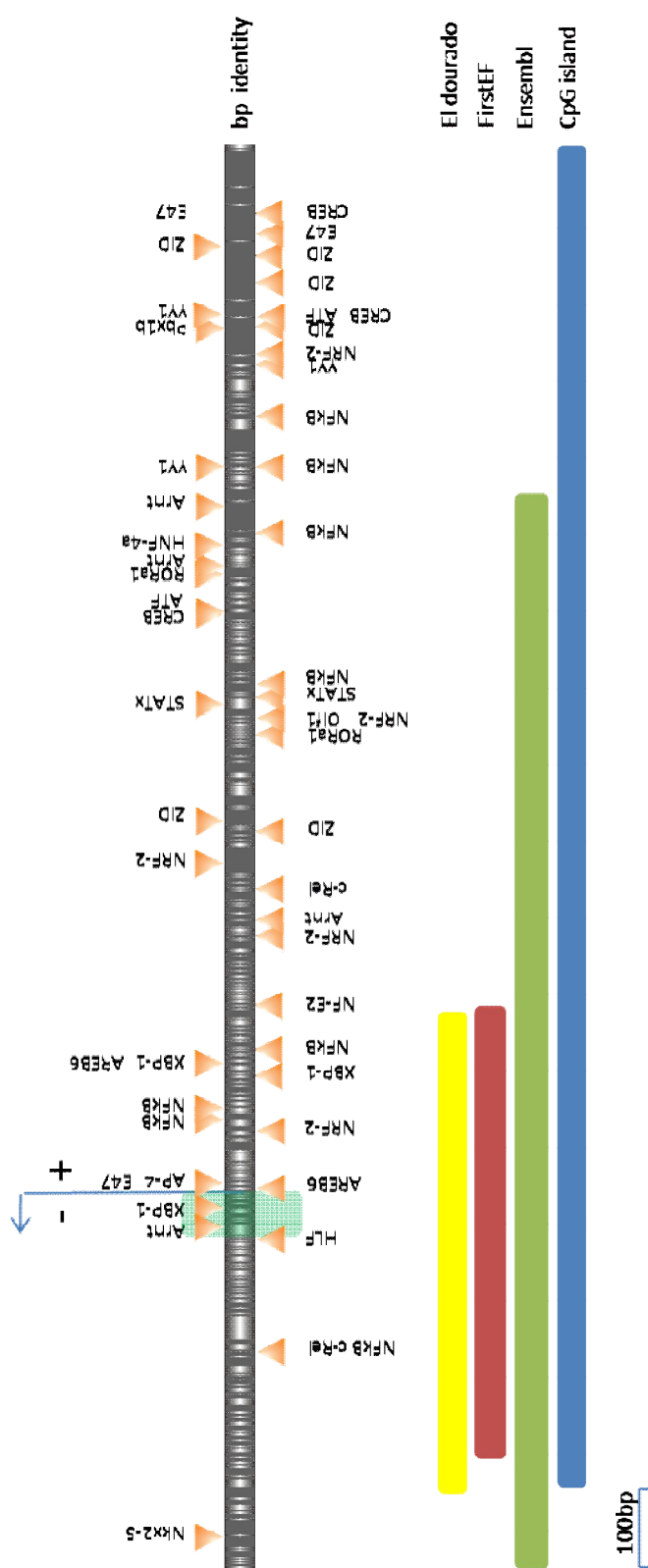


Figure 3.5 Putative promoter region and regulatory sites prediction for human eEF1Bδ. The databases and prediction tools listed were used to identify a putative promoter region, indicated by different colours. Regulatory sites and respective transcription factors represented were predicted as top scores by P-match weight based search on the TRANSFAC database. Identical base pairs between human and mouse sequences are shown in black. The first exon is shaded green and the arrow indicates the beginning of the gene.

3. *IN SILICO* CHARACTERISATION OF EEF1B SUBUNITS

predict a promoter region. The CpG island prediction only overlapped with exon 1 and extended up to 916bp upstream of the gene. Note that the predicted promoter region is not conserved between human and mouse from 1000bp upstream of the gene. Several transcription factor binding sites were predicted with maximum score and these are known to be involved in cell cycle and cell growth (ATF, CREB, STAT, Elk-1, Hox-1.3, RREB and YY1), immune response (NFkB, c-Rel, XBP-1, E47, BSAP and IRF-1), stress (ATF, NF-E2, XBP-1, E47, Elk-1, RREB and NRF-2) and muscle expressed (E47 and YY1) (Figure 3.6).

There are also regulatory motifs embedded in mRNA such as 5' and 3' UTRs, splice sites and miRNA target sites. To search for putative regulatory elements in the UTR region, the 5' and 3' UTR human and mouse sequences of each eEF1B subunit coding gene were analysed by UTRscan tool (Chapter 2). The human and mouse mRNA sequence of each eEF1B was also analysed by the RegRNA tool for further prediction of regulatory elements and prediction of miRNA target sites by microCOSM (Chapter 2).

The UTRscan did not find any regulatory motif in any of the eEF1B subunits 5' and 3' UTRs. RegRNA tool however predicted 5' terminal oligopyrimidine (5'TOP) sequences in all three subunits. Several miRNAs target sites were predicted by microCOSM but none has a known function (Appendix 5).

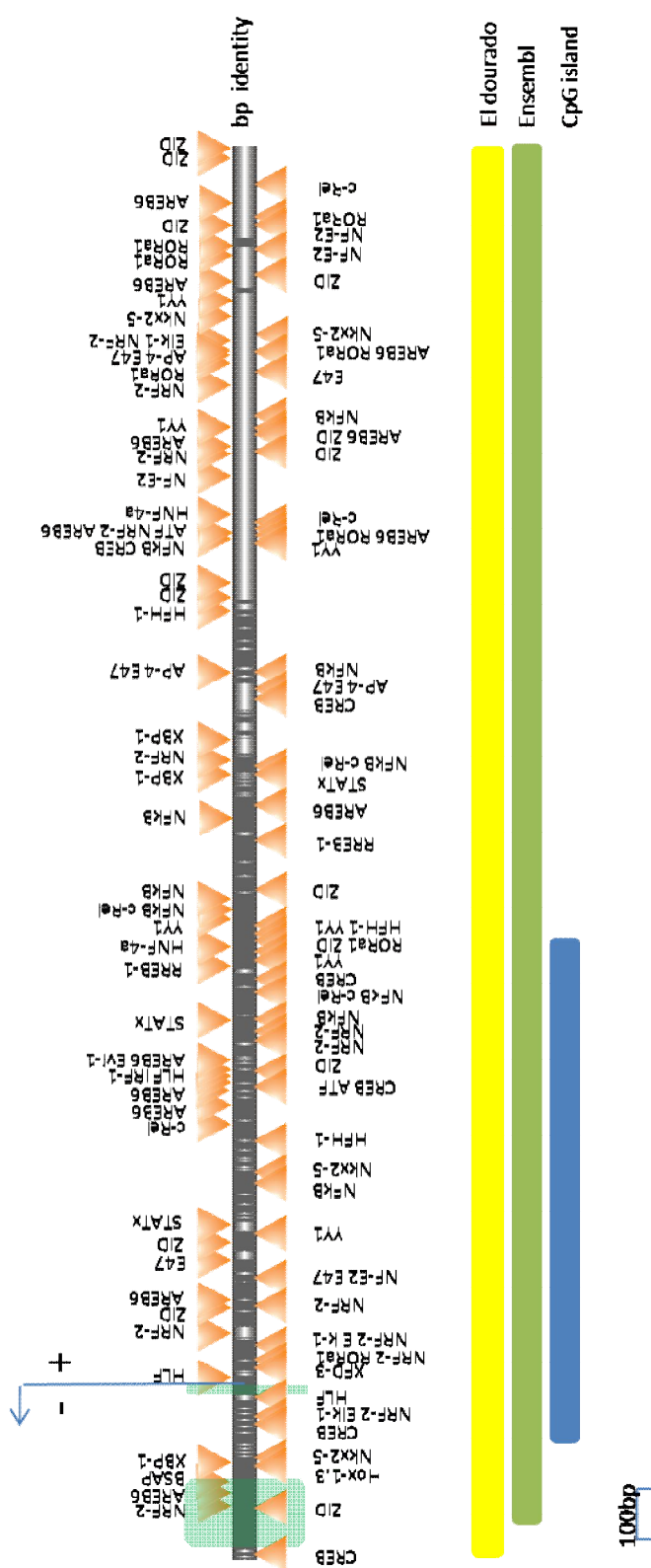


Figure 3.6 Putative promoter region and regulatory sites prediction for human *eEF1B*. The databases and prediction tools listed were used to identify a putative promoter region, indicated by different colours. Regulatory sites and respective transcription factors represented were predicted as top scores by P-match weight based search on the TRANSFAC database. Identical base pairs between human and mouse sequences are shown in black. The first exon is shaded green and the arrow indicates the beginning of the gene.

3.2.5 Comparison between subunits

Cataloguing characteristics at the gene and mRNA level are important but at the protein level it is essential to further understand the biology. It is essential to determine how similar / identical the subunits are to each other and how conserved the several eEF1B δ protein isoforms are. This was achieved by producing multiple sequence alignments using ClustalW with the eEF1B subunits protein sequences as the input (Chapter 2 for more details).

eEF1B subunits have no similarity to eEF1A variants. However between the eEF1B subunits, eEF1B α shows some homology at the C-terminal with eEF1B δ with around 50% identity (table 3.1). The eEF1A interaction with eEF1B α has been mapped previously and on Figure 3.7 can be seen that two of those interacting residues are different in the eEF1B δ C-terminus. In contrast, eEF1B γ showed no similarity with any of the subunits.

Table 3.1 Percentage of identity between the human eEF1B subunits

	eEF1B α	eEF1B δ iso a	eEF1B δ iso b	eEF1B δ iso c	eEF1B γ
eEF1B α	X	56	52	51	7
eEF1B δ iso a		X	100	85	5
eEF1B δ iso b			X	91	6
eEF1B δ iso c				X	6
eEF1B γ					X

Figure 3.8 shows a multiple sequence alignment of all the mouse eEF1B δ putative isoforms, where isoform a and b are present in databases and all the others were derived from translating *in silico* the ESTs.

3.2.6 Protein homologues

Since eEF1B α and eEF1B δ show homology at the C-terminus whilst eEF1B γ has no resemblance to any of the eEF1B subunits, it is interesting to investigate in which eukaryotic species are the eEF1B subunits present and how evolutionary conserved they are throughout species?

To answer these questions, BLASTp was used to search GenBank protein and UniProt databases to determine the protein sequence of each eEF1B subunit from a variety of species. Then, the protein sequences were compared by using the ClustalW tool.

eEF1B α homologues are found in unicellular eukaryotes up to humans. Appendix 6.1 shows a table with all eEF1B α eukaryotic homologues. Their protein sequence is conserved, mainly the C-termini. eEF1B α protein sequences were found to have a percentage identity between 36% (*Trypanosoma cruzi* and humans) and 98% (human and rabbit). Figure 3.9 shows a protein sequence alignment from representative species.

However, eEF1B δ was found to be absent from protozoa, fungi and worms. It has homologues in sea urchins, insects, frogs, fish and mammals (Appendix 6.2). More than one eEF1B δ protein was found in sea urchin, *Xenopus laevis* and *Brachydanio rerio*. The two eEF1B δ copies are similar to the human and mice isoforms b and c. All the homologous sequences were found to be at least 29% identical (sea urchin compared to the human protein sequence) (Figure 3.10). The C-terminus was found to be highly conserved amongst species. Interestingly, several species had the longer isoform (isoform a) of eEF1B δ , previously only described in human and mouse (Figure 3.11). A tBLASTn search against ESTs from eukaryotes (except human and mouse – previously described) showed all ESTs to be from testis and brain, except ESTs extracted from cows where some were found in liver. This might indicate possible tissue-specific expression but careful analysis is required since it might be restricted to the ESTs library availability.

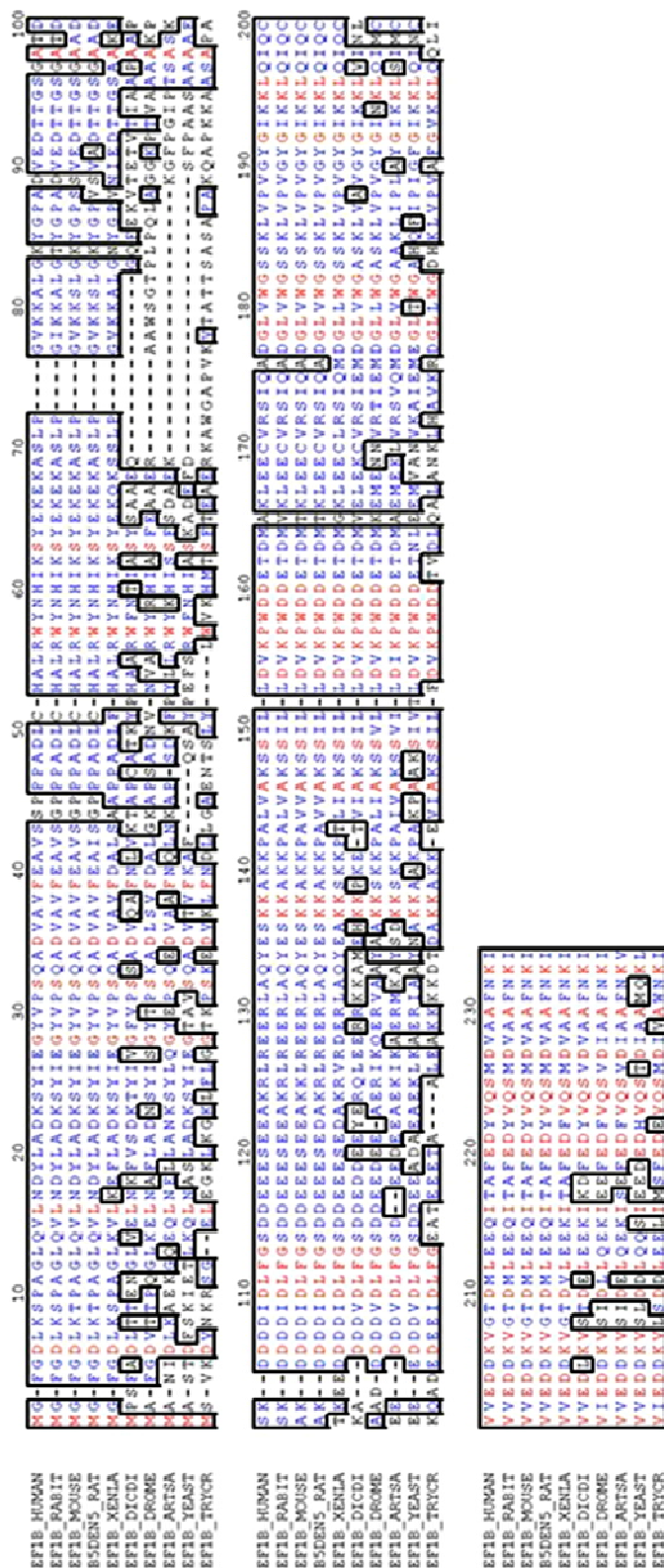


Figure 3.9 Multiple eEF1B α protein sequence alignment from 10 different eukaryotic species. The C-terminus of eEF1B α is very conserved across species. There are 48 invariant residues in this alignment highlighted in red. Highlighted in blue are the residues with less than 50% variance across species. Sequence identifiers are the proteins UNIPROT ID. EF1B - eEF1B α

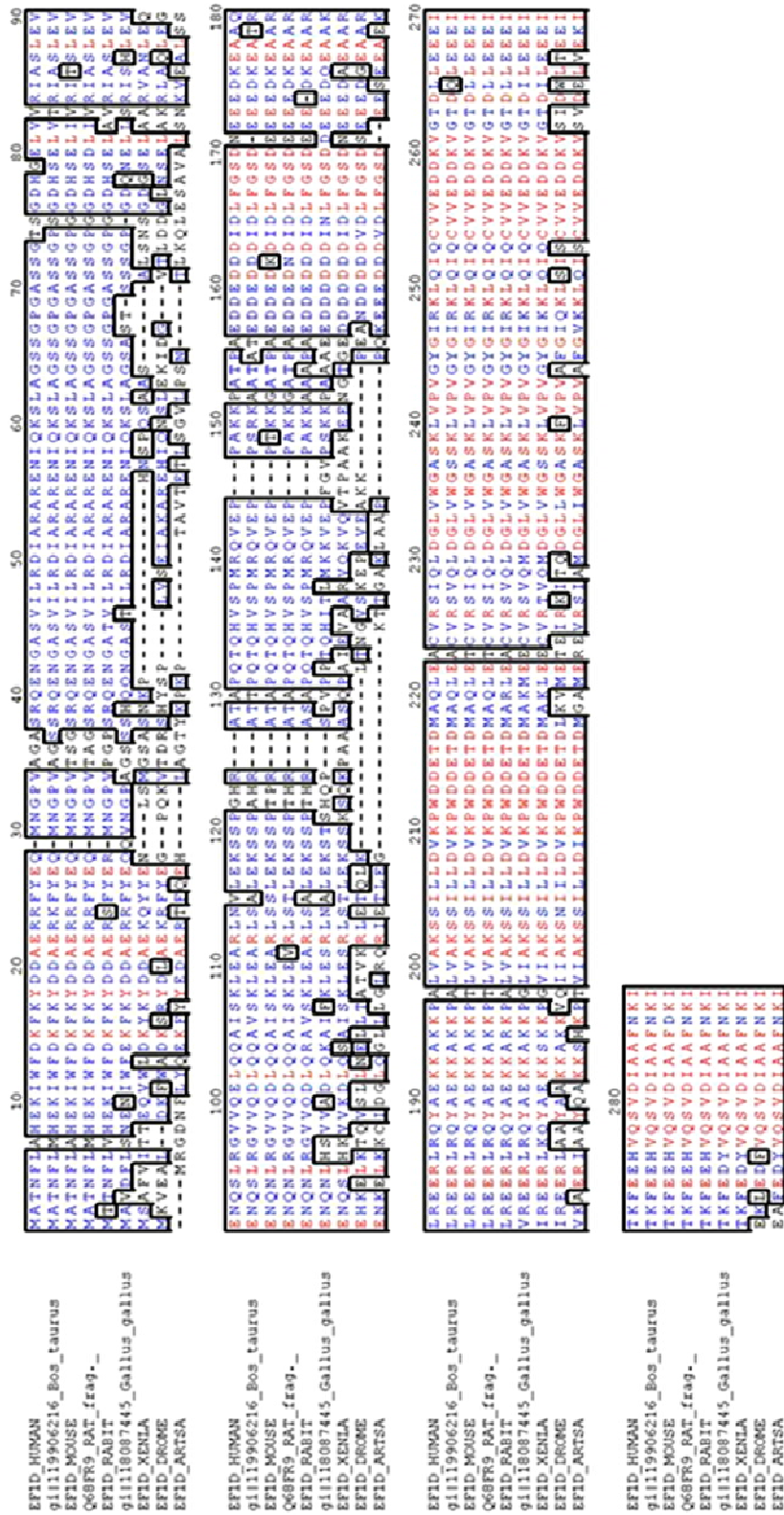


Figure 3.10 Multiple sequence alignment of eEF1B δ isoform b from 9 different eukaryotic species. The C-terminus of eEF1B δ is very conserved across species. There are 82 invariant residues in this alignment highlighted in red. Highlighted in blue are the residues with less than 50% variance across species. Sequence identifiers are the proteins UNIPROT ID. EF1D – eEF1B δ

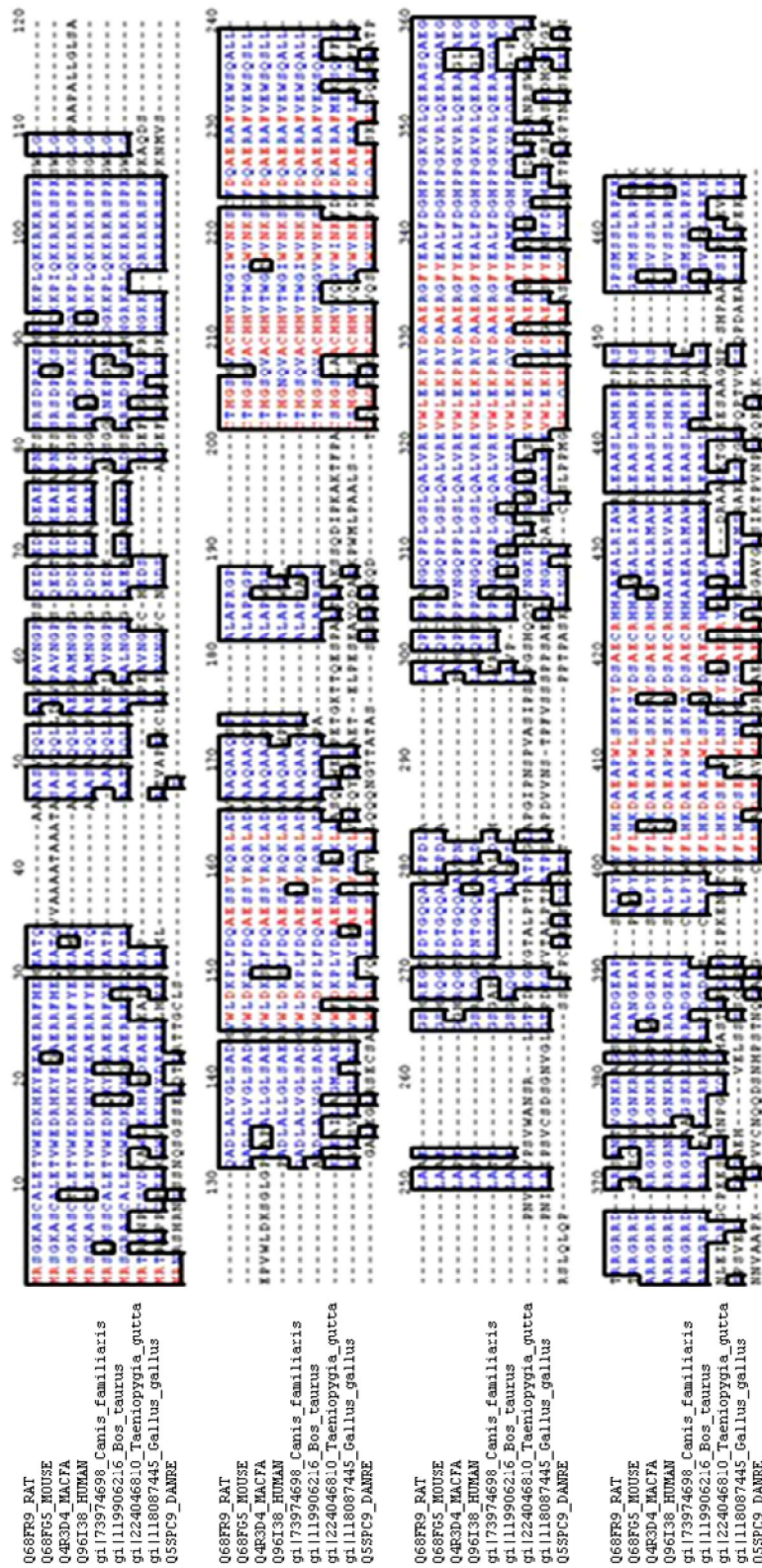


Figure 3.11 Multiple sequence alignment of eEF1Bδ isoform a N-terminus from 9 different eukaryotic species. The N-termini of eEF1Bδ isoform a are variable across species with the exception of 42 invariant residues in this alignment highlighted in red. Highlighted in blue are the residues with less than 50% variance across species. Sequence identifiers are the proteins UNIPROT ID. EF1D – eEF1Bδ

3. *IN SILICO* CHARACTERISATION OF EEF1B SUBUNITS

In plants, particularly *Arabidopsis thaliana* and rice plant *Oriza sativa* there are 4 proteins similar to both eEF1B α and eEF1B δ which can be grouped into two groups. These have been named as eEF1B α and eEF1Bb (Appendix 6.3). All the 4 proteins are equally identical (41-44%) to both human eEF1B α and eEF1B δ .

eEF1B γ was found to have homologues ranging from protozoa up to human (Appendix 6.4). Yeast *Saccharomyces cerevisiae* has two eEF1B γ homologues, as does the plant *Arabidopsis thaliana*. The rice plant *Oryza sativa* has three eEF1B γ proteins. By performing multiple sequence alignment using ClustalW, all the homologous sequences were found to have a percentage of identity above 28% (protozoa compared to human) (Figure 3.12).

As the cross species conservation for the eEF1B subunits has been determined, it is of interest to search for similar protein motifs.

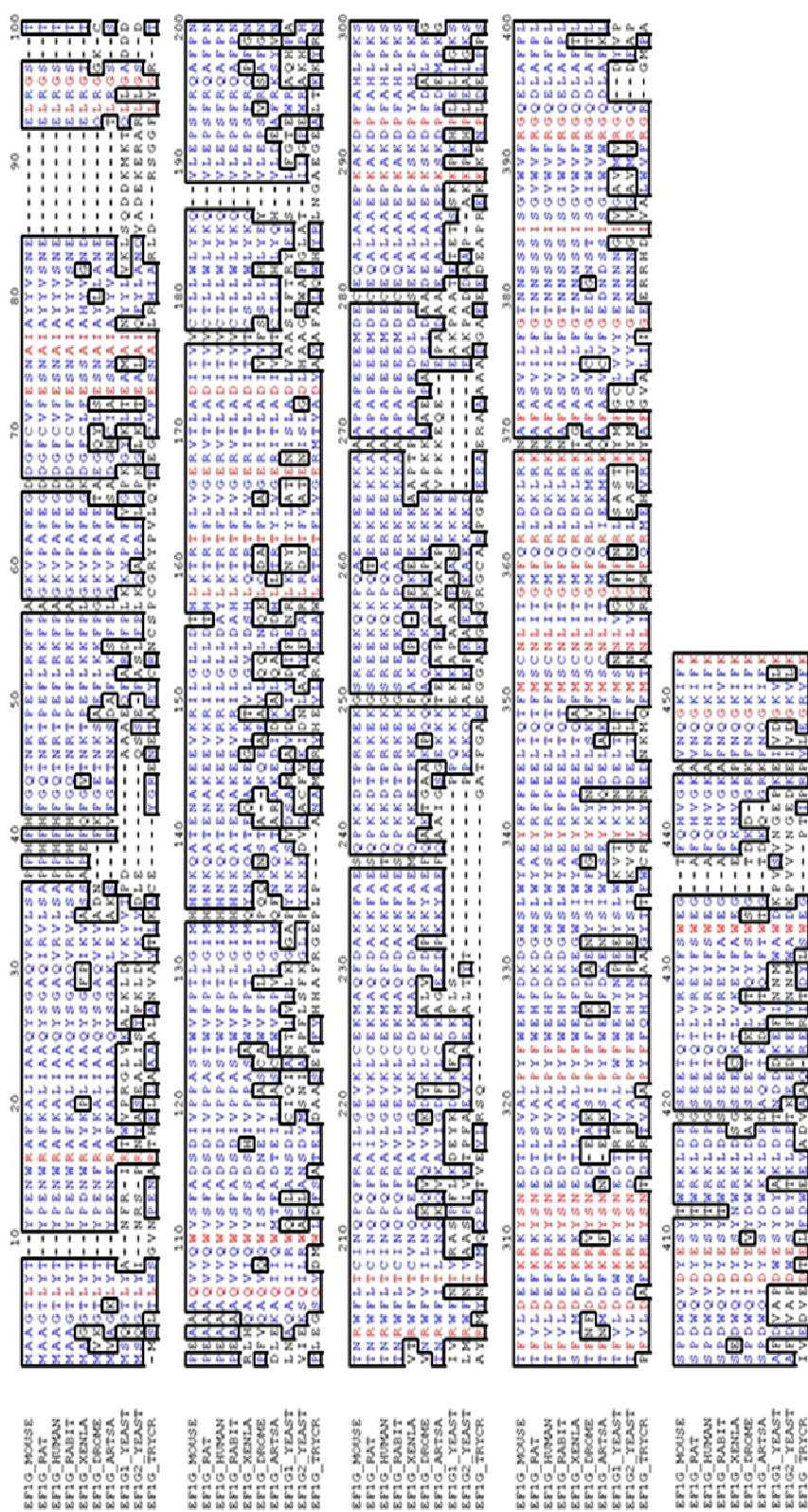


Figure 3.12 Multiple eEF1By protein sequence alignment from 10 different eukaryotic species. There are 44 invariant residues in this alignment highlighted in red. Highlighted in blue are the residues with less than 50% variance across species. Sequence identifiers are the proteins UNIPROT ID. EFIG - eEF1By

3.2.7 Similar proteins to eEF1B subunits and domains

Similar proteins/protein regions and domains provide valuable information indicating possible large regions and architectures that have the same or similar function. The eEF1B subunits protein sequences were compared to other proteins by BLASTp and PSI-BLAST to search for distantly related proteins. The eEF1B subunits protein sequences were also compared against Pfam domain database and InterPro integrated domains and patterns database.

No similar proteins were retrieved by BLASTp or PSI-BLAST search. However, comparison against domains showed several known domains and one unknown domain (Figure 3.13).

eEF1B α belongs to the InterPro family Eukaryotic translation elongation factor 1, beta/beta'/delta chain (IPR 001326) and Pfam family EF1_GNE (PF00736) between amino acids 138-224, as well as Pfam EF1_beta_acid (PF10587) between residues 103 and 130. It was also identified as belonging to the GST C-terminal-like SUPERFAMILY SSF47616 (IPR010987) between 8 and 69. eEF1B δ isoforms were found to belong to the InterPro family Eukaryotic translation elongation factor 1 beta/beta'/delta chain and to Pfam family EF1_GNE, as well as Pfam EF1_beta_acid (PF10587). A ZIP protein domain was found to be similar to eEF1B δ between residues 79 and 113 but did not reach a significant level. No domain was found to be similar to the N-terminus of eEF1B δ . Besides the eukaryotic translation elongation factor 1 gamma chain domain from both InterPro (IPR001662) and Pfam domain (PF00647) between 274 and 380, eEF1B γ also belongs to InterPro families Glutathione S-transferase N (IPR004045) and C terminal (IPR004046) from 3 to 80 and from 92 to 197 respectively. These domains are conserved throughout species. The only exception is eEF1B α and eEF1B β in plants. eEF1B α in plants lacks the EF1_beta_acid domain but has the GST C-terminal domain whereas eEF1B β in plants does not have the any other domains except the GEF domain and the EF1_beta_acid domain. Summary table as appendix 7.

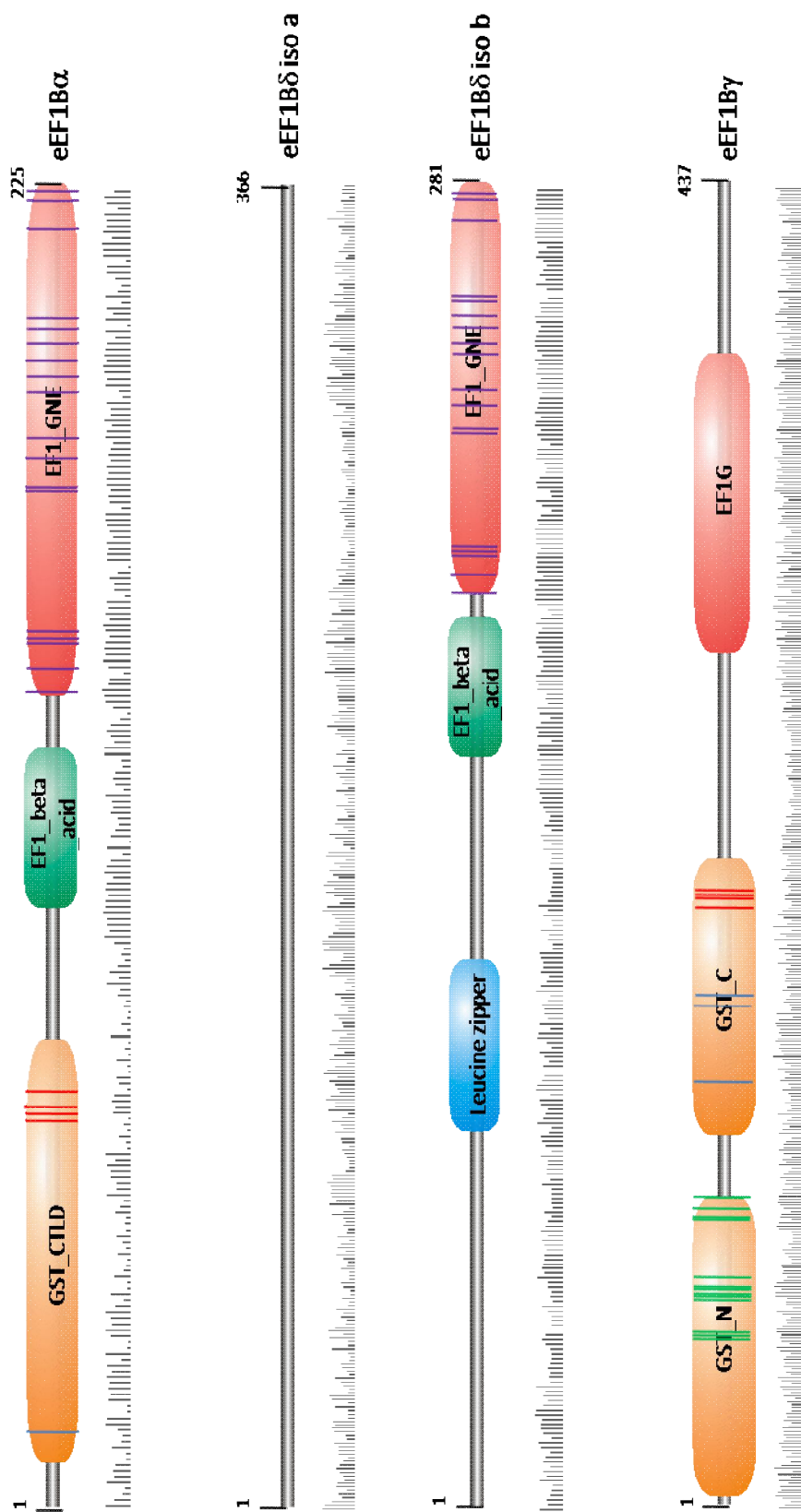


Figure 3.13 eEF1B subunit domain prediction, amino acid sequence variation and known functional residues. Domains were predicted by InterPro and Pfam. Domains are represented by rectangles where the translation elongation domain is in red (EF1_GNE – eEF1A guanine exchange activity; EF1G – eEF1By domain), GST-like domains in orange (GST_C – GST C-terminal domain; GST_N – GST N-terminal domain) and other domains/motifs in green (EF1 – eEF1B domain). Amino acid variation was calculated from multiple sequence alignments where the higher the bar is, the more conserved is the amino acid at that location. Residues with a known function, obtained from the domain information, are represented by a bar across the domains: blue for involvement in GST dimer formation, red for GST N-terminal interaction, green for GST C-terminal interaction and purple for eEF1A interaction.

3.2.8 Secondary structure and other structural features

Not much information is known about the structural features of the eEF1B subunits. Only the translation catalytic domains structures have been solved. PHD from Predict Protein and Jpred tools were used to predict the secondary structure (Chapter 2 for more details). Other structural features such as di-sulphide bonds, low complexity regions, protein disorder, transmembrane domains, amino acid properties and residue accessibility were also predicted using a variety of tools explained in chapter 2 and compared taking into consideration the conservation of the residues.

eEF1B α secondary structure was predicted to be mainly loops (48 %), with 12% β -sheets and 40% α -helices. About 70% of the amino acids were predicted to be exposed particularly a stretch of amino acids in the centre of the eEF1B α protein which includes the small eEF1B beta_acid domain and a small region of the GST C-terminus like domain. This same region was classified as a low complexity region with almost all disordered regions sitting on the exposed area. The conservation of this large exposed region is poor on the N-terminus but extremely high on the C-terminus indicating a possible conserved GEF function (Figure 3.14).

The N-terminus of eEF1B δ isoform a was predicted to be mainly loops (63.4%). It was predicted to have an extremely high number of exposed residues (64%). Three repeats, similar to the residues on the N-terminus of other isoforms, were found scattered around the protein N-terminus which corresponded to highly conserved regions indicating a potential function. Several low complexity regions and disordered regions were predicted, in addition to two di-sulphide bonds spanning almost the entire N-terminus of the eEF1B δ isoform a (Figure 3.15).

The C-terminus of eEF1B δ isoform a, which is similar to the full length isoforms b and c and the putative isoforms d and e, has a secondary structure that was predicted to be mainly loops (around 46%) and α -helices (around 45%) for all the isoforms. All the isoforms were predicted to have greater than 60% exposed

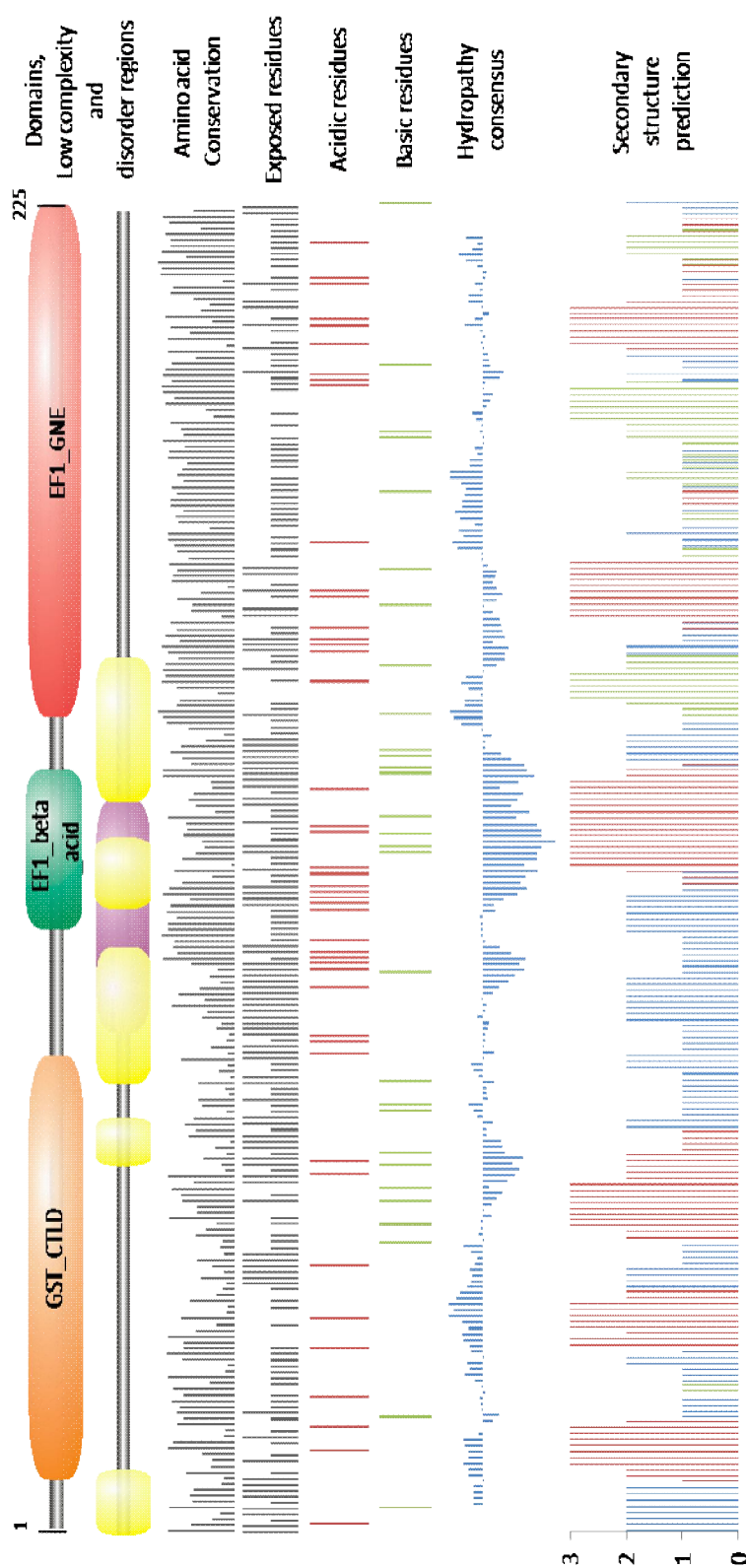


Figure 3.14 eEF1B α structural features and secondary structure prediction. Domains are represented by rectangles where the translation elongation domain is in red (EF1_GNE – eEF1A guanine exchange activity), GST-like domains in orange (GST_CTD – GST C-terminal domain) and other domains /motifs in green (EF1 – eEF1B domain). Disordered regions, represented by yellow rectangles, were predicted by DisEMBL and low complexity regions, represented by purple rectangles, were predicted using the SEG tool. Amino acid variation was calculated from multiple sequence alignments where the higher the bar is, the more conserved is the amino acid at that location. Exposed residues were predicted by Prof_acc, where highly exposed residues are indicated by the highest bar, putatively exposed are indicated by the shortest bar at that location and buried residues are not represented. Amino acid properties such as acidic (red) and basic (green) were calculated using the PepInfo tool. Hydropathy consensus plot was obtained from PepInfo tool. Secondary structure prediction plot was derived from the consensus of PISPRED, PROF (PredictProtein) and Jpred. The plot indicates by how many of these tools, a particular secondary structure was predicted at that location.

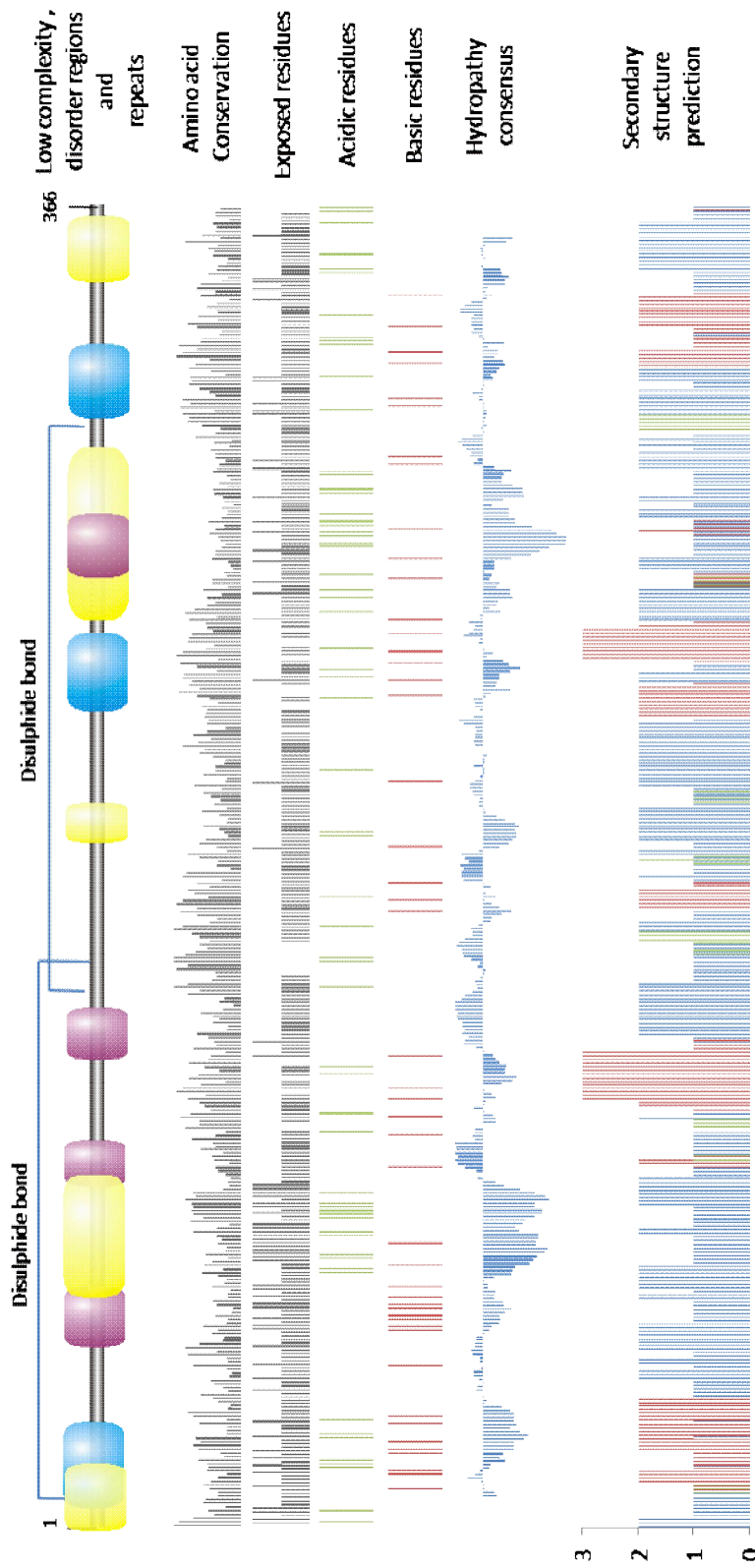


Figure 3.15 eEF1B δ isoform a N-terminus structural features and secondary structure prediction. Disordered regions, represented by yellow rectangles, were predicted by DisEMBL. Low complexity regions, represented by purple rectangles, were predicted using the SEG tool. Disulphide bonds were predicted by Disulfind. Repeats, represented by blue rectangles, were predicted by RPT tool. Amino acid variation was calculated from multiple sequence alignments where the higher the bar is, the more conserved is the amino acid at that location. Exposed residues were predicted by Prof_acc, where highly exposed residues are indicated by the highest bar, putatively exposed are indicated by the shortest bar at that location and buried residues are not represented. Amino acid properties such as acidic (red) and basic (green) were calculated using the Pepinfo tool. Hydropathy consensus plot was obtained from Pepinfo tool. Secondary structure prediction plot was derived from the consensus of PSPRED, PROF (PredictProtein) and Jpred. The plot indicates by how many of these tools, a particular secondary structure was predicted at that location. Red indicates alpha-helices, green indicated beta-sheets and blue indicates loops.

3. IN SILICO CHARACTERISATION OF EEF1B SUBUNITS

amino acids and the centre of the protein had once again a stretch of exposed residues which are conserved and may have a potential function. In this exposed region several disordered regions were predicted, as well as a low complexity region and a coiled-coiled region. The coiled-coiled region corresponded to the EF1_beta_acid domain in eEF1B δ but was not predicted to be coiled-coiled in the same domain present on eEF1B α . In addition, other low complexity regions and disordered regions were predicted, as well as a leucine zipper region. None of the isoform specific regions were predicted to have any structural feature (Figure 3.16).

The secondary structure for eEF1B γ was predicted to be mainly loops (48%), with 41 % α -helices and 11% β -sheets. Just over half of the amino acids (53%) were predicted to be exposed. The region between the EF1G domain and the GST domain was predicted to have two disordered regions and a low complexity region which lie on the less conserved and highly exposed area of the eEF1B γ protein. A small conserved disordered region on the exposed C-terminal tail was predicted as well as another small highly conserved disordered region on the GST C-terminal domain. This latter disordered region is lying adjacent to a predicted buried transmembrane region, and another transmembrane region was predicted in the EF1G domain by one of the two predicting tools (Figure 3.17). eEF1B subunits structural features summary table is shown in appendix 8.

The prediction of secondary structure and structural features provides valuable information on possible structurally conserved regions which may have a particular function, with disordered regions often found to be the site for protein-protein interactions and post-translational modifications (reviewed in Russel and Gibson, 2008).

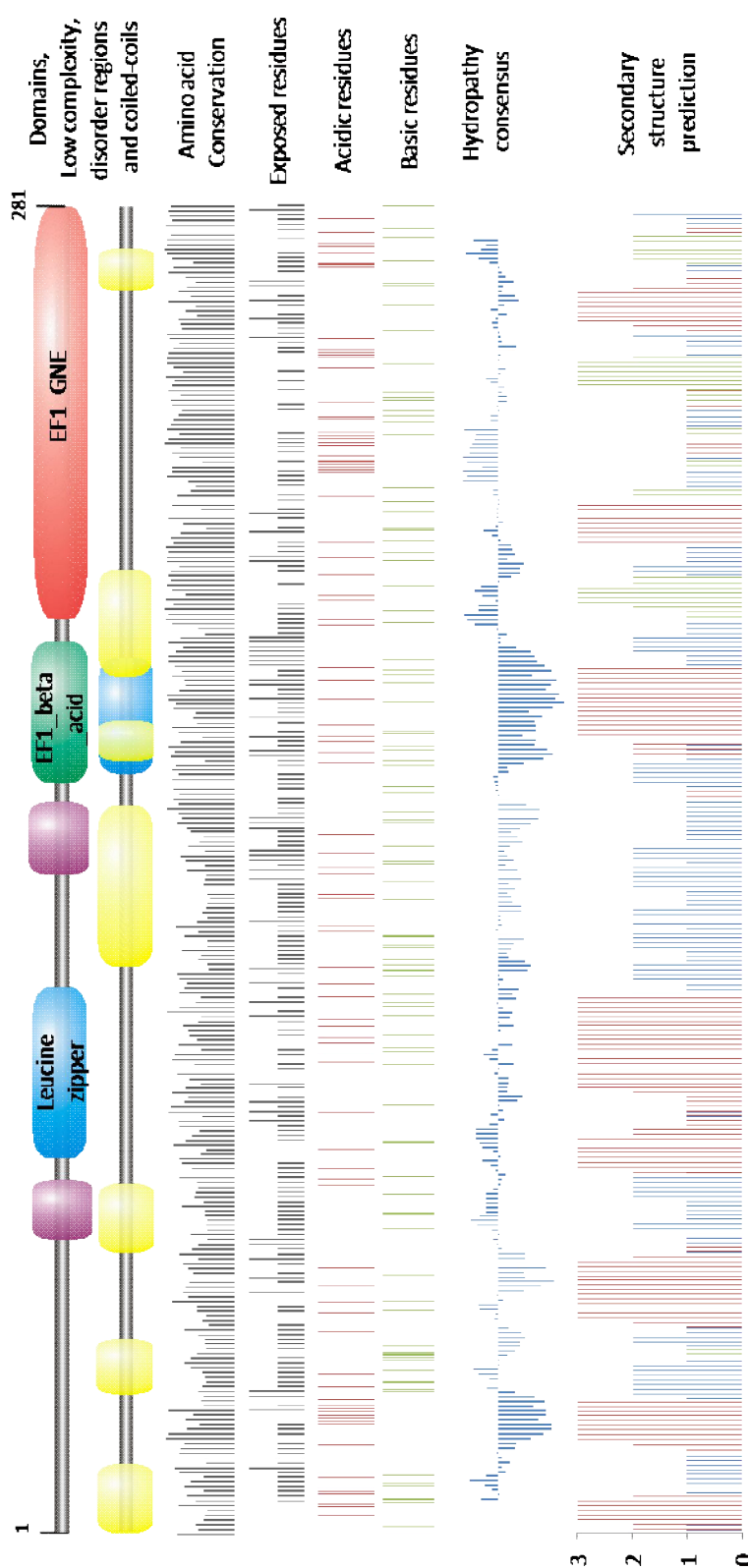


Figure 3.16 eEF1B δ isoform b structural features and secondary structure prediction. Domains represented by rectangles where the translation elongation domain is in red (EF1_GNE – eEF1A guanine exchange activity) and other domains /motifs in green (EF1 – eEF1B domain). Disordered regions, represented by yellow rectangles, were predicted by DisEMBL, low complexity regions, represented by purple rectangles, were predicted using the SEG tool, and coiled-coils regions, represented by blue rectangles, were predicted by Coils tool. Amino acid variation was calculated from multiple sequence alignments where the higher the bar is, the more conserved is the amino acid at that location. Exposed residues were predicted by Prof_acc, where highly exposed residues are indicated by the highest bar, putatively exposed are indicated by the shortest bar at that location and buried residues are not represented. Amino acid properties such as acidic (red) and basic (green) were calculated from Pepinfo tool. Hydropathy consensus plot was obtained using the Pepinfo tool. Secondary structure prediction plot was derived from the consensus of PSIPRED, PROF (PredictProtein) and Jpred. The plot indicates by how many of these tools, a particular secondary structure was predicted at that location. Red indicates alpha-helices, green indicated beta-sheets and blue indicates loops. Amino acid 1 is equivalent to amino acid 367 in figure 3.15

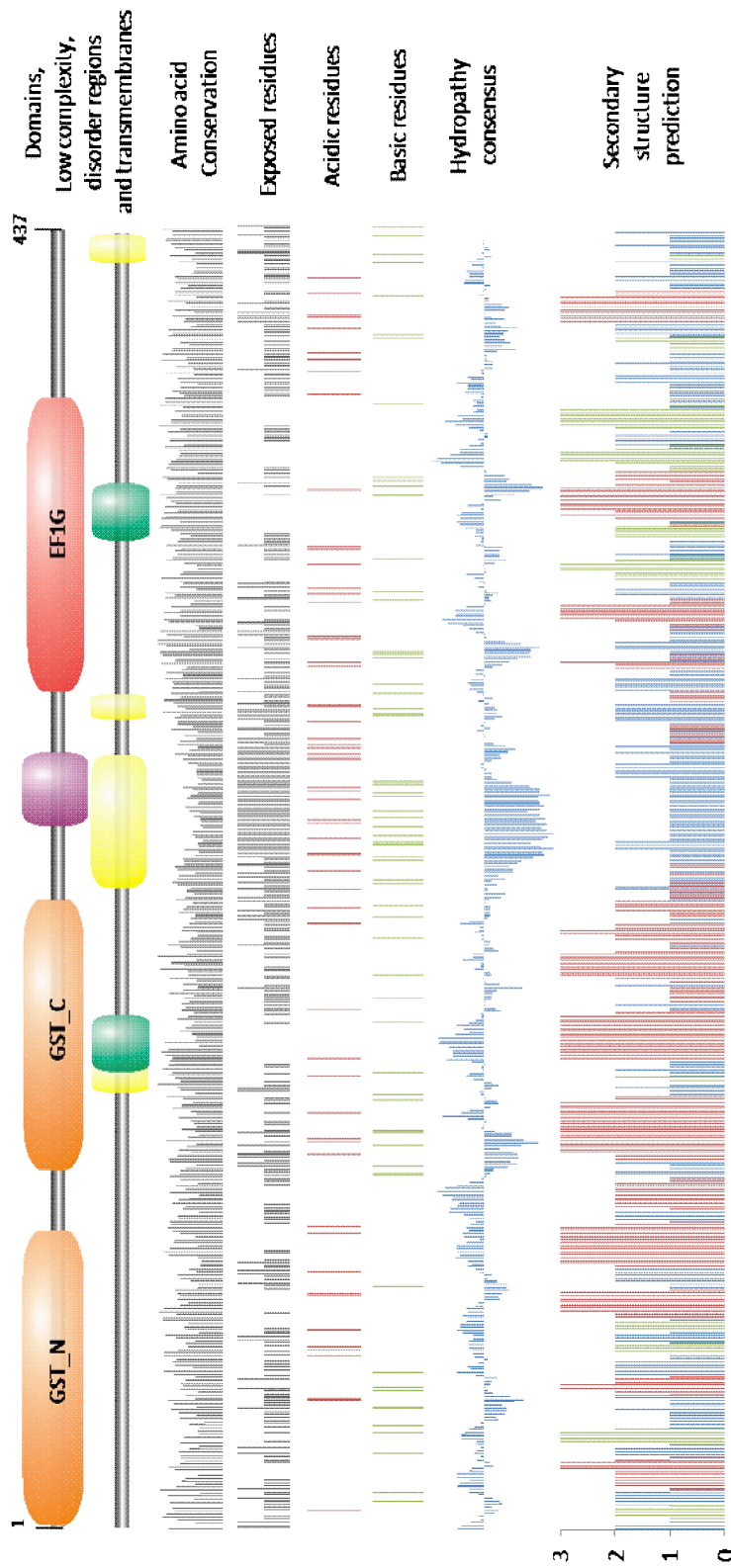


Figure 3.17 eEF1B γ structural features and secondary structure prediction. Domains represented by rectangles where the translation elongation domain (EF1G – eEF1B γ domain) is in red and GST-like domains in orange (GST_C – GST C-terminal domain; GST_N – GST N-terminal domain). Disordered regions, represented by yellow rectangles, were predicted by DisEMBL, low complexity regions, represented by purple rectangles, were predicted using the SEG tool, and transmembrane regions, represented by green rectangles, were predicted by Phdhtm (Prediction Protein) and TMPred. Amino acid variation was calculated from multiple sequence alignments where the higher the bar is, the more conserved is the amino acid at that location. Exposed residues were predicted by Prof_acc, where highly exposed residues are indicated by the highest bar, putatively exposed are indicated by the shortest bar at that location and buried residues are not represented. Amino acid properties such as acidic (red) and basic (green) were calculated from PeplInfo tool. Hydropathy consensus plot was obtained using the PeplInfo tool. Secondary structure prediction plot was derived from the consensus of PSIPRED, PROF (PredictProtein) and Jpred. The plot indicates by how many of these tools, a particular secondary structure was predicted at that location. Red indicates alpha-helices, green indicates beta-sheets and blue indicates loops.

3.2.9 3D structure prediction and folding

Although secondary structure prediction gives valuable information, prediction of 3D structure folding gives a greater insight into protein structure in a non-denatured environment. Each eEF1B subunit protein sequence was compared to the crystallised proteins database PDB by BLAST search (Chapter 2 for more details).

The PDB database BLAST search retrieved the eEF1B crystallised catalytic domains structures as the most similar protein fold. For eEF1B α and all the eEF1B δ isoforms, the crystallised structure PDB:1b64 was predicted to be the most similar to the predicted structure between 135-224aa in human eEF1B α and between 181-280 in human eEF1B δ isoform b. BLAST searches of eEF1B γ protein sequence against PDB identified the PDB:1PBU to be the most similar to the eEF1B γ C-terminus. These results were expected since PDB:1b64 is the crystallised structure of the human eEF1B α C-terminal domain and PDB:1PBU is the solution structure of the C-terminal domain of the human eEF1B γ subunit. Taken together, this suggest that the human C-terminal domains of all the eEF1B subunits have been crystallised, the N-termini have no known three-dimensional structure. Hence, the protein sequences were submitted to a number of folding comparison/prediction tools (Chapter 2 for more details). Agape tools predicted a possible protein fold for the eEF1B α N-terminus between 8 and 77 to have a Glutathione S-transferase (GST) C-terminal domain folding (SCOP:d1aw9_1) with a E-value 7.00E-07. eEF1B δ N-terminus did not show any similarity to any known protein folding structures, whereas a putative GST folding (PDB:1BYE) with a E-value 1.6E-10 was predicted for eEF1B γ N-terminus between residues 5 and 207.

Since the structure of the human eEF1B α C-terminus had been crystallised, this structure model was used to predict a 3-D structure model for the identical GEF domain in the eEF1B δ C-terminus by using Modeller (Chapter 2 for more details on the method) (Figure 18a). The structure of the eEF1B δ C-terminus was very similar

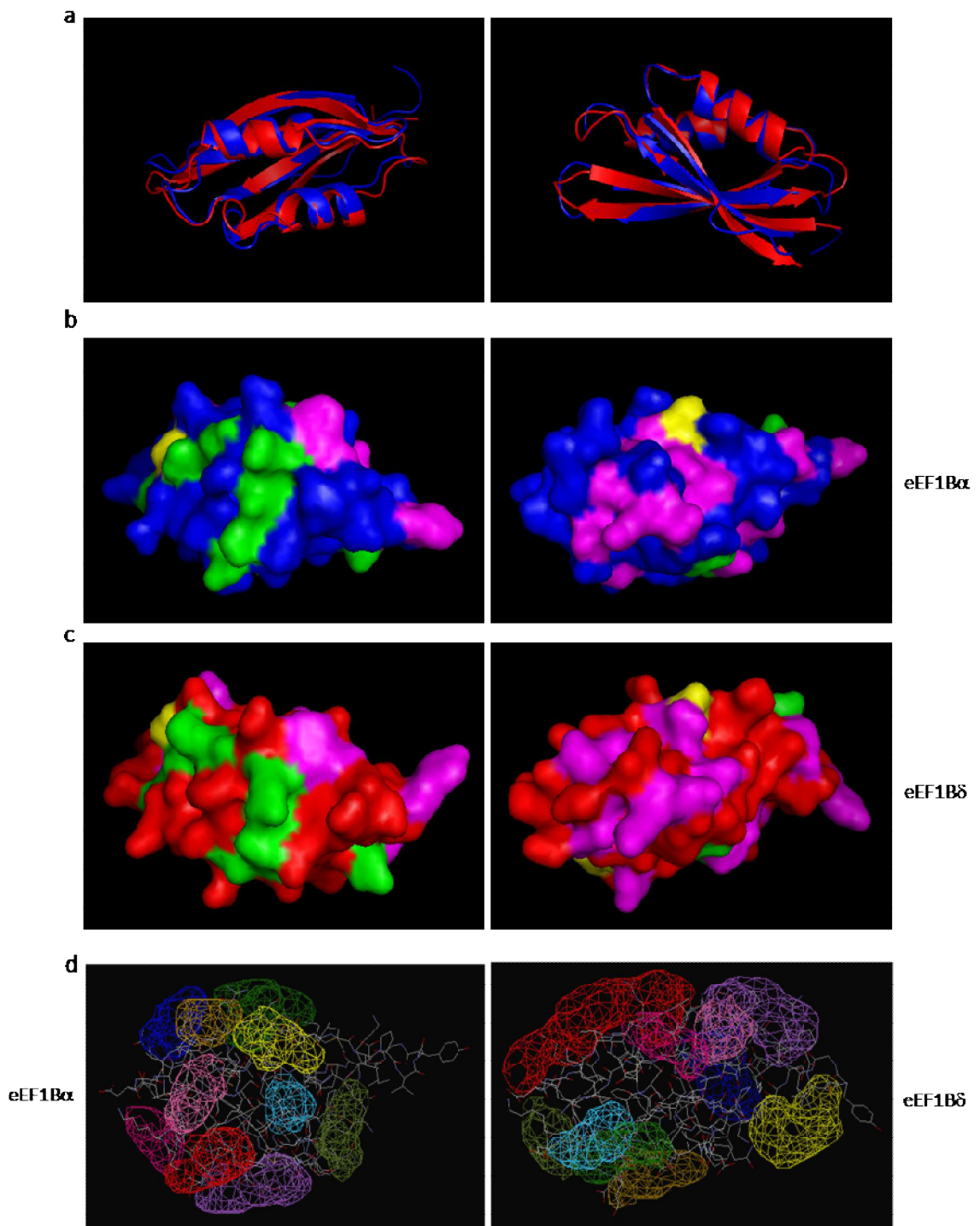


Figure 3.18 Human eEF1B α and eEF1B δ C-terminal 3-D protein structure model. (a) comparative modelling of eEF1B δ C-terminus (blue) to the eEF1B α C-terminus 3-D protein structure (red) by MODELLER and visualised in cartons by PyMol. Surface structure of both sides of (b) eEF1B α and (c) eEF1B δ C-terminus with variant residues shown in green, eEF1A interacting residues in pink, and variant and eEF1A interacting residues in yellow, visualised by PyMol. (d) Prediction of clefts of putative protein binding by ProFunc for eEF1B α C-terminus 3-D structure and eEF1B δ C-terminus 3-D structure model.

to eEF1B α C-terminus with a few conformational changes. These changes alter slightly the surface exposure of some eEF1A interacting residues (Figure 18b and 18c). The ProFunc prediction tool was used to predict the location and volume of possible protein binding clefts (Chapter 2 for more details). Although the primary, secondary and 3-D structure of the eEF1B δ C-terminus was found to be similar or almost identical to the eEF1B α C-terminus, the protein binding clefts' locations and volumes changed considerably between the eEF1B α and eEF1B δ C-termini.

The protein folding prediction can be compared against other proteins and if high similarity is found between folding regions is likely that the regions have the same or similar functions. However, these results suggest that although eEF1B δ and eEF1B α share the C-terminus domain, the protein binding sites might be completely different.

3.2.10 eEF1B post-translational modifications and motifs

Gene expression can also be regulated by protein-protein interactions and post-translational modifications such as phosphorylation. Most post-translational modifications can be predicted by the presence of specific motifs. Motifs are conserved elements of a sequence alignment, which are likely to be a structural or functional region, and can be used to predict further the occurrence of similar motifs on other protein sequences. I have previously mentioned the identification of the leucine zipper motif on eEF1B δ . Other motifs related to protein-protein interactions including post-translational modifications and targeting signals remain to be predicted. Several tools were used to predict likelihood of phosphorylation and the occurrence of other post-translational modifications as well as prediction of regions of the eEF1B protein subunits that are similar or identical to motifs with known function, such as specific proteins or kinases binding sites and targeting signals (Chapter 2 for more details).

Some form of glycosylation was predicted for all the eEF1B subunits. Sulfation was predicted in eEF1B γ and in the N-terminus of eEF1B δ isoform a. Protein methylation was predicted in eEF1B α . Another post-translation modification, acetylation of internal lysines and glycation (non-enzymatic glycosylation) were also predicted in all eEF1B subunits. SUMOylation motif was predicted in eEF1B α and eEF1B γ (Appendix 9). Furthermore, none of the eEF1B subunits was predicted to have a signal peptide on the N-terminus.

Multiple phosphorylation sites and phosphorylation kinases motifs were predicted for each eEF1B subunit, where a score of 1 indicates the highest probability to be phosphorylated and 0 the lowest (Appendix 10). eEF1B subunits are predicted to be phosphorylated by the same kinases, except eEF1B α which is predicted to be phosphorylated by JAK2 on Y56 (likelihood score of 0.066; where 1.0 is maximum likelihood of being phosphorylated) and on Y172 (score of 0.005) but not eEF1B δ or eEF1B γ . Four conserved phosphorylation sites were predicted in the

3. IN SILICO CHARACTERISATION OF EEF1B SUBUNITS

GEF domain of eEF1B α that weren't present in the equivalent eEF1B δ residue position. eEF1B α phosphorylation site S112 (score of 1.0 – maximum likelihood) was predicted to be phosphorylated by CKII, where as phosphorylation site S128 (score of 0.443) was predicted to be phosphorylated by PKC, phosphorylation site S174 (score of 0.057) was predicted to be phosphorylated by PKC and Y213 was not predicted to be phosphorylated. Phosphorylation sites were also predicted in the protein regions coded by eEF1B δ exons 5 and 6 where the highest score site (score of 0.351) was predicted to be phosphorylated by ERK, GSK3 and CKD5.

Targeting signals for several organelles were predicted, including a nuclear localization signal (NLS) at position 85 for eEF1B δ isoform a and a Leucine-rich nuclear export signal (NES) binding to the CRM1 exportin protein at eEF1B γ residues 161-174 (Appendix 11).

Summary diagrams of the predicted post-translational modifications for each eEF1B subunit are on Figures 3.19-3.22.

In addition to all the motifs derived from post-translational modifications already described above, by using the same tools, other protein-protein interaction motifs were also predicted such as STAT5 binding sites on eEF1B α and eEF1B γ , and 14-3-3, TRAF2 and TRAF6 binding sites on eEF1B δ and eEF1B γ (appendix 11).

Although these motif search tools used already have an algorithm that indicates the likelihood of a false positive result, it is particularly difficult to interpret since motifs are usually only a few residues long and are very common.

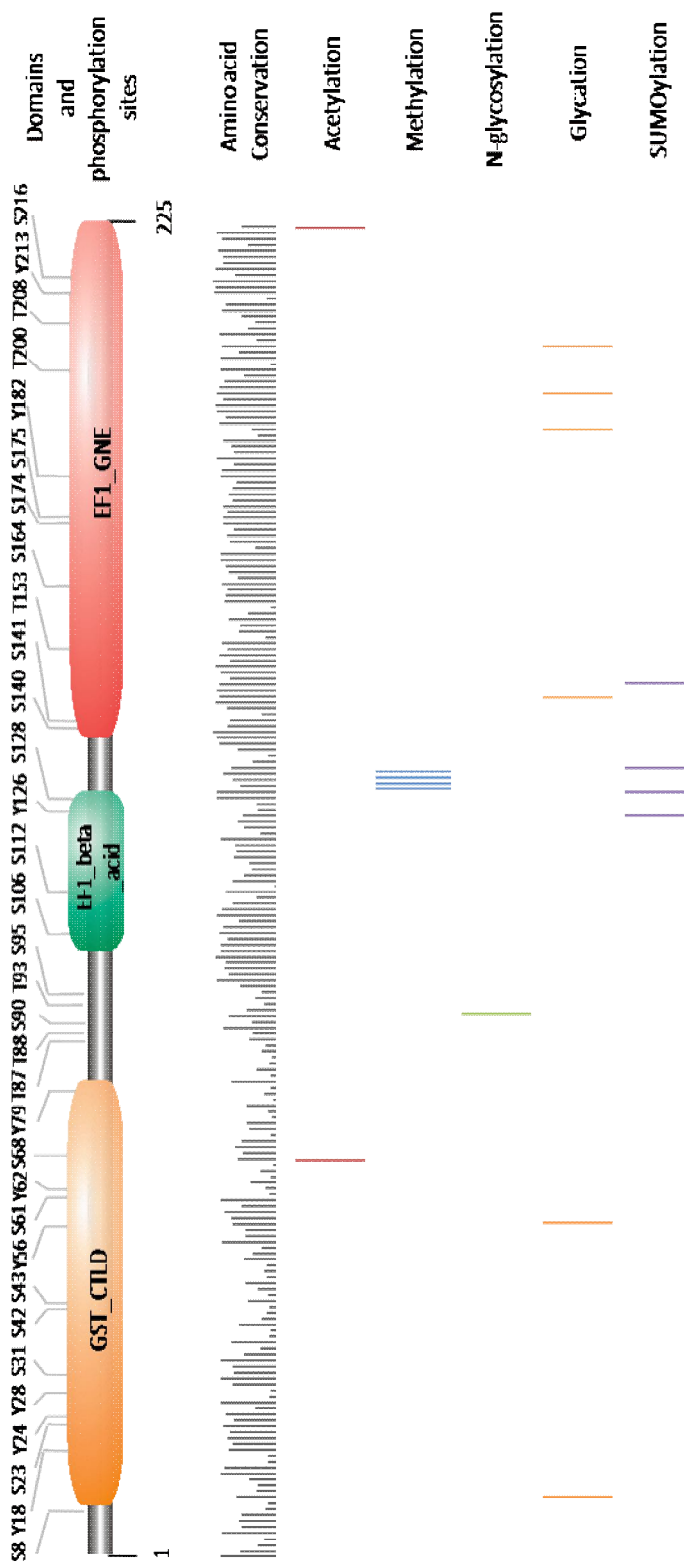


Figure 3.19 Diagram of the post translational modifications predicted for human eEF1B α . Domains are represented by rectangles where the translation elongation domain is in red, GST-like domains in orange and other domains /motifs in green. Prediction phosphorylation sites shown in grey. Amino acid variation was calculated from multiple sequence alignments where the higher the bar is, the more conserved is the amino acid at that location. Predicted methylation sites are represented by blue bars, acetylation sites by red bars, N-glycosylation sites by green bars, SUMOylation sites by purple bars and glycation by orange bars.

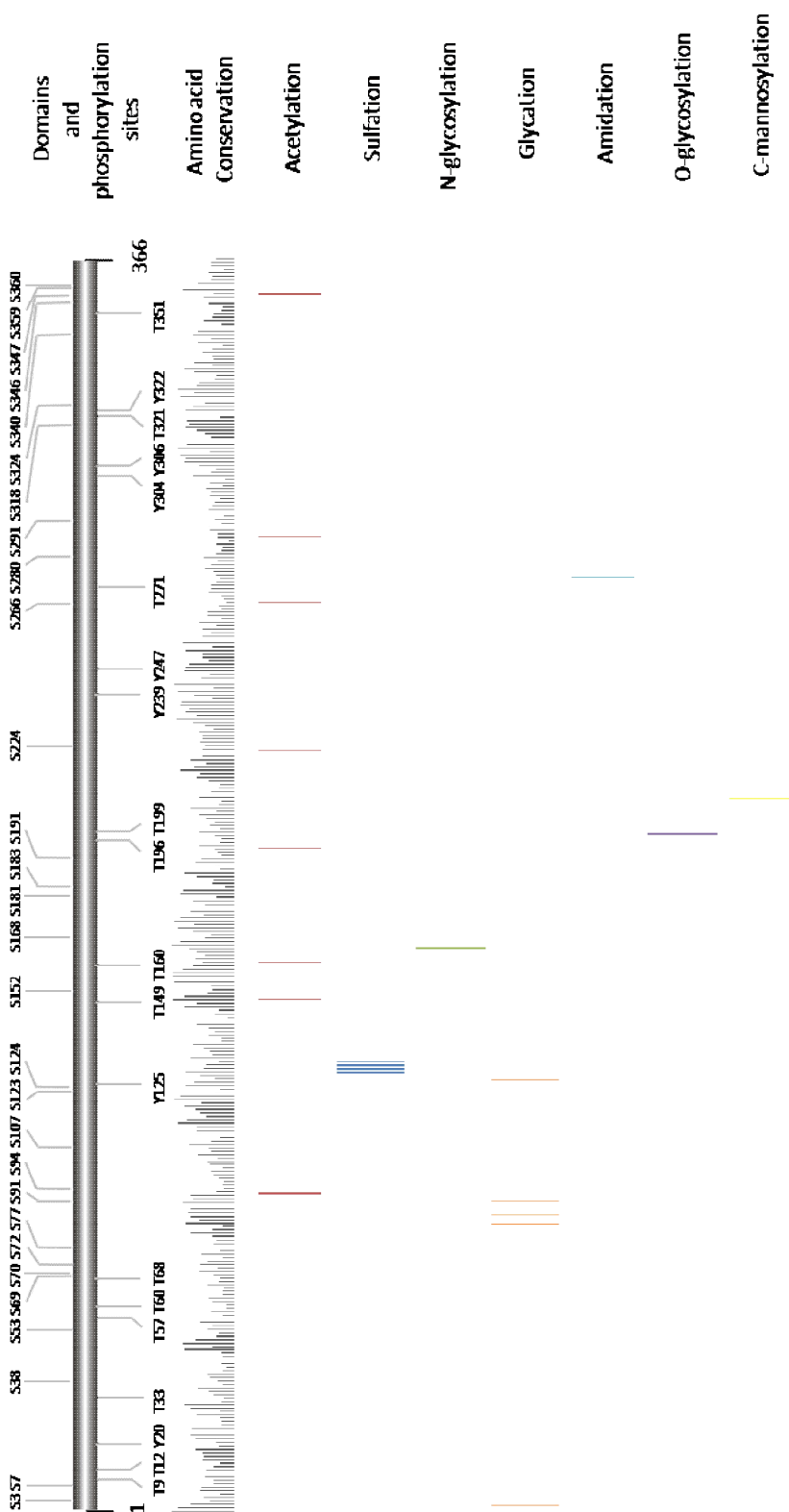


Figure 3.20 Diagram of the post translational modifications predicted for human eEF1Bδ N-terminus isoform a. Prediction phosphorylation sites are shown in grey. Amino acid variation was calculated from multiple sequence alignments where the higher the bar is, the more conserved is the amino acid at that location. Predicted acetylation sites are represented by red bars, sulfation sites by blue bars, N-glycosylation sites by green bars, O-glycosylation sites by purple bars, glycation by orange bars, amidation by light blue bars and C-mannosylation by yellow bars.

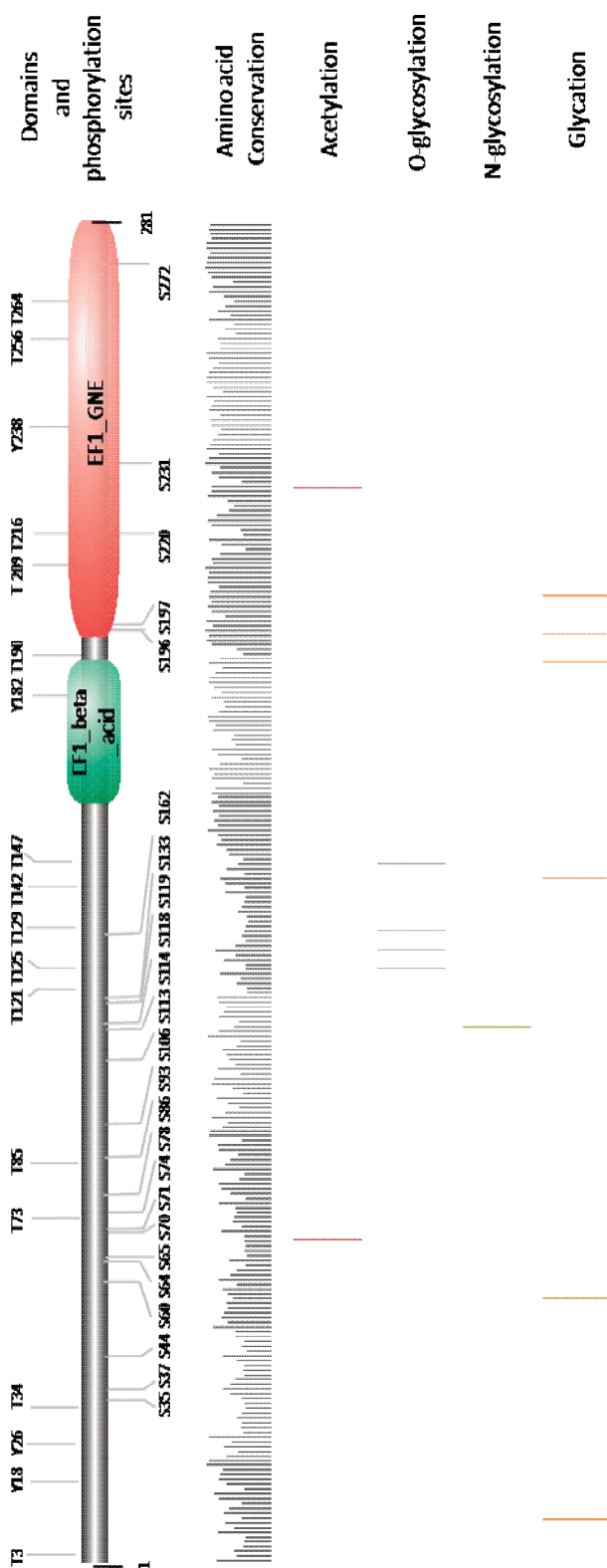


Figure 3.21 Diagram of the post translational modifications predicted for human eEF1B δ isoform b. Domains are represented by rectangles where the translation elongation domain is in red and other domains /motifs in green. Prediction phosphorylation sites are shown in grey. Amino acid variation was calculated from multiple sequence alignments where the higher the bar is, the more conserved is the amino acid at that location. Predicted acetylation sites represented by red bars, N-glycosylation sites by green bars, N-glycosylation sites by orange bars and O-glycosylation sites by purple bars

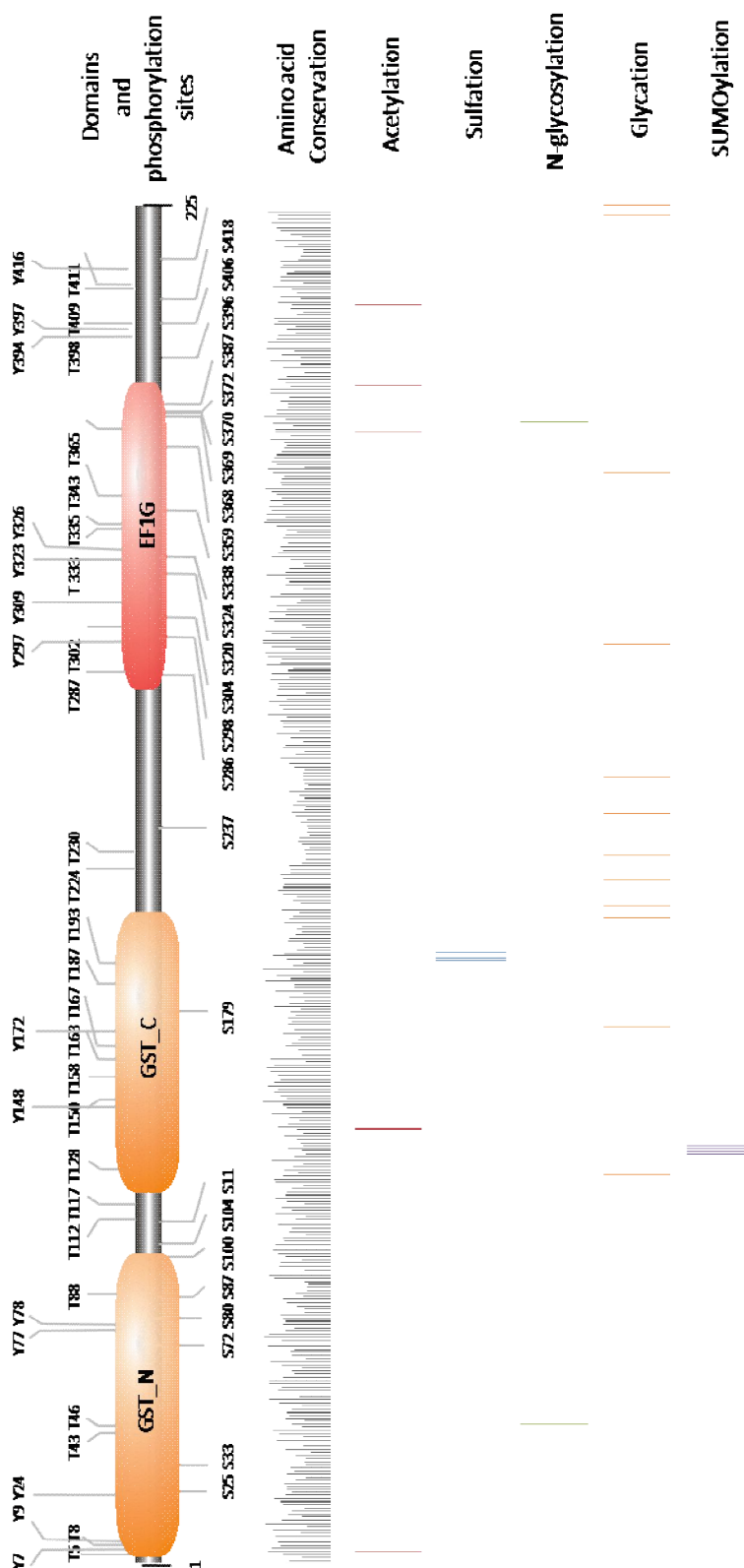


Figure 3.22 Diagram of the post translational modifications predicted for human eEF1B γ . Domains are represented by rectangles where the translation elongation domain is in red and GST-like domains in orange. Prediction phosphorylation sites shown in grey. Amino acid variation was calculated from multiple sequence alignments where the higher the bar is, the more conserved is the amino acid at that location. Predicted acetylation sites are represented by red bars, N-glycosylation sites by green bars, sulfation by orange bars, glycation by orange bars and SUMOylation by purple bars

3.2.11 protein-protein interactions

Valuable information about the biological importance of protein association can be gained from the study from protein-protein interactions with regulatory proteins or proteins with other functions. Data from genome-wide and comprehensive protein-protein interaction studies are available in several databases and can be used to build a network of interactions and possibly even predict putative functions. To build a network of interaction data for each eEF1B subunit and a network with all common interactors between eEF1 subunits the Cytoscape tool was used (Chapter 2 for more details). Cytoscape BINGO plugin (Chapter 2) was used to compare the Gene Ontology classifications from all the interactors and determine molecular functions and biological processes that are overrepresented in a particular network.

eEF1B α was found to interact in two studies with itself and initiation factor 4A2, in three studies with histidyl-tRNA synthetase and in six studies with eEF1B γ (Figure 3.23). The molecular functions which were more represented in the eEF1B α interactors network were translation initiation, translation elongation, GTP binding, IkappaB kinase, aminoacyl-tRNA ligase activity and helicase activity, while the biological processes were regulation of translation initiation and elongation, nuclear transport, and proteolysis.

eEF1B δ was found to interact with cdc2, CTBP1 and aspartate-tRNA synthetase in two studies, with itself, eEF1B γ , CTBP2, kinectin, glycyl-tRNA synthetase and lysyl-tRNA synthetase in three studies, and with valyl-tRNA synthetase in four (Figure 3.24). The molecular functions that were found to be overrepresented in the eEF1B δ interactors network were transcription factor activity, translation elongation activity, NAD binding, NFkB kinase activity, tRNA ligase activity. In addition, the biological processes were mitotic G2 checkpoint, regulation of apoptosis, regulation of development, regulation of immune response, viral genome replication, translation elongation, ubiquitination.

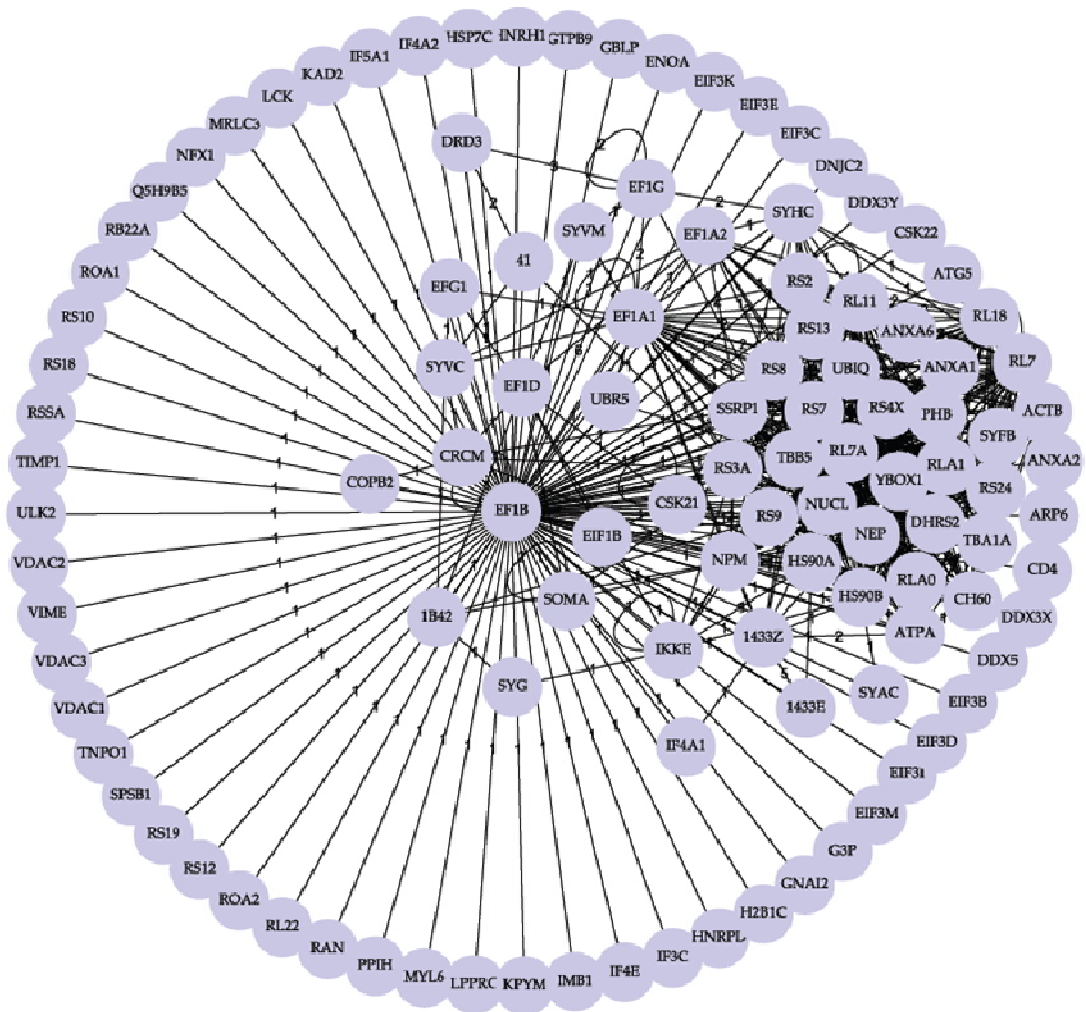


Figure 3.23 eEF1B α protein-protein interactions network. The interactions were retrieved from DIP, BIND, BioGrid, HPRD, IntAct and MINT databases. The interactions were analysed and visualised using Cytoscape. Sequence identifiers are the proteins' UNIPROT IDs.

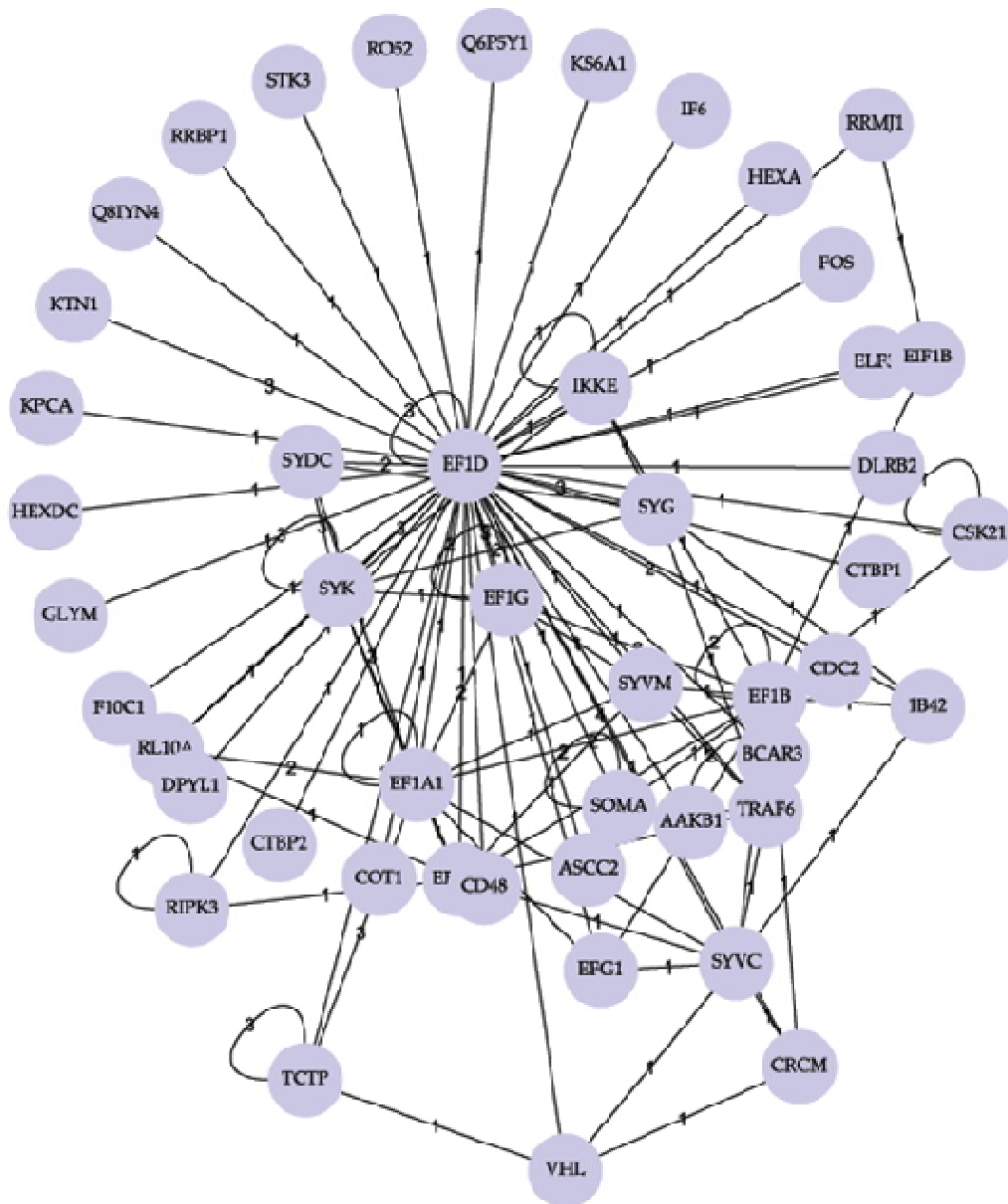


Figure 3.24 eEF1B δ protein-protein interactions network. The interactions were retrieved from DIP, BIND, BioGrid, HPRD, IntAct and MINT databases. The interactions were analysed and visualised using Cytoscape. Sequence identifiers are the proteins' UNIPROT IDs.

3. *IN SILICO* CHARACTERISATION OF EEF1B SUBUNITS

eEF1B γ was found to interact with a variety of proteins in two studies including a CoA isomerase, histone-4, heat shock protein (HSP90b), pre-mRNA splicing factor, tubulin and two different E3 ubiquitin ligases (Figure 3.25). eEF1B γ was found to interact in three studies with an coatmer subunit, dopamine receptor, eEF1B δ , a GTP-binding protein, an cAMP-dependent protein kinase, cysteinyl-tRNA synthetase, glutamyl and prolyl-tRNA synthetase, histidyl-tRNA synthetase and leucyl-tRNA synthetase. Translationally-controlled tumour protein (TCTP) was found to interact with eEF1B γ as well as eEF1B γ self interaction was found in four studies and eEF1B α in six studies. All the other eEF1B subunits interactions had only been observed in a single large scale study. Besides the expected eukaryotic translation elongation factor activity, RNA binding activity, telomerase activity and helicase activity were shown to be the most significant molecular functions of the eEF1B γ interactors. Translation, mRNA processing, nuclear import, transport and response to DNA damage were the most significant biological processes.

Only one or two studies reported interactions between eEF1B subunits and eEF1A1 and eEF1A2 specifically. This low number of reports may reflect the fact that only a couple of genome-wide interaction studies differentiate between eEF1A1 and eEF1A2, thus careful interpretation of the interaction with eEF1A variants is essential. Figure 3.26 shows the minimal protein-protein interaction network between eEF1B α , eEF1B δ , eEF1B γ , eEF1A1 and eEF1A2. A summary of the biological processes and molecular functions is in appendix 12.

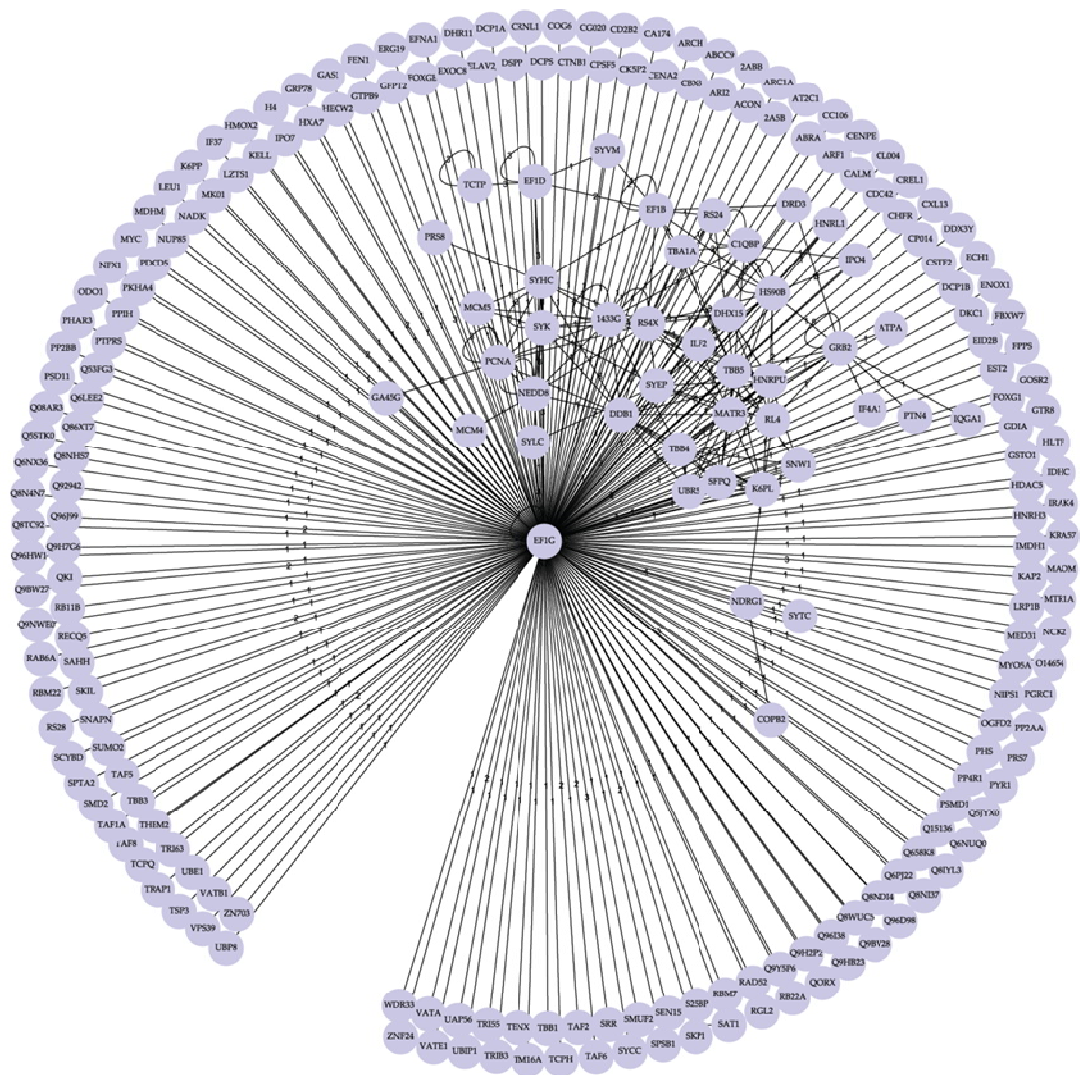


Figure 3.25 eEF1B γ protein-protein interactions network. The interactions were retrieved from DIP, BIND, BioGrid, HPRD, IntAct and MINT databases. The interactions were analysed and visualised using Cytoscape. Sequence identifiers are the proteins' UNIPROT IDs.

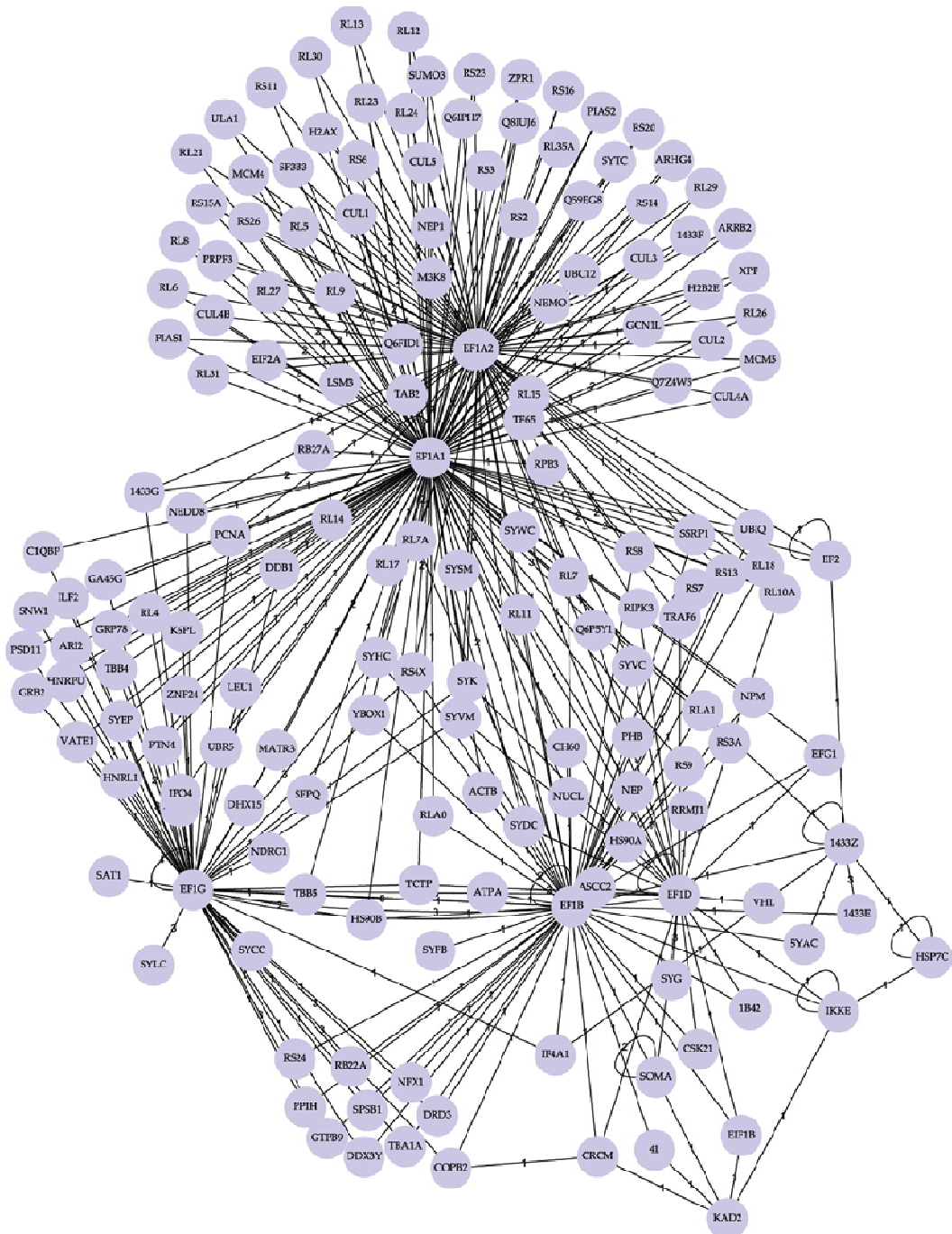


Figure 3.26 eEF1 subunits minimal protein-protein interactions network. The interactions were retrieved from DIP, BIND, BioGrid, HPRD, IntAct and MINT databases. The interactions were analysed and visualised using Cytoscape. Sequence identifiers are the proteins' UNIPROT IDs.

3.3 Discussion

The majority of previous studies of eEF1B subunits focused on the biochemistry of the complex, mainly in lower eukaryotes. It was essential to catalogue the characteristics the eEF1B subunits in higher eukaryotes. In this chapter, *in silico* analysis of the eEF1B subunits described the related sequences or pseudogenes, that are thought not to be expressed. It revealed several eEF1B δ transcript variants in both humans and mice with a possible tissue-restricted expression. This study also focused on the similarities and differences between the subunits at the DNA, RNA and protein level as well as gene regulation and protein-protein binding (interactome).

3.3.1 eEF1B and related sequences

Several eEF1B subunit gene-related sequences were identified both in human and mouse. However all of these sequences had different gene organisation when compared to the structural genes (intronless or just one intron) which suggests that just one gene encodes each of the eEF1B subunits and that these related sequences did not arise due to duplication (non-processed pseudogenes). In contrast, eEF1A has been found to have two protein variants encoded by two different genes in a tissue-specific manner (Knudsen et al., 1993).

All of the eEF1B subunits' putative pseudogenes had differences in the translated amino acid sequence and were not evolutionary conserved between mouse and human. Most had frame-shifts, truncated at the 5' and had internal stop codons. Furthermore, the lack of identical mRNA sequences and ESTs suggests that expression is not likely, or is only at very low levels.

Pizzuti et al. (1993) previously described two human eEF1B α -related sequences, named eEF1B1 and eEF1B3. They suggest that eEF1B3 was a paralogue of eEF1B α expressed at the mRNA level in brain and muscle (Pizzuti et al., 1993).

3. IN SILICO CHARACTERISATION OF EEF1B SUBUNITS

Later, it was suggested that eEF1B1 was a pseudogene derived from a retrotransposition event and suggested that eEF1B3 was a intronless paralogue (Chambers et al., 2001). However, with the sequencing data from both mouse and human now freely available, it is clear that eEF1B3 has in-frame stop codons. Also there is no evidence of eEF1B3 like protein sequences on non-redundant protein databases indicating that even if parts of the eEF1B3 pseudogene were transcribed in certain tissues, these are unlikely to be translated, or are translated at a low frequency, or at a restricted developmental stage. It is likely that eEF1B3, just like all of the putative pseudogenes identified for eEF1B subunits and eEF1B1, is a recent processed pseudogene derived from integration of mature eEF1B subunit mRNA into the genome. Although eEF1B subunit related sequences are thought to be non-coding, it is important to take their sequence into consideration when for example, PCR primers are designed to amplify the coding-genes.

3.3.2 eEF1B δ alternative splicing and expression

Two independent studies by Sanders et al. (1991) and von der Kammer et al. (1991) identified and cloned the human nucleotide sequence of eEF1B α at the same time. These, although they were predicted to code for identical amino acid sequences, had different 5'UTR sequences derived from alternative non-coding exons. The sequences of the different 5'UTRs as well as the 3'UTR did not show any UTR regulatory element, however the difference in size of the 3'UTRs might suggest different mRNA stability or localisation (Fred and Welsh, 2009). This study failed to identify any more transcript variants and all the ESTs and mRNA sequences on databases encoded for an identical protein, suggesting that the eEF1B α gene only codes for one protein.

GenBank indicates two transcript variants and respective protein isoforms for eEF1B δ , that are evolutionary conserved in human and mouse. Here I showed that isoform a is present in fish, birds and mammals whereas isoform b is present in

all of those as well as frogs, insects and crustaceans. Another isoform, named isoform c for simplicity, was also identified in both humans and mouse. It appeared to be derived from alternative splicing, lacking eEF1B δ exon 5. This isoform had previously been found to exist in sea urchins and in *Xenopus* oocytes (Minella et al., 1996b, Le Sourd et al., 2006b). By analyzing gene structure using ESTs, an extra exon, named exon 5a, was identified between mouse eEF1B δ exon 5 and 6 and the respective amino acid sequence was identified in the non-reference protein sequence database. Although information on these transcript variants was derived from hundreds of high quality EST sequences, it is possible that more eEF1B δ transcript variants may exist. They just might be expressed at low-levels, might have spatially and temporally restricted expression.

Both eEF1B α and eEF1B δ seemed to have transcript variants derived from alternative splicing, but there is no evidence for eEF1B γ transcript variants. Furthermore, the ESTs tissue source indicates that all eEF1B subunits and their respective transcript variants are widely expressed except eEF1B δ transcript variant a, that includes exon 1, 2 and 3, which seems to be restricted to eye, testis and brain. As mentioned previously, tissue restricted expression in eukaryotic translation elongation factors has been previously described for eEF1A1 and eEF1A2 variants (Knudsen et al., 1993). Extensive eEF1B subunit expression pattern and distribution analysis will be described in the next chapter.

3.3.3 Similarities and differences between subunits

When eEF1B δ was cloned and sequenced in the crustacean *Artemia* it was described as having a similar C-terminal to eEF1B α (van Damme et al., 1990) and found to have guanine nucleotide exchange function (Cormier et al., 1993). The C-termini of eEF1B α and eEF1B δ , which contain the GEF domains, have a few amino acid differences, including two eEF1B α specific potential phosphorylations sites which are not present in eEF1B δ , and two eEF1A interaction residues which are

3. *IN SILICO* CHARACTERISATION OF EEF1B SUBUNITS

different. Since the eEF1A interaction residue information was derived from the eEF1B α C-terminal NMR structure (Perez et al., 1999) and no structure was ever solved for the eEF1B δ C-terminal, it is difficult to determine if those eEF1A interaction residues in the equivalent position in eEF1B δ are still interacting and if they have a similar interaction strength. The secondary structure prediction was identical between both C-termini. In an attempt to analyse the amino acid variants, the eEF1B δ C-terminal structure was modelled onto the known eEF1B α 3-D structure. It was found that although the eEF1B α and eEF1B δ C-termini are extremely evolutionarily conserved at the primary, secondary and 3-D structures, the few amino acid variations are enough to alter completely the prediction of size and number of protein-binding clefts. This indicates that the different protein-binding clefts might have an effect on different functions or more likely on the affinity for eEF1A or affinity for one of the eEF1A variants. Interestingly, eEF1A2 had been found not to interact with any eEF1B protein by yeast-two-hybrid, whereas eEF1A1 was found to interact with both eEF1B α and eEF1B δ (Mansilla et al., 2002). No other large-scale interactions studies reported interaction of eEF1A1 and eEF1B subunits, however one study reported interaction of eEF1A2 with eEF1B α and eEF1B δ (Ewing et al., 2007). This study only used eEF1A2 as bait for the immunoprecipitation of FLAG-tagged proteins and not eEF1A1. In addition, the Mansilla et al. study did not report any eEF1A2 interaction or any positive control. Hence, further studies are required to determine if both eEF1A variants bind to eEF1B α and/or eEF1B δ .

eEF1B δ has a leucine zipper pattern which may be involved in protein-protein binding or even in self-association (Sanders et al., 1993). eEF1B δ was found in several large scale protein-protein interaction studies to self-associate. Also a further conserved coiled-coiled region was identified. Guerruci and colleagues suggested that eEF1B δ originated from an ancestral (Guerruci et al., 1999) eEF1B α gene duplication and fusion with a leucine zipper protein. The size and sequence of

3. *IN SILICO* CHARACTERISATION OF EEF1B SUBUNITS

introns are not conserved between the eEF1B δ and eEF1B α at the 3' end but the similarity in the gene structure supports this hypothesis. All eEF1B subunits have multiple low complexity regions and disordered regions that are known to facilitate protein binding (Russel and Gibson, 2008). The eEF1B δ isoform a has repeats in the N-terminus which are also likely to be involved in protein binding (Russel and Gibson, 2008). The other eEF1B δ isoforms identified in this study do not have any striking characteristic or feature that may indicate a possible difference in function or activity.

Both eEF1B α and eEF1B γ have a GST N-terminus domain, in addition, eEF1B γ has a GST C-terminus domain. The GST domain was previously identified in eEF1B γ and several conflicting reports exist about the possible GST activity (Chapter 1). The N-terminus of eEF1B α had been previously suggested to be similar to eEF1B γ and multi-synthetase complex auxiliary protein p18 by Quevillon and Mirande (1996) although they didn't identify the domain as being the GST domain (Quevillon and Mirande, 1996). Quevillon and Mirande suggested that p18, one of the three multi-synthetase complex auxiliary proteins, should be changed to eEF1Be because of N-terminus similarity and hence the possibility of interaction between p18 and eEF1B α and eEF1B γ . Another multi-synthetase complex auxiliary protein, p38, also has a GST-C terminal domain and a leucine zipper domain. It has been proposed to bind p18 and the coiled-coiled region on the third multi-synthetase complex auxiliary protein (p43) and is hence thought to be involved in the scaffolding of the multi-synthetase complex (Ahn et al., 2003). The yeast eEF1B γ region suggested by Jeppesen et al. (2003) to be involved in the eEF1B γ dimer formation consists of a coiled-coiled region that is not conserved between yeast and mammals. The location of the eEF1B α and eEF1B γ interaction that was suggested by Jeppesen and colleagues is in the very poorly conserved GST C-terminal domain between yeast and mammals (Jeppesen et al., 2003). It seems likely that if proteins

3. *IN SILICO* CHARACTERISATION OF EEF1B SUBUNITS

that share the GST-C-terminal domain have the potential to bind to each other, then the binding of the N-terminus of eEF1B α with the N-terminus of eEF1B γ might be mediated by the conserved GST C-terminal domain present in both proteins.

Moreover, Valyl-tRNA synthetase, thought to be part of the eEF1H complex in certain conditions (Chapter 1 for more details) has a GST C-terminus and N-terminus domain. The GSTs are known to dimerise strongly, mainly with hydrophobic substrate domains (Rossjohn et al., 1998). Interestingly, valyl-tRNA synthetase is thought to bind only eEF1B δ in the eEF1B complex (Motorin Yu et al., 1988, Jiang et al., 2005) in mammals. It is thought that this binding only occurs in higher eukaryotes that have a valyl-tRNA synthetase N-terminal extension (Bec et al., 1994). Another eEF1B δ strong interactor is eEF1B γ , which also has both GST C- and N-terminus domains. Due to the similarity of the domains between valyl-tRNA synthetase and eEF1B γ , it is possible to postulate that both the GST N-terminus domain of valyl-tRNA synthetase and eEF1B γ bind to eEF1B δ . This hypothesis is backed up by the fact that binding of eEF1B α and eEF1B δ to eEF1B γ is non-competitive, indicating that the proteins have different binding sites on the eEF1B γ N-terminus (Chapter 1). Also, the binding of valyl-tRNA synthetase and eEF1B γ also appears to be non-competitive since purification of the complex and three dimensional reconstruction of the complex shows equal molar proportions (Bec et al., 1994, Jiang et al., 2005).

Plants have four sets of GEF proteins that are grouped into two groups of two proteins each, and that during the last few years have changed nomenclature frequently. Two have no EF1_beta_acid domain but have a GST C-terminal domain, while the other two have an EF1_beta_acid domain but no leucine zipper domain. Guerrucci et al. (1999) suggested that eEF1Bb and eEF1Bb' arose from a duplication of the ancestor gene in plants. Guerrucci and colleagues, however, didn't suggest which ancestor gene the plants GEF are derived from (Guerrucci et al., 1999). I suggest that the groups should have their own nomenclature since they are equally different from eEF1B α and eEF1B δ .

3.3.4 Putative non-canonical functions

Data from large-scale protein-protein interactions are freely available and together with the prediction of DNA-, RNA-, protein- and phosphorylation-binding motifs, are very helpful in pinpointing possible regulatory events or even functions. All eEF1B subunits are known to be phosphorylated, with eEF1B δ showing several forms on SDS-PAGE in *Xenopus* oocytes and a mouse cell line. These were suggested to be due to hyper-phosphorylation forms (Chang and Traugh, 1998, Minella et al., 1996b).

As discussed in chapter 1, there are multiple reports of non-canonical functions for translation factors. Both eEF1B α and eEF1B γ have GST domains which if active, might be implicated in oxidative stress (Chapter 1). Interestingly, binding sites of transcription factor known to be involved in stress responses were predicted for the putative promoter regions of all eEF1B subunits. Stress-related proteins were also identified as eEF1B interactors and predicted to phosphorylate eEF1B subunits. In addition, transcription factors and proteins known to regulate the cell cycle were found to bind to or were predicted to phosphorylate eEF1B subunits.

Careful analysis is needed when inferring information from protein interaction data and prediction tools. Computational prediction is based on statistical models built with selected biological data, followed by testing and validation usually on another set of biological data. Although most prediction tools are reasonably accurate, they might not be appropriate for particular searches due to the restricted set of data on which they were tested. The number of interactions of human proteins is estimated to be around 650,000, however less than 10% are thought to have been identified (Hart et al., 2006, Stumpf et al., 2008). Large scale protein-protein interaction studies give rise to a high number of false positives. Abundant proteins such as transcription and translational factors are often contaminants or are included as a result of non-specific binding (Bernhard et al., 2004, Nguyen and Goodrich, 2006). False positive interactions can also arise from

3. *IN SILICO* CHARACTERISATION OF eEF1B SUBUNITS

differences between *in vitro* and *in vivo* interactions, and if two proteins are part of a larger complex but do not directly physically interact. For example, eEF1A2 was reported to bind to several proteins that are part of the TNF- α /NF- κ B signal transduction pathways (Bouwmeester et al., 2004). However this result might be slightly biased since the only baits were proteins involved in the TNF- α /NF- κ B signalling pathway. These false positive interactions can be reduced by repeated experiments (consistency) and by only considering high quality baits and preys, switching baits with preys and by treating samples with micrococcal nuclease to increase the interaction confidence intervals (Bernhard et al., 2004, Nguyen and Goodrich, 2006, Kriegsheim et al., 2008). The ultimate test would be to use several different independent protein-protein interaction techniques individually both *in vivo* and *in vitro* on potential each pair of interactors and test for baits or preys mutants.

A catalogue of features and characteristics of eEF1B subunits was identified and *in silico* tools used enabled to suggest regulatory events that may affect the expression and function of eEF1B subunits. However, it is vital to confirm or dismiss these hypotheses by performing *in vitro* and *in vivo* experiments.

Chapter 4 – Expression of the eEF1B subunits

4.1 Introduction

In the previous chapter, ESTs and SAGE data, indicative of mRNA expression, showed widespread expression for all eEF1B subunits. None of the pseudogenes and homologues analysed in the previous chapter showed evidence of being expressed however data retrieved from databases showed evidence of multiple transcript variants for eEF1B δ in mouse and human. With the exception of studies that mention one of the eEF1B subunits as being expressed in a particular cell type or organism, no thorough study of expression of each eEF1B subunit has yet been published.

Determining the expression pattern and distribution in mouse and human tissues as well as cell lines is important to obtain biological information that can be the basis of future studies. In order to characterise the eEF1B subunits *in vivo* and *in vitro*, mRNA expression in tissues was investigated paying particular attention to possible transcript variants. To determine the protein levels, peptides were designed and antibodies raised against the peptides. These antibodies were then used to explore possible isoforms including tissue-specific forms to determine specific cell type expression in adult mice and human tissues as well as during different mice developmental stages, to investigate the sub-cellular localisation of each subunit, and to assess expression during cell cycle and in wasted mice which lack eEF1A2.

In this study eEF1B subunits were found to be present in all tissues and cell lines tested and to have several forms, including tissue-specific isoforms. The expression of eEF1B subunits is largely correlated although some clear uncoupled expression is seen during development and in terms of tissue distribution in both mouse and human. Sub-cellular distribution in tissues varied, including signs of nuclear distribution, whereas in cell lines eEF1B subunits were always cytoplasmic under the specific conditions tested.

4.2 Results

4.2.1 eEF1B α and eEF1B γ mRNA are ubiquitously expressed in mouse tissues

EST information for eEF1B α and eEF1B γ retrieved from databases does not suggest the presence of any transcript variants (chapter 3) however it is important to verify this is by determining expression *in vivo*. To examine the eEF1B α and eEF1B γ mRNA expression pattern, RNA was extracted from mouse tissues, cDNA synthesis and RT-PCR was performed. GAPDH primers were used as controls. No cDNA was used as a negative PCR control and -RT as a DNA contamination control.

eEF1B α mRNA is expressed in all the tissues tested (Figure 4.1a). mRNA of eEF1B γ was also found to be present in all the tissues tested (Figure 4.1b). A single band was consistently obtained by RT-PCR with various primer pairs targeting different exons for both eEF1B α and eEF1B γ (Figure 4.1c and d). The minus RT control showed no genomic DNA contamination and the no cDNA control showed no contamination from any of the PCR solutions.

Both alpha and gamma eEF1B subunits are ubiquitously expressed in all the mouse tissues studied. In order to determine the relative mRNA level, quantitative RT-PCR was carried out in a variety of mouse tissues. No cDNA was used as a negative control and -RT as blank control. Efficiency curves were calculated for each tissue extracted, and experiments were carried out in triplicate. Actin, 18S rRNA and β -2-microglobulin were used as reference genes, and data were normalised against the reference genes. Eight mice were analysed, four of each sex, and a mean was taken from these eight.

Efficiency was consistently between 95% and 105% (Figure 4.2e-f) with a high correlation of 3.999. The single melting curve shown on Figure 4.2c-d is indicative of just one transcript variant. No significant difference in mRNA expression between tissues was observed for either eEF1B α (Figure 4.2g) or eEF1B γ (Figure 4.2h). Thus, eEF1B α and eEF1B γ are expressed at the mRNA level at a similar level in a variety of mouse tissues with no evidence of transcript variants. No statistical difference was found between males and females by performing students t-test analysis.

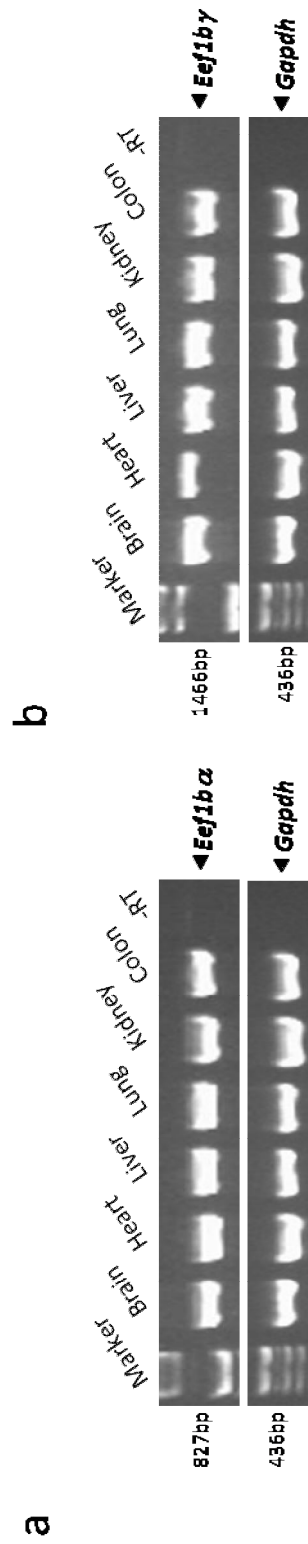
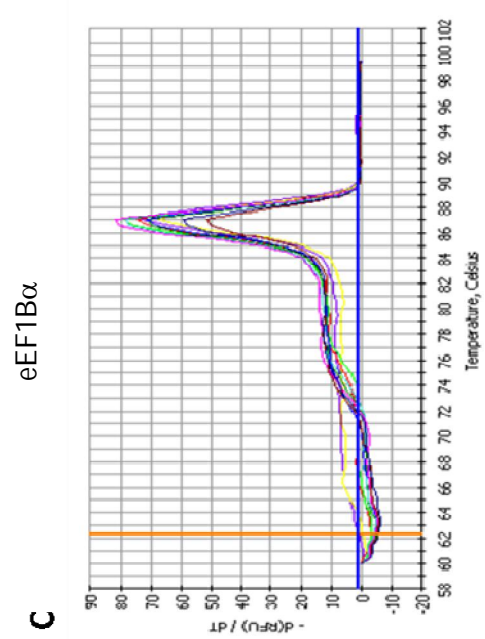
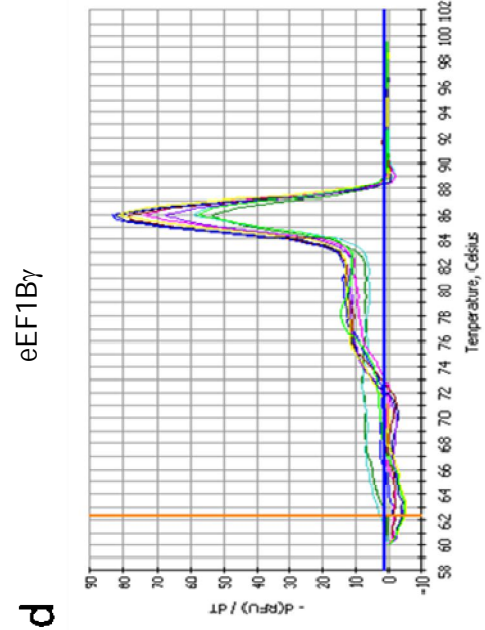
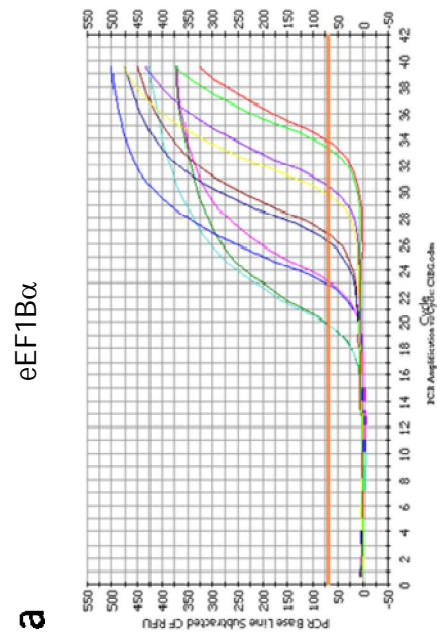
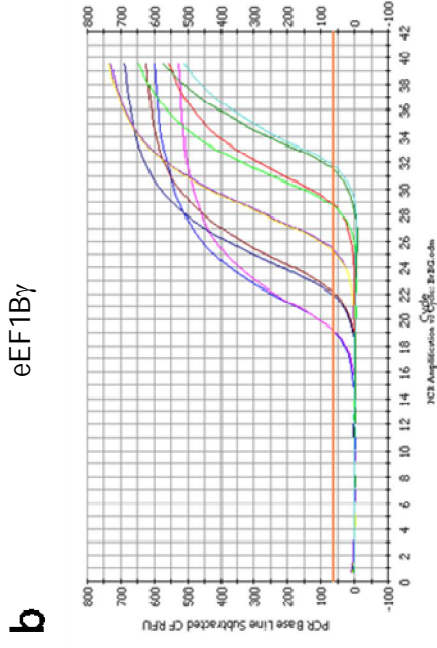


Figure 4.1 eEF1B α and eEF1B γ mRNA expression in normal mouse tissues. RNA was extracted from mouse tissues followed by cDNA synthesis and analysed for (a) *Eef1b α* and (b) *Eef1b γ* mRNA expression by semi-quantitative RT-PCR. *Gapdh* was used as a loading control and Minus RT as a RT-PCR control.



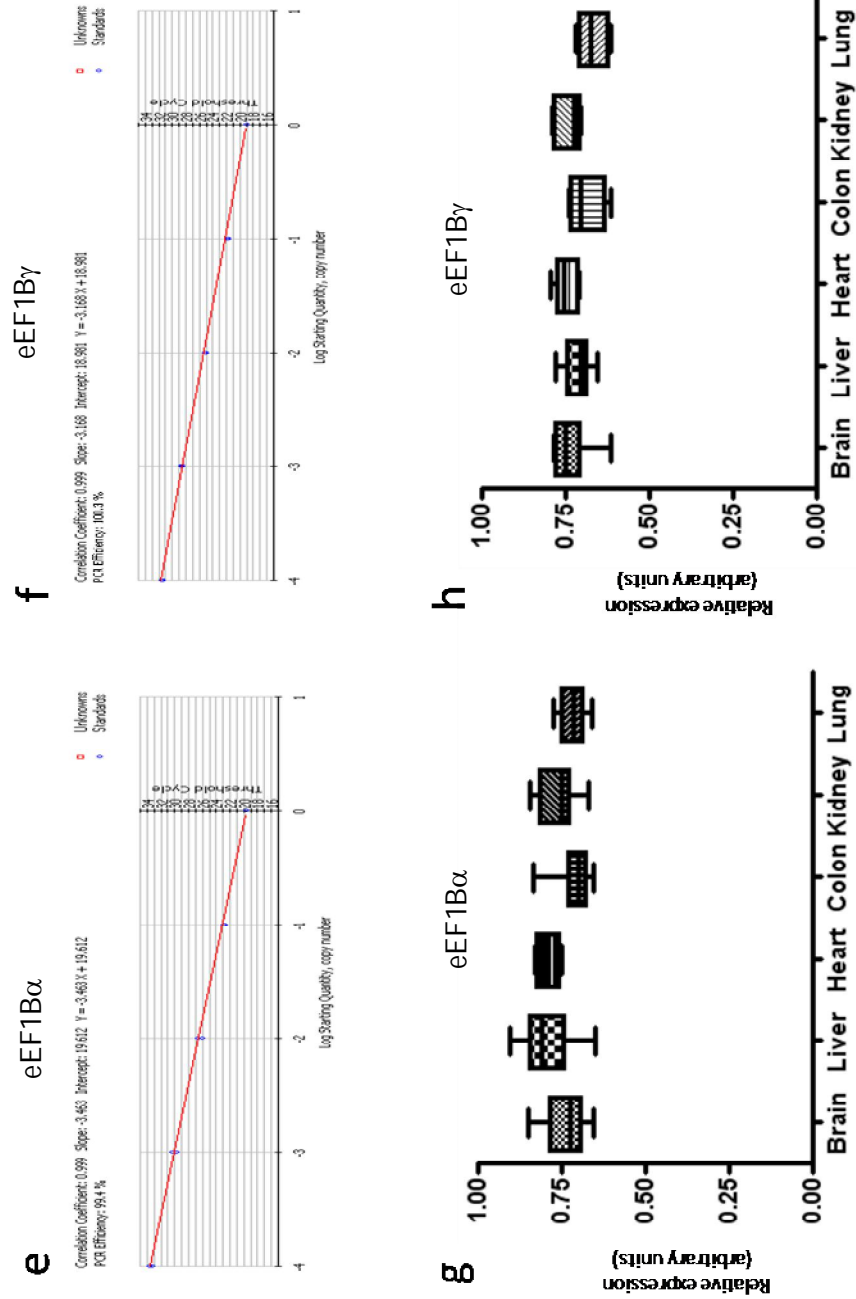


Figure 4.2 Eef1b α and Eef1b γ quantitative mRNA expression in normal mouse tissues. RNA was extracted from mouse tissues followed by cDNA synthesis and analysed for Eef1b α and Eef1b γ mRNA expression by using real-time RT-PCR. B-actin, 18S rRNA and b-2-microglobulin were used as reference genes. Graphs representative of amplification curves indicating no difference in ct score or the shape of the curves (**a-b**), melting curves showing amplification of only one product and no primer dimers (**c-d**) and standard curves showing high efficiency of Eef1b α and Eef1b γ respectively. Whisker graph showing the relative expression of Eef1b α (**g**) and Eef1b γ (**h**) between tissues with data obtained from eight mice (four male and four female). $P > 0.005$ between tissues and between females and males

4.2.2 eEF1B δ has multiple mRNA transcripts some of which show tissue-specificity

In contrast with eEF1B α and eEF1B γ , there is evidence of transcript variants for eEF1B δ . In the Genbank database, eEF1B δ has two reference mRNA sequence variants both in mouse and human, and the *in silico* data described in the previous chapter suggest even more transcript variants. Are the transcript variants ubiquitously expressed in mouse tissues? Is there any suggestion of further transcript variants in mouse tissues? To attempt to answer these questions, RNA was extracted from mouse tissues, cDNA synthesis and RT-PCR was performed as before.

Primers designed specifically to amplify eEF1B δ transcript variant a (exon 3 to any other exon), only showed a single band of the expected size in brain and not in any other mouse tissues studied (Figure 4.3a). RT-PCR with primers targeting any other exons except exon 3 consistently showed multiple bands in all the studied tissues. These results indicate the presence of tissue specific transcript variants and possibly the existence of previously unsuspected transcript variants.

Taking in consideration the *in silico* data (Chapter 3) which suggested the presence of a further exon between exon 5 and 6, primers were designed to target exon 5a. RT-PCR with these primers and primers targeting further down exons amplified a band at the predicted *in silico* size (Figure 4.3b). Negative controls showed no contamination.

Quantitative RT-PCR as previously described for eEF1B α and eEF1B γ was also attempted for eEF1B δ using a variety of primer sets. All the primer sets showed multiple melting curves (Figure 4.3c-d), so it was not possible to accurately quantify eEF1B δ mRNA expression in mouse tissues.

Both the amplification of multiple bands and multiple melting curves with different primer sets suggest the possible presence of more transcript variants. To confirm that the RT-PCR amplified bands were eEF1B δ transcript variants, the bands were gel extracted, cloned into pcDNA2.1 (TA cloning) and sequenced. Figure 4.3e shows a diagram of sequenced mRNA transcripts.

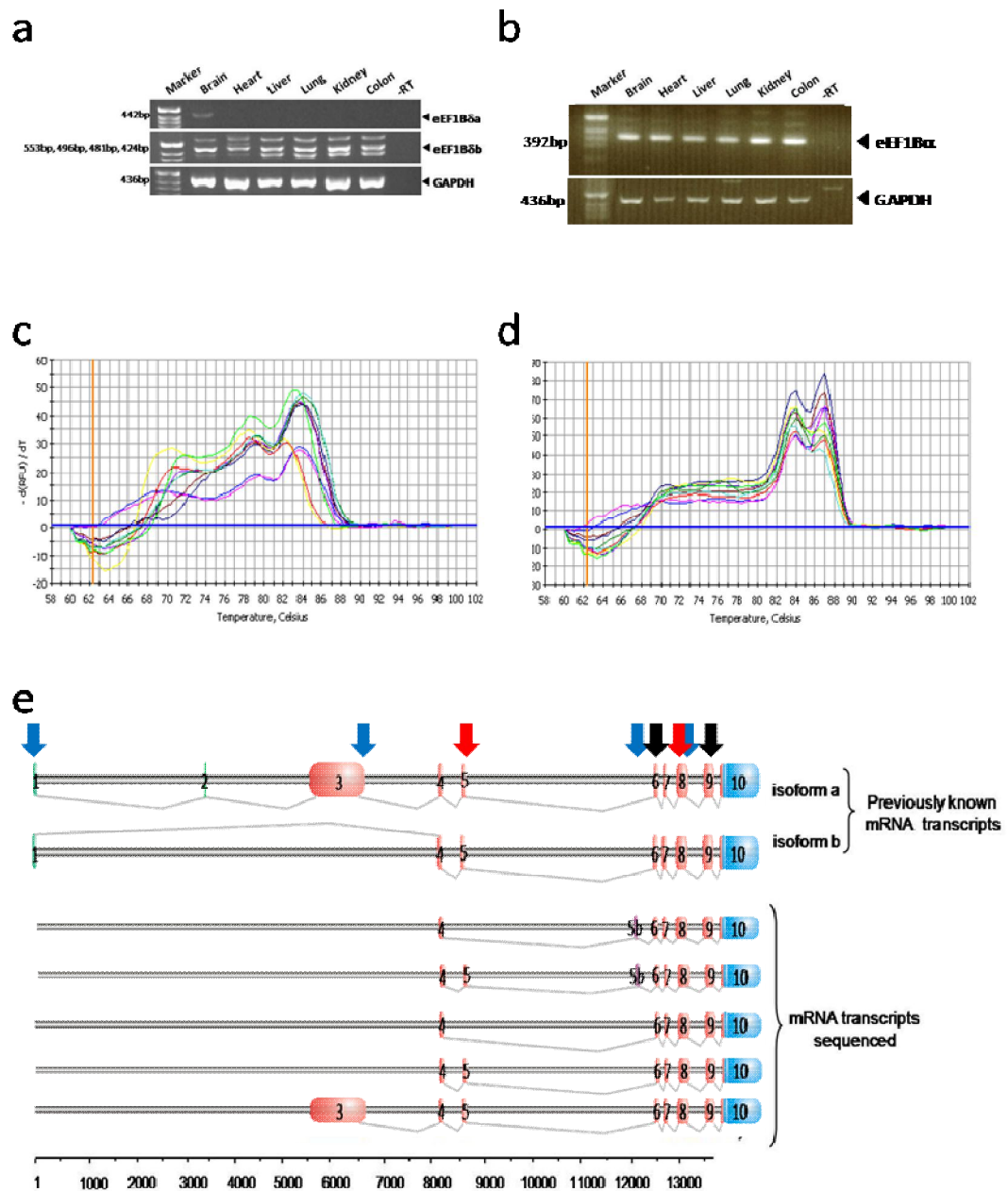


Figure 4.3 *Eef1bδ* mRNA expression in normal mouse tissues. RNA was extracted from mouse tissues followed by cDNA synthesis and analysed for *Eef1bδ* (a) exon 1 or exon 3/4 to exon 8/9; (b) exon 5b to exon 8/9 mRNA expression by using semi-quantitative RT-PCR (blue arrows). GAPDH was used as a loading control and minus RT as a RT-PCR control. *Eef1bδ* mRNA expression analysed by using real-time RT-PCR. *b-actin*, *18S rRNA* and *b-2-microglobulin* were used as reference genes. Graphs representative of melting curves of exon 5 to exon 8 (red arrows) (c) and exon 6 to exon 9 (black arrows) (d) indicating the presence of multiple amplified products. Diagram of cloned and sequenced transcript variants where arrows represent promoters location (e)

4.2.3 Peptide design and antibody production

To attempt to study protein expression, antibodies against each of the subunits had to be produced as no commercially antibodies were available at the beginning of my PhD.

The peptide sequences chosen to generate antibodies were selected by taking in consideration amino acid conservation between human and mouse, similarities to other proteins, particularly between subunits, and avoiding both mouse and human SNPs that alter coding sequence. Although the complete three-dimensional structure of either mouse or human proteins has not yet been determined, the peptide sequence selection also took in consideration the predicted secondary structure, exposed and flexible amino acids and antigenicity properties. These properties are important to help the access of the antigen by the antibody. A peptide was designed against eEF1B α , eEF1B δ isoform 1, both known eEF1B δ isoforms and eEF1B γ (Figure 4.4).

A terminal C-terminal cysteine was added to each peptide to allow for conjugation to keyhole limpet hemocyanin (KLH) improving antigenicity of the peptide and allowing the conjugation of the peptide to a SulfoLink column for subsequent immunoaffinity purification.

The KLH-conjugated peptide was then injected into a rabbit as described in chapter 2, and the sera from the bleeds was obtained for each peptide. ELISA was used to determine if the sera would recognise each specific peptide. Different concentrations of sera were tested against different concentrations of peptide. Pre-immune serum, obtained from the same animal prior to immunisation with the peptide, was used as a negative control. An immunoaffinity purified anti-eEF1A2 antibody obtained through the same process (Helen Newbery, PhD thesis) was also used as a control.

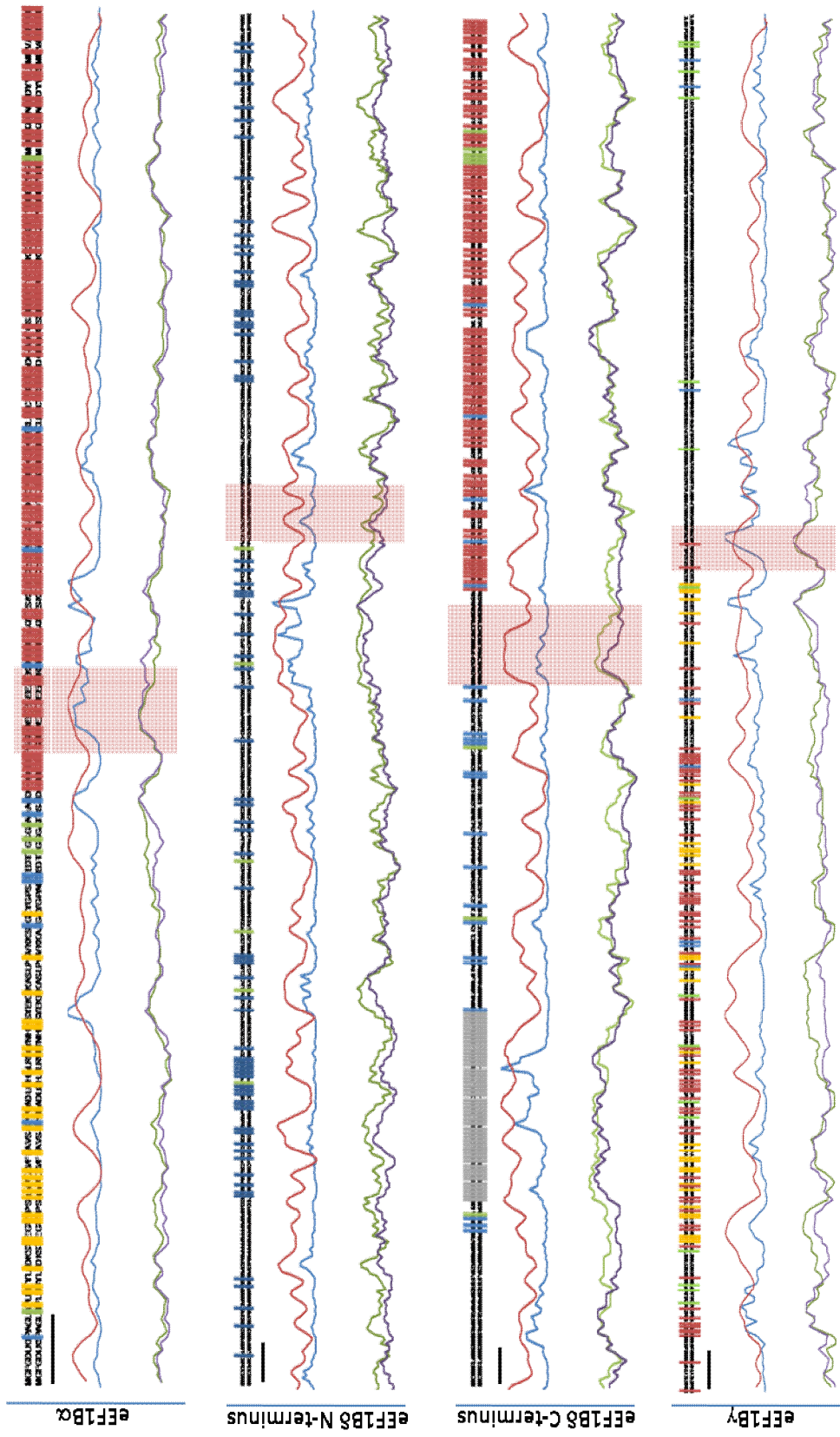


Figure 4.4 Protein characteristics and features and peptide sequence for each eEF1B subunit. Mouse and human aligned protein sequences, in which non-conserved residues are indicated in blue, SNPs in green, GST identical residues in yellow and eEF1B α , eEF1B δ , eEF1B γ or valyl-tRNA synthetase identical residues to eEF1B α , eEF1B δ and eEF1B γ respectively in red. Amino acids surface plotted in red, flexibility plotted in blue, Parker hydropathy plotted in green and

The ELISA showed greater response (higher absorbance at 450nm) of the sera raised against the peptide compared to the pre-immune serum or the anti-eEF1A2 antibody (Figure 4.5), suggesting specificity of the sera for the peptide against which it was raised.

To obtain the immunoglobulin component of the sera, the antibodies were purified using the ammonium sulphate precipitation. They were further purified against the peptide using a SulfoLink column to remove all non-specific bands on a Western blot.

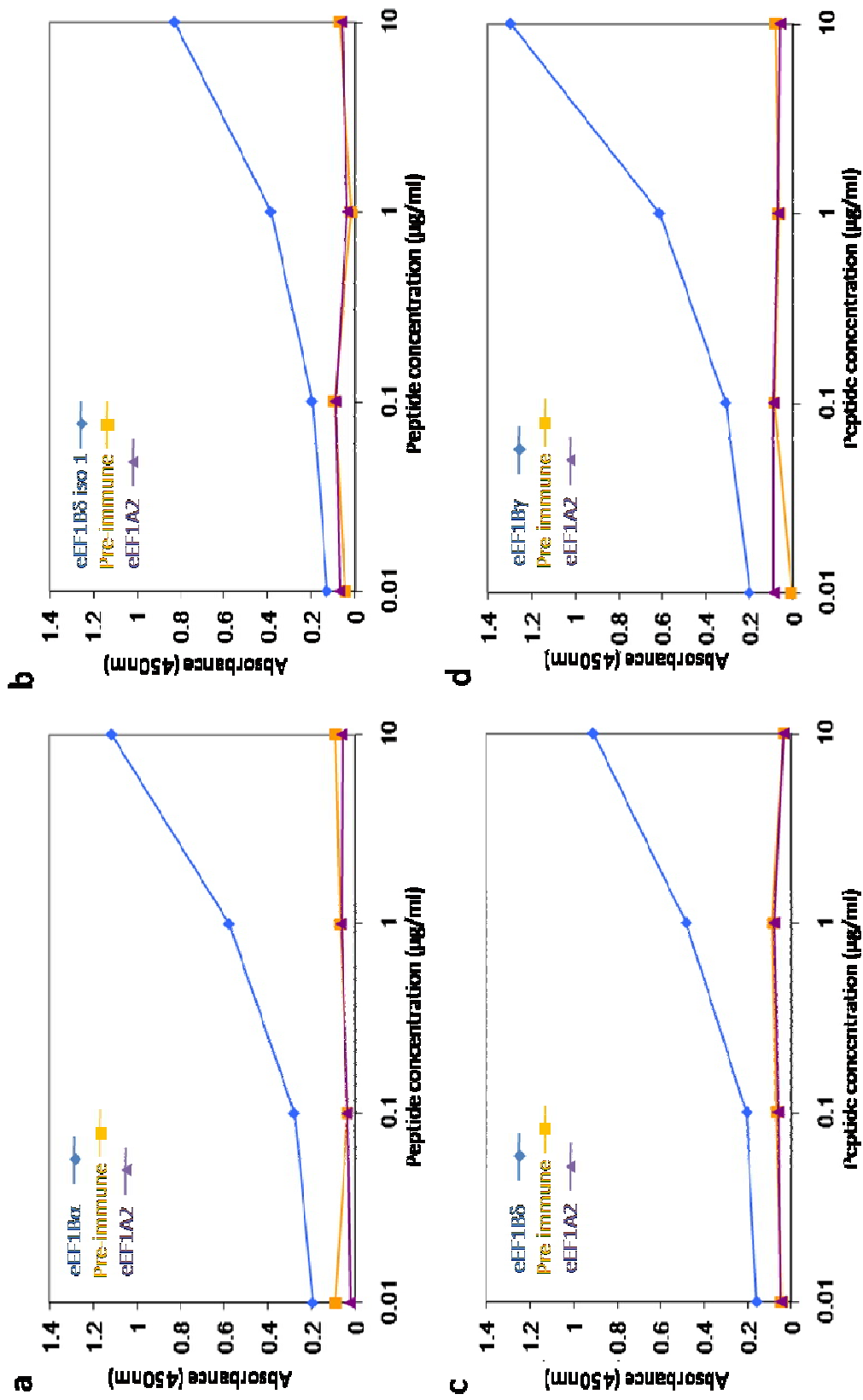


Figure 4.5 Antibody specificity for the peptide it was raised against measured by ELISA under peptide titration. Peptide was diluted at different concentrations, the antibodies that detect (a) eEF1B α , (b) eEF1B δ , (c) all isoforms of eEF1B δ and (d) eEF1B γ were incubated with the peptide, incubated with OPD substrate and absorbance read at 450nm. Increase in absorbance reflects increase in the binding of the antibody to the peptide. Pre-immune serum and anti-eEF1A2 antibody were used as a negative controls.

4.2.4 Protein expression in adult mouse tissues and cell lines

Although mRNA expression is important and showed ubiquitously expression of eEF1B α , eEF1B δ and eEF1B γ , with eEF1B δ showing multiple transcript variants, little is known about the expression of the cognate proteins. To determine the pattern of eEF1B subunit protein expression, proteins were extracted from a variety of mouse tissues and protein expression was analysed by Western blot with antibodies for eEF1B subunits and GAPDH as a control. Anti- α -tubulin, anti-eEF1A1 and anti-eEF1A2 antibodies were also used as tissue expression controls. In addition, commercial antibodies were later available from PTG (polyclonal anti-eEF1B2 and anti-eEF1D) and Abnova (nonoclonal anti-eEF1G) and most recently, the same samples were also analysed with Abcam monoclonal anti-eEF1B2, and Bethyl monoclonal anti-eEF1D and anti-eEF1G antibodies.

eEF1B α

Western blotting using the anti-eEF1B α antibody showed a band in brain and spinal cord tissues of around 50kDa and a smaller band of just above the predicted size (29 kDa; predicted 24.7kDa) in all tissues only when overexposed (Figure 4.6). A similar pattern was observed with the anti-eEF1B2 polyclonal antibody from PTG with the exception that the 50 kDa band was also consistently present in the heart and skeletal muscle tissues. The higher bands were consistently present even at extreme protein denaturing conditions such as DTT and β -mercaptoethanol and SDS. In addition, this higher band tissue expression correlates with eEF1A2 tissue-specific expression. However, the same tissue samples analysed with anti-eEF1B2 monoclonal antibody from Abcam only showed the smaller band of the predicted size in all the tissues tested. The eEF1B α 29kDa band seems to be weaker in heart and skeletal muscle tissues with all the antibodies.

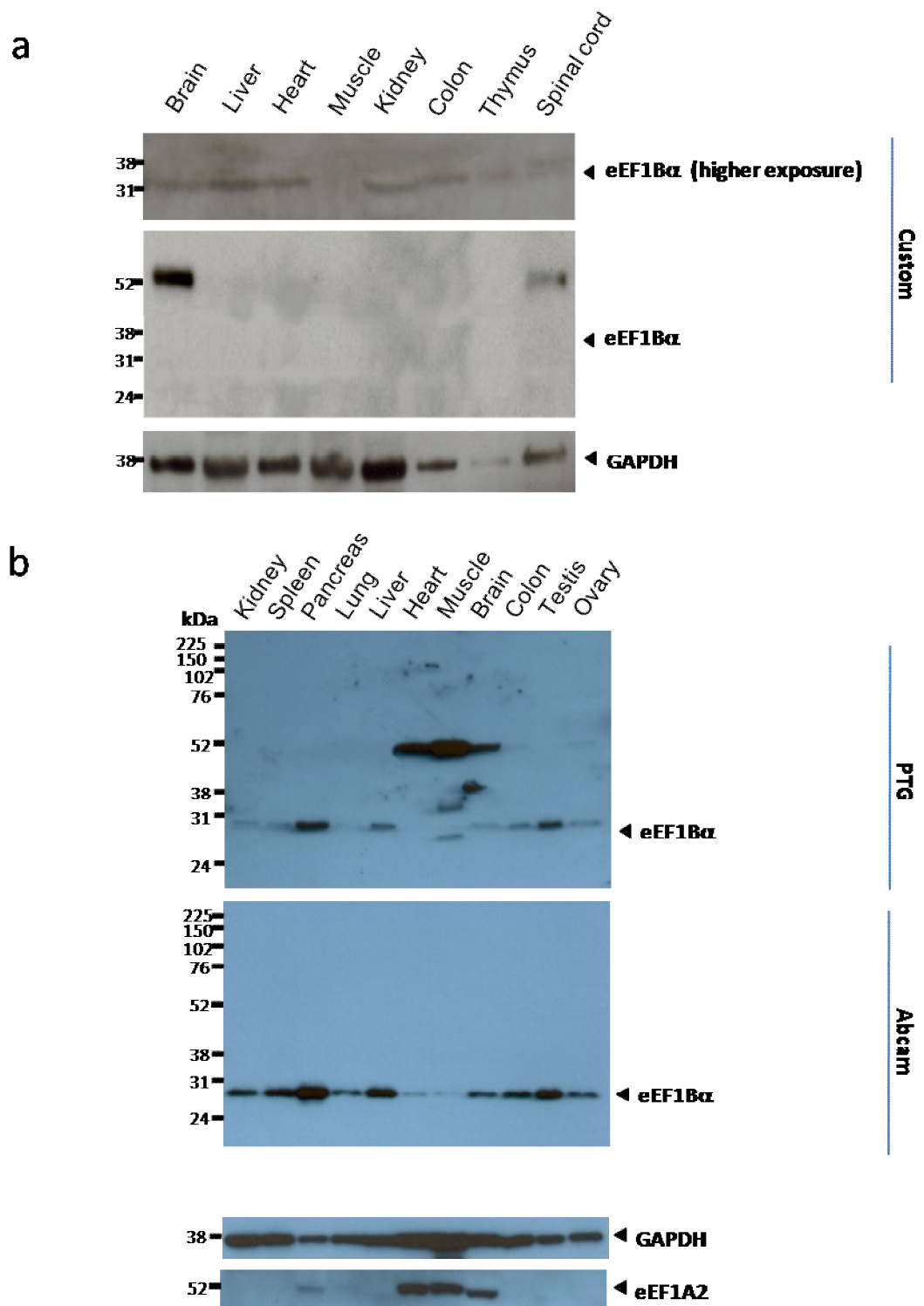


Figure 4.6 Immunoblot of eEF1B α expression in a mouse tissue panel. Protein was extracted from mouse tissues and analysed for eEF1B α protein expression by (a) eEF1B α antibody and by the (b) commercial eEF1B α antibodies from PTG (polyclonal) and Abcam (monoclonal), and eEF1A2 expression. GAPDH was used as a loading control.

eEF1B δ

Although the eEF1B δ antibodies recognised the peptide against which it was raised, it did not reveal any recognisable bands of the correct size using Western blotting hence those antibodies were not investigated further. Both anti-eEF1D antibodies from PTG and Bethyl detected several bands between 31kDa and 38kDa in all the tissues, the predicted size for transcript variant b being 31.3kDa (Figure 4.7). A slightly higher band around 38kDa was observed consistently on mouse skeletal muscle tissue but not in any of the other tissues. A higher band of around 75kDa was also observed in testis, brain and spinal cord tissues at longer exposure time with the predicted size for transcript variant a being 72.9kDa.

eEF1B γ

All the antibodies for eEF1B γ showed bands of the predicted size (50.1kDa) in all tissues (Figure 4.8). The anti-eEF1G antibody raised in rabbit showed similar amounts of eEF1B γ in all mouse tissues with exception of muscle tissue which showed lower protein expression compared with GAPDH. The commercial antibodies from Abnova and Bethyl showed similar amounts of eEF1B γ in all mouse tissues compared with GAPDH. In addition, since both of these antibodies were raised in mouse, bands around 52kDa and 25kDa are also present and are assumed to correspond to the immunoglobulin heavy chain and light chain respectively and the variance observed between tissues a reflection of the amount of immunoglobulin found in those tissues.

GADPH protein expression was detected in all the tissues tested, and eEF1A1 and eEF1A2 showed their expected tissue specific protein expression.

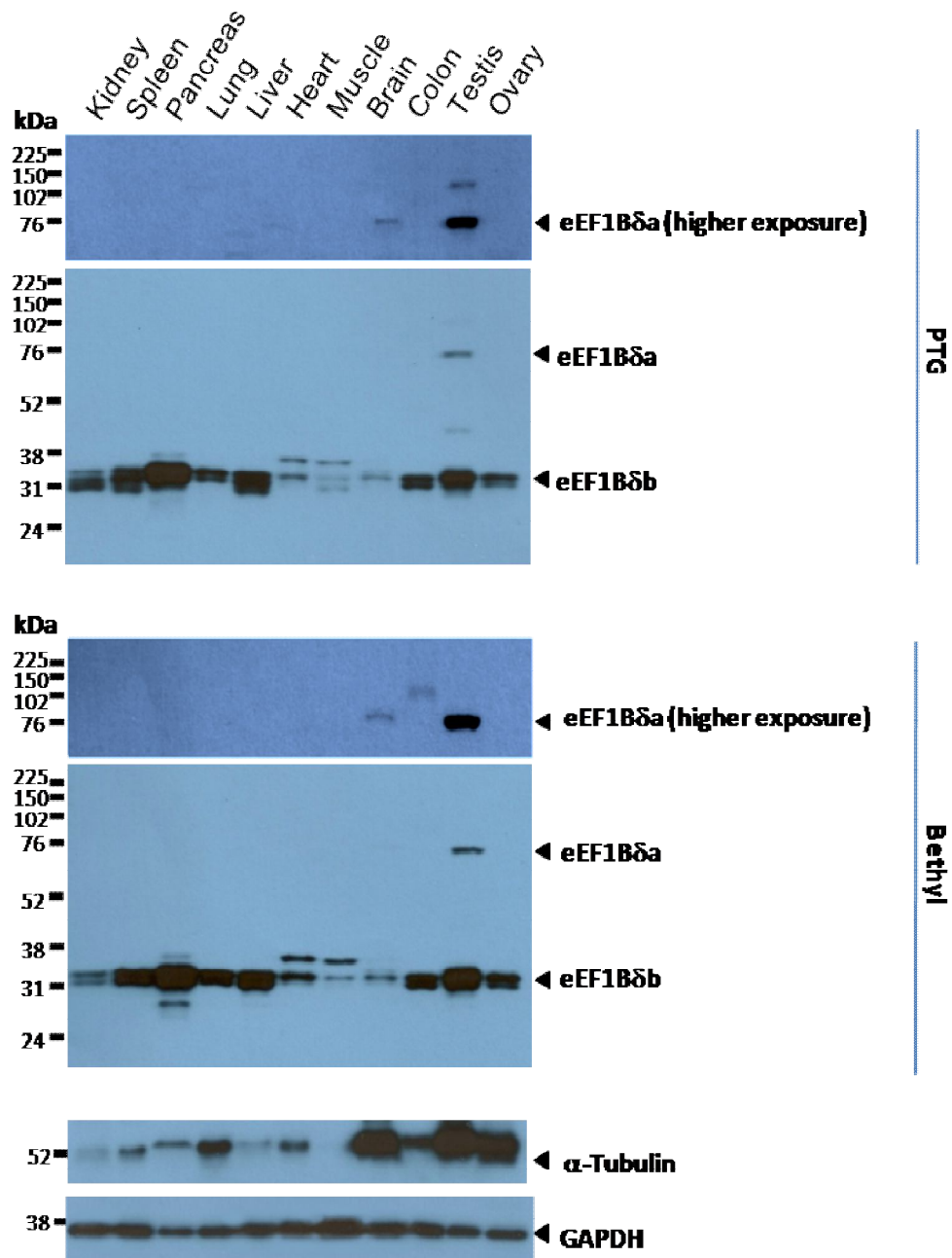


Figure 4.7 Immunoblot of eEF1B δ expression in a mouse tissue panel. Protein was extracted from mouse tissues and analysed for eEF1B δ protein expression by the commercial eEF1B δ antibodies from PTG (polyclonal) and Bethyl (monoclonal), and α -tubulin expression. GAPDH was used as a loading control.

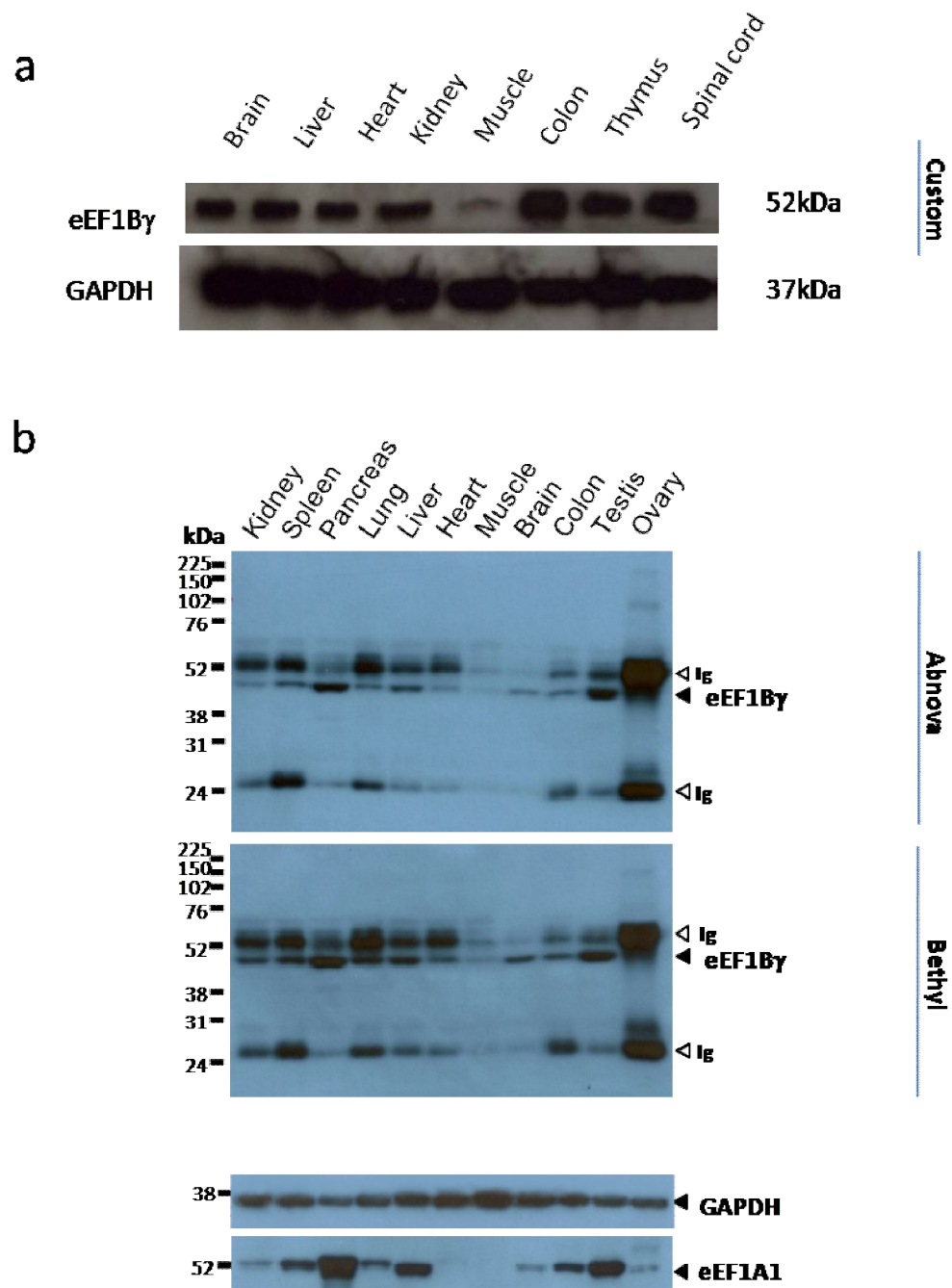


Figure 4.8 Immunoblot of eEF1B γ expression in a mouse tissue panel. Protein was extracted from mouse tissues and analysed for eEF1B γ protein expression by (a) eEF1B γ antibody and by the (b) commercial eEF1B γ antibodies from PTG and Bethyl, and eEF1A1 expression. GAPDH was used as a loading control. Immunoglobulins (Ig) both heavy and light chains can be observed because the antibodies were raised in the same species as the samples (mouse).

eEF1B subunits are present in all mouse tissues tested. These results suggest that eEF1B α has a possible heavier tissue specific isoform although there is no evidence from *in vitro* studies nor from mRNA transcripts. eEF1B δ has tissue specific isoforms and possibly the existence of more protein isoforms or post-translational modifications to account for the several bands seen in Western blots. In contrast, eEF1B γ appears to have only one protein isoform.

After purification of one bleed, the SulfoLink column kit was discontinued and replaced with another kit which involved a series of centrifugation steps and lower amounts. I was not able to obtain antibody concentration any higher than 0.1mg/ml. Even using dilutions as low as 1:2 it was not enough to visualise the bands on a Western blot that I had previously obtain with the sera purified with the previous kit. Commercial antibodies against eEF1B α and eEF1B δ from PTG and against eEF1B γ from Abnova were available by then and all of the experiments described in this thesis were done using those commercial antibodies unless otherwise stated.

Since the eEF1B subunits were found to be present in all adult mouse tissues studied, a variety of cell lines from different tissue origins and different species were examined for the expression of eEF1B subunits proteins analysed by Western blot with antibodies for eEF1B subunits and GAPDH as a control.

All three eEF1B subunits were detected at the protein level in all the cell lines tested (Figure 4.9). The species and cell types from which the cell lines arose are shown in table 2.4 (Chapter 2). eEF1B α showed stronger protein expression in HepG2 and NSC-34 and weaker in Lan5, NIH3T3, SHSY5Y, Rat2 and Cos7 compared with GAPDH. eEF1B α showed only one single band at the predicted size (29kDa). Immunoblotting with the antibody against eEF1B δ showed once again several bands between 31 and 38kDa in all cell lines. Rat2 cells showed very low eEF1B δ expression while all the other cell lines, except NSC-34 and HepG2, showed

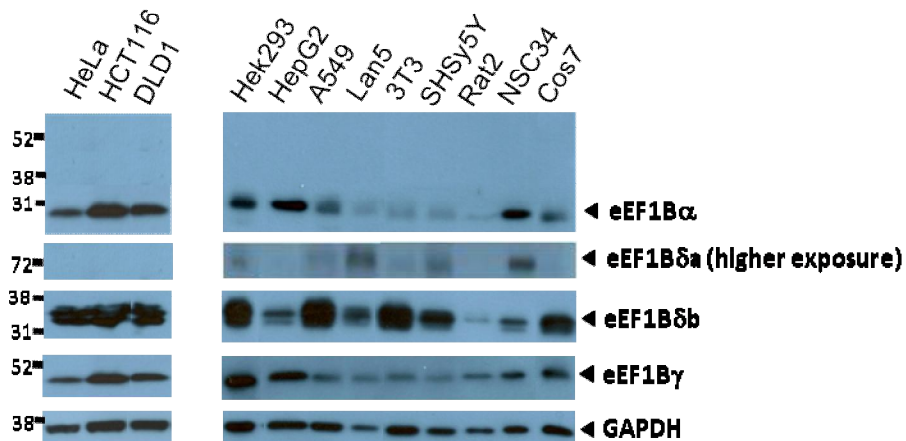


Figure 4.9 Immunoblot of eEF1B subunits expression in a variety of cell lines. Protein was extracted from different cell lines and analysed for eEF1B α , eEF1B δ and eEF1B γ protein expression. GAPDH was used as a loading control.

highly levels of protein expression compared with GAPDH. At a longer exposure time, higher bands of around 75Kda in the cell lines Lan5, SHSY5Y and NSC-34 were observed. eEF1B γ showed a similar expression to eEF1B α , stronger protein expression in HepG2 cell and weaker in A549, Lan5, NIH3T3 and SHSY5Y compared with GAPDH.

eEF1B subunits consistently showed protein expression in all the cell lines studied. The mouse brain, spinal cord and testis tissue-specific eEF1B δ isoform a was found to be present in the human neuroblastomas cell lines (Lan5 and SHSY5Y) and mouse neuroblastoma/motor neuron hybrid (NSC-34) but not in the other cell lines.

4.2.5 Mouse development

The complexity of the eEF1B subunits protein expression in adult mouse tissues together with the fact that expression of eEF1A1 and eEF1A2 change through mouse development (Chapter 1), raises the question of whether eEF1B subunits expression also changes through development and if so when? To address this question, proteins were extracted from a variety of mouse tissues at various stages of development and protein expression was analysed by Western blot with antibodies for eEF1B subunits and GAPDH as a control.

A Western blot with mouse brain and liver tissues ranging from embryonic to 4 months old mice showed protein expression pattern differences for eEF1B α and eEF1B δ but not eEF1B γ (Figure 4.10a) compared with GAPDH protein expression. eEF1B α were shown to be absent or at very low levels in both brain and liver from embryos 15.5 days. The protein levels of eEF1B α in post-natal brain and liver tissues were detectable and similar amongst all the development stages tested. Expression of eEF1B δ proteins ranging from 31-38kDa showed high levels in the embryonic stage and post-natal day 1 while all the other developmental stages tested showed moderate protein levels compared with GAPDH. GAPDH protein was present in all the tissues studied.

To study the protein expression of young mice before the eEF1A1/eEF1A2 switch, protein was extracted from 10days post natal mouse tissues and analysed by Western blot as previously described. No obvious difference in the protein expression of eEF1B subunits was observed from 10 days post-natal mice (Figure 4.10b) compared with adult mouse tissue protein expression (Figure 4.6-4.8).

To further investigate the protein expression change of eEF1B α and eEF1B δ in embryonic (E15.5 and E16.5) and new born mice (post-natal day 1), immunohistochemistry with eEF1B commercial antibodies was used to study the expression distribution in brain tissues. Immunohistochemistry using different antigen retrieval techniques was performed and always gave identical results indicating the likelihood of the signal being specific for each antibody. Incubation

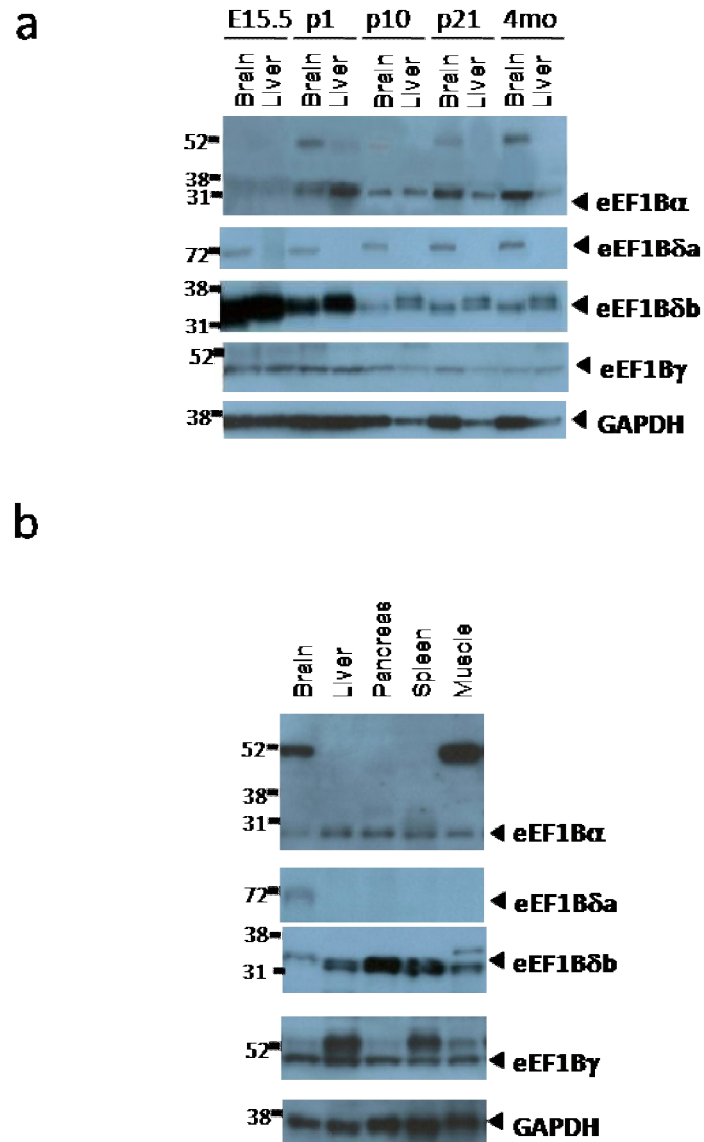


Figure 4.10 Immunoblot of eEF1B subunits expression during various mouse developmental stages. Protein was extracted from mouse tissues at different developmental stages and analysed for eEF1B α , eEF1B δ and eEF1B γ protein expression. **(a)** Brain and liver tissue eEF1B protein expression during embryonic and adult stages. **(b)** eEF1B protein expression in various tissues from P10 mice. GAPDH was used as a loading control.

with secondary antibody and in the absence of any primary antibody was used as a negative control.

Immunohistochemistry of transverse sections on embryonic brain mouse tissues, performed by Chris Beirne, showed consistently strong eEF1B α staining throughout the brain at E16.5 (Figure 4.11g-h) but absent or highly reduced staining at E15.5 (Figure 4.11e-f). The eEF1B α staining appeared to be cytoplasmic. eEF1B δ showed strong staining throughout the brain at E15.5 (Figure 4.11i-j) and E16.5 (Figure 4.11k-l) embryonic stages studied. The eEF1B δ staining at both embryonic stages was cytoplasmic although at E16.5 there is some potential nuclear staining. eEF1B γ showed strong staining in embryonic brain, similar at both E15.5 (Figure 4.11m-n) and E16.5 (Figure 4.11o-p) stages and it appeared to be both cytoplasmic and nuclear staining. The expression level of the eEF1B α higher molecular weight band correlated with the lower expected molecular weight suggesting dimer formation or a close relation. The negative control showed no staining (Figure 4.11a-d).

Immunohistochemistry of sagittal section of post-natal day 1 mouse brain showed strong expression of all eEF1B subunits. Anti-eEF1B α antibody stained strongly neurons in the brain cortex and moderate staining of the hippocampus (Figure 4.11s). eEF1B α also showed very strong cytoplasmic and nuclear staining in Purkinje cells and moderate to strong staining of the granular cells (Figure 4.11t). A similar staining profile was showed by eEF1B δ , with strong staining of neurons in the cortex, moderate staining in the hippocampus (Figure 4.11u), strong staining in Purkinje cells and some granular cells in addition to some areas of the molecular layer of the cerebellum (Figure 4.11v). As with eEF1B α , eEF1B δ also showed cytoplasmic and nuclear staining. The eEF1B γ staining in the hippocampus was weak and in brain cortex neurons was weak to moderate (Figure 4.11w). eEF1B γ stained strongly the cytoplasm and nuclei of Purkinje cells and weakly to moderately stained of the granular cells in the cerebellum (Figure 4.11x). The secondary only control showed no obvious staining (Figure 4.11q-r).

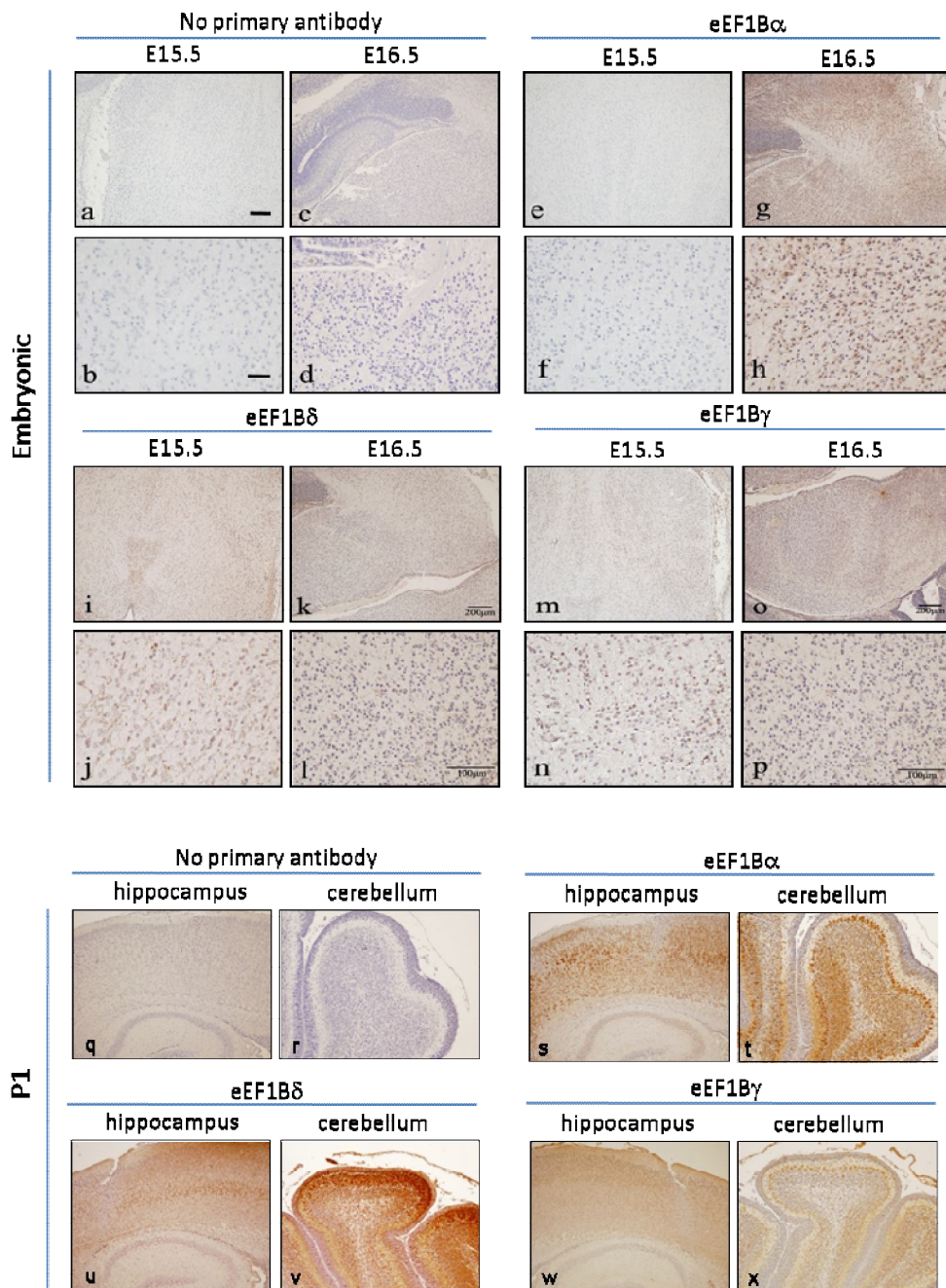


Figure 4.11 Immunohistochemical analysis of eEF1B subunits protein distribution in embryonic and post-natal day 1 mice. Proteins detected through primary antibody incubation, HRP mouse+rabbit secondary antibody and subsequent incubation with DAB. Positive signal is indicated by the presence of brown DAB reaction product. eEF1B α (e - h), eEF1B δ (c - g) and eEF1B γ (d - h) protein expression in E15.5 and E16.5 embryonic stage at two different magnifications. Performed by Chris Beirne. Incubation with secondary antibody only was used as negative control (a - e). Bar (top left micrograph) represents 200 and 50 μ m respectively. eEF1B α (s and t), eEF1B δ (u and v) and eEF1B γ (w and x) protein expression in post-natal day 1 mouse hippocampus and cerebellum. Incubation with secondary antibody only was used as negative control (q and r). Representative images shown. Bar (top left micrograph) represents 200 μ m.

These results point out that expression of eEF1B subunits differs throughout development, particularly with eEF1B α and eEF1B δ . The reduced eEF1B α protein expression at E15.5 was confirmed by Western blot and by immunohistochemistry. These results also suggest that the generally accepted eEF1B complex tertiary structure may be different at different stages of development as only eEF1B δ and eEF1B γ are detectable at E15.5. It is possible that a heterodimer eEF1B $\delta\gamma$ exists at some stages. Furthermore, these results also suggest the presence of eEF1B subunits in the cytoplasm and nuclei of some cells *in vivo*.

4.2.6 Immunohistochemical analysis of eEF1B subunits in a variety of mouse and human tissues

To better characterise the eEF1B subunits it was essential to study the expression distribution profile of eEF1B subunits in different cell types using normal adult mouse and human tissues. In order to investigate this, immunohistochemical analysis using eEF1B antibodies on a variety of mouse and human tissues was performed. The human tissues are from different ages and sex as shown in table 2.6 while the mouse tissues are all from the same mice. Secondary antibody only was used as a control. For the sake of simplicity, the analysis of tissues which were obtained from correspondent human and mouse organs are presented first, followed by the tissues for which a corresponding human sample was not available.

4.2.6.1 Liver

The liver has a diversity of functions including absorption, storage, synthesis and breakdown of a variety of substances. This includes, synthesis and secretion of plasma proteins, production and secretion of bile, storage of glycogen, synthesis of urea and degradation of drugs and toxic substances. The bulk of the liver is organized into lobules with a central vein and hepatocytes surrounding it. Hepatocytes are polygonal in shape, with distinct round nuclei, one or two prominent nucleoli and large cytoplasm. Hepatocytes can be in contact with either sinusoids or neighboring hepatocytes. The bile canaliculi network passes through the intercellular spaces of some neighboring hepatocytes, collecting and carrying bile towards bile ducts.

In the cross section of the human liver, eEF1B α showed weak staining in the cytoplasm of hepatocytes (Figure 4.12b). eEF1B δ also stained the cytoplasm of hepatocytes (Figure 4.12c). eEF1B γ presented widespread staining with some hepatocyte nuclei staining strongly (Figure 4.12d). Incubation with secondary

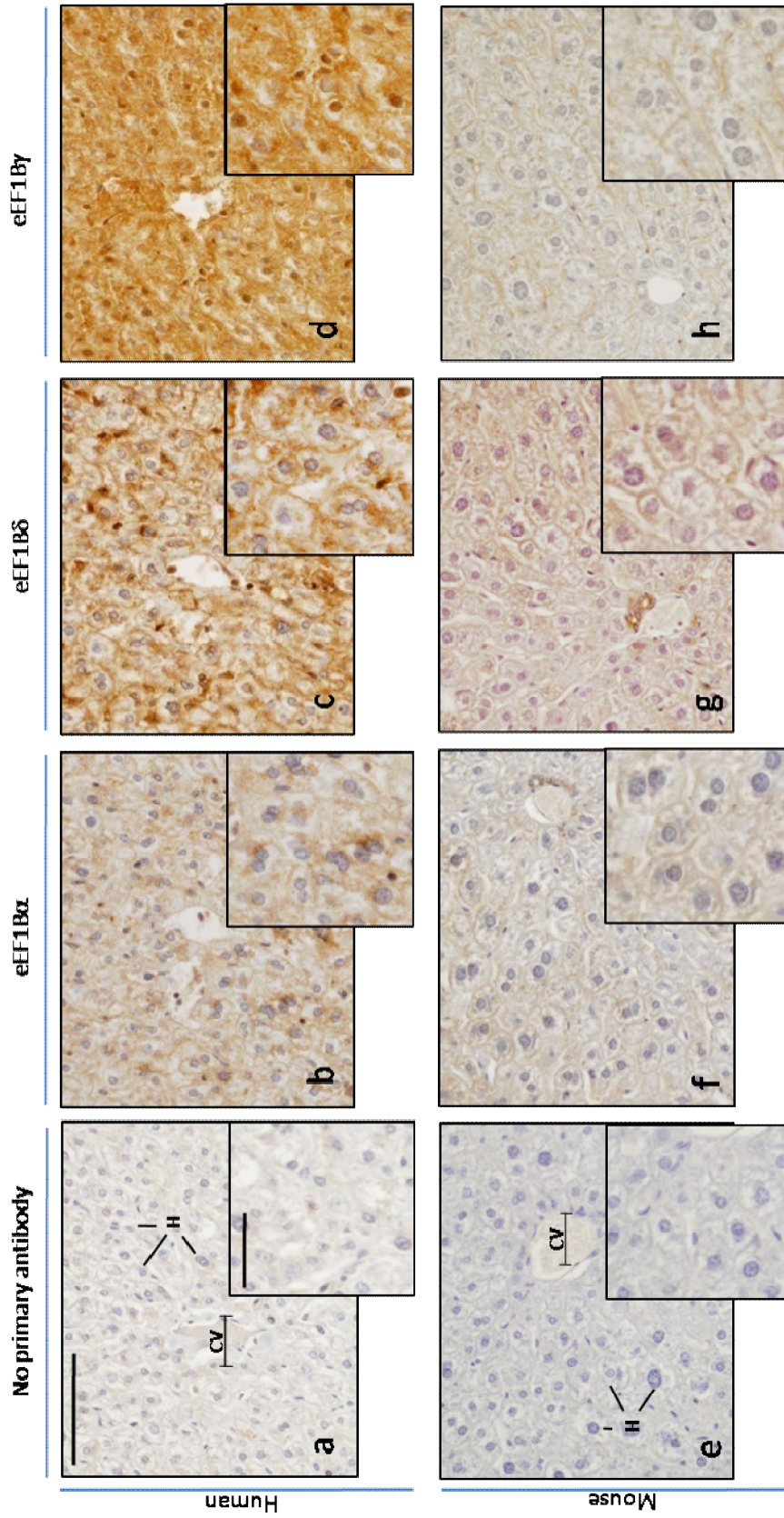


Figure 4.12 Immunohistochemical analysis of eEF1B subunits protein distribution in mouse and human liver. Proteins detected through primary antibody incubation, HRP mouse+rabbit secondary antibody and subsequent incubation with DAB. Positive signal is indicated by the presence of brown DAB reaction product. eEF1B α (b and f), eEF1B δ (c and g) and eEF1B γ (d and h) protein expression in human and mouse liver respectively at two different magnifications. Incubation with secondary antibody only was used as negative control (a and e). Representative images shown. Bar (top left micrograph) represents 100 and 50 mm respectively. CV – central vein; H – hepatocytes.

antibody, in the absence of any primary antibody, showed very weak staining restricted to the central vein (Figure 4.12a).

In mouse liver cross sections, the cytoplasm of hepatocytes were weakly stained by the anti-eEF1B α antibody (Figure 4.12f). eEF1B δ (Figure 4.12g) and eEF1B γ (Figure 4.12h) show a similar pattern of staining to eEF1B α . The no primary antibody control showed very weak staining restricted to the central vein (Figure 4.12e).

4.2.6.2 Lung

In the lung, large bronchioles are lined by ciliated columnar epithelium and smaller bronchioles by non-ciliated columnar epithelium. Small bronchioles branch into a cluster of alveoli where the gas exchange occurs. Alveoli consist mainly of single epithelial layer, numerous capillaries and connective tissue. Besides macrophages, in alveoli there are two major cell types. Pneumocytes type I are flattened cells which are unable to replicate. They form the simple squamous epithelium, thin lining that facilitates the gas exchange. Pneumocyte type II cells are cuboidal in shape and contain cytosomes, the source of pulmonary surfactant that coats alveoli essential to prevent collapsing of the alveoli.

In cross sections of the human lung, showing a number of alveoli, eEF1B α was found to stain strongly the cytoplasm of what appear to be pneumocyte type II cells and most of the pneumocyte type I cells as well apparent nuclear staining (Figure 4.13b). eEF1B δ stained heavily the cytoplasm of pneumocyte cells, including nuclear staining in a few cells (Figure 4.13c). eEF1B γ showed widespread staining both cytoplasmic and nuclear staining (Figure 4.13d). The negative control showed no staining (Figure 4.13a).

In the mouse lung cross sections, in addition to the alveoli, a large bronchiole and smooth muscle could be identified. Smooth muscle, the cytoplasm of pneumocyte cells and the nucleus of some pneumocyte cells were stained strongly by the anti-eEF1B α antibody (Figure 4.13f). Ciliated columnar epithelium

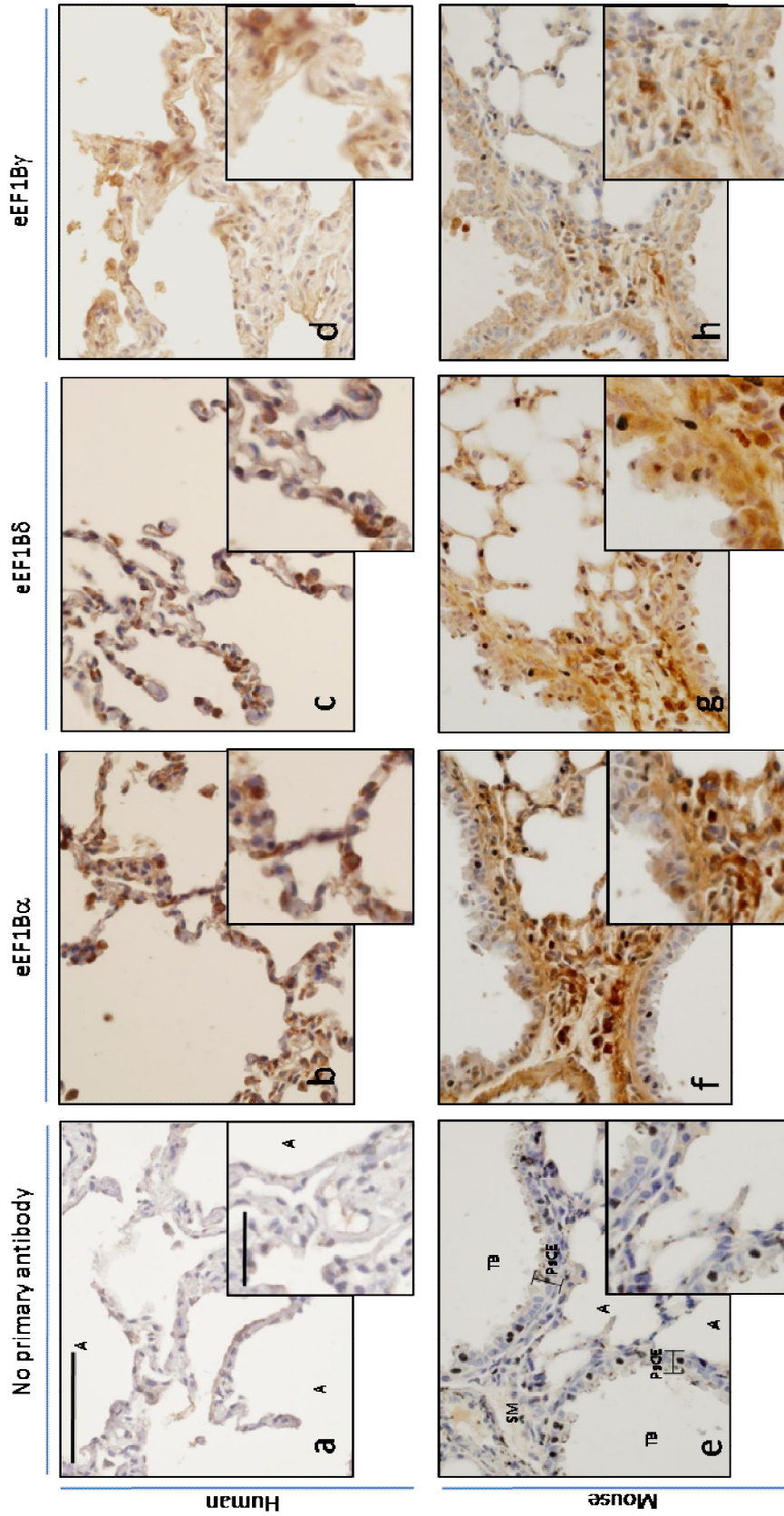


Figure 4.13 Immunohistochemical analysis of eEF1B subunits protein distribution in mouse and human lung. Proteins detected through primary antibody incubation, HRP mouse+rabbit secondary antibody and subsequent incubation with DAB. Positive signal is indicated by the presence of brown DAB reaction product. eEF1B α (b and f), eEF1B δ (c and g) and eEF1B γ (d and h) protein expression in human and mouse lung respectively at two different magnifications. Incubation with secondary antibody only was used as negative control (a and e). Representative images shown. Bar (top left micrograph) represents 100 and 50 mm respectively. A – alveolus; TB – terminal bronchiole; SM – smooth muscle; PsCE – pseudo-stratified columnar epithelium

from the large bronchiole present in this section showed little to no eEF1B α staining. eEF1B δ stained in smooth muscle, and showed widespread cytoplasmic expression of pneumocytes, nuclear expression in some pneumocytes and weak staining in the ciliated columnar epithelium of the bronchiole (Figure 4.13g). eEF1B γ showed smooth muscle staining, widespread cytoplasmic staining of pneumocytes and ciliated columnar epithelium of the bronchiole, with some pneumocytes showing stronger nuclear staining (Figure 4.13h). The secondary antibody only control showed some very dark staining nuclei (Figure 4.13e). This might indicate that the nuclear staining observed in some pneumocytes may be an artefact.

4.2.6.3 Spleen

The spleen has two major functional zones, the white pulp and red pulp. Around a central artery, the white pulp is arranged as a cylindrical sheath of lymphocytes, called periarteriolar lymphoid sheath (PALS) which is rich in T-lymphocytes. Follicles with a germinal centre may also be present rich in B-lymphocytes. The red pulp surrounds the white pulp. The red pulp consists of cords of Billroth (also known as splenic cords) surrounded by sinusoids and the red pulp is where the mechanical filtration of red blood cells occurs.

In human spleen, eEF1B α was found to stain heavily the white pulp, namely the cytoplasm of some lymphocytes, and in a few cases the cytoplasm and nucleus (Figure 4.14b). No eEF1B α staining was present in the red pulp. eEF1B δ staining was similar to eEF1B α (Figure 4.14c). eEF1B γ showed no or little staining in the white pulp (Figure 4.14d). However, eEF1B γ stained some splenic cells nuclei in the red pulp. The control secondary antibody showed some dark staining nuclei which may indicate that nuclear staining observed with the specific antibodies might be an artefact (Figure 4.14a).

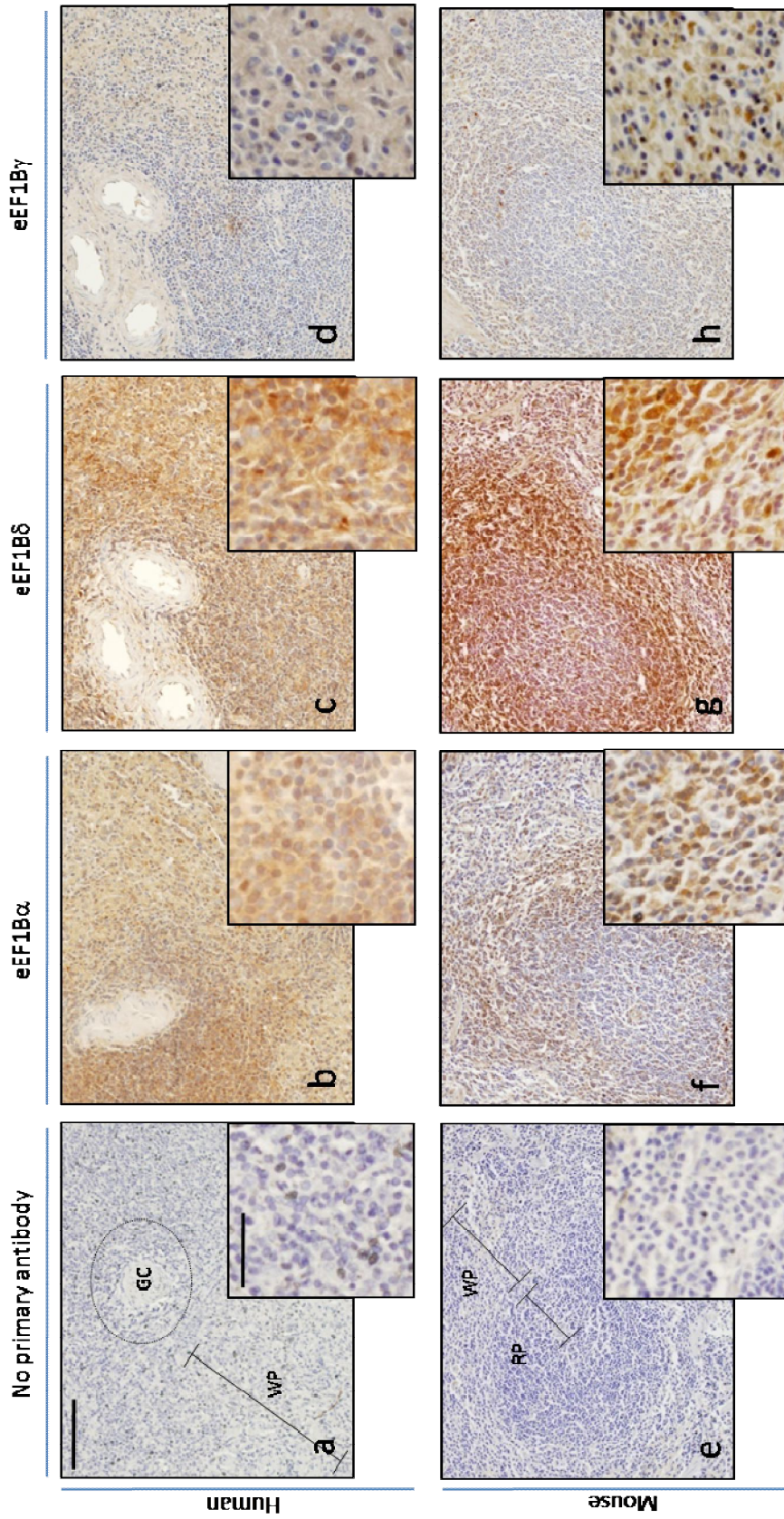


Figure 4.14 Immunohistochemical analysis of eEF1B subunits protein distribution in mouse and human spleen. Proteins detected through primary antibody incubation, HRP mouse+rabbit secondary antibody and subsequent incubation with DAB. Positive signal is indicated by the presence of brown DAB reaction product. eEF1B α (b and f), eEF1B δ (c and g) and eEF1B γ (d and h) protein expression in human and mouse spleen respectively at two different magnifications. Incubation with secondary antibody only was used as negative control (a and e). Representative images shown. Bar (top left micrograph) represents 200 and 50 mm respectively. GC – germinal center; WP – white pulp; RP – red pulp.

In mouse spleen cross sections, eEF1B α strong staining was found to be restricted to some lymphocytes, some of these showed exclusively cytoplasmic staining while others showed both cytoplasmic and nuclear staining (Figure 4.14f). The splenic red pulp was not stained by the anti-eEF1B α antibody. eEF1B δ stained strongly the cytoplasm and nuclei of lymphocytes and stained weakly the red pulp splenic cells (Figure 4.14g). eEF1B γ showed little staining of the white pulp. Heavy eEF1B γ staining was present in the red pulp splenic cells with some staining in the nuclei and cytoplasm (Figure 4.14h). The no primary antibody incubation control showed no staining (Figure 4.14e).

4.2.5.1 Kidney

The Nephron is the functional unit of the kidneys. It consists of a renal corpuscle and renal tubules. Renal corpuscles produce a plasma filtrate that is processed into urine by the tubules. The Bowman's capsule is the outer epithelial wall. The glomerulus is the little nest of cells which makes most of the corpuscle. It contains numerous capillaries and epithelial cells covering the capillaries called podocytes. Proximal tubules are long tortuous tubes that carry the fluid away from the Bowman's space. They reabsorb most minerals and other nutrients. Proximal tubules are lined by a simple cuboidal epithelium with microvilli at the apical end to provide increased surface area. The distal tubules are also convoluted but shorter than proximal tubules, with a smoother apical surface and smaller cells. Therefore it is more likely that in a section one will see a nucleus in every profile of distal tubules. In contrast, proximal tubule cells profiles may not show as many nuclei. It's lined by a simple cuboidal epithelium whose cells, unlike those of proximal tubules, have a smoother apical surface, conferring the appearance of a larger and clearer lumen.

eEF1B α in human kidney showed strong mostly cytoplasmic staining in distal tubules and podocytes and weak staining in the proximal tubules (Figure

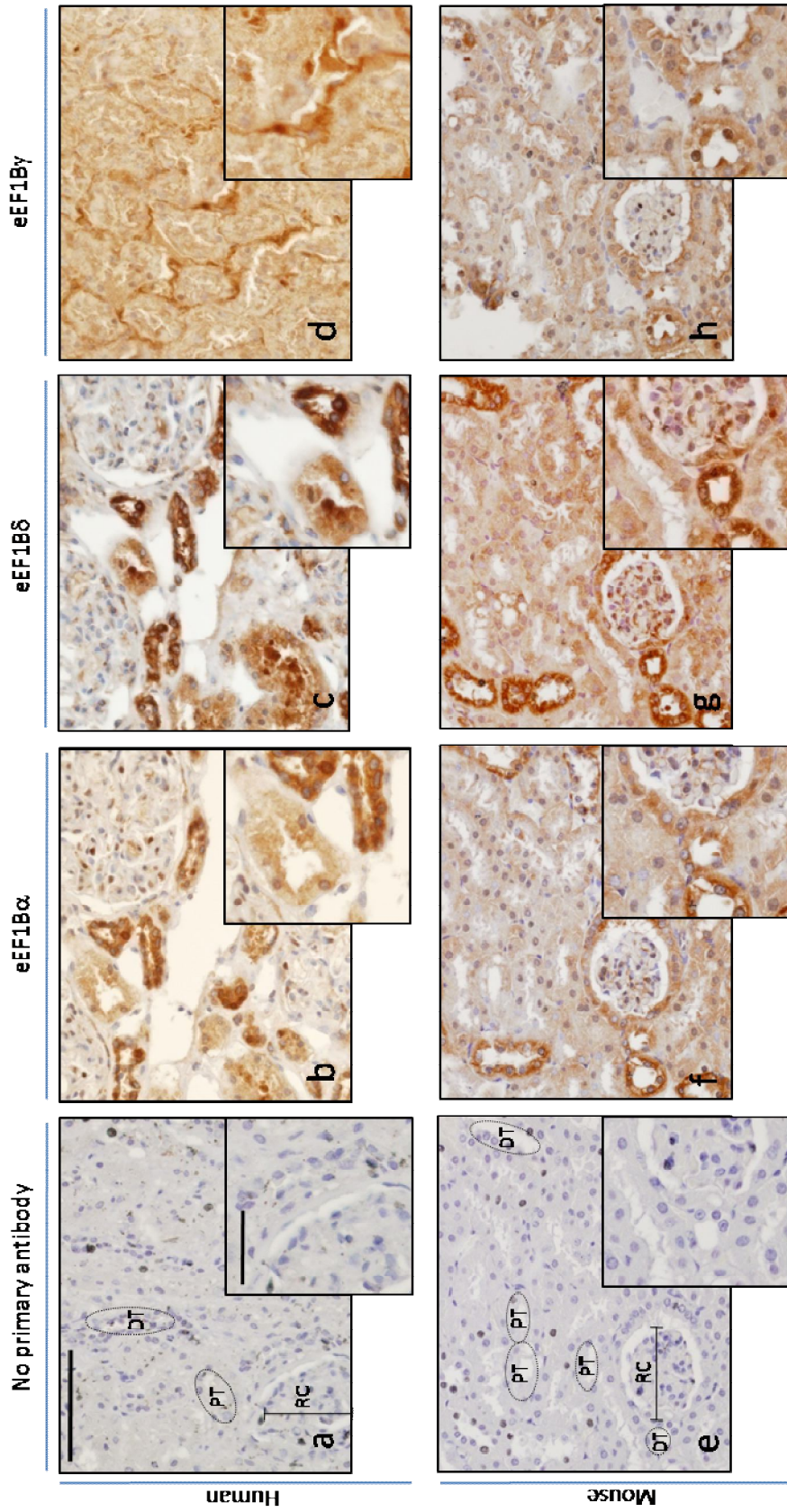


Figure 4.15 Immunohistochemical analysis of eEF1B subunits protein distribution in mouse and human kidney. Proteins detected through primary antibody incubation, HRP mouse+rabbit secondary antibody and subsequent incubation with DAB. Positive signal is indicated by the presence of brown DAB reaction product. eEF1B α (b and f), eEF1B δ (c and g) and eEF1B γ (d and h) protein expression in human and mouse kidney respectively at two different magnifications. Incubation with secondary antibody only was used as negative control (a and e). Representative images shown. Bar (top left micrograph) represents 100 and 50 mm respectively. RC – renal capsule; DT – distal tubulue; PT – proximal tubule

4.15b). In some distal tubules cells and podocytes, eEF1B α staining seemed to be nuclear as well as cytoplasmic. eEF1B δ expression pattern was found to be similar to eEF1B α in human kidney (Figure 4.15c). eEF1B γ showed widespread staining (Figure 4.15d). The control showed no staining (Figure 4.15a).

In mouse kidney, eEF1B α was found to stain strongly the cytoplasm of distal tubules, podocytes and Bowman's capsules epithelial cells and to stain weakly the proximal tubules (Figure 4.15f). eEF1B δ showed very strong cytoplasmic staining of the distal tubules epithelia, strong staining of the podocytes, moderate staining of the Bowman's capsules epithelia and weak staining of the proximal tubules epithelia (Figure 4.15g). Some cells of distal tubules and podocytes appeared to show cytoplasmic and nuclear staining. eEF1B γ showed wide spread staining, stronger in the cytoplasm of epithelial cells from distal tubules, podocytes and Bowmans's capsule epithelia (Figure 4.15h). Some cells appeared to have nuclear staining. The secondary antibody only control showed no staining (Figure 4.15e).

4.2.6.4 Pancreas

Pancreas is both an endocrine and exocrine gland. The exocrine part of the pancreas consists of tubuloacinar glands made up of pyramidal shapes cells clusters designated acini. These cells synthesise and secrete proteolytic enzymes into the intestine. The endocrine secretion of several hormones into blood is by the cells of the islets of Langerhans. Islets of Langerhans are small nests of cells scattered throughout the pancreas. The islets of Langerhans contain several endocrine cell types secreting insulin (beta cells), glucagon (alpha cells), somatostatin (delta cells), and pancreatic polypeptide (PP cells). These endocrine cells are difficult to distinguish in routine preparations but may be identified with special stains. Insulin stimulates the synthesis of glycogen, protein and fatty acids.

eEF1B α in cross section of the human pancreas showed widespread weak staining throughout the pancreas and very strong staining in all endocrine cells present in the pancreatic islets (Figure 4.16b). eEF1B δ expression is similar to eEF1B α with the exception that in the islets of Langerhans it stains moderately some endocrine cells (Figure 4.16c). On the other hand, eEF1B γ showed weak widespread staining, once again stronger in the pancreatic islets, in particular some endocrine cells (Figure 4.16d). The negative control showed no staining (Figure 4.16a).

In mouse pancreas, the islets of Langerhans stained very strongly for eEF1B α showing both cytoplasmic and nuclear staining (Figure 4.16f). eEF1B δ showed weak to moderate staining in some nuclei of pancreatic cells, moderate staining of the nuclei pancreatic islets and some endocrine cells were stained strongly (Figure 4.16g). eEF1B γ showed a similar pattern of expression to eEF1B δ except that more pancreatic cells were stained strongly (Figure 4.16h). The no primary antibody incubation control showed no staining (Figure 4.16e).

4.2.6.5 Skeletal muscle

Skeletal muscle consists of long, tubular cells also designated muscle fibers. In muscle fiber is a multinucleate cell where most nuclei are located in the periphery of the muscle fiber.

In longitudinal sections of human skeletal muscle, where cross-striations may be seen, eEF1B α showed cytoplasmic weak staining (Figure 4.17b), as did eEF1B δ (Figure 4.17c) and eEF1B γ (Figure 4.17d). The negative control showed no staining (Figure 4.17a).

Both eEF1B α (Figure 4.17f) and eEF1B δ (Figure 4.17g) showed staining of the cytoplasm in mouse skeletal muscle sections, whereas eEF1B γ stained weakly the cytoplasm and strongly the nuclei of muscle cells (Figure 4.17h). The no primary antibody incubation control showed no staining (Figure 4.17e).

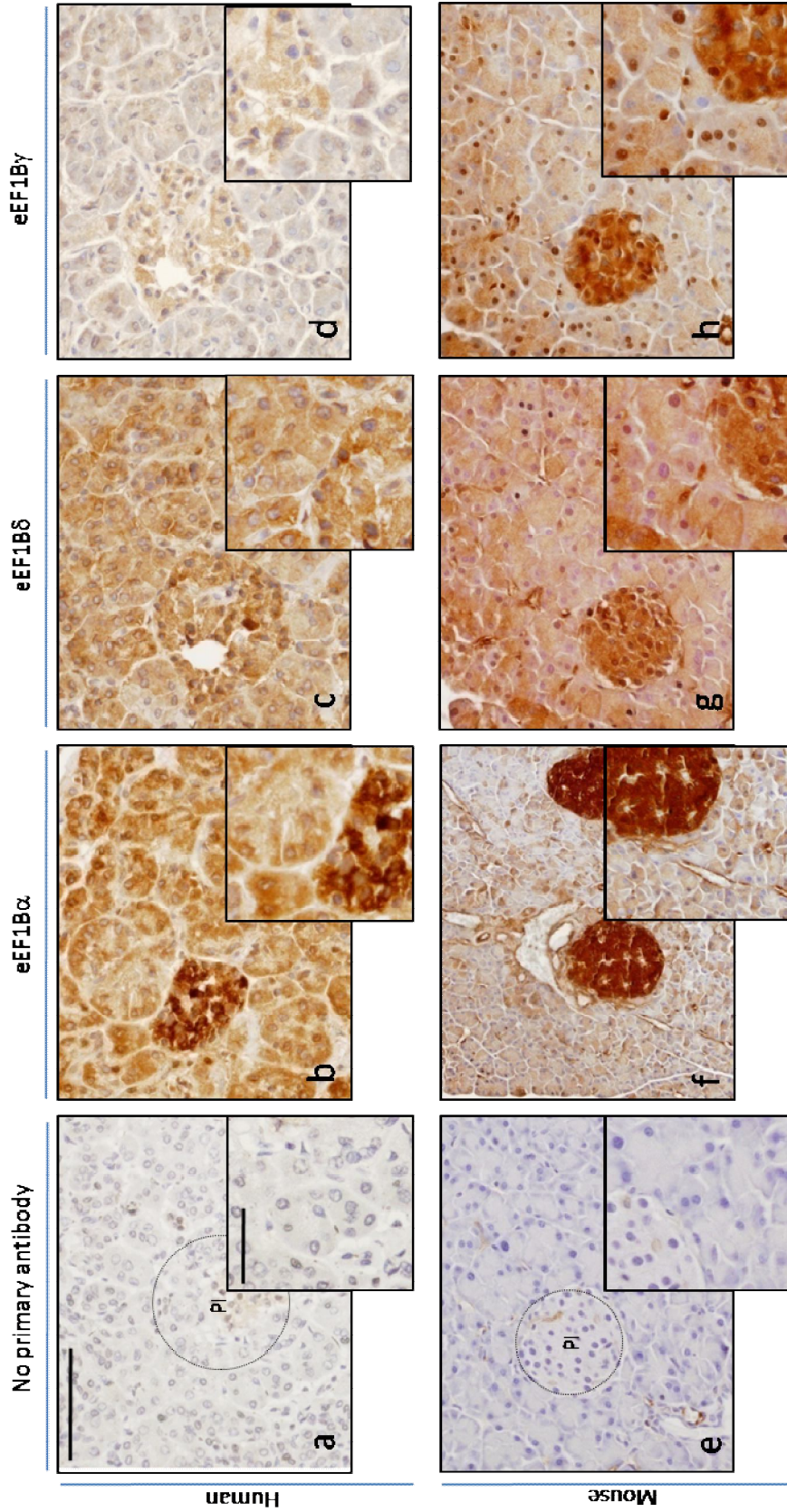


Figure 4.16 Immunohistochemical analysis of eEF1B subunits protein distribution in mouse and human pancreas. Proteins detected through primary antibody incubation, HRP mouse+rabbit secondary antibody and subsequent incubation with DAB. Positive signal is indicated by the presence of brown DAB reaction product. eEF1B α (b and f), eEF1B δ (c and g) and eEF1B γ (d and h) protein expression in human and mouse pancreas respectively at two different magnifications. Incubation with secondary antibody only was used as negative control (a and e). Representative images shown. Bar (top left micrograph) represents 100 and 50 mm respectively. PI – pancreatic islets

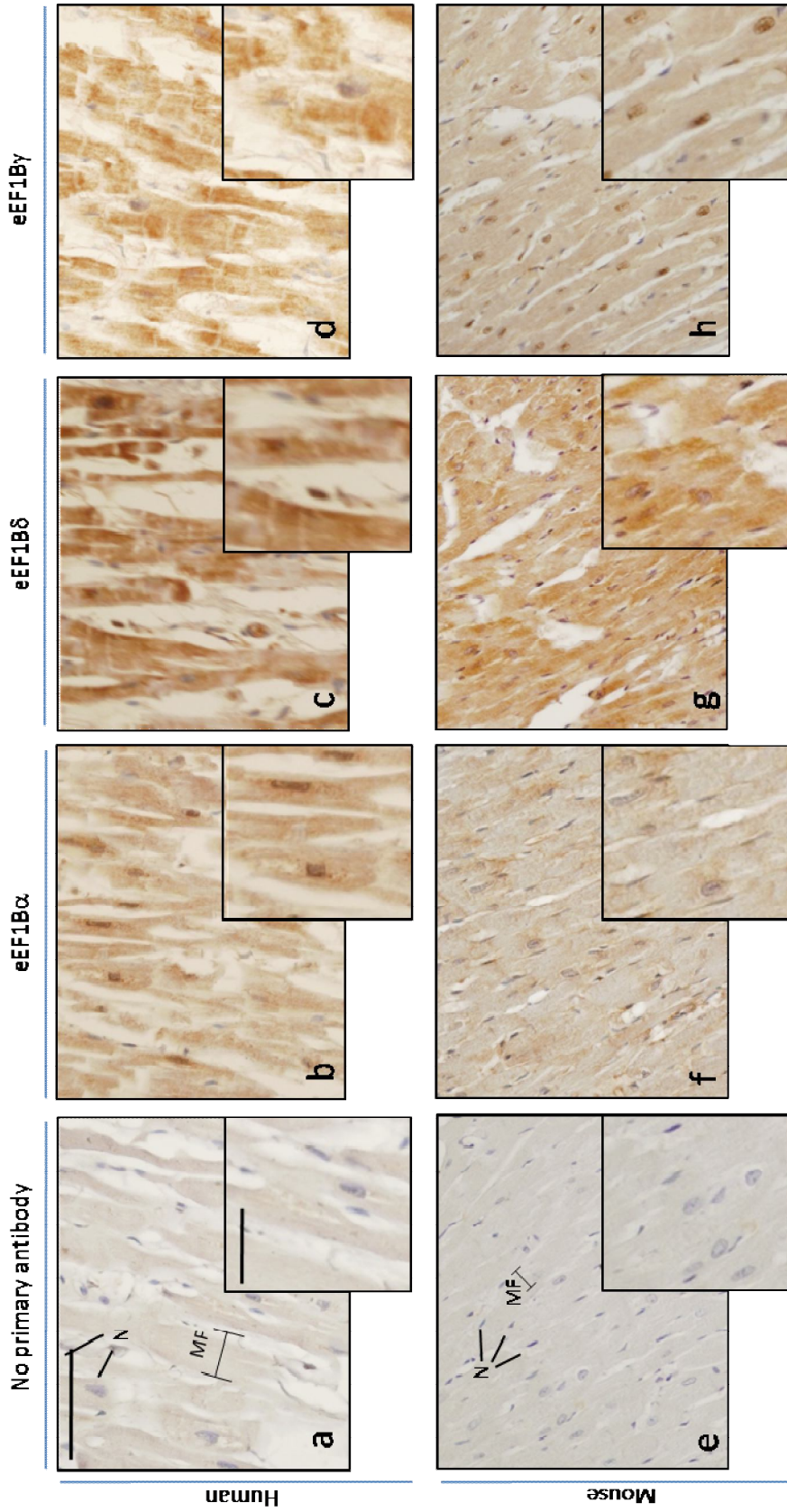


Figure 4.17 Immunohistochemical analysis of eEF1B subunits protein distribution in mouse and human skeletal muscle. Proteins detected through primary antibody incubation, HRP mouse+rabbit secondary antibody and subsequent incubation with DAB. Positive signal is indicated by the presence of brown DAB reaction product. eEF1B α (b and f), eEF1B δ (c and g) and eEF1B γ (d and h) protein expression in human and mouse skeletal muscle respectively at two different magnifications. Incubation with secondary antibody only was used as negative control (a and e). Representative images shown. Bar (top left micrograph) represents 100 and 50 μ m respectively. MF – muscle fiber; N – nuclei of muscle cells

4.2.6.6 Heart

Cardiac muscle consists of muscle cells with one central nucleus. Cardiac muscle cells often form acute angles and are connected by intercalated discs. Unlike skeletal muscle, each cardiac muscle cell may attach to two or more other cells giving the appearance of branching. Cross-striations may also be seen.

eEF1B α showed widespread cytoplasmic staining with some nuclei staining strongly in a cross section of human heart muscle (Figure 4.18b). A similar expression pattern was observed for eEF1B δ (Figure 4.18c) and eEF1B γ (Figure 4.18d). The secondary antibody only control showed no staining (Figure 4.18a).

Longitudinal sections of mouse heart muscle incubated with eEF1B α antibody showed cytoplasmic staining, particularly strong around the nucleus (Figure 4.18f). Furthermore, eEF1B δ showed widespread cytoplasmic staining of the heart muscle cells (Figure 4.18g). However, eEF1B γ showed in addition to widespread cytoplasmic staining, strong staining in some nuclei but absent in others (Figure 4.18h). The negative control showed no staining (Figure 4.18e).

4.2.6.7 Brain

The cerebral cortex has a complex composition, with many different nerve cell types. These include many local interneurons, such as stellate and granule cells, as well as much larger and conspicuous pyramidal cells. The cerebral cortex is traditionally divided into layers with roughly similar features. The molecular layer (layer I) is the outermost layer, which contains relatively few nerve cell bodies. It is composed largely of dendrites, axon terminals and glial cells. The outer granular layer (layer II) typically contains many small cells (granule cells). The outer pyramidal layer (layer III) contains the cell bodies of small pyramidal cells. The inner granular layer (layer IV) contains axons such as sensory axons from the thalamus. The inner pyramidal layer (layer V) contains cell bodies of large pyramidal cells. Axons from pyramidal cells typically project to more distant

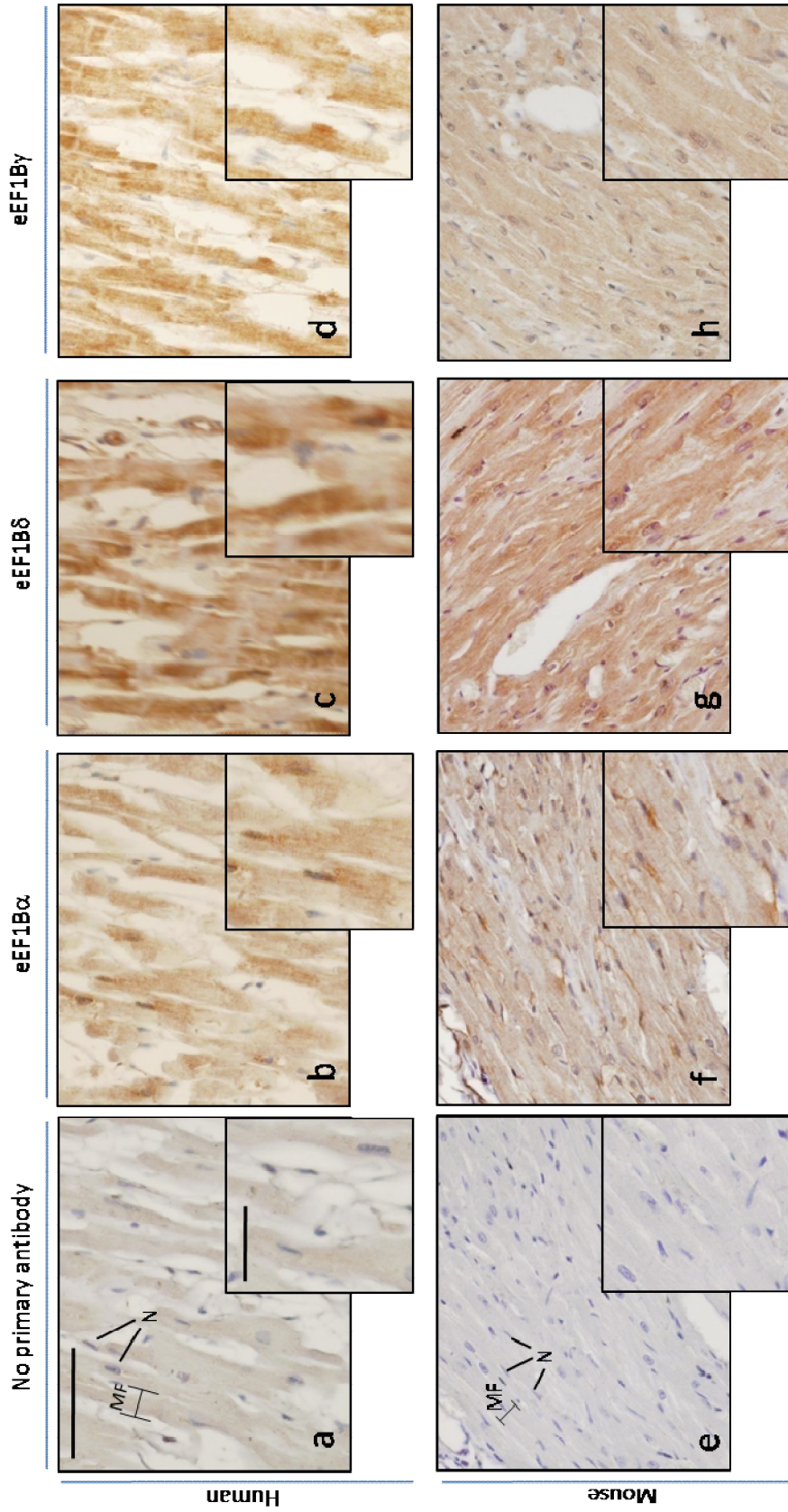


Figure 4.18 Immunohistochemical analysis of eEF1B subunits protein distribution in mouse and human cardiac muscle. Proteins detected through primary antibody incubation, HRP mouse+rabbit secondary antibody and subsequent incubation with DAB. Positive signal is indicated by the presence of brown DAB reaction product. eEF1B α (b and f), eEF1B δ (c and g) and eEF1B γ (d and h) protein expression in human and mouse cardiac muscle respectively at two different magnifications. Incubation with secondary antibody only was used as negative control (a and e). Representative images shown. Bar (top left micrograph) represents 100 and 50 μ m respectively. MF – muscle fiber; N – nuclei of muscle cells

cortical regions, to other parts of the brain or to lower centres such as spinal motor neurons. Layer VI is a layer of pleiomorphic cells, containing cells of varied size and shape. The cytoplasm of many neurones contains fairly large amounts of rough endoplasmic reticulum which may aggregate to form Nissl-bodies. Axons are processes specialised for conducting signals from one nerve cell to another. Dendrites are processes specialised for receiving and integrating signals from other nerve cells.

CNS tissue also contains several types of non-neuronal, supporting cells, neuroglia. Astrocytes (or astroglia) are star-shaped cells that provide metabolic and physical support to the neurones. Oligodendrocytes (or oligoglia) have fewer and shorter processes and they form myelin sheaths around axons. Microglia are small cells with complex shapes and their function is similar to macrophages. Glial cell nuclei are smaller than those of neurones, oval in shape with heterochromatin bundles, and no obvious cytoplasm.

In a human section of the brain eEF1B α showed strong cytoplasmic and moderate nuclear staining in some neurones and no staining in others (Figure 4.19b). eEF1B δ was found to stain very strongly the cytoplasm of some neurones, showed moderate nuclear and cytoplasmic staining of another sub-population of neurones and no staining in others (Figure 4.19c). eEF1B γ showed weak cytoplasmic staining of neurones as well as staining of the axons (Figure 4.19d). The no primary antibody incubation control showed no staining (Figure 4.19a).

eEF1B α in a mouse brain section showed cytoplasmic staining in a sub-population of neurones and in other neuronal cells no signal was detected (Figure 4.19f). Once again, eEF1B δ showed varied staining of neurones, some cytoplasmic staining, some strong nuclear staining and others no staining was observed (Figure 4.19g). eEF1B γ also showed a varied staining of the neurones with some staining and others not (Figure 4.19h). The control secondary antibody showed no staining (Figure 4.19e).

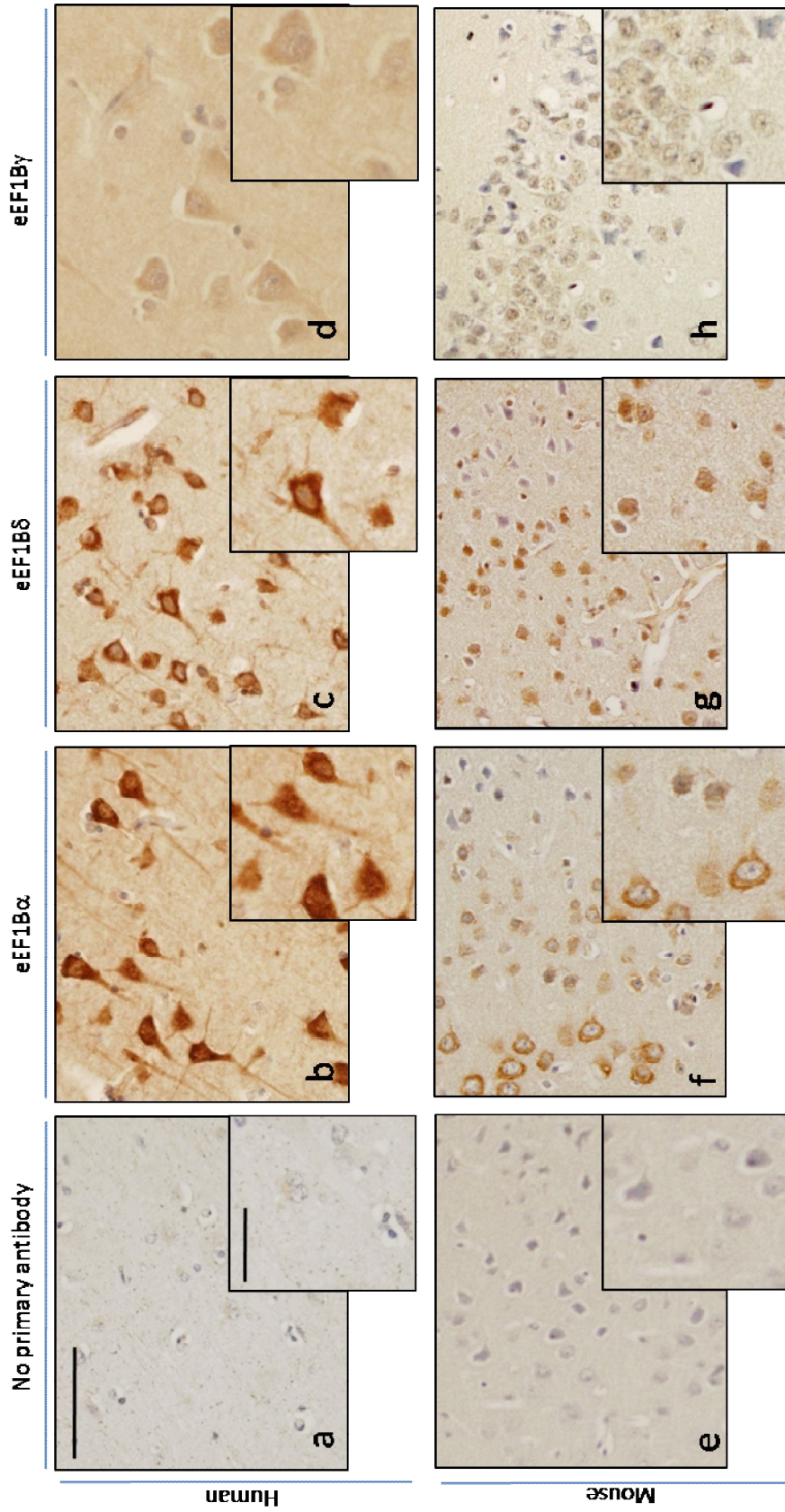


Figure 4. 19 Immunohistochemical analysis of eEF1B subunits protein distribution in human brain and mouse frontal lobe cortex brain. Proteins detected through primary antibody incubation, HRP mouse+rabbit secondary antibody and subsequent incubation with DAB. Positive signal is indicated by the presence of brown DAB reaction product. eEF1B α (b and f), eEF1B δ (c and g) and eEF1B γ (d and h) protein expression in human and mouse brain respectively at two different magnifications. Incubation with secondary antibody only was used as negative control (a and e). Representative images shown. Bar (top left micrograph) represents 100 and 50 mm respectively.

4.2.6.8 Spinal cord

Spinal cord consists of white matter surrounding the dorsal and ventral horns, and the grey matter where the neurons are present. Spinal motor neurons are present in the ventral horn and have very long axons in the peripheral nerves extending out to the muscles.

In a mouse spinal cord transverse section eEF1B α showed very strong cytoplasmic and nuclear staining in some motor neurons, slightly weaker in others and just perinuclear staining or no staining in others (Figure 4.20b). eEF1B δ showed a similar expression pattern to eEF1B α but with stronger nuclear than cytoplasmic staining (Figure 4.20c). eEF1B γ showed weak cytoplasmic and strong nuclear staining in some motor neurons and moderate cytoplasmic and nuclear in other motor neurons, in addition, it showed apparently nuclear staining in other cells (Figure 4.20d). NeuN stained neurons and was used as a neuronal specific marker (Figure 4.20e). The negative control showed no staining (Figure 4.20a).

4.2.6.9 Colon

The main function of the colon is the reabsorption of water and inorganic salts. The mucosa has a simple columnar epithelium shaped into straight tubular crypts, crypts of Lieberkuhn. The Goblet cells are interspersed among absorptive cells and secrete mucus. The crypts are separated by the lamina propria, consisting of connective tissue, white blood cells, capillaries and smooth muscle. The muscularis mucosa forms a thin layer of muscle fibres beneath the ends of the crypts and the mucosa externa consists of smooth muscle.

A transverse or cross section of mouse colon tissue shows the packed arrangement of glands in the mucosa, in which eEF1B was detected in the columnar

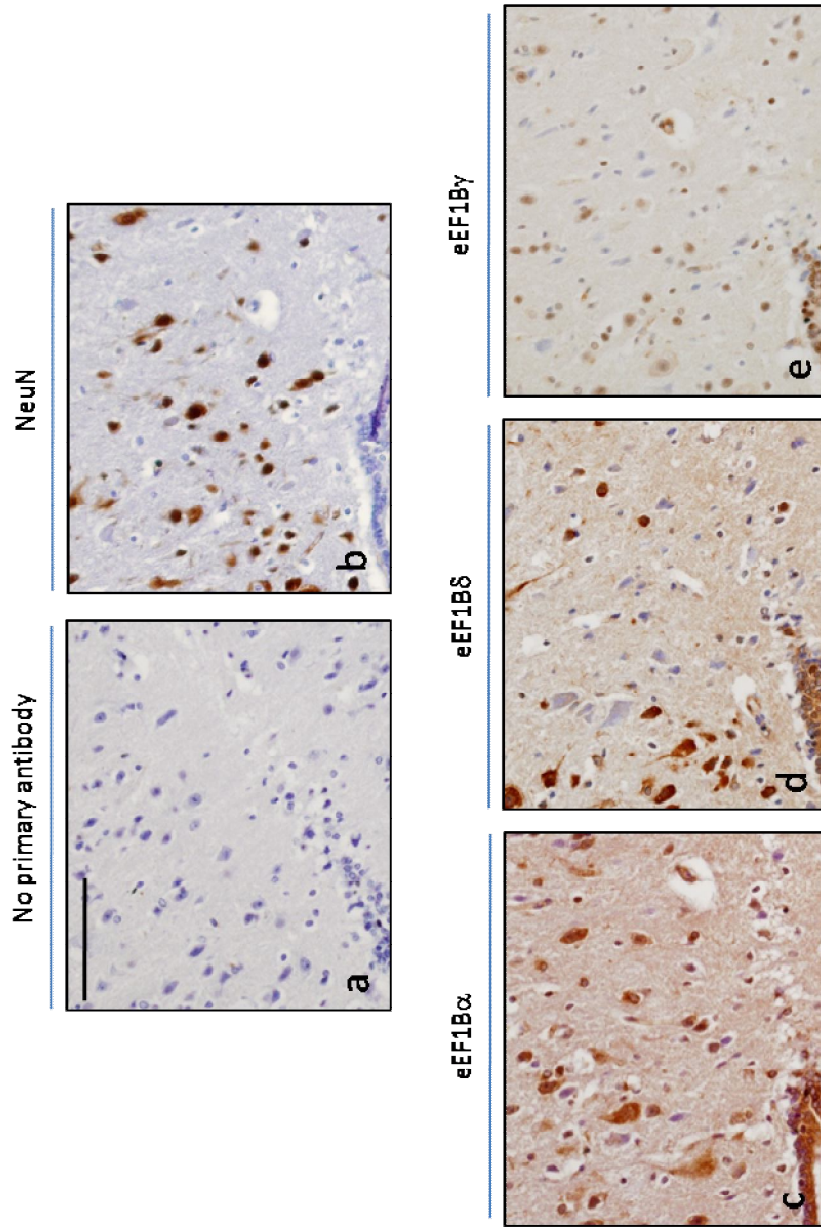


Figure 4.20 Immunohistochemical analysis of eEF1B subunits protein distribution in mouse spinal cord. Proteins detected through primary antibody incubation, HRP mouse+rabbit secondary antibody and subsequent incubation with DAB. Positive signal is indicated by the presence of brown DAB reaction product. eEF1B α (c), eEF1B δ (d) and eEF1B γ (e) protein expression in mouse spinal cord. Incubation with secondary antibody only was used as negative control (a). NeuN was used as a neuronal specific marker (b). Representative images shown. Bar (top left micrograph) represents 100 μ m.

epithelium of the mucosa. eEF1B α (Figure 4.21b), eEF1B δ (Figure 4.21c) and eEF1B γ (Figure 4.21d) showed varied staining that is difficult to interpret. The secondary antibody only control showed no staining (Figure 4.21a).

4.2.6.10 Testis

The testis is responsible for the production of the spermatozoa and the secretion of hormones. The testis is surrounded by a capsule, the tunica albuginea and the bulk consists of lobules with seminiferous tubules. Interstitial cells that lie in the space between adjoining tubules consist mostly of Leydig cells (small round nucleus), the main source of testosterone in the male. Sertoli cells are non-proliferating cells easily recognised by their elongated, pale-staining nucleus and conspicuous nucleolus. The spermatogenic cells consist of successive generations arranged in concentric layers. The spermatogonia are found at the periphery. Spermatocytes, which have large round nuclei with a distinctive chromatin pattern (reorganised chromatin), lie above the spermatogonia. The spermatid population consists of one or two generations and are located closest to the lumen.

Cross sections of mouse testis showed strong cytoplasmic staining for eEF1B α (Figure 4.22b) and eEF1B δ (Figure 4.22c) in the lobular cells with some cells also showing weak staining that appears to be nuclear, whereas eEF1B γ showed a strong nuclear and weak cytoplasmic staining (Figure 4.22d). The no primary antibody incubation control showed no staining (Figure 4.22a).

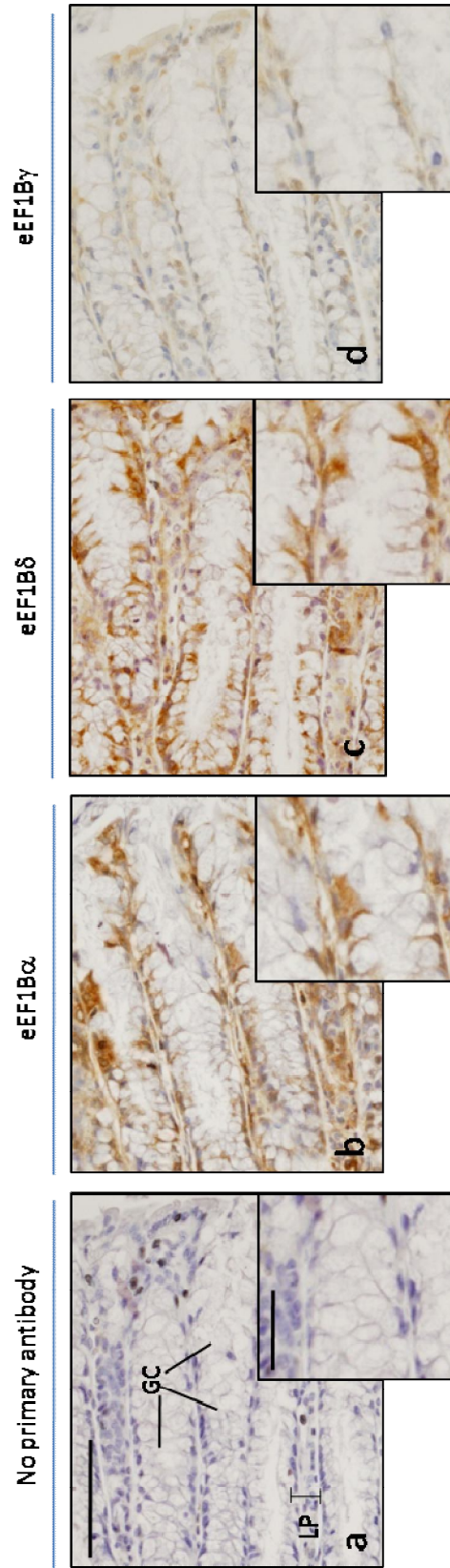


Figure 4.21 Immunohistochemical analysis of eEF1B subunits protein distribution in mouse colon. Proteins detected through primary antibody incubation, HRP mouse+rabbit secondary antibody and subsequent incubation with DAB. Positive signal is indicated by the presence of brown DAB reaction product. eEF1B α (b), eEF1B δ (c) and eEF1B γ (d) protein expression in mouse colon. Incubation with secondary antibody only was used as negative control (a). Representative images shown. Bar (top left micrograph) represents 100 μ m and 50 μ m respectively. LP – lamina propria; GC – goblet cells.

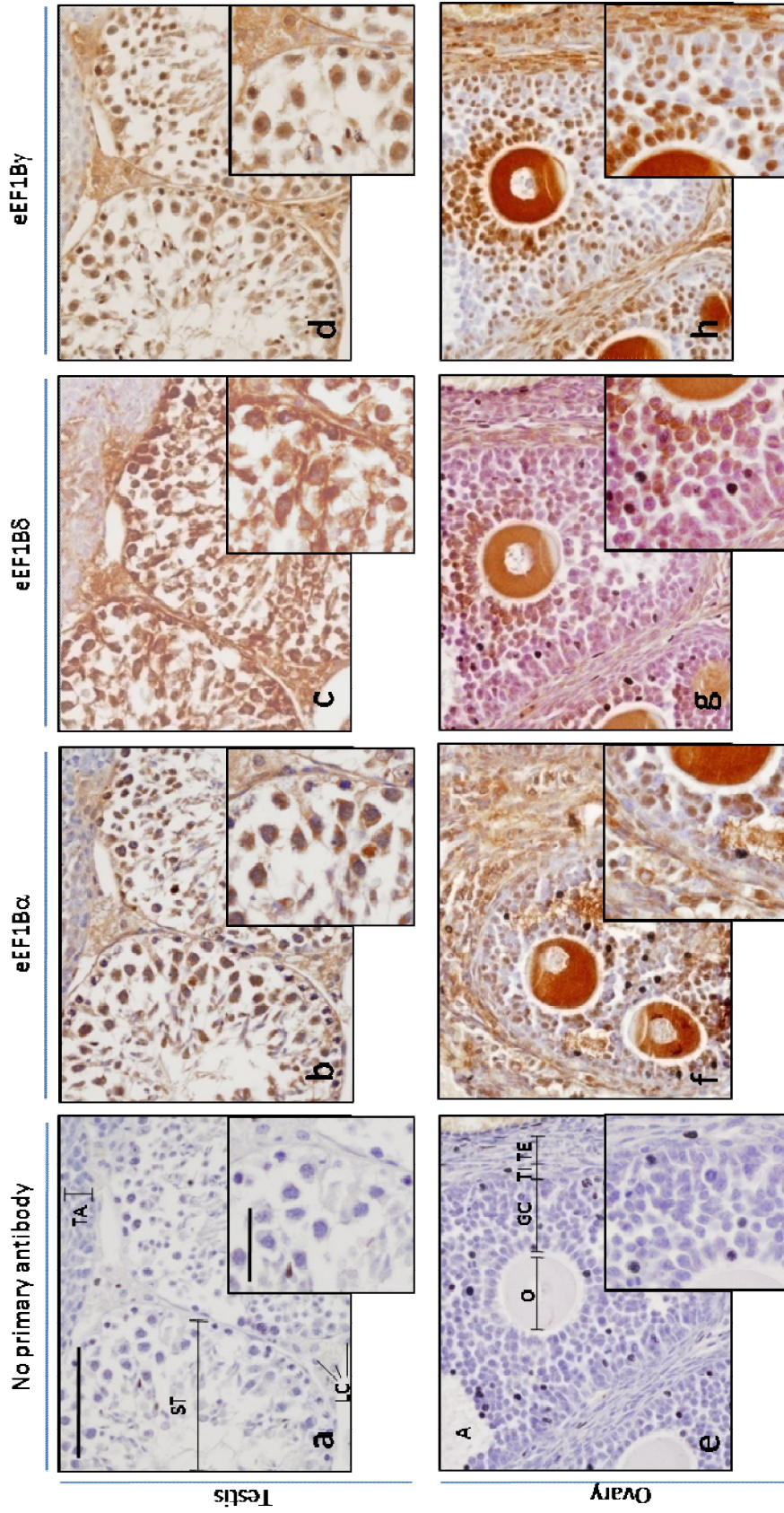


Figure 4.22 Immunohistochemical analysis of eEF1B subunits protein distribution in mice testis and ovary. Proteins detected through primary antibody incubation, HRP mouse+rabbit secondary antibody and subsequent incubation with DAB. Positive signal is indicated by the presence of brown DAB reaction product. eEF1B α (b and f), eEF1B δ (c and g) and eEF1B γ (d and h) protein expression in mouse testis and ovary respectively at two different magnifications. Incubation with secondary antibody only was used as negative control (a and e). Representative images shown. Bar (top left micrograph) represents 100 and 50 mm respectively. TA – tunica albuginea; ST – seminiferous tubule; LC – Leydig cells; A – antrum; O – oocyte; GC – granulosa cells; TE – theca externa.

4.2.6.11 Ovaries

The ovaries have two major functions, production of oocytes and secretion of hormones. Ovaries consist of an outer cortex where the follicles are embedded and an inner medulla which contains blood vessels and nerves. The follicles can be at different stages of development. The cross section of mouse ovary shows a secondary follicle with an oocyte surrounded by granulosa cells, with a fluid-filled antrum. The theca folliculi differentiates into a theca interna, cuboidal oestrogen producing cells and a theca externa, connective tissues with smooth muscle.

In cross sections of mouse ovaries, all eEF1B subunits showed similar strong cytoplasmic staining in the follicular cells of the primary follicles (Figure 3.22f-h), and both eEF1B α and eEF1B γ appear to stain some nuclei. The control secondary antibody showed no staining (Figure 3.22e).

4.2.7 Wild-type and wasted mice brain expression

To assess the possible effect of eEF1A2 knockout on expression of eEF1B subunits, the expression of eEF1B subunits was compared between wild-type and wasted mice brain. The protein was extracted from brain tissues of three wild-type and three wasted mice at P21-P24 and analysed by Western blot by Chris Beirne for the expression of eEF1B subunits and GAPDH was used as a control. Both eEF1B α and eEF1B γ protein expression showed no or little difference between wild-type and wasted mice compared with GAPDH (Figure 4.23a). In contrast, eEF1B δ showed a decreased protein expression in wasted mice compared with wild-type mice. Densitometry analysis of the eEF1B δ immunoblot expression bands normalised against GAPDH showed a mean of 44% protein expression decrease in wasted mice.

To investigate if the other tissues of wasted mice also showed lower eEF1B δ protein expression, a pilot study was carried out where protein was extracted from tissues of wild-type and wasted P21 mouse and analysed by Western blot for the expression of eEF1B subunits as above. eEF1B δ expression was decreased by around 50% in wasted brain compared with wild-type as previously. It was also decreased by around 25% in wasted skeletal muscle but not in any of the other tissues studied (Figure 4.23b). All the other subunits did not show any significant protein expression difference between wild-type and wasted mice tissues.

To determine the eEF1B expression pattern, immunohistochemical analysis was conducted by Chris Beirne using eEF1B antibodies on coronal whole brain sections of P24 wild-type and wasted mice. Immunohistochemistry of wild-type mice showed moderate staining of eEF1B α and eEF1B δ throughout the brain, strong staining in the neurons of the hippocampus (Figure 4.24c-f) and in some Purkinje cells of the cerebellum (Figure 4.25e-l). eEF1B δ showed a slight reduction in staining throughout the brain when comparing wild-type with wasted mice. However, eEF1B γ showed absent or little staining of both wild-type and wasted mice sections

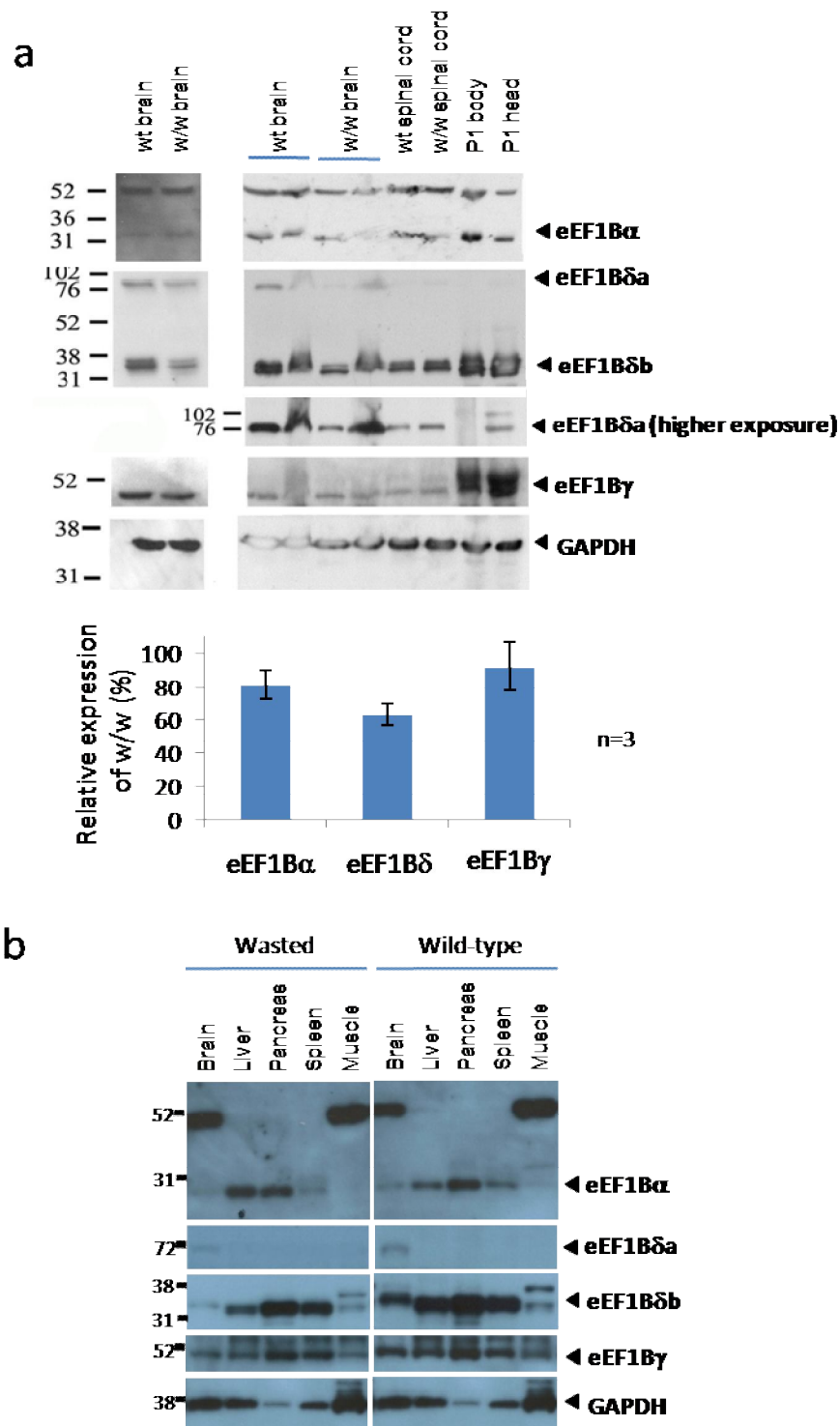


Figure 4.23 Immunoblot of eEF1B subunits protein expression in wasted and wild-type mice. Protein was extracted from mouse tissues and analysed for eEF1B α , eEF1B δ and eEF1B γ protein expression. **(a)** eEF1B protein expression of three wasted and three wild type brain tissues and the relative expression of wasted expression compared to wild type normalised against GAPDH. Performed by Chris Beirne. **(b)** eEF1B protein expression in various tissues from wasted and wild type mouse. GAPDH was used as a loading control.

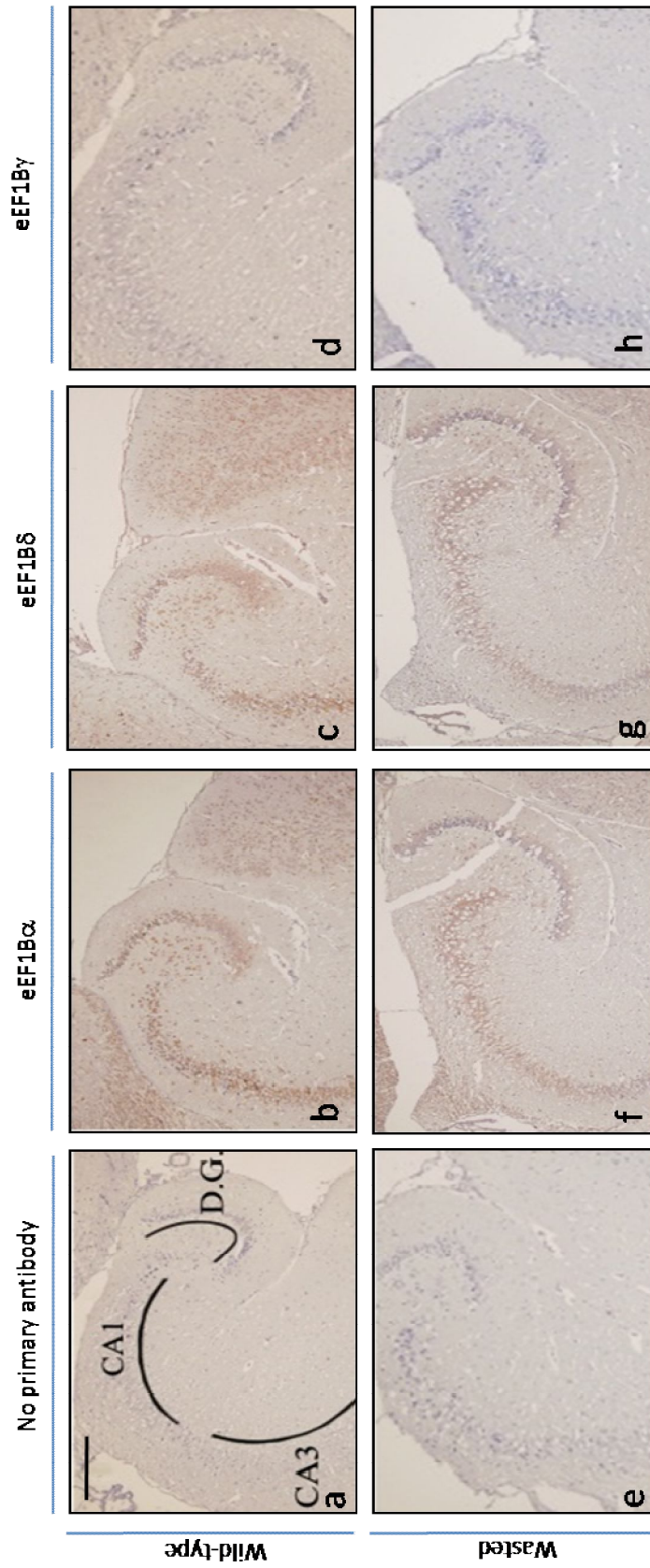


Figure 4.24 Immunohistochemical analysis of eEF1B subunits protein distribution in wasted and wild-type hippocampus (p21). Proteins detected through primary antibody incubation, HRP mouse+rabbit secondary antibody and subsequent incubation with DAB. Positive signal is indicated by the presence of brown DAB reaction product. eEF1B α (b and f), eEF1B δ (c and g) and eEF1B γ (d and h) protein expression in mouse hippocampus. Incubation with secondary antibody only was used as negative control (a and e). Performed by Chris Beirne. Representative images shown. Bar (top left micrograph) represents 200 μ m.

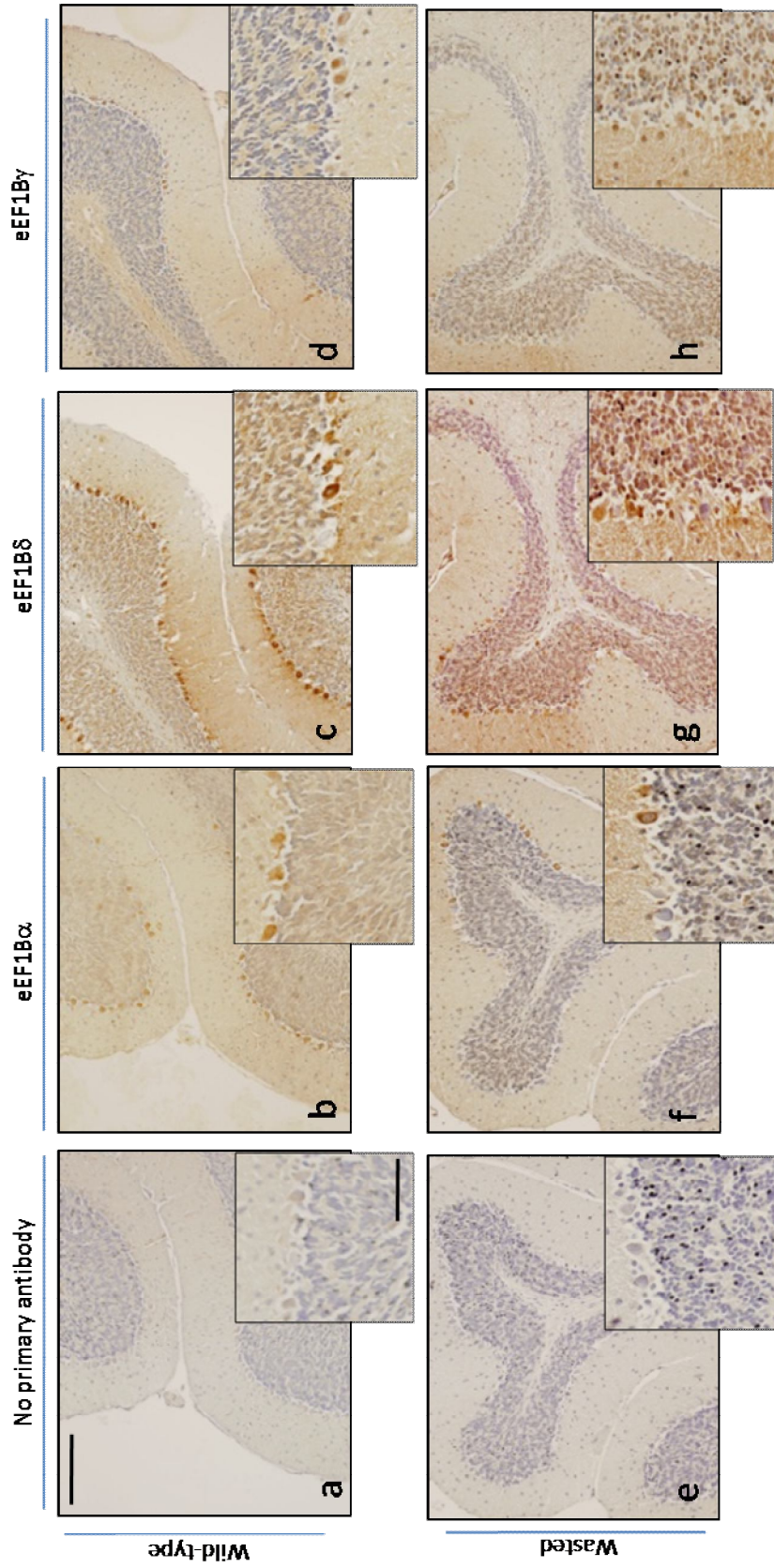


Figure 4.25 Immunohistochemical analysis of eEF1B subunits protein distribution in wasted and wild-type cerebellum. Proteins detected through primary antibody incubation, HRP mouse+rabbit secondary antibody and subsequent incubation with DAB. Positive signal is indicated by the presence of brown DAB reaction product. eEF1B α (b and f), eEF1B δ (c and g) and eEF1B γ (d and h) protein expression in mouse hippocampus at two different magnifications. Incubation with secondary antibody only was used as negative control (a and e). Representative images shown. Bar (top left micrograph) represents 200 and 50 mm respectively.

(Figure 4.24g-h). In the cerebellum, the anti-eEF1B γ antibody showed very weak nuclear staining of some Purkinje cells in both wild-type and wasted mouse sections and weak staining of granular cells in wasted mice (Figure 4.25m-p). The secondary antibody only control showed no staining (Figure 4.24a-b; Figure 4.25a-d).

Although the pattern of expression of eEF1B subunits in mouse brain does not change significantly between wild-type and wasted mice, eEF1B δ expression level was shown to be reduced by around 50% in all the wasted brain tissues tested and around 25% in muscle tissue although further testing is necessary. These results indicate that the knockout of eEF1A2 may affect the eEF1B δ expression or that the wasted phenotype on these tissues by p21 when is undergoing shrinking and cellular loss affects the eEF1B δ expression.

4.2.8 Cytoplasmic and nuclear expression in tissues

In the immunohistochemical analysis of the mouse and human tissues described in this chapter, eEF1B subunits are located mostly in the cytoplasm however in some cells the staining is unexpectedly nuclear. To investigate further the nuclear and cytoplasmic expression of the eEF1B subunits, 10ng of nuclear and cytoplasmic extracts of brain and liver tissues from human and mice (Chapter 2) were analysed by Western blot using the eEF1B antibodies, α -tubulin as a marker for cytoplasmic proteins and Lamin A and C as a marker for nuclear proteins.

In mouse brain tissues, eEF1B α and eEF1B γ are detected in the cytoplasmic extract but not in the nuclear extract whereas eEF1B δ is detected in both extracts (Figure 4.26). In mouse liver tissues, eEF1B α was only detected in the cytoplasm while both eEF1B γ and eEF1B δ were present strongly in the cytoplasm and weaker in the nuclear extract. In human brain tissue, all three subunits were detected in the nuclear extract. eEF1B α and eEF1B γ showed stronger protein levels in the cytoplasmic extract, whereas eEF1B δ showed similar levels in both extracts. In human liver extracts, eEF1B δ and eEF1B α showed stronger cytoplasmic expression than nuclear. However, eEF1B γ showed stronger nuclear expression compared with cytoplasmic.

The mouse nuclear extracts had small amounts of cytoplasmic protein contamination as the presence of weak α -tubulin protein expression demonstrates but the human nuclear extracts show little to no α -tubulin expression. The contamination of nuclear proteins into the cytoplasmic extracts could not be assessed as the antibody used as nuclear marker did not show any signal. Although the extracts were quantified (as described in chapter 2) it is possible that uneven loading might be, at least in part, responsible for the expression pattern.

The nuclear expression of eEF1B subunits previously observed by immunohistochemical analysis was confirmed by Western blot analyses on nuclear

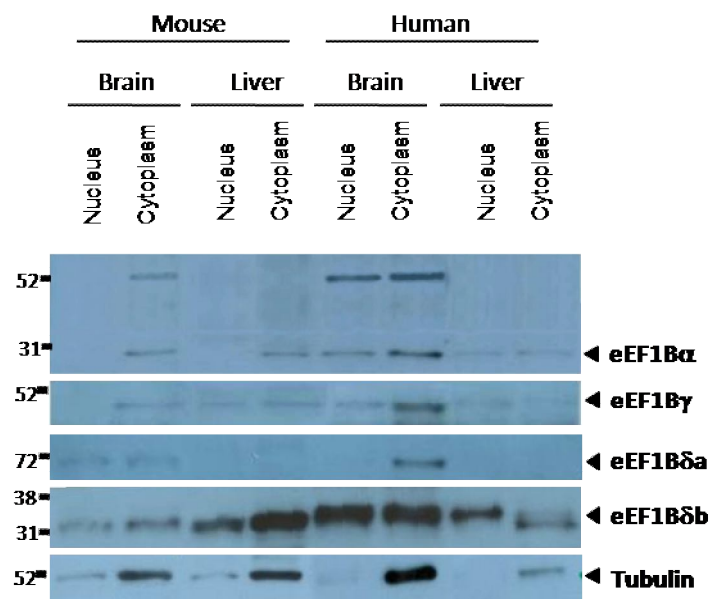


Figure 4.26 Immunoblot of eEF1B subunits protein expression in nuclear and cytoplasmic fractions from mice and human of brain and liver tissues. Protein nuclear and cytoplasmic fractions were extracted from brain and liver mouse tissues and together with human fractions of brain and liver tissues were analysed for eEF1B α , eEF1B δ and eEF1B γ protein expression. α -tubulin was used as a control.

protein extracts from tissues. The fractionation correlated with the immunohistochemistry analysis was performed in human and mouse brain and liver tissues. However, since no markers for other organelles were examined, microsomes and endoplasmatic reticulum may be present in the fractions examined making it difficult to interpret the exact sub-cellular localisation of the complex.

4.2.9 Sub-cellular localisation

Although the sub-cellular localisation of each eEF1B subunit is known in human fibroblast cells (Minella et al., 1996a), is it the same in different cell lines? To determine the sub-cellular localisation of each eEF1B subunit in cells, unsynchronised cells were subjected to co-immunofluorescence with eEF1B antibodies, cytoskeleton staining with α -tubulin, and nuclear staining with 4',6-diamidino-2-phenylindole (DAPI).

Immunofluorescence with anti-eEF1B α antibody in HeLa cells showed staining throughout the cytoplasm, stronger peri-nuclear localisation (Figure 4.27a). Co-immunofluorescence of merged eEF1B α and alpha-tubulin showed co-localisation (in yellow) of the microtubules where they are more condensed around the nucleus with eEF1B α staining (Figure 4.27d). eEF1B δ staining was detected throughout the cytoplasm, with strong perinuclear staining (Figure 4.27f). α -tubulin and eEF1B δ merged immunofluorescence staining showed co-localisation of eEF1B δ and the microtubules around the nuclei (Figure 4.27i). eEF1B γ showed a similar staining pattern to eEF1B δ and eEF1B α (Figure 4.27k). Co-immunofluorescence staining of eEF1B γ and alpha-tubulin merged image also showed co-localisation around the nuclei (Figure 4.27n). A negative control in which primary antibody was omitted showed no fluorescence except nuclear blue DAPI staining (Figure 4.27e, j and o). eEF1B subunits showed a similar sub-cellular localisation restricted to the cytoplasm of all cell lines studied (data not shown; table 2.4).

To study the localisation of eEF1B α and eEF1B δ compared with eEF1B γ , HeLa cells were subjected to co-immunofluorescence with eEF1B α and eEF1B γ , or eEF1B δ and eEF1B γ antibodies, and nuclear staining with DAPI.

eEF1B α (Figure 4.28a), eEF1B δ (Figure 4.28f) and eEF1B γ (Figure 4.28b and g) all showed the expected cytoplasmic staining, stronger around the nuclei. eEF1B α and eEF1B γ showed strong co-localisation around the nuclei of HeLa cells

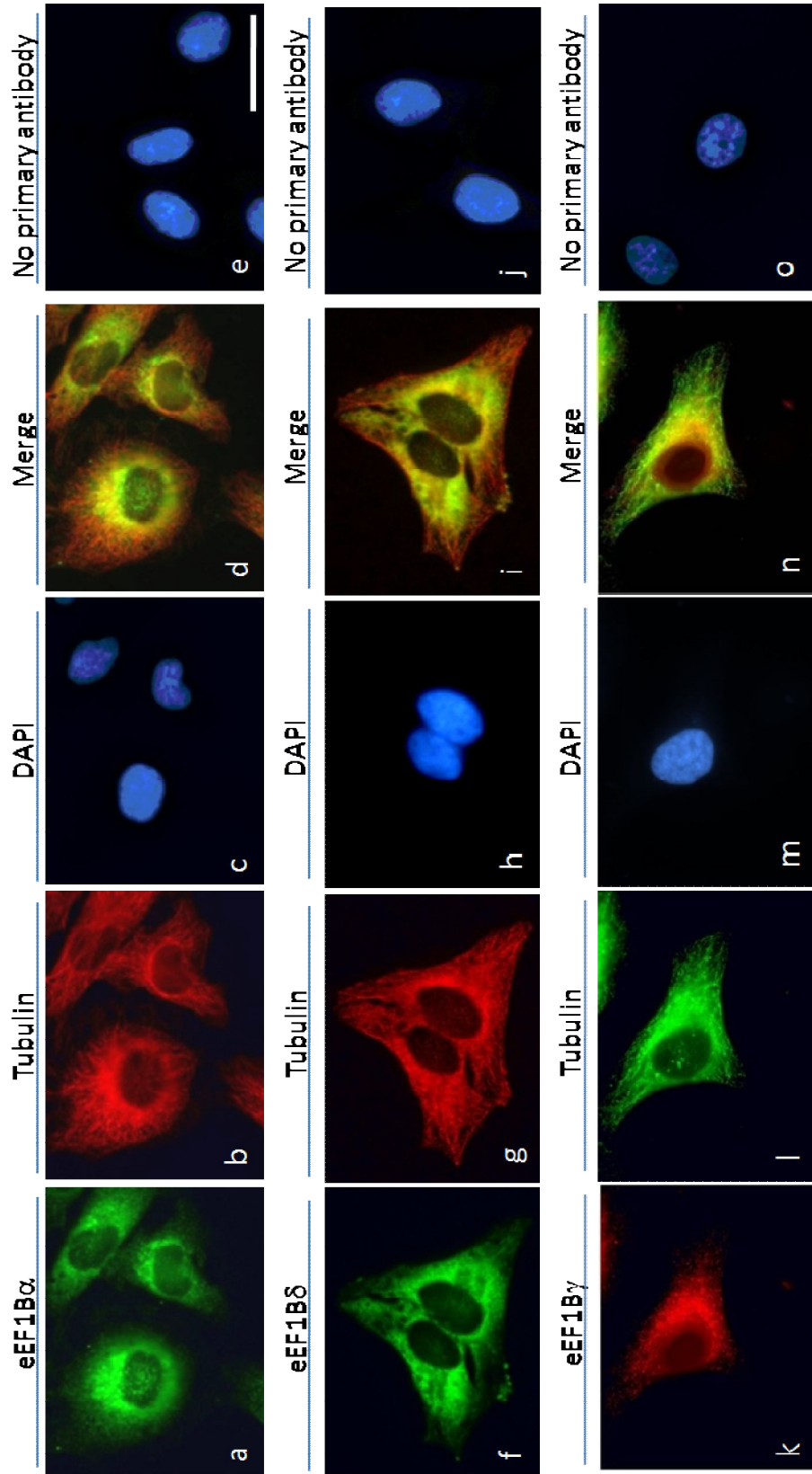


Figure 4.27 eEF1B subunits show cytoplasmic staining in double immunofluorescence on HeLa cells. Unsynchronised HeLa cells were subjected to double-immunofluorescence with eEF1B α in green (**a-d**), eEF1B δ in green (**f-i**) or eEF1B γ in red (**k-n**) and α -tubulin as a control. Incubation of secondary antibody only was used as a fluorescence negative control (**e,j,o**). Representative images shown. Bar (top right micrograph) represents 25 μ m.

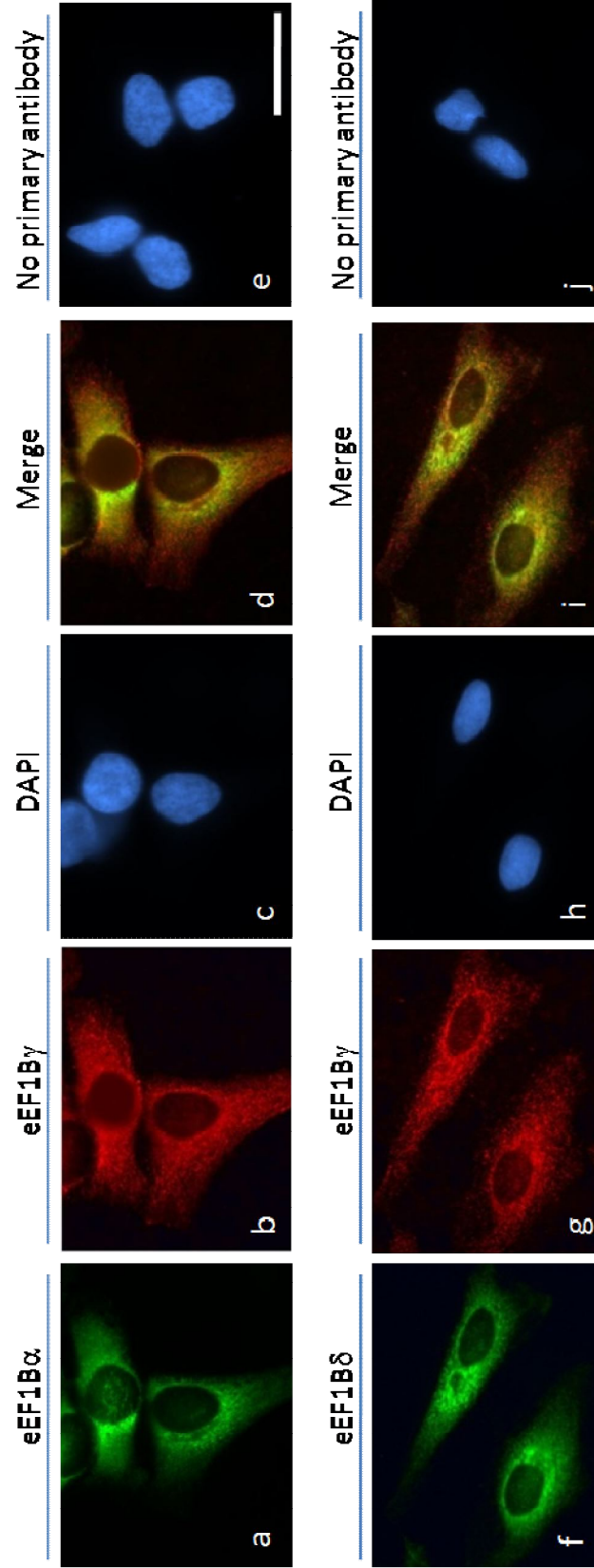


Figure 4.28 Perinuclear co-localisation of eEF1B subunits in HeLa cells. Unsynchronised HeLa cells were subjected to double-immunofluorescence with eEF1B α in green and eEF1B γ in red (**a-d**) and with eEF1B δ in green and eEF1B γ in red (**f-i**). Incubation of secondary antibody only was used as a fluorescence negative control (**e,j**). Representative images shown. Bar (top right micrograph) represents 25 μ m.

and dispersed co-localisation throughout the cytoplasm (Figure 4.28d). Co-localisation around the nuclei was also detected by immunofluorescence of eEF1B δ and eEF1B γ with some scattered co-localisation around the cytoplasm (Figure 4.28i). The negative control showed no fluorescence except nuclear blue DAPI staining (Figure 4.28e and j).

Immunofluorescence of eEF1B subunits showed the expected ER-like sub-cellular localisation, co-localising around the nuclei with microtubules and not detectable in the nuclei. eEF1B γ was also found to partially co-localise with the other eEF1B subunits.

4.2.10 Cell cycle expression

eEF1B δ and eEF1B γ have been suggested to be involved in cell cycle progression (Chapter 1). Does the protein expression of eEF1B subunits change during the cell cycle? To address this question, HeLa cells were synchronised in S-phase by treatment with Aphidicolin, which inhibits DNA replication blocking cell cycle at the S-phase (Berger et al., 1979), and then the cells were allowed to enter the normal cell cycle by the removal of Aphidicolin from the media. Unsynchronised cells were used as control. To confirm the cell cycle stage, cells were incubated with propidium iodide and analysed by flow cytometry (Figure 4.29a). Protein was extracted from the cells and eEF1B subunit protein expression was analysed by immunoblotting. GAPDH was used as a control.

eEF1B α and eEF1B γ protein levels do not change over the cell cycle in HeLa cells whereas eEF1B δ showed strong protein expression in S-phase arrested cells, moderate levels at G2/M and lower protein levels in G0/G1 phase cells compared with GAPDH (Figure 4.29b).

eEF1B α and eEF1B γ subunits protein expression does not seem to be related to the cell cycle stage *in vitro* although eEF1B δ protein expression is increased in S-phase cells.

Due to the possible link of eEF1B subunits to the cell cycle and the nuclear expression in sub-population of cells from mouse and human tissues, we hypothesised that eEF1B subunits might change sub-cellular localisation during the cell cycle. The cells described above were subjected to co-immunofluorescence with eEF1B antibodies and cytoplasmic staining with α -tubulin, and nuclear staining with DAPI. Secondary antibody only was used as a control. Proliferating Cell Nuclear Antigen (PCNA) changes sub-cellular expression pattern, cytoplasmic to nuclear during S-phase. An anti-PCNA antibody was used as a cell cycle dependent sub-cellular distribution positive control.

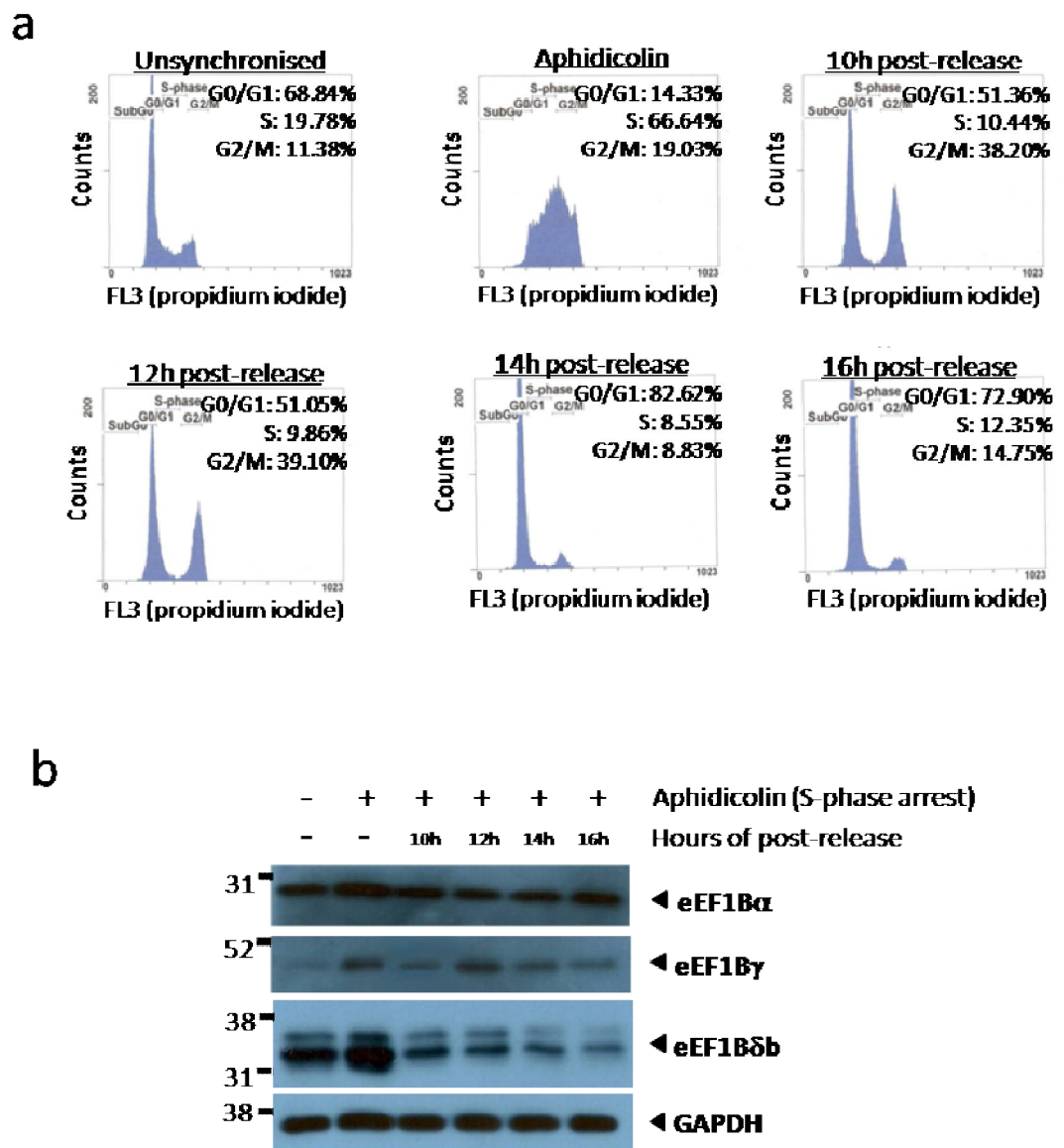


Figure 4.29 eEF1B protein levels during cell cycle. Cells were treated with Aphidicolin for 24h resulting in S-phase arrest. Cells in S-phase arrest by Aphidicolin were released by adding new media and every two hours, cells were collected. **(a)** Unsynchronised and collected cells were labelled with propidium iodide and subjected to flow cytometry. Representative images of the flow cytometry analysis. **(b)** Collected cells were harvested and analysed for eEF1B subunits and GAPDH protein expression by immunoblotting.

During the cell cycle, eEF1B α (Figure 4.30a,h,o and v), eEF1B δ (Figure 4.30c,j,q and x) and eEF1B γ (Figure 4.30b, i, p and w) showed cytoplasmic staining and no obvious difference in the expression distribution pattern. Alpha-tubulin (Figure 4.30d, k, r and y) and DAPI (Figure 4.30 e, l, s and z) also showed specific cytoplasmic and nuclear staining respectively. PCNA showed strong nuclear staining in S-phase arrested cells and cytoplasmic staining in non S-phase cells (Figure 4.30f, m, t and aa). The negative controls showed no fluorescence except nuclear DAPI staining (Figure 4.30g, n, u and ab).

These results suggest that cell cycle differences are not responsible for the change in eEF1B subunits sub-cellular localisation that is observed in some *in vivo* cells. However, it may be that the behaviour of HeLa cells does not fully recapitulate that seen in cells within tissues.

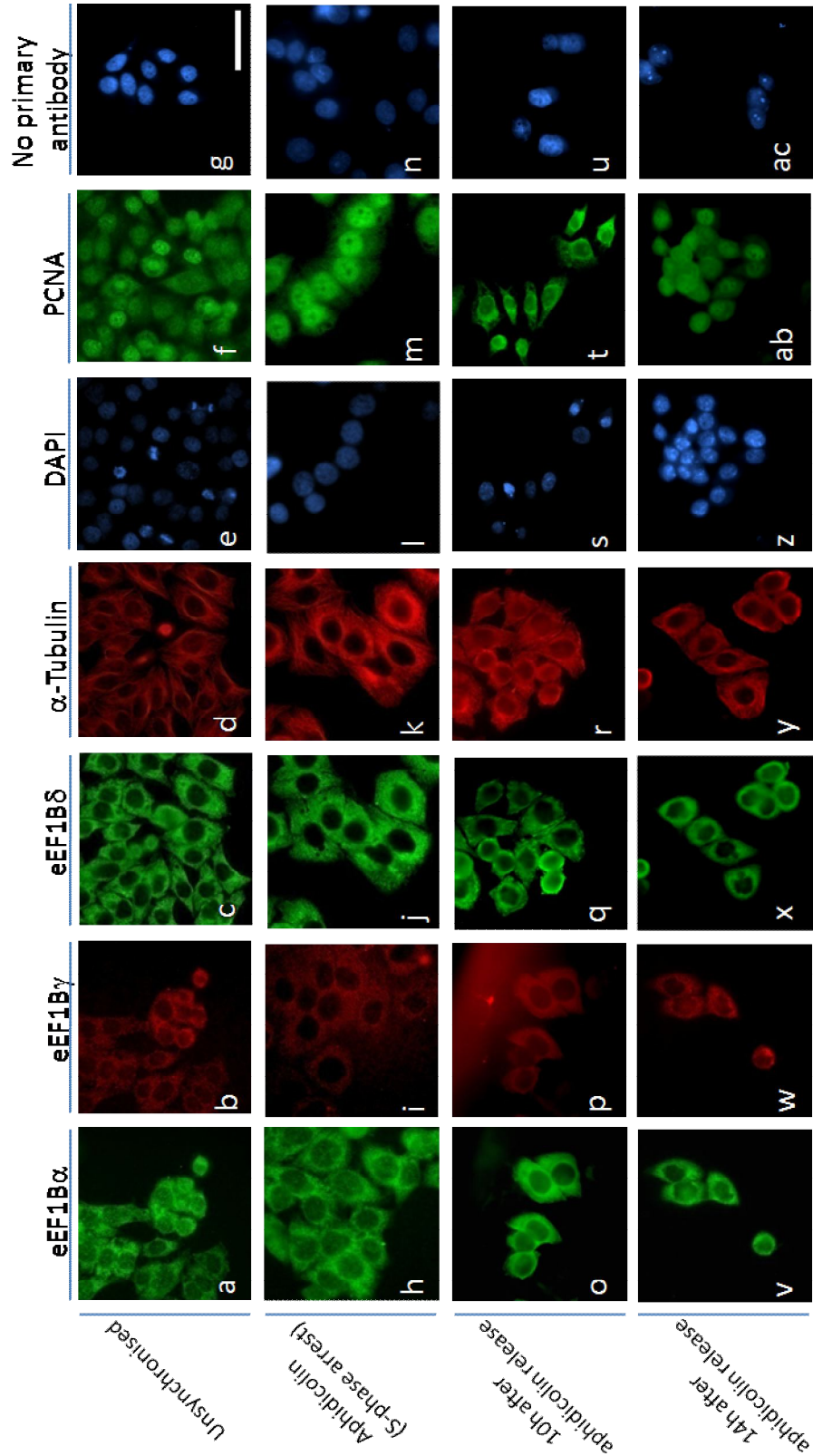


Figure 4.30 Cytoplasmic staining present for all the eEF1B subunits through out cell cycle. HeLa cells were treated with Aphidicolin for 24h resulting in S-phase arrest. Cells were released from S-phase by adding new media and every two hours, cells were collected and eEF1B subunits sub-cellular localisation was observed by immunofluorescence. Double-immunofluorescence microscopy of eEF1B α (green) and eEF1B γ (red); eEF1B δ (green) and α -tubulin (red); PCNA (green) and nuclei stained with DAPI (blue) and secondary antibody as a control. As a cell cycle control, PCNA was used since that its nuclear expression peaks at S-phase. Representative images are shown. Bar (top right micrograph) represents 50 μ m.

4.3 Discussion

No previous studies have focused on the expression pattern and precise expression distribution within tissues of each eEF1B subunit. In this chapter, eEF1B factor expression in mouse and human tissues was examined. Expression of eEF1B subunits through different mouse developmental stages and their expression in wasted mice which lack eEF1A2 were also studied as well as the expression of the subunits in different cell lines and during the cell cycle in HeLa cells.

4.3.1 Expression levels and multiple variants in translation

Translation factors are considered to be housekeeping genes, expected to be expressed in all tissues at similar levels - eEF1B γ showed evidence of exactly that. mRNA evidence supported the idea of one transcript variant, present in all studied tissues with no significant change between tissues both at mRNA and protein levels determined by three different antibodies. Unsurprisingly, eEF1B γ was also expressed in all cell lines tested. However, eEF1B α and eEF1B δ expression was more complex.

eEF1B α showed a 29kDa band in all mouse tissues tested with all the antibodies, slightly heavier than the estimated molecular weight of 24kDa. Only a few studies reported raising antibodies against eEF1B α . In a investigation by Furukawa (2001) about the link between eEF1B α and the cytoskeleton in slime mold *Dictyostelium discoideum*, a polyclonal antibody was raised against a 17kDa eEF1B α fragment and a 29kDa band was observed by Western blots. In *Xenopus* oocytes, an antibody raised against eEF1B α also showed a band with a molecular weight of around 30,000 (Minella et al., 1996a). When eEF1B α was cloned from *Sacharomyces cerevisiae* and further characterised (Hiraga et al., 1993), eEF1B α was detected as a 33kDa protein although it was expected to be 22kDa protein, which they suggested to be due to the unusual structural features of eEF1B α . Interestingly, one of the monoclonal antibodies and the polyclonal antibody tested for the

purpose of this thesis also show consistently a substantially heavier band (50kDa) in brain and the polyclonal also showed in both heart and skeletal muscles but not in any of the cell lines tested. There is no evidence from bioinformatic analyses or any mRNA evidence for the existence of another transcript variant or another gene that might encode a similar protein. eEF1B α appears to have the ability to form homodimers in rabbit and rat liver cells and recombinant eEF1B α eluted as a 50kDa (Bec et al., 1994, Sheu and Traugh, 1997). However even with protein lysates treated with high concentration of β -mercaptoethanol, DTT and SDS to break di-sulphide bonds and keep the proteins in a denatured state, the eEF1B α heavier band was always present. Antibody specificity and cross reactivity with another protein might also be the cause for the heavier band seen in Western blots using two of the three antibodies. However, siRNAs against eEF1B α were able to reduce the protein level detected by these two antibodies confirming specificity (more details on chapter 5). The location of the peptides to which the third commercial eEF1B α antibody was raised that does not detect the higher form is not known making it difficult to postulate about it. The nature of the heavier band observed in certain mouse tissues remains unclear where homodimer formation which is difficult to dissociate in tissues, cross reactivity or even large post-translational modifications cannot be excluded as possible causes.

eEF1B δ however gave evidence of multiple transcript variants, including a brain tissue-specific variant which corresponds to the known isoform a. Several other transcripts expressed in all the studied tissues were identified and agree with the ESTs/mRNA data from databases (chapter 3). Isoform a shows restricted expression to brain, spinal cord and testis, while up to four eEF1B δ forms were present in all the tissues with sizes ranging from 31 to 38 kDa, including a muscle-specific form at 38kDa. These multiple bands and identical expression pattern were detected by both antibodies used for the Western Blot analyses. Two or three forms ranging from 31 to 38kDa were also present in all cell lines studied. eEF1B δ isoform

a was restricted to neuroblastoma cell lines which agrees with the brain and testis specific expression, and previously known expression in neuroblastoma tumours (De Bortoli et al., 2006). Multiple bands for eEF1B δ have been previously detected by Western blot in several species. In sea urchins, 2 forms were identified at 35 and 37kDa derived from eEF1B δ isoform b and isoform c (Le Sourd et al., 2006b) described in chapter 3 in more detail. (Minella et al., 1996b) and colleagues reported three forms of eEF1B δ present in *Xenopus* oocytes derived from eEF1B δ isoform b, isoform c and the third form due to phosphorylation. Two of the three eEF1B δ forms denominated p34, p36 and p38 observed in mouse cell line NIH3T3 were found to be due to phosphorylation (Chang and Traugh, 1998). Two forms were also detected in human fibroblast cells using a polyclonal antibody against eEF1B δ (Sanders et al., 1996). However, (Kruse et al., 2000) reported in human Hep2 cells a single band using an eEF1B δ antibody and a double band using an eEF1B α antibody. The two bands described in this investigation by Kruse as having been obtained using an eEF1B α antibody are all identical to the pattern reported in this thesis and observed by others for eEF1B δ . In addition, the sizes of the proteins were not indicated making it impossible to verify if the immunoblots were correctly labelled. eEF1B δ seems to exist as several isoforms that differ in their migration in SDS gels *in vivo* and *in vitro*, most likely as a result of alternative splicing and possibly phosphorylation, however their true nature needs to be ascertained.

Besides eEF1A1 and eEF1A2 variants, although not very common, other translation factors also show multiple forms such as eIF5A-1 and the rare variant eIF5A-2 (Jenkins and Fuerst, 2001), and eIF4GI which is known to have at least five isoforms in HeLa cells derived from alternative start codons, alternative promoter and alternative splicing (Byrd et al., 2002). It is unclear why eEF1B δ exists in so many forms. The presence of multiple forms could mean redundancy or reflect a more complex role for eEF1B δ than previously thought.

4.3.2 Correlation of expression between eEF1 factors and assess implications for eEF1B function

eEF1B subunits were found to be present in all tissues analysed at the mRNA level as analysed by RT-PCR and at the protein level by Western blot and immunohistochemical analysis. They were found to be widely expressed with strong expression mainly in major endocrine cells in the pancreas, colon, testis and ovaries, and cells with stable shape such as motor neurons and Purkinje cells. Immunohistochemistry was performed using different antigen retrieval techniques and always gave identical results indicating the likelihood of the signal being specific for each antibody. However careful interpretation of brain, heart and muscle immunostaining is needed since that the origin of the higher molecular weight band observed on Western blots is unclear. The immunohistochemistry performed in a variety of human tissues cannot be compared between tissues since the tissues are from different sources that vary in age and sex (refer to chapter 2 for more details). Although a recent investigation to eEF1B γ mRNA expression in crayfish found eEF1B γ to be expressed in all tissues, showing the lowest expression levels in hepatopancreatic cells and the highest in cardiac muscle cells (Gillen et al., 2008) and ESTs data from databases indicate the presence of eEF1B subunits mRNA transcripts in all tissues (chapter 3 for more details), no previous studies analysed the precise cell types in which eEF1B subunits are present, although most of the eEF1B subunits were purified from rat and rabbit hepatocytes (chapter 1).

Throughout mouse development, eEF1B δ shows stronger expression pre-natally or early post-natally, eEF1B α is not detectable at early developmental stages and eEF1B γ is present at all stages tested at similar protein levels. This different pattern of expression amongst the different eEF1B subunits was not expected. This un-coupled expression was further observed in the expression distribution analysed by IHC on mouse and human tissues. The eEF1B subunits appear to be expressed sometimes in different cell types, cell sub-populations and even have different sub-

cellular localisation (discussed below). Staining with cell specific markers would be important to determine exactly which cell types there are staining such as neurons, pneumocytes, pancreatic endocrine cells.

The protein expression pattern and distribution of eEF1A1 and eEF1A2 is different from the one observed for eEF1B subunits that make up the GEF activity complex. The eEF1A2 variant appears to have a restricted expression to central nervous system cells - neurons, motor neurons and Purkinje cells, muscle cells and in specific endocrine cells present in the pancreatic islets, colon and stomach (Newbery et al., 2007). Whereas eEF1A1 has a mutually exclusive expression pattern with eEFA2 except in tumour cells and some cell lines. eEF1B expression seems to correlate strongly with eEF1A2 in the pancreatic islets, muscle and brain tissues but it is also correlated with eEF1A1 in other tissues suggesting that eEF1B might be part of the GEF for both eEF1A1 and eEF1A2. The eIF2B which is the GEF in the initiation phase of protein translation is ubiquitously expressed in all human tissues but mutations of its subunits can cause tissue-specific diseases (Pavitt, 2005).

During development, in contrast with the eEF1A1 and eEF1A2 shift, no apparent change in eEF1B subunits protein expression is detectable. The lack of correlation eEF1B with eEF1A at the mRNA level was observed by Delalande and colleagues in sea urchin early developmental stages. They showed eEF1B δ high expression during the first hours of development, an abrupt decrease up to 10 hours after eEF1A increased before eEF1B δ mRNA levels increased to a similar ratio as eEF1A. Interestingly, the high eEF1B δ mRNA levels observed by Delalande during sea urchin development correlate with the increased protein synthesis and increased elongation rate seen (Delalande et al., 1998). However, in adult slime mold, eEF1B α was found to have an identical expression distribution to eEF1A (Furukawa et al., 2001).

In wasted mice which lack eEF1A2, the expression of eEF1B α and eEF1B γ subunits at the protein level was found not to change considerably compared with wild type mice, whereas eEF1B δ protein expression was found to be down-regulated in brain tissues and moderately down-regulated in skeletal muscle protein lysates from wasted mice. eEF1A2 transgenes are able to rescue the wasted mice phenotype and hence eEF1A2 is fully responsible for the wasted phenotype (Newbery et al., 2007), however lack of eEF1A2 in those tissues might lead to changes in expression of other proteins or the wasted phenotype on those tissues when they undergo shrinking and cellular loss affects the eEF1B δ expression directly. Further comprehensive testing is required to assess the change in eEF1B δ expression in tissues affected by the wasted deletion or by cellular shrinkage or loss.

In cell lines, expression of eEF1B subunits is restricted to the cytoplasm, strongly expressed in the peripheral nuclear area of cells similar to the expression pattern observed by (Sanders et al., 1996) in which eEF1B subunits were found to co-localise with ER in human fibroblasts. This expression pattern is also similar to the one described by Cans 2003 in HeLa cells. (Cans et al., 2003) also suggested that it was a similar expression pattern to TCTP and eEF1A although the antibody used for eEF1A did not differentiate between the eEF1A variants. Immunofluorescence of eEF1A1 or eEF1A2 was not possible as antibodies available are not specific when used for immunofluorescence (Tomlinson, 2006). Furthermore, eEF1B subunits also showed an apparent co-localisation with alpha-tubulin in the peripheral nuclear area of HeLa cells. eEF1B has been reported to interact physically and co-localise with cytoskeleton proteins (chapter 1). Further testing to determine if eEF1B physically bind to alpha-tubulin and other cytoskeleton proteins is needed to further study the potential non-canonical function of eEF1B subunits in cytoskeleton remodelling/assembly.

4.3.3 Nuclear and cell cycle dependent translation

The nuclear location of eEF1B subunits in some sub-populations of cells in mouse and human tissues was evident by both immunohistochemical analysis and Western blot analysis of nuclear and cytoplasmic extracts. eEF1B subunits never have been reported to be present in the nucleus *in vivo*, but eEF1A1 has been reported to have nuclear expression in some motor neurons (Newbery et al., 2007).

In silico, the eEF1B γ mouse and human protein was predicted to show nuclear localisation since it has a lysine rich motif that may act as a nuclear localisation sequence. This has also been suggested by (Kim et al., 2007).

Nevertheless the eEF1B nuclear expression was not observed in cell lines. Since the nuclear staining appeared to be restricted to sub-populations of cells and since eEF1B δ and eEF1B γ had been found to be regulated during the cell cycle (Chapter 1 for review) we hypothesised that sub-cellular localisation might change during the cell cycle as reported in sea urchins (Boulben et al., 2003). However, nuclear expression of eEF1B was not observed in any of the cell line studies with either unsynchronised growth and cell cycle synchronised growth. Although it is thought that at mitosis cells cap-dependent translation rate is reduced and increased IRES-dependent translation, protein levels during the G2/M phase, the phase at which eEF1B δ and eEF1B γ are thought to be regulated (Chapter 1), showed no change. eEF1B δ was the only eEF1B subunit that showed a slight increase in protein expression during a particular cell cycle stage, the S-phase.

Only under specific conditions are translation factors known to redistribute to the nucleus. An eEF1B γ homologue in yeast shows nuclear expression during oxidative stress which is suggested to be due to the possible GST like activity (refer to chapter 1)(Hanbauer et al., 2003, Grosshans et al., 2000). Although eEF1B subunits have been linked to oxidative stress and DNA damage (Chapter 1) and eEF1B α and eEF1B γ possess a GST-like domain, it is unclear if they have non-canonical functions that might explain the nuclear expression. eEF1A was also found to have nuclear expression in human A431 cells in which it binds to ZPR1

and is redistributed to the nucleus by EGF treatment (Gangwani et al., 1998). In addition, both in yeast and in human Hep2 cells, eEF1A is part of the nuclear and cytoplasmic tRNA binding protein complex (tRNP) possibly involved in nuclear export of tRNA (Kruse et al., 2000), while eEF1B α , eEF1B δ and eEF1B γ are only part of the cytoplasmic tRNP complex. Furthermore, (Bohnsack et al., 2002) and colleagues investigated nuclear expression of several translation factors by adding nuclear localisation signals and specific inhibition of nuclear export by treatment with drugs. A couple of initiation factors showed nuclear expression, while eEF1A was found to show a Exportin5-dependent nuclear exclusion and most of the other translation factors also show Exportin1(CRM1)-dependent nuclear exclusion. Only eEF1B α and eEF2 showed CRM1-independent nuclear exclusion. Although several initiation, elongation and termination factors have been shown to have nuclear expression under certain conditions (Bohnsack et al., 2002, Dahlberg et al., 2003), with some reports claiming the protein synthesis also occurs in the nucleus - nuclear translation is controversial (Dahlberg and Lund, 2004, Iborra et al., 2004). In addition to that, many of these factors with nuclear expression also have non-canonical functions in the nucleus which might explain their presence there (Dahlberg and Lund, 2004).

All these data suggest that eEF1B subunits may exist under a different quaternary structural model and may have potentially non-canonical functions. More in depth studies are necessary to determine the possible links of eEF1B subunits with cell cycle, cytoskeleton and stress conditions. In the absence of the GEF eEF1B α and eEF1B δ , eEF1A guanine nucleotide exchange activity still exists, but to a much lesser extent (Bec et al., 1994, Motorin Yu et al., 1988, Venema et al., 1991b). Together with the lack of consistent staining, this may indicate the presence of another GEF with a reciprocal expression pattern. It is therefore necessary to further analyse the eEF1B activity during translation elongation.

Chapter 5 – eEF1B function

5.1 Introduction

Understanding the molecular mechanisms involved in the overexpression of eEF1B subunits and the involvement of eukaryotic translation elongation factors in tumourigenesis (refer to chapter 1) may help to identify biomarkers and potentially develop more effective treatments for cancer.

To evaluate the biological changes that result from down and up-regulation of eEF1B subunits, siRNA-mediated RNAi and overexpression of each eEF1B subunit were carried out in cell lines and cell proliferation, cell cycle distribution and apoptotic ratio were assayed.

In this study, knockdown of each eEF1B subunit inhibited cell proliferation and induced apoptosis in several cell lines and overexpression of each subunit increases cell proliferation and viability. These findings better establish the view that eEF1B plays a role in tumourigenesis.

5.2 Results

5.2.1 RNAi used to successfully knockdown eEF1B subunits at mRNA level

siRNAs trigger mRNA degradation to varying extents and with variable efficiency. For that reason the effectiveness of siRNAs require validation at both mRNA and protein level. The mRNA and protein level of the relevant gene should not be affected by transfection of non-targeting siRNAs or by the siRNA delivery method (mock transfection) so all siRNA experiments should include controls designed to test this.

To validate the siRNAs designed to target each eEF1B subunit at the mRNA level, the mRNA levels of each eEF1B subunit from cells transfected with three different siRNAs targeting each eEF1B subunit mRNA and a non-targeting siRNA (chapter 2 for more details) were compared by RT-PCR, with GAPDH mRNA expression as a expression control. This was achieved by transiently transfecting HeLa cells with three different siRNAs targeting each eEF1B subunit mRNA, transfecting the same cells with a non-targeting siRNA and also transfecting the cells with no siRNAs. siRNAs transfected were at a concentration of 30nM using the Amaxa nucleofection as a delivery method. Cells were harvested 48 hours after transfection following the manufacturer's recommended conditions (chapter 2).

The mRNA level of eEF1B α was completely knocked down by all three siRNAs targeting eEF1B α compared to cells transfected with non-targeting siRNA (Figure 5.1a). Cells transfected with eEF1B δ and eEF1B γ targeting siRNAs showed a great reduction of eEF1B δ and eEF1B γ mRNA expression respectively compared to controls (Figure 5.1b-c). GAPDH showed equivalent expression levels in each sample, showing no mRNA level change.

To ascertain that the delivery of siRNAs and the transfection method does not affect the expression of the relevant genes, mRNA levels of cells transfected with non-targeting siRNA, cells transfected with no siRNAs and untransfected cells

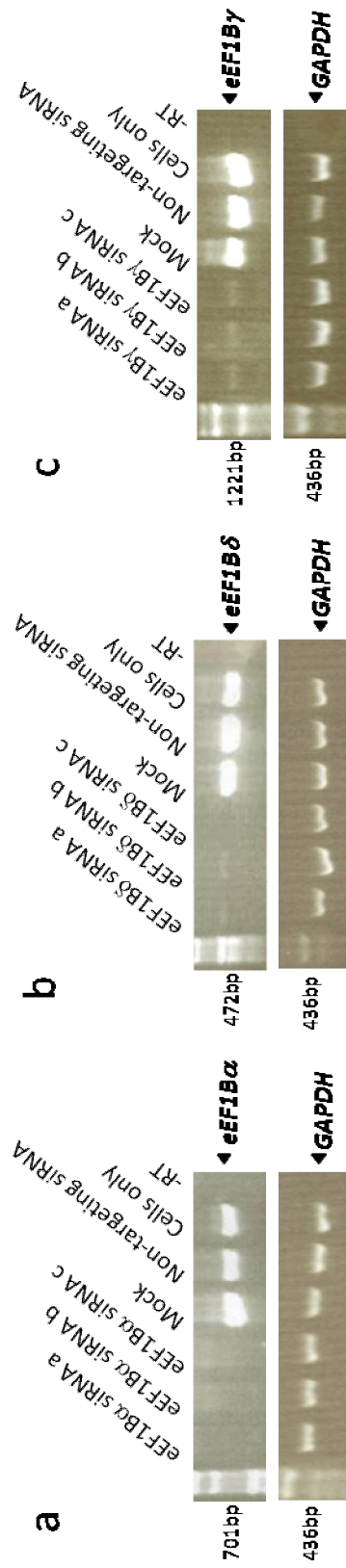


Figure 5.1 eEF1B subunits knockdown of mRNA level by sequence specific siRNAs. eEF1B mRNA is efficiently knocked down by all eEF1B targeted siRNAs. HeLa cells were transfected with 30nM of either a siRNA oligonucleotide targeting a particular eEF1B subunit or a non-targeting control by nucleofection. Cells were harvested 48h after transfection, RNA extracted, followed by cDNA synthesis and analysed for (a) eEF1B α , (b) eEF1B δ and (c) eEF1B γ mRNA expression by using semi-quantitative RT-PCR. GAPDH was used as a expression control. -RT was used as a PCR control.

were compared. mRNA expression of eEF1B subunits and GAPDH did not change in cells with scrambled siRNA, mock transfected cells and untreated cells. In addition, the minus RT control for RT-PCR showed no evidence of DNA contamination

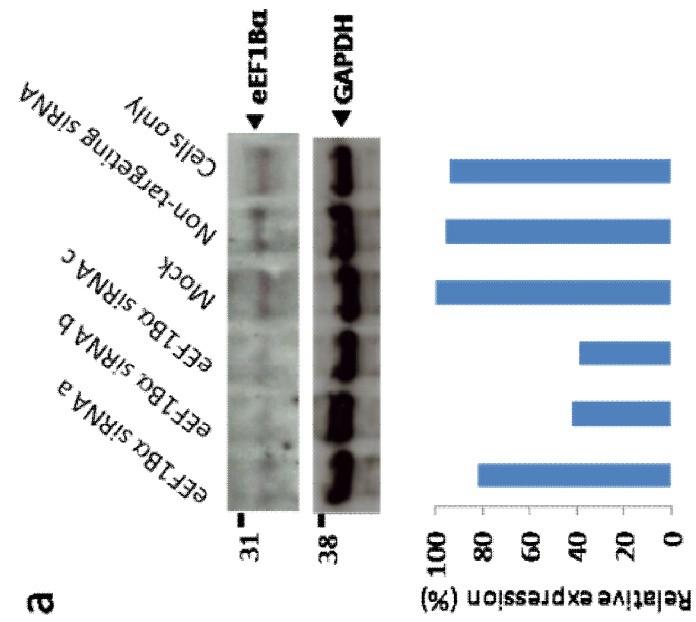
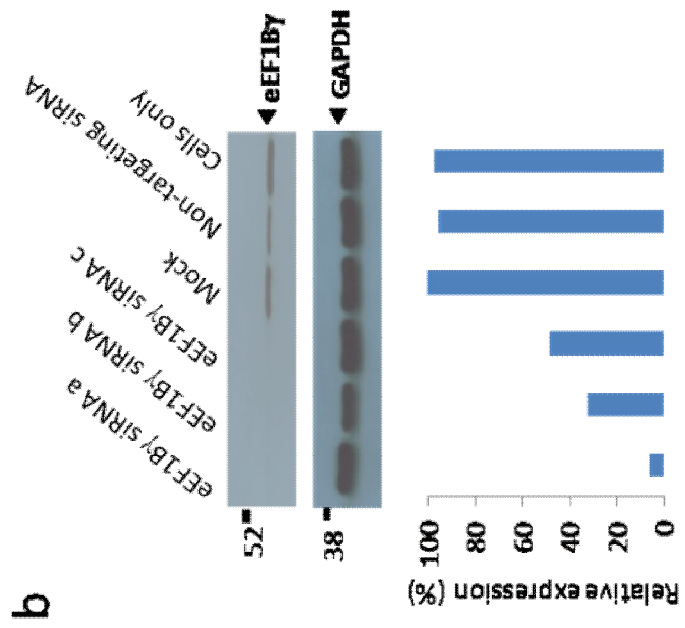
5.2.2 siRNA mediated knockdown of eEF1B subunits at protein level

All the siRNAs were able to knockdown efficiently each eEF1B subunit at mRNA level in HeLa cells. Furthermore, the nucleofection siRNA delivery method does not affect mRNA expression of GAPDH nor any of the eEF1B subunits. However the protein level is more important as it is more functionally relevant, since depending on the stability of the protein, even total depletion of the mRNA level may not result in loss of protein.

To determine if the mRNA reduction effect observed was reflected in the protein level, the protein expression of each eEF1B subunit and GAPDH from cells transiently transfected with three different siRNAs for each of the eEF1B subunits and a scrambled siRNA were compared by Western blot. To determine the protein expression of eEF1B α and eEF1B γ , initially anti-eEF1B α and anti-eEF1B γ antibodies described previously were used, as well as the commercial antibodies anti-eEF1B2 (PTG cat. no. 10483-1-AP), anti-eEF1G (Abnova cat. no. H00001937-M01) and anti-eEF1D (PTG cat. no. 10630-1-AP).

All three siRNAs targeting eEF1B α reduce substantially eEF1B protein detected with the anti-eEF1B2 antibody. The level is not affected in cells treated with scrambled siRNA, mock transfected or cells only when compared with GAPDH (Figure 5.2a). eEF1B γ protein levels detected with anti-eEF1G were considerably reduced in cells transfected with each siRNA targeting eEF1B γ in contrast with cells transfected with non-targeting siRNA, cells transfected with no siRNAs and non-transfected cells (Figure 5.2b). GAPDH expression was equivalent in each case.

Identical cell extracts were analysed with the commercial antibodies and gave similar results, with reduced eEF1B α in cells treated with all three siRNAs targeting eEF1B α (Figure 5.2c) and eEF1B γ (Figure 5.2e). The protein level of the eEF1B δ subunit was drastically reduced in cells with eEF1B δ siRNAs compared with the negative controls (Figure 5.2d). GAPDH protein expression did not change.



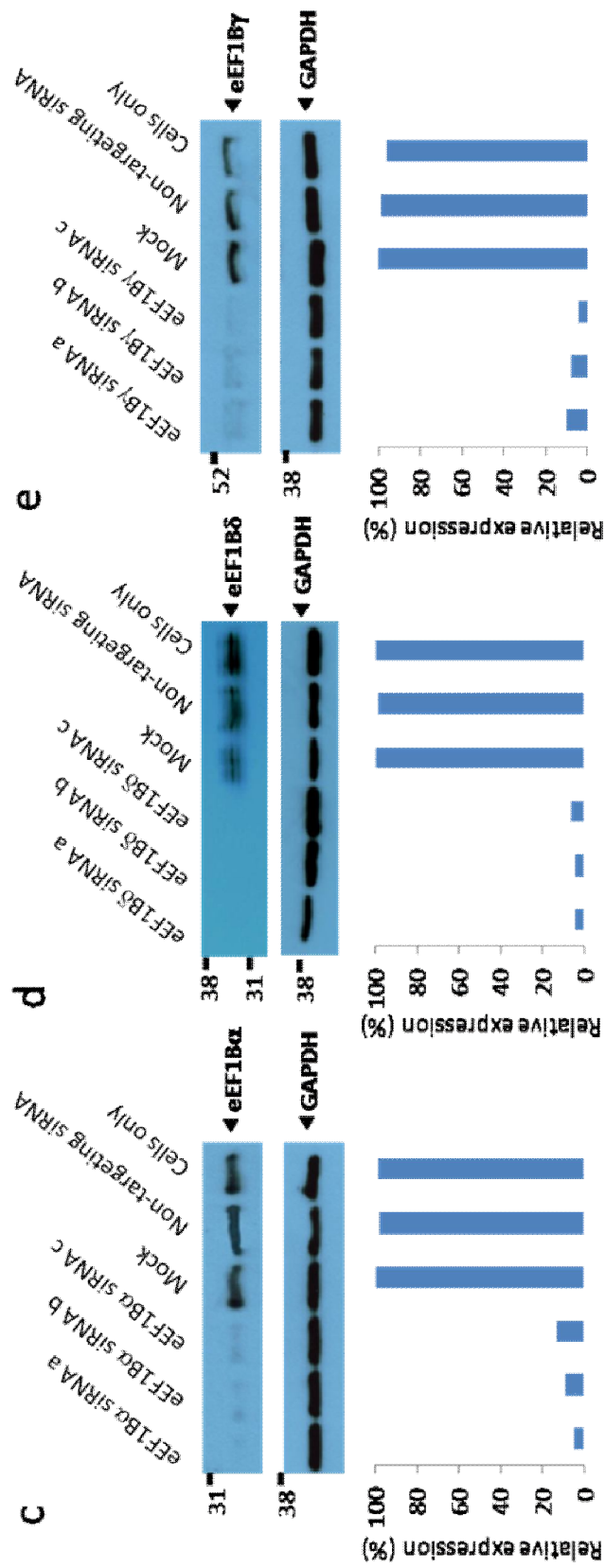


Figure 5.2 eEF1B subunits protein knockdown by sequence specific siRNAs. eEF1B α , eEF1B γ and eEF1B δ protein level efficiently knockeddown by three different siRNAs. HeLa cells were transfected with 30nM of either a siRNA oligonucleotide targeting a particular eEF1B subunit or a non-targeting control by nucleofection. Cells were harvested 72h after transfection and analysed by Western blot, using anti-eEF1B2 (a), anti-eEF1B γ (b), anti-eEF1B from PTG (c), anti-eEF1D from Abnova (e) and anti-eEF1G from Abnova (e) and anti-GAPDH as a loading control and relative expression of each of the eEF1B subunits normalised against GAPDH

Expression of GAPDH and eEF1B subunits was not altered in cells transfected with non-targeting siRNA, mock transfected cells and cells only, indicating that the nucleofection siRNA delivery method does not affect protein expression of GAPDH nor any of the eEF1B subunits. The Amaxa nucleofection system was used for subsequent experiments unless otherwise mentioned.

These results indicate that all siRNAs are able to efficiently silence each eEF1B subunit at the mRNA and protein level in HeLa cells, validating the siRNAs as well as demonstrating the specificity of anti-eEF1B2 and anti-eEF1G and the commercial antibodies. Due to the previously successful antibody purification kit being discontinued (chapter 4), I was not able to purify successfully more anti-eEF1B2 and anti-eEF1G antibodies. For this reason, the commercial antibodies were used for all the remaining experiments described in this chapter.

5.2.3 Optimisation of eEF1B subunits siRNA mediated knockdown

Although siRNAs were successful in knocking down eEF1B subunits using the nucleofection method using the manufacture's recommended protocol, further optimisation was required.

To determine the lowest siRNA concentration that gives a reasonable level of knockdown to reduce possible off-target effects, HeLa cells were transfected with 2nM, 5nM and 10nM of pooled siRNAs targeting each eEF1B subunit, 10nM of non-targeting siRNA or no siRNA. Cells were lysed 48 hours after transfection and protein expression was analysed by Western blot with antibodies for eEF1B subunits and GAPDH.

For eEF1B α , the lowest concentration of siRNAs that gave a substantial silencing of eEF1B α was 10nM (Figure 5.3a). The siRNAs targeting eEF1B δ gave a high reduction of eEF1B δ protein level at a concentration of 5nM, however at a concentration of 10nM the eEF1B δ protein expression was further reduced (Figure 5.3b). This was also the lowest concentration of siRNAs targeting eEF1B γ that gave substantial knockdown (Figure 5.3c). Cells transfected with non-targeting siRNAs and transfected with no siRNAs showed no reduction in eEF1B subunit protein expression.

Having established the optimal concentration of siRNA for silencing, it was important to define the time interval over which silencing takes place, so that a particular time point at which knockdown is maximal could be targeted for biological assays. In addition, knockdown results should be confirmed by multiple individual and pooled siRNAs for the same target gene.

In order to measure the effect of individual and a mixed population of siRNAs on protein levels over a time course, HeLa cells were transfected transiently by nucleofection with individual and a pool of all siRNAs targeting each eEF1B subunit, with a non-targeting siRNA, and with a siRNA targeting β -actin as a

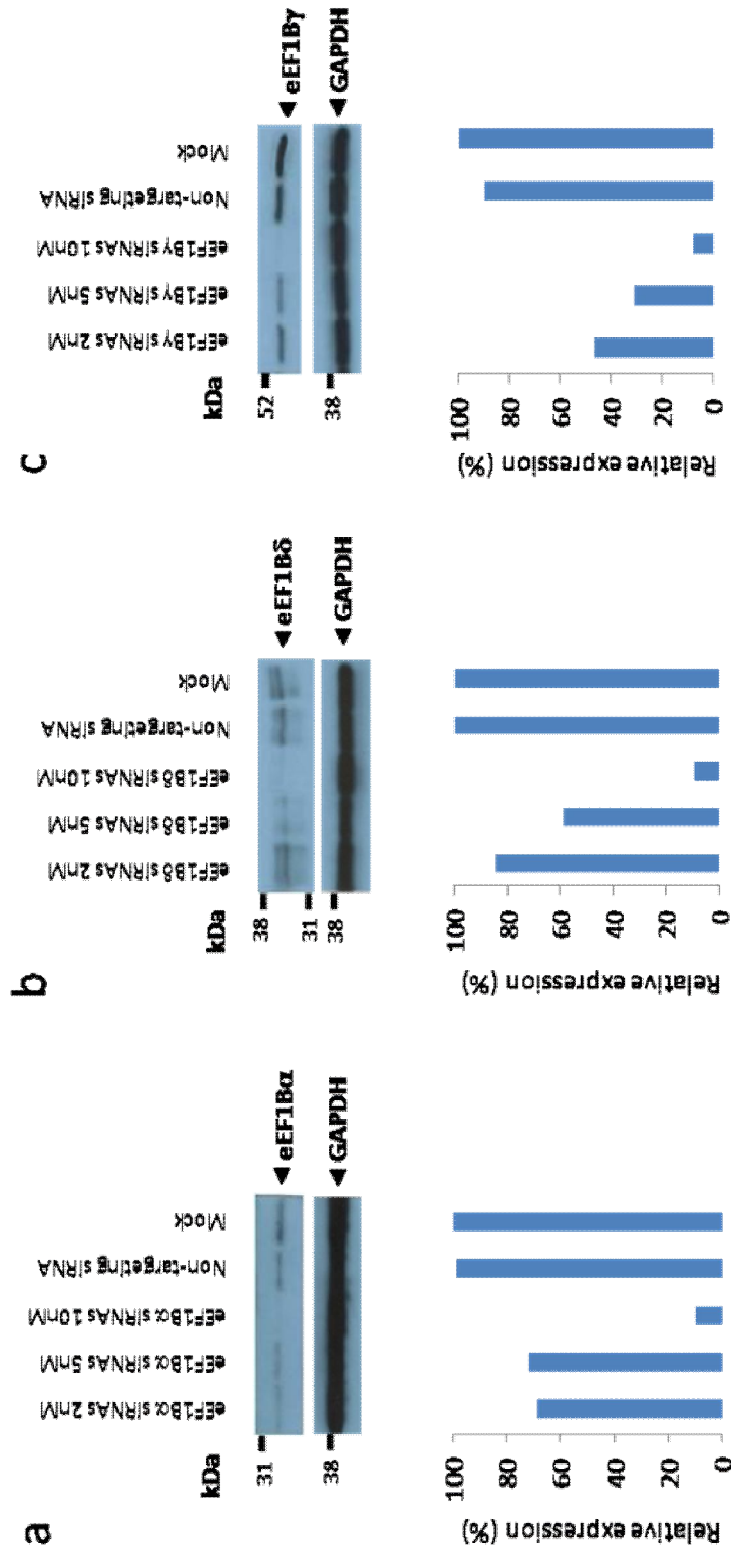


Figure 5.3 eEF1B subunits knockdown using different siRNA concentrations. HeLa cells were transfected by nucleofection with 10nM non-targeting siRNA as a control and 2nM, 5nM and 10nM pooled siRNA oligonucleotides targeting (a) eEF1B α , (b) eEF1B δ or (c) eEF1B γ . Cells were harvested 72h after transfection and analysed by Western blot, using anti-eEF1B α , anti-eEF1B δ , anti-eEF1B γ or anti-eEF1B δ , anti-GAPDH as a loading control and the relative expression of each of the eEF1B subunits normalised against GAPDH.

positive control, in addition to mock transfected and non-treated cells. Western blot analysis was carried out on cell lysates for eEF1B subunits, beta-actin and GAPDH protein expression 24, 72 and 120 hours after transfection.

The time course of eEF1B α depletion showed evidence of a small decrease in eEF1B α protein levels compared to GAPDH 24 hours after transfection (Figure 5.4a). Substantial silencing was observed 72 and 120 hours after transfection. No noticeable difference was observed in reduction of eEF1B α protein level between single siRNA and mixed population of siRNAs. Cells transfected with non-targeting siRNA showed increased eEF1B α protein expression at 120 hours but not at 24 or 72 hours after transfection, but was not reproducible so it might have been due to experimental variation. eEF1B δ showed a small protein reduction at 24 hours, a considerable reduction at 72 hours and a smaller reduction at 120 hours post-transfection in cells transfected with siRNAs targeting eEF1B δ when compared to beta-actin (Figure 5.4b). The reduction of eEF1B δ protein level was slightly delayed using pooled siRNAs when compared with individual siRNAs. In addition, eEF1B δ protein expression was restored slightly more quickly with individual siRNAs than with pooled siRNAs. This was probably due to experimental variation since this effect was not observed on other occasions. eEF1B γ protein reduction was visible 24 hours after transfection but a drastic knockdown was observed 72 and 120 hours after transfection (Figure 5.4c). The mixed population of the three siRNA targeting eEF1B γ gave a similar protein expression reduction compared with individual siRNAs. All the controls showed no change in eEF1B subunit protein expression except actin in some experiments showed a reduction in the protein level when eEF1B δ was knocked down as highlighted on figure 5.4b.

These results indicate no major difference between single and pooled siRNAs, with the maximal reduction of eEF1B subunit protein expression being achieved 72 hours after transfection and with substantial reduction lasting up to 120h after transfection. Unless otherwise stated, in the RNAi experiments described in this chapter, the time-point 72 hours after transfection was used to assay biological changes with pooled siRNAs at a concentration of 10nM.

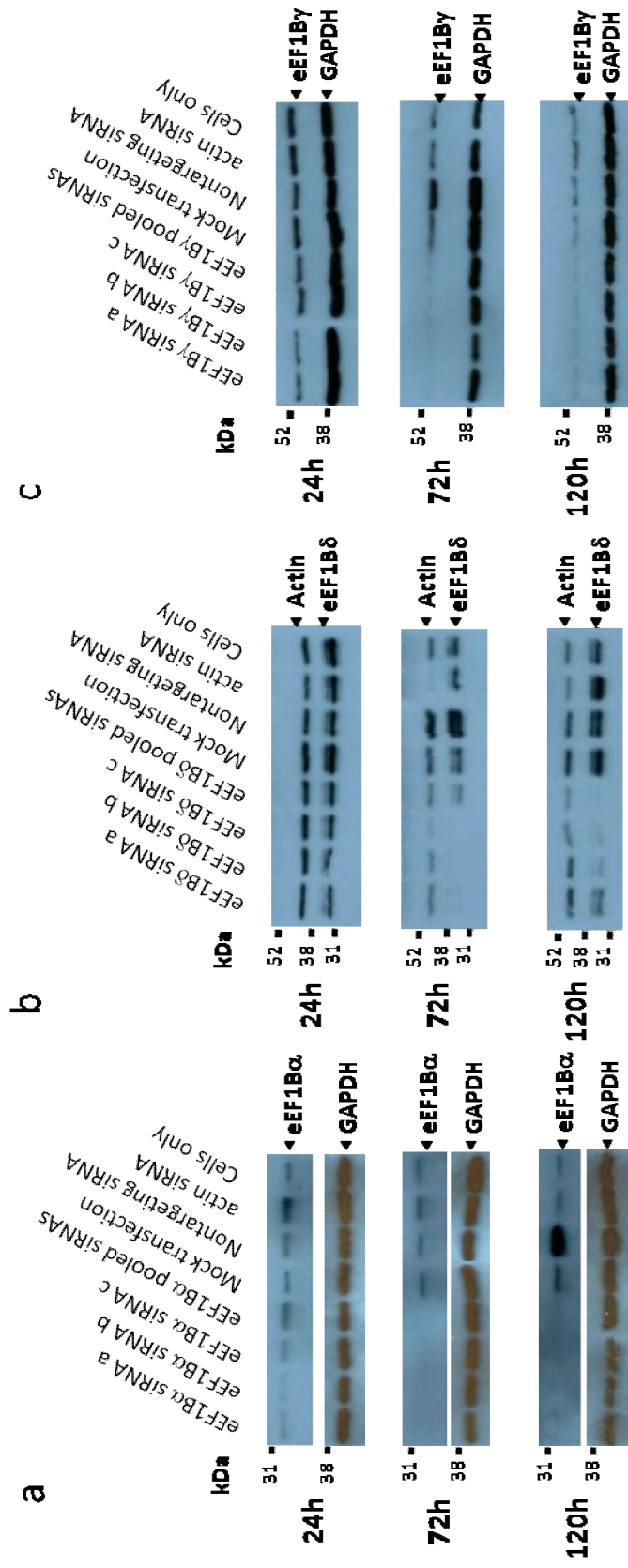


Figure 5.4 Immunoblot of a time course transient transfection of siRNAs targeting eEF1B subunits. Individual and pooled siRNAs targeting (a) eEF1B α , (b) eEF1B δ and (c) eEF1B γ efficiently knockdown the protein, with the best knockdown timepoint being 72h after transfection. Individual and pooled siRNAs (10nM) targeting each of the eEF1B subunits, scrambled non-targeting siRNA and a siRNA targeting actin, were transfected into HeLa cells by nucleofection. Cells were harvested 24h, 72h, and 120h after transfection and were analysed for eEF1B subunits, GAPDH and actin protein expression by immunoblotting. Relative expression

5.2.4 Knockdown of either eEF1B α or eEF1B δ reduce expression of eEF1B γ

After optimisation of siRNA-induced down regulation of eEF1B α , eEF1B δ and eEF1B γ , I hypothesised that the silencing of each individual subunit might affect the expression of other eEF1B complex subunits. To test this hypothesis, HeLa cells were transfected with siRNAs targeting each eEF1B subunit, siRNA targeting beta actin and non-targeting siRNAs. These together with mock transfected cells and were harvested and analysed by RT-PCR for the mRNA expression of each eEF1B subunit, actin and GAPDH as an expression control.

siRNAs targeting each individual eEF1B subunit reduced the mRNA level of that particular subunit but not that of any other eEF1B subunit (Figure 5.5a). Actin siRNA only reduced actin mRNA expression. No DNA contamination was detected by RT-PCR in the minus RT control.

This result suggests that the siRNAs are specific to each eEF1B subunit that they target at mRNA level in HeLa cells. However, it does not reveal information on the impact at the protein level. In addition, since eEF1B is a multiprotein complex, is it possible to knockdown in parallel the protein subunits in the various combinations? To address these questions, HeLa cells were transfected with siRNAs targeting eEF1B subunits individually and collectively and analysed by Western blot.

Cells transfected with siRNAs targeting eEF1B α or eEF1B δ , besides showing silencing of the target protein, also showed reduced eEF1B γ protein levels (Figure 5.5b). Cells transfected with siRNAs targeting eEF1B γ showed not only a reduction in eEF1B γ protein but also decreased expression of the other two eEF1B subunits. Transfection of cells with siRNAs targeting both eEF1B α and eEF1B δ resulted in a reduction of all eEF1B proteins. The same result was obtained with siRNAs targeting both eEF1B δ and eEF1B γ subunits. However siRNAs targeting both eEF1B α and eEF1B γ did not reduced eEF1B δ protein expression. These results were reproducible in more than three experiments. Actin protein expression was only reduced in cells transfected with siRNAs targeting actin.

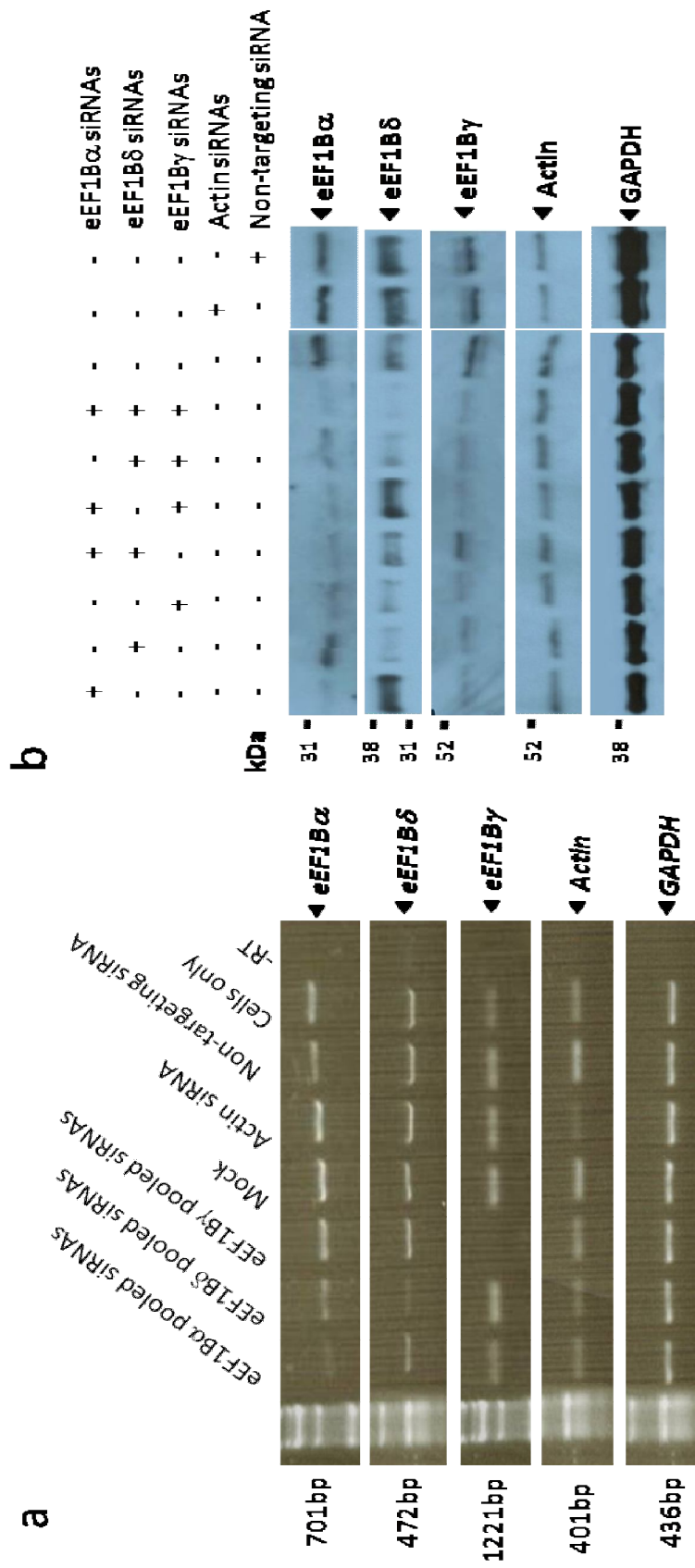


Figure 5.5 The expression of eEF1B subunits when a particular subunit has been knockeddown changes post-transcription. (a) Knockdown of each eEF1B subunits reduces mRNA expression of that particular subunit only. Cells were harvested forty-eight hours after transfection, RNA was extracted, followed by cDNA synthesis and analysed by semiquantitative RT-PCR comparing eEF1B subunits, actin and GAPDH mRNA levels. (b) Reduced endogenous eEF1B α and eEF1B δ protein levels independently by RNAi decrease expression of eEF1B γ and knockdown of eEF1B γ reduced both eEF1B α and eEF1B δ expression in HeLa cells. Each eEF1B subunit was knockeddown individually or in combination with the other eEF1B subunits by transient transfection of pooled siRNAs in HeLa cells. The oligos used in any one experiment are summarised by the '+' and '-' above each lane. Scramble siRNA and actin siRNA were used as controls. Cells were harvested 72h after transfection and analysed for eEF1B subunits, GAPDH and actin protein expression by immunoblotting.

Since the siRNAs targeting eEF1B subunits are specific at the mRNA level, and changes in the expression of other eEF1B subunits are only seen at the protein level, post-transcriptional mechanism must be involved. In the light of these observations, and since the presence or absence of eEF1A2 might potentially change the expression of eEF1B subunits, tests were carried out in three different cell culture systems: in HCT116 cells, which like HeLa cells express both eEF1A1 and eEF1A2, and in DLD1 and HepG2 cells which lack eEF1A2 expression.

Transfection efficiency differs in different cell culture systems. For this reason it is important to optimise further transfection of each cell lines used. An eGFP plasmid was used obtain a crude measure of cell line transfection efficiency as measured by flow cytometry. While HeLa, HCT116 and DLD1 cells consistently gave efficiencies of 70%, efficiency of transfection in HepG2 cells was always lower, varying from 40 to 60%. To test the effect of knocking down each subunit on the other subunits, cells were transfected using various amounts of lipofectamine 2000 (Chapter 2) with 10nM siRNAs targeting each eEF1B subunit and with 10nM non-targeting siRNA. Cells transfected with no siRNAs and untransfected cells were used as controls.

As in HeLa cells, knockdown of eEF1B α in HCT116, DLD1 and HepG2 cells considerably reduced protein expression of eEF1B γ (Figure 5.6). In HCT116 and DLD1 cells, as in HeLa cells, knockdown of eEF1B δ strongly reduced eEF1B γ protein levels. However knockdown of eEF1B δ in HepG2 cells reduced the expression of eEF1B α and eEF1B γ only to a moderate degree. eEF1B γ knockdown in HepG2, as in HeLa cells, reduced to some extent the protein expression of the other two subunits. The low transfection efficiency for HepG2 may be part of the cause of poorer knockdown in HepG2 cells. In contrast, in HCT116 cells, eEF1B γ knockdown only partially reduced eEF1B α protein levels. And in DLD1 cells, eEF1B γ knockdown did not change any of the other eEF1B subunits protein expression.

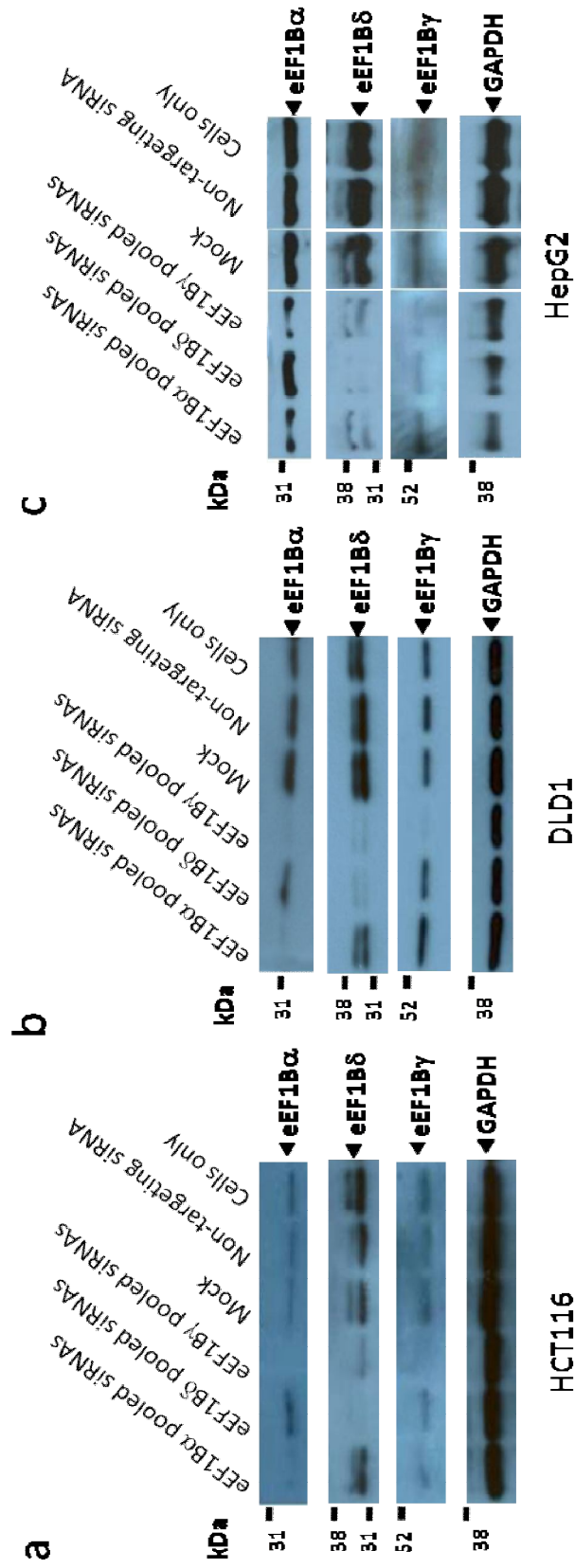


Figure 5.6 Efficient knockdown of eEF1B subunits in HCT116, DLD1 and HepG2 cells. Knockdown of eEF1B α reduces expression of eEF1B γ in all cells lines tested. Pooled siRNAs (10nM) targeting each eEF1B subunit and a non-targeting siRNA were subject to transient transfection into (a) HCT116, (b) DLD1 and (c) HepG2 cells. Cells were harvested 72h after transfection and analysed by Western blot for the expression of each eEF1B subunit and GAPDH was used as a loading control.

These results show some variability in the degree of depletion of eEF1B subunits in different cell lines, which does not seem to be related to the presence or absence of eEF1A2. The variation might be due at least in part to the diversity of tumour cells from which the cell lines derived. The expression of eEF1A1 and eEF1A2 was not verified in these samples due to problems with antibody specificity.

5.2.5 No apparent phenotypic abnormalities demonstrated by immunofluorescence microscopy

To determine any phenotypic changes results from the downregulation of eEF1B subunits using previously optimised siRNA mediated knockdown of eEF1B subunits, HeLa cells were transfected with siRNAs targeting each eEF1B subunit and non-targeting siRNA. These and mock transfected cells were analysed then by immunofluorescence for the presence of the respective eEF1B subunit, cytoplasmic staining with alpha-tubulin and nuclear staining with DAPI.

eEF1B α

Most cells transfected with eEF1B α targeted siRNAs were negative for eEF1B α protein except a few cells, however α -tubulin and DAPI stained all cells examined (Figure 5.7a-c). eEF1B α knockdown gives no evident phenotypic change compared with cells transfected with non-targeting siRNA (Figure 5.7e-g). A negative control in which primary antibody was omitted showed no fluorescence except nuclear blue DAPI staining (Figure 5.7d; 5.7h).

eEF1B δ

Only a very small number of cells transfected with siRNAs targeting eEF1B δ had noticeable eEF1B δ fluorescence while all the cells stained for α -tubulin and DAPI (Figure 5.9a-c). A few cells with a drastic eEF1B δ knockdown appeared to show α -tubulin arranged in small clumps. Tubulin protein-levels were never examined by immunoblot. Cells transfected with non-targeting siRNA showed strong fluorescence of eEF1B δ , α -tubulin and DAPI (Figure 5.9e-g). Immunofluorescence negative control showed no fluorescence apart from nuclear DAPI staining (Figure 5.9d; 5.9h).

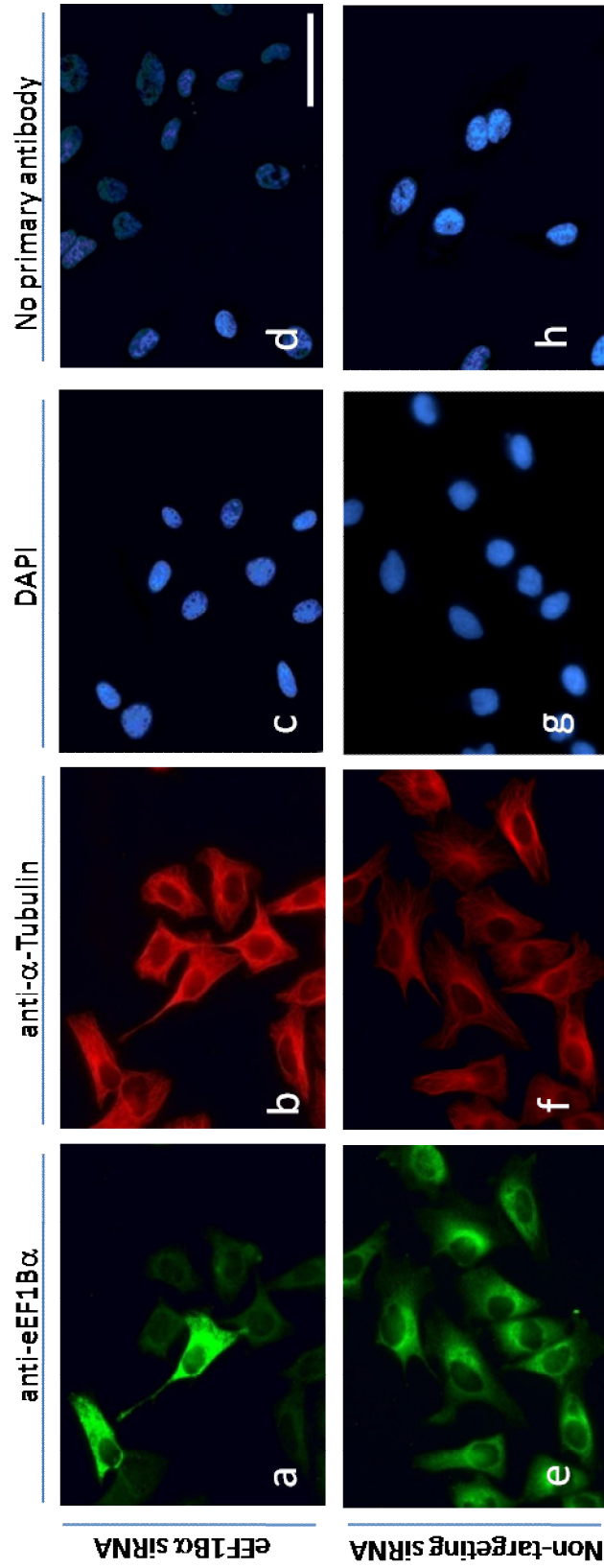


Figure 5.7 No obvious phenotypic abnormalities observed by immunofluorescence microscopy 72h after transfection with 10nM siRNAs targeting eEF1B α in HeLa cells by nucleofection. Double-Immunofluorescence microscopy of anti-eEF1B α (green), anti- α -tubulin (red) and nuclei stained with DAPI (blue). As a control, cells were incubated only with secondary antibodies. Immunofluorescence on cells transfected with eEF1B α siRNA (a-d) and with non-targeting siRNA (e-g) at x400 magnification. Representative images are shown. Bar (top right micrographs) represents 50 μ m.

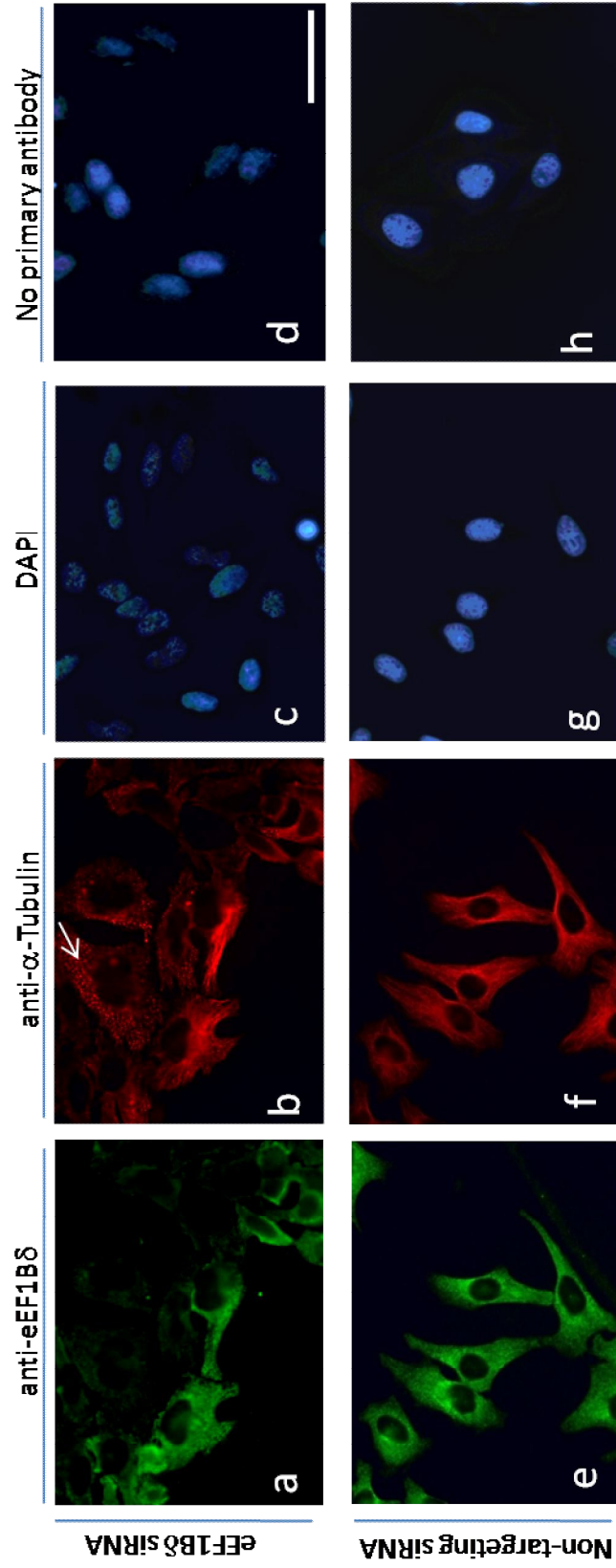


Figure 5.8 Alpha-tubulin appears to be disrupted in some cells observed by immunofluorescence microscopy 72h after transfection by nucleofection with 10nM siRNAs targeting eEF1B δ in HeLa cells indicated by the white arrow. Double-immunofluorescence microscopy of anti-eEF1B δ (green), anti- α -tubulin (red) and nuclei stained with DAPI (blue). As a control, cells were incubated only with secondary antibodies. Immunofluorescence on cells transfected with eEF1B δ siRNA (a-d) and with non-targeting siRNA (e-g) at x400 magnification. Representative images are shown. Bar (top right micrographs) represents 50 nm.

eEF1B γ

DAPI and α -tubulin fluorescence are present in all the cells transfected with siRNAs targeting eEF1B γ , in contrast with eEF1B γ itself, which was only detectable in a few cells (Figure 5.8a-c). No apparent phenotypic abnormality was observed in cells with reduced eEF1B γ protein levels compared with cells transfected with scrambled siRNA (Figure 5.8e-g). Only DAPI fluorescent cell nuclei was observed in the immunofluorescence control with secondary antibodies only (Figure 5.8d; 5.8h).

Immunofluorescence on cells transfected with siRNAs targeting eEF1B subunits showed a reduction of staining with anti-eEF1B subunit antibodies in most cells, indicating an effective protein knockdown. No apparent phenotypic gross abnormalities were observed for depletion of the eEF1B subunits in HeLa cells by immunofluorescence with the exception of a few cells showing an apparent change in the distribution of α -tubulin. Additional assays were then used to assess the biological impact of knocking down eEF1B subunits.

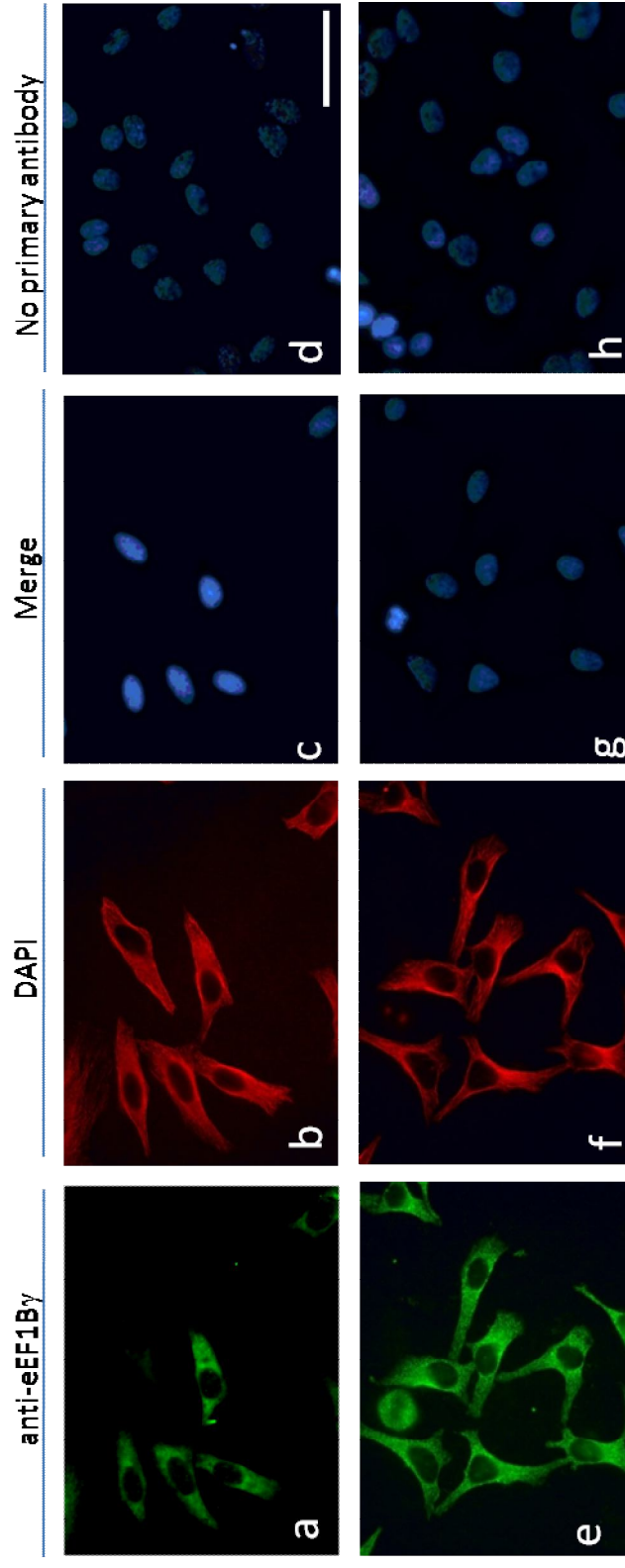


Figure 5.9 No obvious phenotypic abnormalities observed by immunofluorescence microscopy 72h after transfection by nucleofection with 10nM siRNAs targeting eEF1B γ in HeLa cells. Immunofluorescence microscopy of anti-eEF1B γ (red) and nuclei stained with DAPI (blue) and merged image. As a control, cells were incubated only with secondary antibody. Immunofluorescence on cells transfected with eEF1B γ siRNA (a-d) and with non-targeting siRNA (e-g) at x400 magnification. Representative images are shown. Bar (top right micrographs) represents 50 μ m.

5.2.6 Significant reduction of cell metabolism in cells with eEF1B down-regulation

To study the impact of the depletion of eEF1B subunits on cell proliferation, cellular metabolism was assessed by Alamar blue assay when a substantial down-regulation of eEF1B subunits was observed by Western blot. The mean of at least three independent experiments was plotted as a relative percentage of cell metabolism of mock transfected cells and statistical student t-tests were used to analyse statistical significance of cells transfected with eEF1B subunits targeting siRNAs compared to non-targeting siRNA (chapter 2 for more details on the statistical analysis). Staurosporine was used as a cell growth control since that it is known to induce reduction of cell growth leading to apoptosis by activation of caspase-3 (***) .

Knockdown of all eEF1B subunits in HeLa cells reduced cell metabolism ($p < 0.05$) compared with cells transfected with scrambled siRNA (Figure 5.10a). Knockdown with oligos targeted to eEF1B α reduced cell metabolism by more than 14%, with those targeted to eEF1B δ by more than 17% and with those targeted to eEF1B γ by more than 10% compared to cells transfected with non-targeting siRNA. No statistically significant difference in cell metabolism was observed between individual and pooled siRNAs in HeLa cells (Data not shown).

In HCT116 cells, eEF1B α , eEF1B δ and eEF1B γ siRNA induced knockdown resulted in a reduction of cell metabolism of over 19% ($p < 0.001$), 12% ($p < 0.05$) and 10% ($p < 0.05$) respectively compared with cells transfected with non-targeting siRNAs (Figure 5.10b).

Knockdown of eEF1B subunits decreased to a highly significant degree cell metabolism in DLD1 cells ($p < 0.001$) (Figure 5.10c). A reduction of cell metabolism of greater than 21% was seen after down regulation of eEF1B α , more than 20% for eEF1B δ and more than 14% for eEF1B γ compared to cells transfected with non-targeting siRNA.

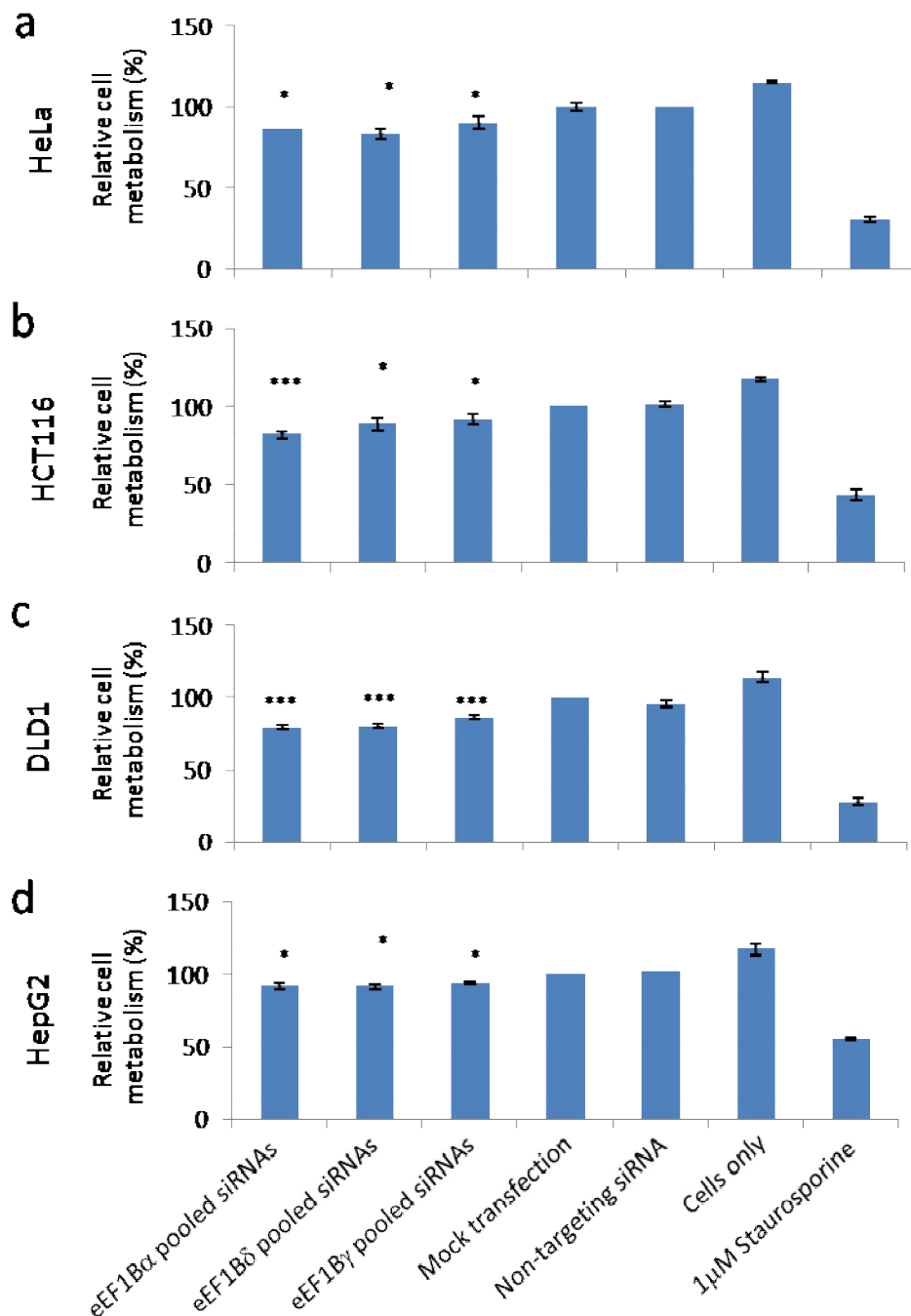


Figure 5.10 Lower cellular metabolism is observed when any of the eEF1B subunit protein level is decreased by siRNAs in HeLa, HCT116, DLD1 and HepG2 cells. Cell metabolism was assessed by the Alamar blue assay. Alamar blue was added to the media 72 hours after transfection. Data are presented as a percentage of mock transfected cells. Staurosporine (1mM) was used as a proliferation control. Data were obtained from the mean of three or more independent experiments in (a) HeLa, (b) HCT116, (c) DLD1 and (d) HepG2 cells, with more than 10 wells each. Error bars indicate \pm SEM; n of wells > 10 ; $n = 3-4$; *, $P < 0.05$; ***, $P < 0.001$ from non-targeting siRNA

Silencing of eEF1B subunits by RNAi in HepG2 cells reduced cell metabolism compared with scrambled siRNAs (Figure 5.10d). Knockdown of eEF1B α and eEF1B δ lead to a decrease of cell metabolism of over 10% ($p < 0.05$) while silencing eEF1B γ decreased cell metabolism by almost 9% ($p < 0.05$).

Transfection of a non-targeting siRNA does not alter the cell growth in comparison with mock transfected cells in any of the cell lines studied. However the siRNA delivery (transfection) method reduces the cell metabolism compared with untreated cells by between 14% and 17%. Staurosporine (1 μ M), which was used as a cell proliferation control, decreased cell metabolism by over 60% compared with cells only.

These results show that knockdown of each eEF1B subunit leads to a statistically significant reduction of cell metabolism in the four different cell lines studied.

5.2.7 Increased G0/G1 phase and reduced S- and G2/M phase cells with eEF1B knock down

With the possible link between the cell cycle and eEF1B subunits (Chapter 1) and the decreased cellular metabolism observed when eEF1B subunits are depleted, I hypothesised that eEF1B knockdown might affect the normal cell cycle distribution leading to decreased proliferation. In addition, the percentage of cells in S-phase also provides information on cellular proliferation.

To address this question, cells were collected 72 hours after transfection, stained with propidium iodide and their cell cycle status was determined by flow cytometry analysis. Representative images of the flow cytometry output can be seen in Figure 5.11a and in Figure 5.12a. Plotted graphs are the mean of at least three independent experiments in which depletion of eEF1B subunits was confirmed by Western blot.

Depletion of eEF1B subunits by RNAi in HeLa cells increased the proportion of cells in G0/G1 phase by more than 7%, decreased cells in S-phase by over 13% and decreased cells in G2/M phase by more than 10% compared with cells transfected with scrambled siRNA ($p < 0.05$; Figure 5.11b). No difference in the cell cycle distribution was detected between HeLa cells transfected with single and pooled siRNAs targeting eEF1B subunits (data not shown).

In HCT116 cells, down-regulation of eEF1B subunits increased the proportion of cell in G0/G1 by over 6%, and reduced cells in S-phase by more than 10% and in G2/M phase by 5% in comparison to cells with scrambled siRNA ($p < 0.05$; Figure 5.12b).

In DLD1 cells, knocking down eEF1B subunits increased by 8% or more the proportion of cells in G0/G1 compared with cells transfected with non-targeting siRNA ($p < 0.05$). Cells in S-phase decreased by over 15% ($p < 0.01$) and cells in G2/M phase decreased by more than 9% ($p < 0.05$; Figure 5.12c).

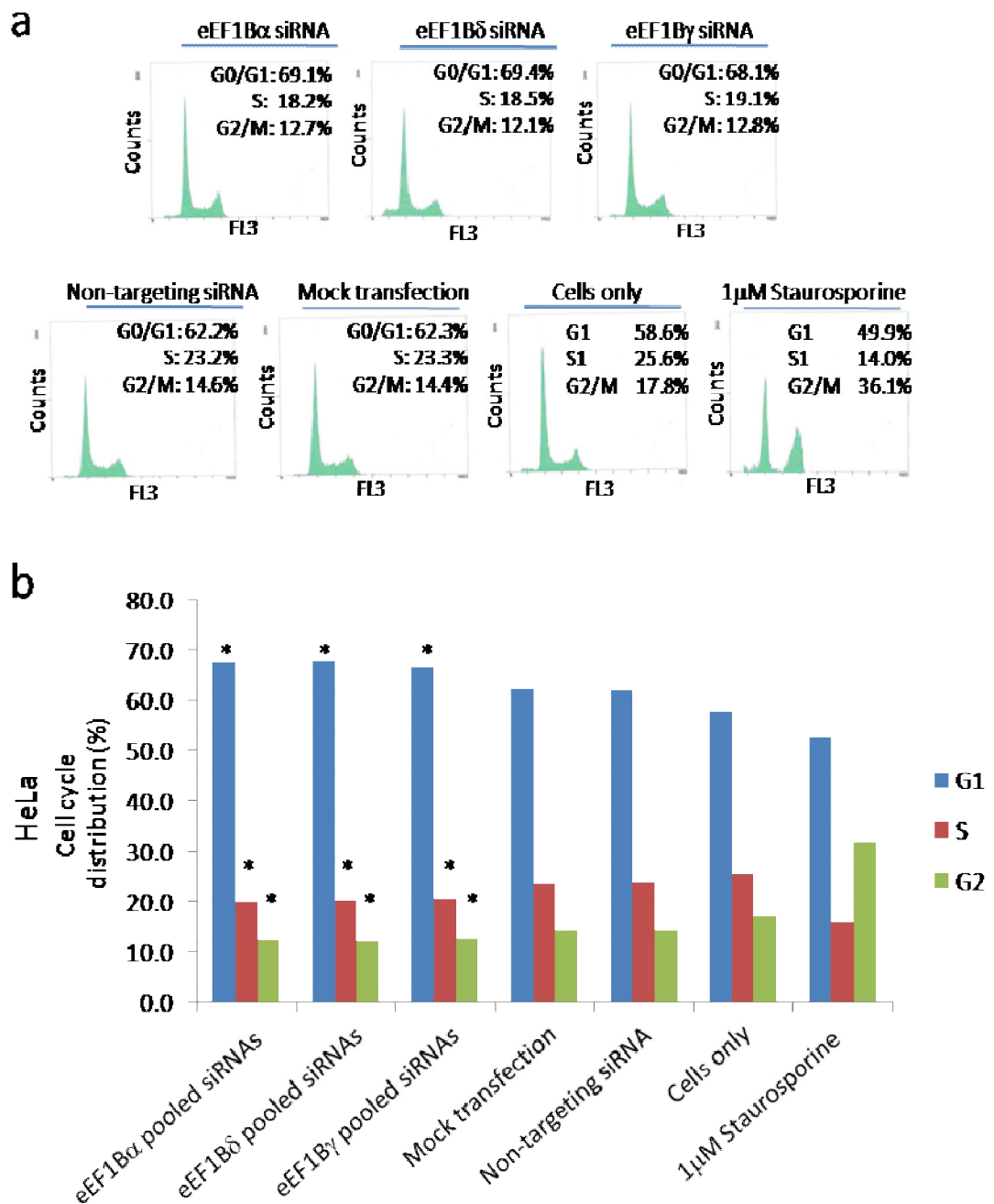


Figure 5.11 Knockdown of eEF1B subunits leads to G0/G1 cell cycle arrest with decreased S-phase and G2/M phase in HeLa cells. Cells were transfected by nucleofection with 10nM siRNAs targeting eEF1B subunits and a scrambled control, labelled with propidium iodide 72h after transfection and subjected to flow cytometry. Staurosporine (1mM) was used as a cell cycle distribution control. (a) Representative images of the flow cytometry analysis. (B) Graphs of the mean percentage obtained from three independent experiments with 10,000 cell counts each. Error bars indicate \pm SEM; $n = 3$; *, $P < 0.05$ from non-targeting siRNA

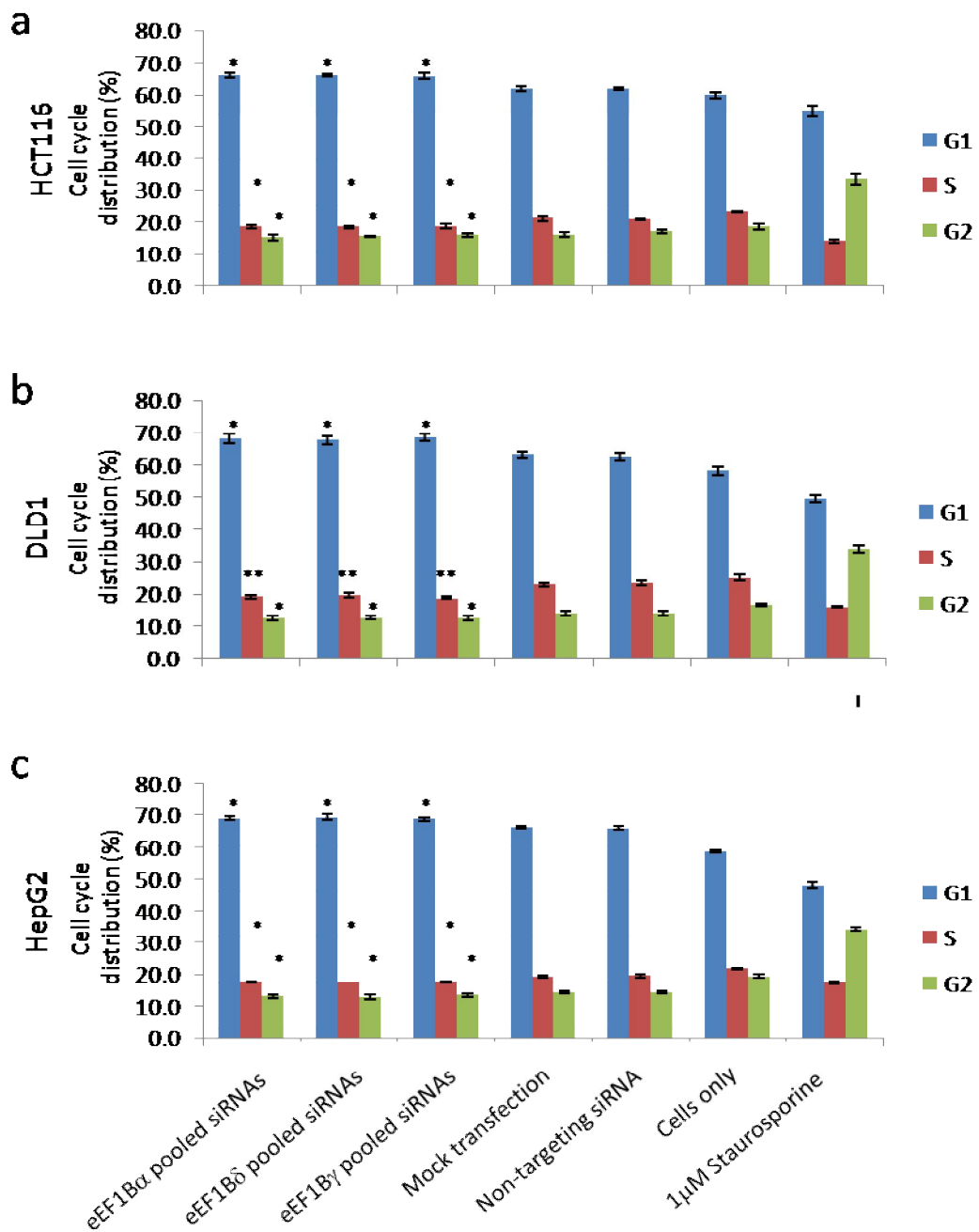


Figure 5.12 Cell cycle distribution of HCT116, DLD1 and HepG2 cells transfected with 10nM siRNAs targeting eEF1B subunits and non-targeting siRNA, measured 72 hours after transfection. The cells were labelled with propidium iodide and subjected to flow cytometry. Staurosporine (1 μ M) was used as a cell cycle distribution control. Graphs of the mean percentage obtained from three independent experiments in (a) HCT116, (b) DLD1 and (c) HepG2 cells with 10,000 cell counts each. Error bars indicate \pm SEM; $n = 3$; *, $P < 0.05$; **, $P < 0.01$ of non-targeting siRNA

HepG2 cells with eEF1B siRNA mediated knockdown showed an increase of more than 9% cells in the G0/G1 stage compared with HepG2 cells transfected with scrambled siRNA, and a decrease of over 4% cells in the S-phase and more than 6% cells in the G2/M phase ($p < 0.05$; Figure 5.12d).

No statistically significant differences were seen in the cell cycle distribution of cells transfected with scrambled siRNA and mock transfected cells. Cells untreated showed a reduced number of cells in G0/G1 and increased in the S- and G2/M-phases compared with mock transfected cells. Staurosporine ($1\mu\text{M}$) was used as a cell cycle distribution control; this gave reduced G0/G1- and S-phase cell number and increased number of cells in the G2/M phase.

In all cell lines studied, eEF1B subunits knockdown lead to a significant decrease in the proportion of cells in S and G2/M phase and increase of cells in G0/G1 phase.

5.2.8 siRNA mediated knockdown of eEF1B enhances apoptosis

Is the low cellular metabolism of cells with low eEF1B expression as measured by Alamar Blue and the increased proportion of cell in the S-phase due to apoptosis? To investigate this, cells were collected after transfection and immediately stained with propidium iodine and annexin V as an early apoptosis detection marker by flow cytometry analysis. Representative images of the flow cytometry output can be seen in Figure 5.13a and in Figure 5.14a. Plotted graphs are the mean of at least three independent experiments in which depletion of eEF1B subunits was confirmed by Western blot.

Flow cytometry analysis detected an increase of the number of apoptotic cells of more than 25% in cells with knocked down eEF1B α ($p=0.003$), over 30% with eEF1B δ down-regulation ($p=0.009$) and almost 25% with eEF1B γ knockdown ($p=0.009$) in HeLa cells compared with cells transfected with scrambled siRNAs (Figure 5.13b).

In HCT116 cells the percentage of apoptotic cells increased by 16% with eEF1B α knockdown ($p=0.04$), by over 14% with eEF1B δ silencing ($p=0.03$) and by more than 13% with eEF1B γ down regulation ($p=0.04$) compared to cells transfected with non-targeting siRNA (Figure 5.14b).

In DLD1 cells, silencing of eEF1B subunits increased the percentage of apoptotic cells by 25% in eEF1B α knockdown ($p=0.004$), 24% in eEF1B δ knockdown ($p=0.005$) and 27% in eEF1B γ knockdown ($p=0.007$) compared with cells transfected with scrambled siRNA (Figure 5.14c).

HepG2 cells with knocked down eEF1B subunits also showed an increase in the percentage of apoptotic cells compared with non-targeting siRNA transfected cells (Figure 5.14d). eEF1B α silencing increased the percentage of apoptotic cells by over 16% ($p=0.04$), eEF1B δ knockdown by more than 15% ($p=0.04$) and eEF1B γ by more than 14% ($p=0.04$).

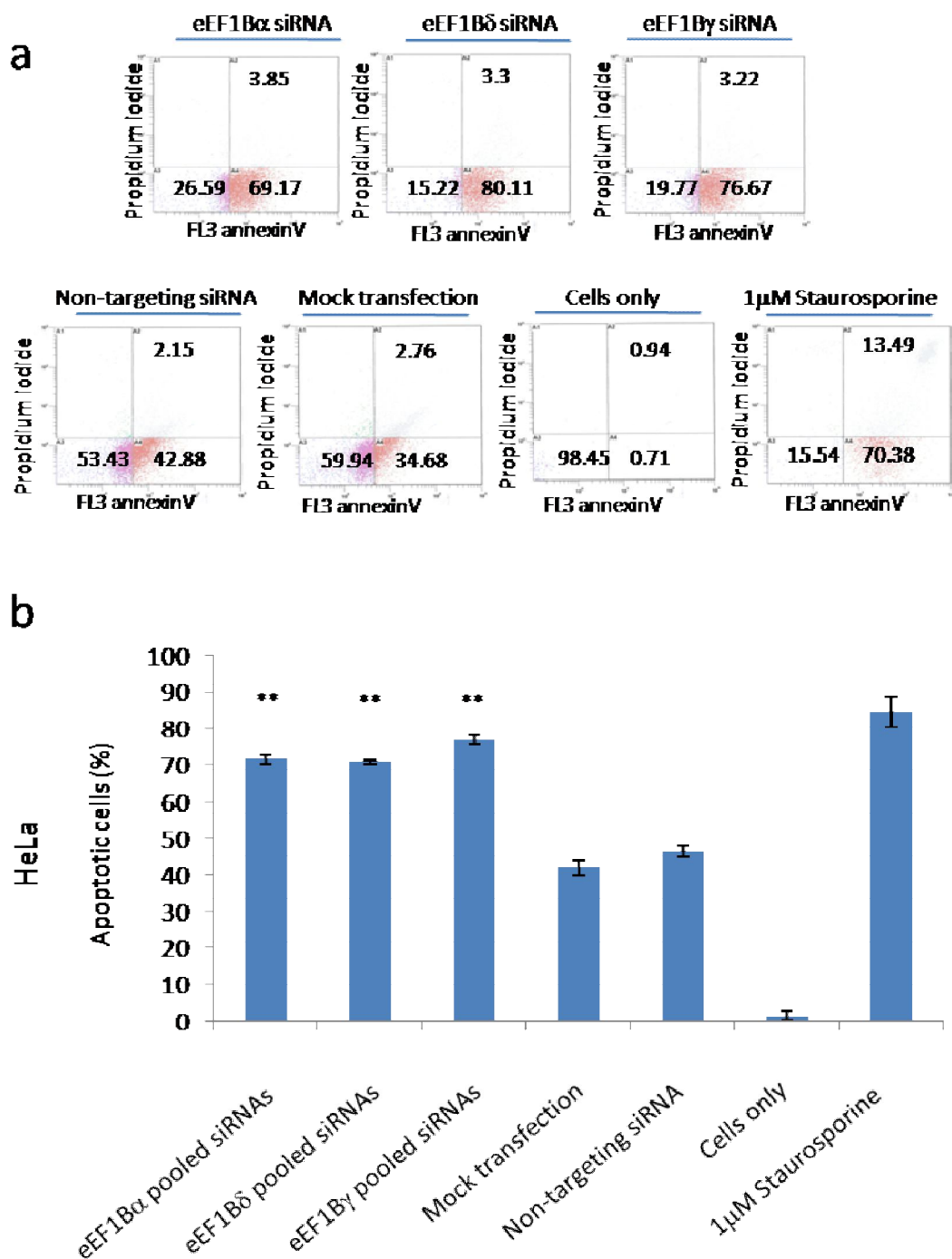


Figure 5.13 Transfection of siRNA targeting eEF1B subunits leads to increased apoptosis compared to non-targeting siRNAs in HeLa cells. Cells were transfected by nucleofection with 10nM siRNAs targeting eEF1B subunits and non-targeting siRNA as a control. Cells were labelled with propidium iodide and annexin V, 72h after transfection and subjected to flow cytometry. Staurosporine (1mM) was used as a apoptosis positive control. (a) Representative images of the flow cytometry analysis. (b) Graphs of the mean percentage obtained from three independent experiments with 10,000 cell counts each. Error bars indicate \pm SEM; $n = 3$; **, $P < 0.01$ from non-targeting siRNA

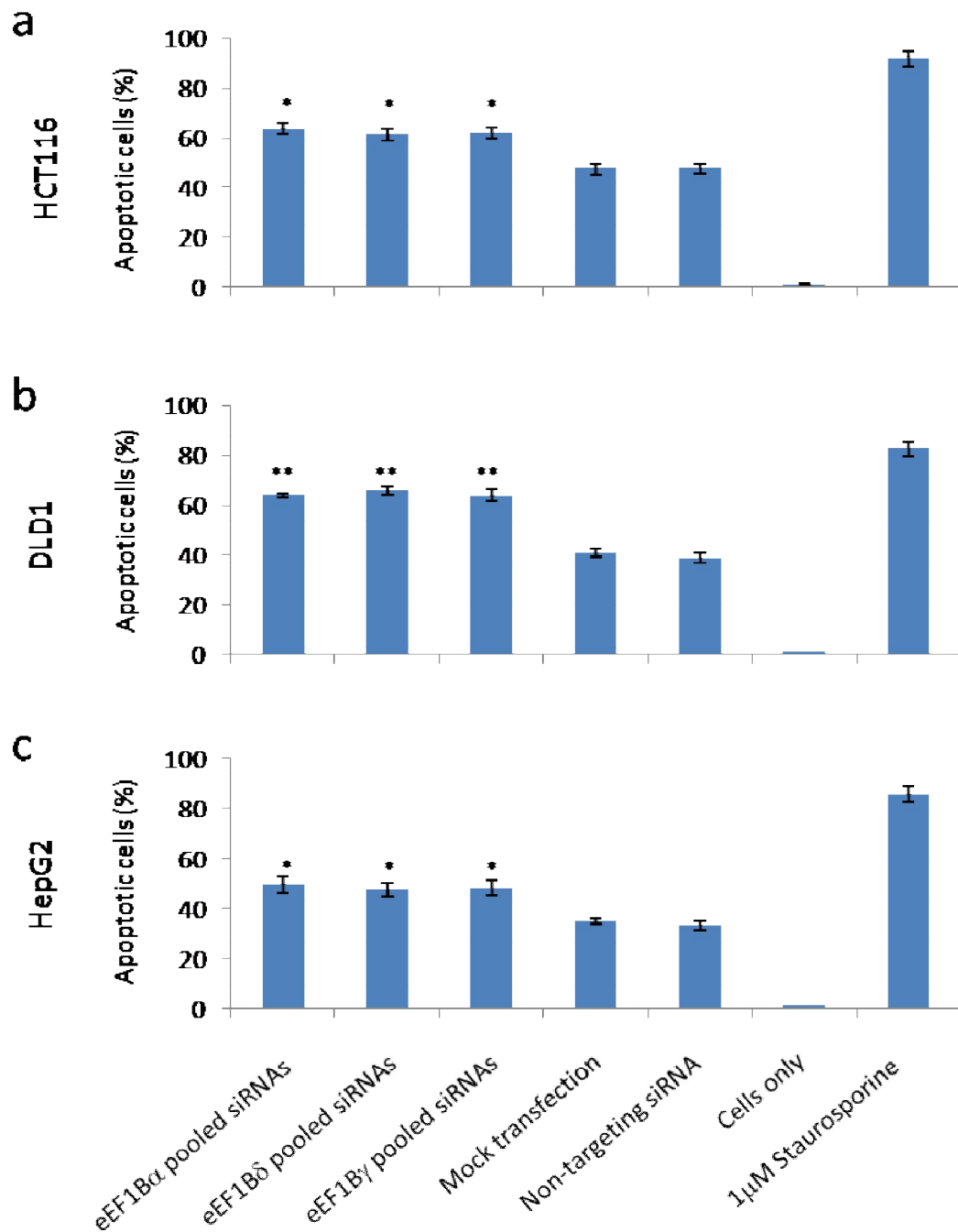


Figure 5.14 Transfection of siRNA targeting eEF1B subunits leads to increased apoptosis compared to non-targeting siRNAs in HeLa, HCT116, DLD1 and HepG2 cells. Cells were transfected with 10nM siRNAs targeting eEF1B subunits and non-targeting siRNA as a control. Cells were labelled with propidium iodide and annexin V, 72h after transfection and subjected to flow cytometry. Staurosporine (1mM) was used as apoptosis positive control. Graphs of the mean percentage obtained from three independent experiments in (a) HCT116, (b) DLD1 and (c) HepG2 cells, with 10,000 cell counts each. Error bars indicate \pm SEM; $n = 3$; *, $P < 0.05$; **, $P < 0.01$; ***, $P < 0.001$ of the non-targeting siRNA

No statistically significant change in the percentage of apoptotic cells was detected by flow cytometry between cells transfected with non-targeting siRNAs and mock transfected cells. Staurosporine (1 μ M) was used as a positive apoptotic control, inducing the percentage of apoptotic cells up to 82% or more compared to a threshold that was set for normal cells of around 1% of apoptotic cells. The elevated number of apoptotic cells can be explained by the method of transfection of cells producing high numbers of apoptotic cells, determined by mock cells and cells transfected with non-targeting siRNA.

Cells transfected with siRNA targeting eEF1B subunits in which the mRNA and protein level of the target was reduced also showed an increased apoptosis as detected with a marker for early apoptotic events. Was this apoptotic effect due to activation of caspases? To explore this question, HCT116 and DLD1 cells were lysed after treatment with siRNAs and analysed by Western blot for the presence of activated caspase-3. DLD1 cells were also submitted to an assay that detects active caspase 3 and caspase 7 by fluorometric analysis.

Immunoblotting of cells with eEF1B subunit knockdown and controls stained with anti-cleaved caspase-3 antibody showed a detectable signal only on the apoptosis positive control (Staurosporine at a concentration of 3 μ M) in DLD1 cells (Figure 5.15a). In all the attempts to repeat this in HCT116 cell line or at a lower staurosporine concentration, a signal could not be detected for active caspase-3.

Fluorometric analysis designed to detect cleaved caspase 3 and caspase 7 showed an increased fluorescence signal in cells with depletion of eEF1B α (33%), eEF1B δ (34%) and eEF1B γ (21%) compared to scrambled siRNA transfected cells (Figure 5.15b). Staurosporine at a concentration of 1 μ M showed a high increase in apoptosis compared with cells only.

siRNA induced knockdown of eEF1B subunits induced apoptosis in all cell lines studied by more than 14% with a statistical significance of $p < 0.05$ using flow

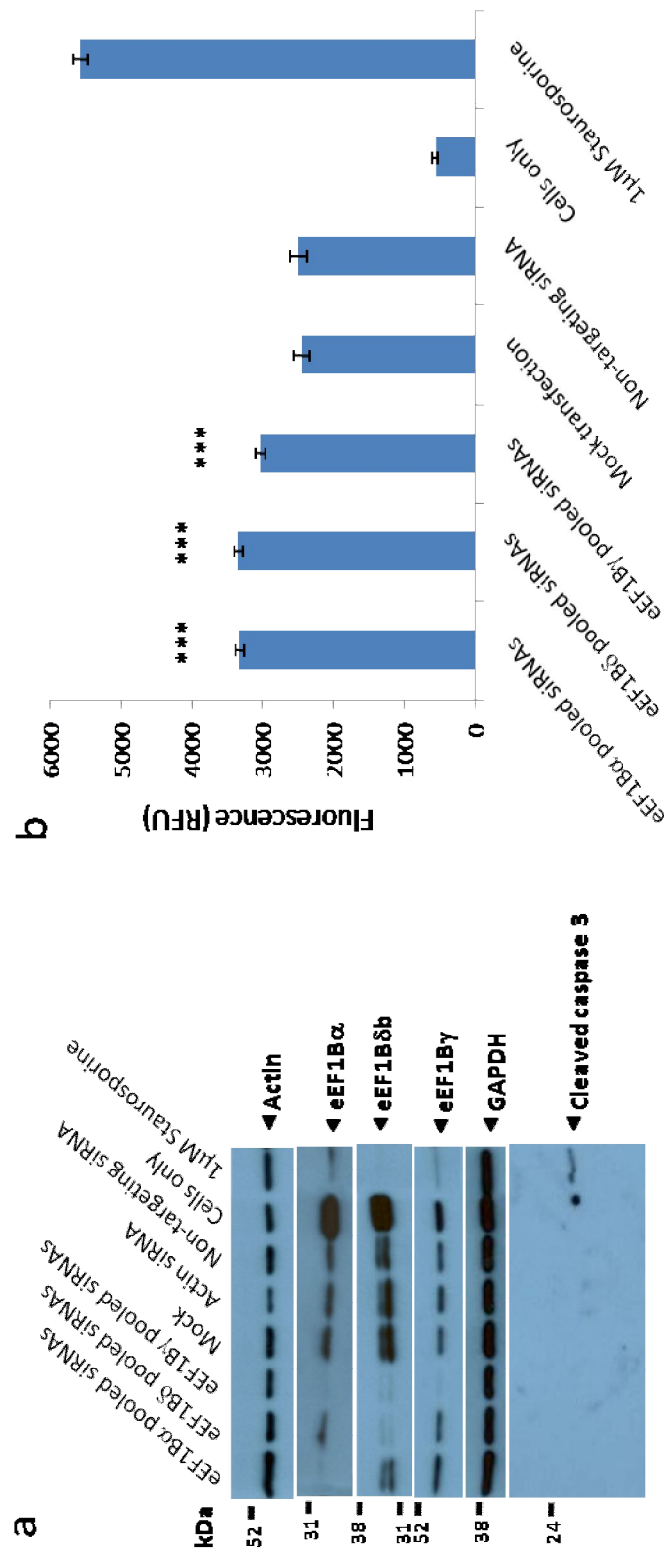


Figure 5.15 RNAi mediated knockdown of eEF1B in DLD1 cells leads to increase of Caspase-3/7 cleavage by fluorescence based assay but not Caspase-3 by Western Blot. DLD1 cells were transfected with siRNAs targeting eEF1B subunits and non-targeting siRNA control. (a) Western blot showing knockdown of all the eEF1B subunits and cleaved-caspase 3 detection only in the lane of cells treated with 3 μ M staurosporine. Cells were harvested 72h after transfection and analysed by Western blot with anti-eEF1B2, anti-eEF1D, anti-eEF1G, anti-GAPDH, anti-actin and anti-cleaved-Caspase 3. Staurosporine (3mM) was used as a positive apoptosis control. (b) Graph showing increased fluorescence on samples transfected with eEF1B subunits specific siRNAs compared with non-targeting siRNA. Increased fluorescence signal is indicative of caspase3/7 cleavage. Seventy-two hours after transfection, cleavage of Caspase 3 and 7 was measured by Apo-ONE Caspase-3/7 assay. Staurosporine (1mM) was used as a control. Graph of the mean fluorescence readings obtained from two independent experiments with 5 wells each. Error bars indicate +- SEM; n = 2 ; ***, P < 0.001 of non-targeting siRNA

cytometry with an early apoptosis marker. DLD1 cells also showed increased apoptosis with a fluorometric analysis based on a later apoptosis marker. However the same apoptotic marker was not detected by Western blot.

These observations are summarised in the Table 5.1 and strongly suggest that specific silencing of eEF1B in HeLa, HCT166, DLD1 and HepG2 is sufficient to cause an increase of apoptosis. However, these effects may be due entirely to the loss of eEF1B γ alone since the increased apoptosis is no worse than when both eEF1B α and eEF1B γ , or eEF1B δ and eEF1B γ proteins are reduced by siRNAs.

Table 5.1 – Relationship between protein expression, proliferation, cell cycle distribution and apoptosis for each eEF1B subunit knocked down in each cell line. Protein expression was determined by densitometry of Western blots. Proliferation was assayed by Alamar blue. Cells were stained with propidium iodine and assayed by flow cytometry to determine the cell cycle distribution. Apoptosis ratio was determined by staining with Annexin V and propidium iodine and analysed by flow cytometry. Table showing the mean values of at least 3 independent experiments normalised against non-targeting siRNA +/- SD.

		Protein reduction (%)	proliferation reduction (%)	S-phase reduction (%)	G0/G1 increase (%)	apoptosis increase (%)
eEF1B α	HeLa	92.3+/-7.8	13.7+/-2.9	16.3+/-3.5	9.1+/-1.7	27.0+/-3.2
	HCT116	89.0+/-9.3	18.6+/-2.7	10.6+/-3.1	6.7+/-1.3	16.1+/-3.7
	DLD1	94.5+/-4.9	20.6+/-1.5	18.3+/-1.0	9.1+/-1.3	24.9+/-1.1
	HepG2	44.4+/-8.6	9.3+/-2.1	9.2+/-1.0	4.6+/-1.0	16.5+/-3.1
eEF1B δ	HeLa	92.0+/-6.9	16.8+/-4.1	15.8+/-3.0	9.5+/-1.4	28.8+/-4.6
	HCT116	94.4+/-6.4	11.6+/-4.1	11.1+/-2.1	6.7+/-0.5	14.5+/-3.9
	DLD1	92.3+/-4.9	19.6+/-1.4	20.4+/-1.3	9.8+/-1.4	24.7+/-2.7
	HepG2	80.7+/-9.8	9.7+/-2.1	10.3+/-0.6	5.2+/-0.7	15.1+/-2.8
eEF1B γ	HeLa	84.0+/-5.6	9.8+/-2.8	13.2+/-3.4	7.5+/-1.3	24.8+/-3.1
	HCT116	77.9+/-5.6	9.6+/-3.5	9.9+/-3.2	6.1+/-1.3	13.7+/-3.4
	DLD1	97.3+/-8.2	14.3+/-1.7	15.0+/-0.7	9.2+/-1.1	26.8+/-4.0
	HepG2	75.0+/-9.5	9.1+/-0.8	9.4+/-1.3	4.1+/-1.1	14.4+/-2.8

5.2.9 Correlation between eEF1B protein level with cell proliferation, cell cycle and apoptosis

In order to correlate the phenotype with the siRNA-induced knockdown of eEF1B subunit protein levels, HeLa cells transfected with siRNAs targeting eEF1B subunits and non-targeting siRNAs were assayed for cellular proliferation, cell cycle distribution and apoptosis over a time course.

Cells transfected with siRNAs targeting each eEF1B subunit showed a decreased cellular proliferation over time compared with cells transfected with non-targeting siRNAs (Figure 5.16a). Decreased cellular proliferation was evident 48 hours after transfection, particularly in cells transfected with eEF1B α targeting siRNAs. The reduction of cell proliferation is more apparent 72 hours after transfection as the protein is effectively reduced, and increased slightly 120 hours after transfection as eEF1B subunit protein levels start to recover.

The cell cycle distribution of cells transfected with siRNAs targeting each eEF1B subunit changed over time compared to cells transfected with scrambled siRNA. Cells transfected with eEF1B targeting siRNAs shifted their cell cycle distribution 24h hours after transfection by a slight increase in the proportion of cells in G0/G1 (Figure 5.16b) and a decrease in the number of cells in G2/M (data not shown) and S phases (Figure 5.16c). The cell cycle distribution difference is more evident 72 hours and 120 hours after transfection as eEF1B protein silencing becomes substantial.

The proportion of apoptotic cells increased over time in cells transfected with siRNAs targeting eEF1B compared with cells transfected with non-targeting siRNAs (Figure 5.16d). A slight increase was detected 24 hours after transfection,

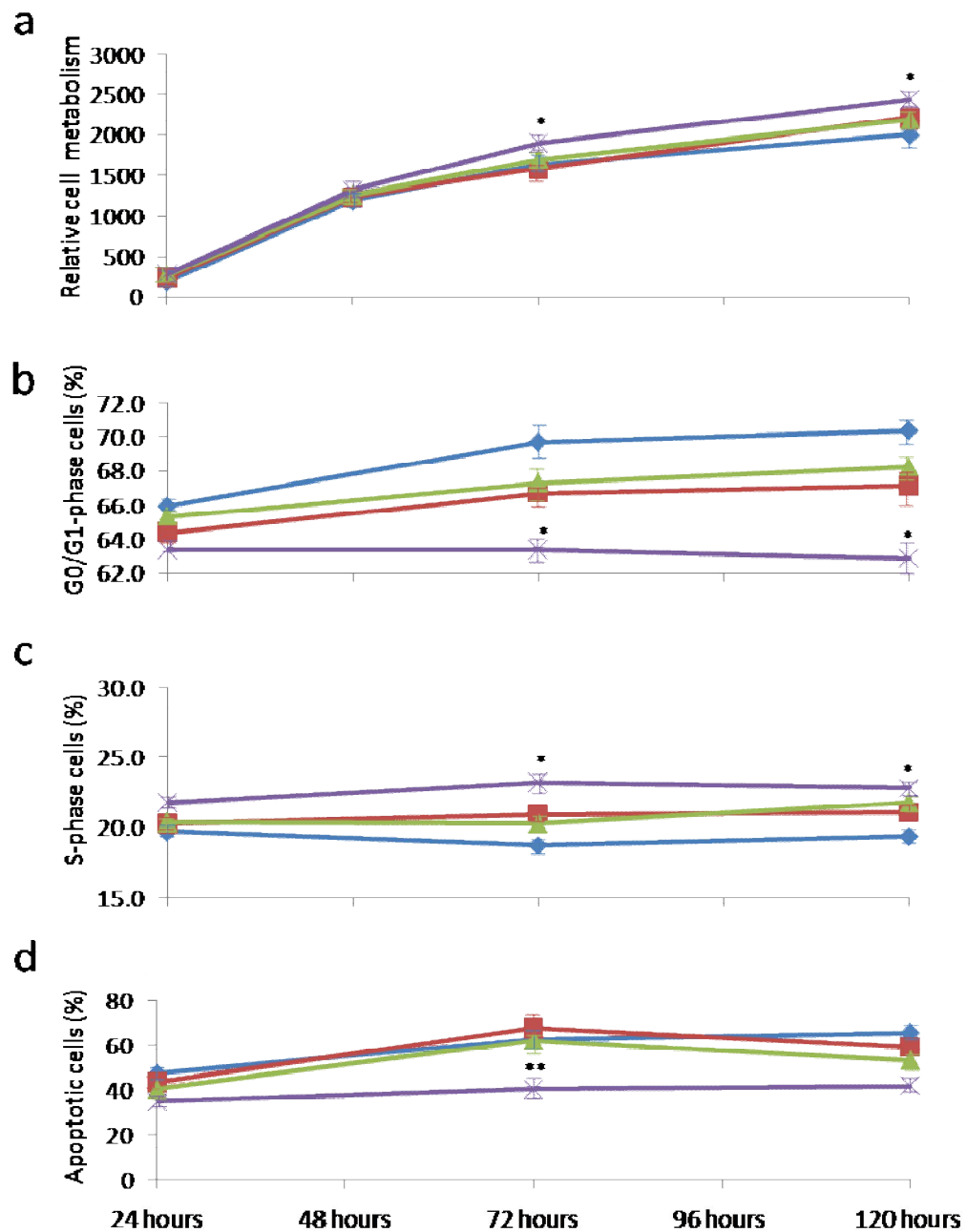


Figure 5.16 Time course of eEF1B knockdown impact on metabolism, cell cycle distribution and apoptosis ratio. Cells were transfected by nucleofection with 10nM siRNAs targeting each eEF1B subunit and non-targeting siRNA. Cells were assayed over a time course of 120 hours. (a) cellular metabolism assayed by Alamar blue. (b) Percentage of cells in G0/G1 phase and (c) percentage of cells in the S- phase measured by flow cytometry analysis of cells stained with PI. (d) percentage of apoptotic cells measured by flow cytometry analysis of cells stained with Annexin V. —◆— eEF1B α pooled siRNAs, —■— eEF1B δ pooled siRNAs, —▲— eEF1B γ pooled siRNA and —×— non-targeting siRNA Error bars indicate \pm SEM; $n = 2$; *, $P < 0.05$; **, $P < 0.01$; ***, $P < 0.001$ of the non-targeting siRNA assessed by student's t test

became more apparent 72 hours after transfection as the eEF1B protein levels are drastically reduced. The percentage of apoptotic cells decreased slightly 120 hours after transfection in cells transfected with eEF1B siRNAs but was still much higher than in cells transfected with scrambled siRNA.

Reduced cell proliferation, an increase proportion of cells in G0/G1 phase and decreased S- and G2/M phase cells and an increase in apoptosis is highest at the time point at which eEF1B protein levels are most reduced.

5.2.10 Overexpression of eEF1B subunits induces proliferation and cell viability

The previous results indicate that siRNA induced knockdown of eEF1B subunits increases apoptosis, and the proportion of cells in the G0/G1 phase, and decreases cell proliferation which leads to the question, does overexpression of eEF1B subunits gives rise to opposite biological changes?

To address this question, full length eEF1B α , eEF1B γ , and eEF1B δ transcript variant b cDNA sequences were cloned into pcDNA-DEST40 with a C-terminal V5 tagged protein (more details Chapter 2). HeLa cells were transiently transfected using the Amaxa nucleofection system with V5 tagged eEF1B α , V5 tagged eEF1B δ transcript variant b, V5 tagged eEF1B γ , V5 plasmid only and transfected with no DNA. Cells were harvested 48h after transfection following the manufacture's recommended conditions.

In order to determine if the constructs were able to direct overexpression of eEF1B subunits, Western blot analysis was used. V5-tagged eEF1B subunits were detected by anti-V5 antibody and increased expression was detected by eEF1B antibodies (Figure 5.17). V5-tagged eEF1B α detected by anti-V5 antibody showed a band at around 30kDa and strong overexpression was detected with the anti-eEF1B α antibody. V5-tagged eEF1B δ signal was detected at around 33kDa and up regulation of eEF1B δ protein detected by anti-eEF1B δ antibody. V5-tagged eEF1B γ was detected at around 50kDa and overexpression of eEF1B γ also detected by the anti-eEF1B γ antibody. GAPDH was detected with anti-GAPDH antibody in all the samples.

These results of overexpression of V5 tagged eEF1B subunits in HeLa cells shown by anti-V5 antibody and anti-eEF1B antibodies moreover again demonstrate the specificity of the eEF1B antibodies.

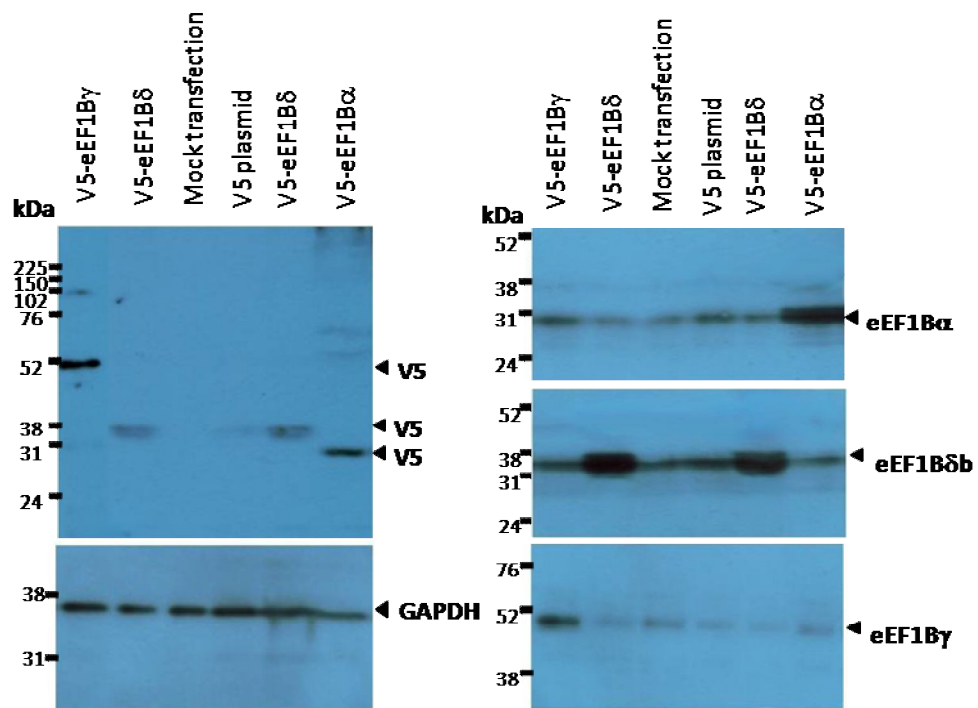


Figure 5.17 Overexpression of eEF1B subunits tagged with V5 in HeLa cells. HeLa cells were transfected with constructs of eEF1B with a V5 tag. eEF1B subunits inserted into a V5 construct and transfected in HeLa cells shows overexpression of eEF1B subunits. Cells were harvested 48h after transfection and analysed by Western blot with anti-eEF1B α , anti-eEF1B γ , anti-eEF1B δ , anti-V5 and anti-GAPDH. V5-eEF1B δ was loaded twice.

Assays were performed to test for cellular proliferation, cell cycle distribution and apoptosis. The cellular proliferation of cells transfected with V5-tagged eEF1B subunits was found to be greater relative to cells transfected with plasmid only (Figure 5.18a). V5-eEF1B α showed an increase in the cell growth around 12% ($p < 0.05$), while V5-eEF1B δ was over 10% ($p < 0.05$) and V5-eEF1B γ almost 8% ($p < 0.05$). Cells transfected with V5 plasmid showed a similar cellular proliferation to mock transfected cells. Cells treated with staurosporine at 1 μ M concentration had a highly reduced cellular proliferation whereas non-treated cells showed 17% more cell growth than with mock transfected cells.

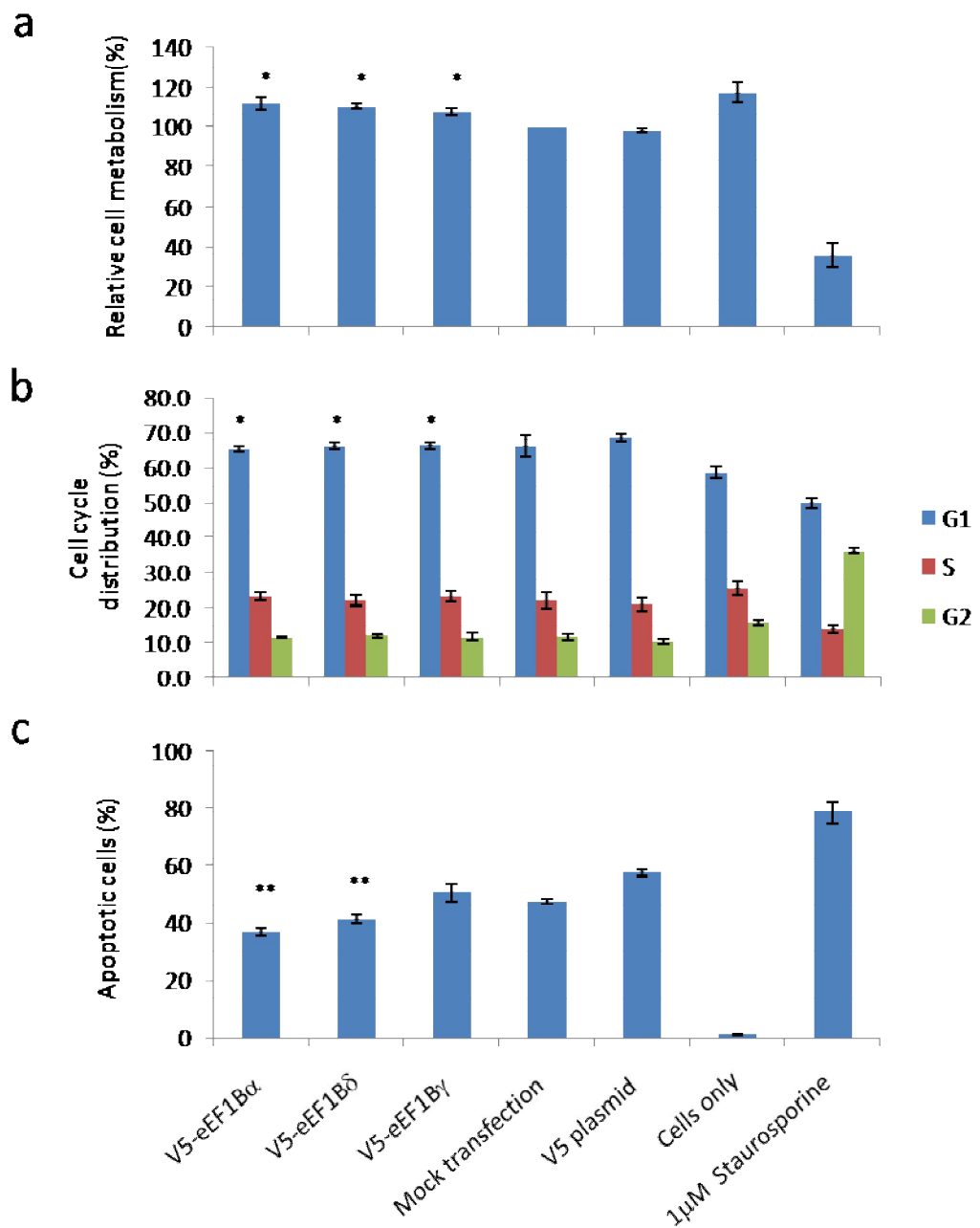


Figure 5.18 Overexpression of eEF1B subunits increases proliferation, in cells in G0/G1 phase and reduces apoptosis compared with V5 plasmid only. HeLa cells were transfected with constructs of eEF1B with a V5 tag. Cells were assayed 48 hours after transfection. **(a)** Graphs of the mean cell growth presented as a percentage of mock-transfected cells. Cell growth was determined by Alamar blue fluorescence. **(b)** Graphs of the mean proportion of cell cycle distribution. The cells were labelled with propidium iodide and subject to flow cytometry. **(c)** Graphs of the mean percentage of apoptotic cells. The cells were labelled with propidium iodide and annexin V and subjected to flow cytometry. Staurosporine (1mM) used as a control. Data obtained from two independent experiments. *Error bars indicate \pm SEM; n = 2; *, P < 0.05; **, P < 0.01 of V5 plasmid*

The proportion of cells in G0/G1 phase increased while the proportion in S- and G2/M phase decreased in HeLa cells transfected with V5 tagged eEF1B subunits in comparison to cells with V5 plasmid only (Figure 5.18b). Up-regulation of eEF1B decreased the number of cells in the G0/G1 phase by around 5% ($p < 0.05$), increased the proportion in S-phase by 9% or more, and increased cells in G2/M phase by over 8%. Cells transfected with V5 plasmid showed a decrease in the proportion of cells in S-phase of around 5% and G2/M phases over by 14% and an increase in the G0/G1 of more than 3%. However, the proportion of S-phase cells in eEF1B overexpressed cells still showed an increase of 4% or more compared with mock transfected cells ($p < 0.05$).

The percentage of apoptotic cells in cells overexpressing eEF1B subunits was decreased compared with cells transfected with V5 plasmid (Figure 5.18c). Compared with V5 plasmid transfected cells, the percentage of apoptotic cells decreased by more than 21% in cells overexpressing eEF1B α ($p = 0.007$), by over 16% in cells with upregulated eEF1B δ ($p = 0.009$) and more than 6% in eEF1B γ overexpressing cells ($p = 0.2$). Once again, cells transfected with V5 plasmid showed increased apoptosis (around 10%) compared with mock transfected cells. However, the eEF1B α and eEF1B δ over-expressing cells still showed a significant decrease of apoptosis compared with mock transfected cells ($p = 0.02$).

The assays performed on cells over-expressing eEF1B subunits, in general, showed the opposite phenotype to the cells with depleted eEF1B subunits. The RNAi gives compound effects in which knockdown of each subunit also affect the expression of the other subunits. Whereas, the protein levels of the eEF1B subunits is not altered in cells over expressing each eEF1B subunit. Overexpression seems to be able to isolate the effects of individual subunits.

Table 5.2 summarises the different assays performed in HeLa cells with knockdown and overexpressed eEF1B subunits.

Table 5.2 – Relationship between protein expression, proliferation, cell cycle distribution and apoptosis for each eEF1B subunit knocked down and up-regulated in HeLa cells. Protein expression was determined by densitometry of Western blots. Proliferation was assayed by Alamar blue. Cells were stained with propidium iodine and assayed by flow cytometry to determine the cell cycle distribution. Apoptosis ratio was determined by staining with Annexin V and propidium iodine and analysed by flow cytometry. Table showing the mean values of at least 2 independent experiments normalised against non-targeting siRNA or plasmid only +/- SD.

		protein expression (%)	proliferation (%)	S-phase (%)	G0/G1- phase (%)	apoptosis (%)
eEF1B α	RNAi	7.7+/-7.8	-13.7+/-2.9	-16.3+/-3.5	9.1+/-1.7	27.0+/-3.2
	Overexpression	187.7+/-17.8	14.0+/-4.0	10.7+/-1.5	-5.2+/-1.2	-22.9+/-5.4
eEF1B δ	RNAi	8.0+/-6.9	-16.8+/-4.1	-15.8+/-3.0	9.5+/-1.4	28.8+/-4.6
	overexpression	153.0+/-15.2	12.5+/-1.3	5.2+/-2.1	-3.9+/-1.3	-18.5+/-4.9
eEF1B γ	RNAi	16.0+/-5.6	-9.8+/-2.8	-13.2+/-3.4	7.5+/-1.3	24.8+/-3.1
	overexpression	150.5+/-22.1	9.8+/-2.6	10.7+/-2.1	-3.7+/-1.3	-8.0+/-4.8

5.3 Discussion

The literature on eEF1B is mainly based on biochemical analysis of its role in protein synthesis and analysis of the overexpression of eEF1B subunits in tumours. In previous chapters of this thesis, some eEF1B subunits were found to have multiple transcript variants, tissue specific expression, varying expression during development, lower expression in wasted mice and nuclear, as well as cytoplasmic, expression in some cells from both human and mouse tissues. This chapter concentrates on functional analysis by siRNA induced knockdown and V5-tagged overexpression of each eEF1B subunit in several human cancer cell lines.

All of the siRNA oligos targeting eEF1B subunits were successful in obtaining extensive mRNA and protein knockdown, validating both the siRNAs themselves and the antibodies raised against eEF1B α and eEF1B γ , as well as the commercial antibodies for all subunits. Cells transfected with siRNAs at a concentration of 10nM 72 hours after transfection were found to give a substantial knockdown of each eEF1B subunit using either single or pooled siRNAs.

In translation elongation, eEF1B subunits act as guanine nucleotide exchange factors on eEF1A, however there is little evidence suggesting which of the two eEF1A variants interact with eEF1B. The one exception is a yeast-two-hybrid experiment where eEF1A1 was found to interact with eEF1B subunits but eEF1A2 did not (Mansilla et al., 2002). If only eEF1A1, but not eEF1A2, needs eEF1B as a GEF, then the effect of biological changes in eEF1B in cells may vary depending on whether they express eEF1A1 or eEF1A2. HCT116 and HeLa cells both express high amounts of all eEF1 subunits, while HepG2 and DLD1 cells lack the eEF1A2 variant (Victoria Tomlinson, PhD thesis, 2007; Jan Bergman, C. Abbot, unpublished data). These four cells lines were used to study the potential biological changes due to reduced protein levels of eEF1B subunits.

To assess the possible effects that each subunit might have on the other eEF1B subunits, each was knocked down and the protein levels of the other subunits were measured. Knockdown of eEF1B α and eEF1B δ independently reduced eEF1B γ protein expression in all cell lines studied. However, in HeLa cells, the mRNA levels were not changed indicating that post-transcriptional mechanisms may be involved. siRNA induced reduction of protein expression of eEF1B δ also reduced eEF1B α protein expression but in HepG2 cells only. eEF1B γ knockdown leads to a reduced protein level of eEF1B α and eEF1B δ in HeLa and HepG2 cells but only eEF1B α in HCT116 cells. In contrast, eEF1B γ knockdown showed no effect on the other subunits in DLD1 cells. The variability observed was most likely due to the variety of tumours from which the cell lines were originally obtained.

Parallel knockdown has recently been suggested to be helpful in analysing pathways (Sahin et al., 2007). In a pilot study, parallel knockdown of eEF1B subunits using different combinations was attempted in HeLa cells. Most combinations showed the expected protein level reduction, knocking down all subunits demonstrating the requirement of each subunit in the formation of the complex. However, one of the siRNA combinations (eEF1B α and eEF1B γ) showed reduced expression for eEF1B α and eEF1B γ but normal protein levels for eEF1B δ . This may have been due to a Western blot artefact or due to variability of knockdown, but since this experiment was only attempted once, repetition is essential to verify its reliability and validity.

Except cells with a strong eEF1B δ reduction which showed an abnormal distribution of α -tubulin, cells with knockdown of eEF1B subunits showed no obvious phenotypic abnormalities by immunofluorescence, although reduced cell proliferation was found as measured by Alamar blue reduction. The Alamar blue assay was chosen to assay the cell viability/proliferation as it is a simple, quick, reliable and sensitive assay that does not affect the cells and does not require cell lysis and therefore can be used to take successive measurements (O'Brien et al.,

2000). It also been reported to have a greater reproducibility and accuracy than MTT assays (Hamid et al., 2004). Low cellular proliferation was further confirmed by determining the proportion of cells in the S-phase in all the cell lines tested. In addition to a decrease in number of cells in the S-phase, down regulation of eEF1B subunits also decreased the number of cells in G2/M phase and increased those in G0/G1 phase.

One of the early features of apoptosis is loss of plasma membrane asymmetry which exposes phosphatidylserine (PS) to the extracellular environment. Annexin V binds exposed PS hence acting as an early marker of apoptosis (Vermes et al., 1995). Annexin V used in conjunction with the vital dye propidium iodide, which detects cell membrane integrity loss, can be detected by flow cytometry and distinguishes between early apoptotic, late apoptotic and dead cells. Since Annexin V staining has to be performed on live cells and changes over time, cells were analysed by flow cytometry immediately after collection and cells with eEF1B knockdown showed an increased apoptosis in all cell lines studied. Induction of apoptosis also activates a cascade of caspases with amongst others Caspase 3 and Caspase 7 as the main effector caspases. Anti-cleaved caspase-3 antibody was used to confirm the eEF1B knockdown induced apoptosis in DLD1 and HCT116 cells. However immunoblotting with this antibody failed to show a signal even in the apoptosis positive control (1 μ M Staurosporine). A signal was only detected when the concentration of Staurosporine was increased to 3 μ M in DLD1 cells but still not in HCT116 cells, while cell lysates with eEF1B subunits knocked down showed no signal. This suggests that the antibody used might not be sensitive enough to detect low levels of caspase-3 activity. To investigate this further, Apo-ONE Homogeneous Caspase3/7 fluorometric assay (Promega) was carried out in DLD1 cells. This assay is a fast, robust and sensitive measurement of the ability of these caspases to cleave a profluorescent substrate. This assay has been used in multiple studies with Staurosporine as an apoptosis positive control, with a few

studies detecting a signal even with doses as low as 0.5 μ M (Piddubnyak et al., 2007) or even 0.1 μ M of Staurosporine (Lakhani et al., 2006). Using this assay, eEF1B siRNA induced knockdown cells and cells treated with 1 μ M Staurosporine were found to have increased caspase-3 and caspase-7 activity with the percentage of apoptotic cells similar to the ones detected by flow cytometry analysis of Annexin V/propidium iodine. These results suggest that silencing of eEF1B subunits leads to increased apoptosis with increased exposed PS and activation of caspase-3 or/and caspase-7.

In addition, the trends in the most obvious phenotypic changes were correlated with the loss of eEF1B protein over time, which is important since the siRNAs were transiently transfected.

In a much smaller scale study, performed in HeLa cells, overexpression of eEF1B subunits tagged to a V5 protein was achieved and once again validated the eEF1B commercial antibodies. Cells overexpressing eEF1B subunits showed almost opposite phenotypic effects when compared to cells with depleted eEF1B subunits in the HeLa cell line. Overexpression of eEF1B subunits leads to increased proliferation, measured by Alamar blue, and a greater proportion of cells in S-phase, and decreased apoptosis detected by Annexin V/propidium iodine flow cytometry analysis, compared with mock transfected cells and cells transfected with V5 plasmid only. pDEST40 V5 plasmid only showed a considerable difference in cell proliferation and apoptosis compared with mock transfected cells suggesting high toxicity of the plasmid. This might have been an artefact or due to contamination such as endotoxin. A pDEST40 V5 plasmid tagged to a protein which is known not to affect proliferation or apoptosis might have been a better control for this study.

The pattern of reduced eEF1B subunit protein levels when an individual subunit is knocked down using RNAi indicates that it is likely that the knockdown of individual subunits alters the folding, stability and consequently function of the eEF1B complex, with eEF1B γ playing a central role in the stability of the complex. eEF1B γ has been previously suggested to somehow be involved in the scaffolding of the complex (Mansilla et al., 2002). A similar result was obtained when knockdown of individual translation initiation factor 3 subunits consistently reduced the expression of the eIF3a subunit (Martineau et al., 2008) which had been previously known to be essential for the eIF3 complex stability and function (Masutani et al., 2007). Furthermore, these results obtained in cell culture system are not wholly consistent with the results described in the previous chapter, in that eEF1B subunits are not all present in the same cells and even in the same sub-cellular localisation both in mouse and human tissue samples.

The effect of the RNAi for each eEF1B subunit on the protein levels of the other subunits does not allow to distinguish completely the effects of individual subunit depletion on cells, because eEF1B γ was reduced by the eEF1B α and eEF1B δ knockdown. In contrast to the knocked down effects, overexpression of individual eEF1B subunits does not alter the protein levels of the other eEF1B subunits. The overexpression results are more reflective of the individual effects of each subunit on HeLa cells.

Knockdown of eEF1B subunits reduced cell metabolism, induced accumulation of cells in G0/G1 phase, and increased proliferation and apoptosis, while overexpression resulted in induced cell metabolism, proliferation and reduced apoptosis. These results are consistent with the multiple reports of overexpression of eEF1B subunits in cancer and their potential as oncogenes. A similar phenotype observed with eEF1B subunit knockdown and overexpression has also been reported with many other oncogenes and translation factors with

oncogenic features. In HCT116, HepG2 and MCF7 cells, c-Myc down regulation reduced cell proliferation and increased apoptosis and also inhibited anchorage-independent colony formation in soft agar and reduced tumour growth in nude mice (Wang et al., 2005). eIF3H knockdown reduced proliferation, increased apoptosis and anchorage-independent growth in soft agar of the breast cancer cell line MDA436 and prostate cancer cell line PC-3 (Zhang et al., 2008) while overexpression of eIF3H in NIH-3T3 cells lead to increased proliferation, reduced apoptosis and resulted in malignant transformation (Zhang et al., 2007). In MCF7 cells, 72 hours after transfection, eIF4E knockdown induced accumulation of cells in G0/G1 phase by around 7%, reduced proliferation by around 24% and increased apoptosis by around 9% (Dong et al., 2009). This phenotype is in all respects similar to the phenotype observed with knockdown of eEF1B subunits. Dong and colleagues went on to find that knockdown of eIF4E also inhibited tumour growth in nude mice. Overexpression of eIF4E is also known to lead to increased cell proliferation, survival and cause malignant transformation in immortal NIH-3T3 cells (Lazaris-Karatzas et al., 1990).

Both actin and tubulin protein expression seemed to be altered/reduced in some RNAi experiments particularly using siRNAs targeting eEF1B δ but although the altered tubulin expression and the speckled DAPI staining may be associated with the phenotype, it was found not to be reproducible. In some RNAi experiments in which neither actin or tubulin seemed to be affected, the knock down effect was always similar to the one observed when actin or tubulin protein expression was altered. However it is not to exclude completely that the effects attributed to the knock-down of eEF1B δ subunit might be due to alterations in actin and tubulin. Therefore, it would be interesting to study to determine if the phenotype of the eEF1B subunits knock down is not related to the altered expression of actin and tubulin by studying its effect on cytoskeletal proteins.

It is not essential to carry out rescue experiments in siRNA-mediated knockdowns, as long as other controls such as, scrambled siRNAs, use of the lowest concentration of siRNAs possible and showing that similar effects are observed with several siRNAs targeting different sites in the same mRNA are present. The ultimate way to fully confirm the phenotype derived from siRNA-mediated knockdown, however, would be to rescue the effect by the addition of a rescue of the target gene that is not affected by the siRNA used. This can be achieved by plasmid caring either a mutation in the siRNA target region or by the use of siRNAs targeting 3' or 5' UTRs (Sarov and Stewart, 2005). Taking into consideration the fact that the transfections were transient and that an *in vitro* system was used, it is interesting that knockdown of eEF1B α lead to increased apoptosis in agreement with eEF1B α knockout which is lethal in yeast *Sacharomyces cerevisiae* (Hiraga et al., 1993). Knockdown by RNAi of eEF1B α in *Caenorhabditis elegans* at the embryonic stage is also lethal with 80% penetrance, knockdown at the larvae stage gives a larva slow growth or larval arrest phenotype (Kamath et al., 2003, Simmer et al., 2003) while in the nematode *Panagrolaimus superbus* knockdown is also embryonic lethal (Shannon et al., 2008).

Knockdown of eEF1B γ leads to apoptosis, however in *S. cerevisiae*, knockout of eEF1B γ or eEF1B γ homologue is viable (Kinzy et al., 1994, Kambouris et al., 1993) but a double knockout has not been reported. In contrast, in *C. elegans*, eEF1B γ knockdown by RNAi at embryonic stage is lethal with 80% penetrance, at the larval stage slow growth is reported and at the adult stage an adult sterile phenotype is found (Simmer et al., 2003, Kamath et al., 2003, Sonnichsen et al., 2005).

In yeast, two genes encode for eEF1A (Schirmaier and Philippsen, 1984) and eEF1B δ is not present in lower eukaryotes. However human eEF1B δ with a mutant CDK1 phosphorylation site is able to suppress the yeast lethal phenotype caused by eEF1B α knockout (Pomerening et al., 2003). Would eEF1B δ rescue eEF1B α depletion phenotype and eEF1B α rescue eEF1B δ knockdown phenotype in human cell lines?

eEF1B α lethal phenotype, in yeast, is overcome by overexpression of eEF1A, but not by overexpression of eEF1B α itself (Kinzy and Woolford, 1995) which raises the question would eEF1A1 or eEF1A2 rescue eEF1B α depletion phenotype in human cell lines? Would they rescue eEF1B δ knockdown phenotype? Since the eEF1B subunit knockdown phenotype might be due at least in part to the reduced protein levels of eEF1B γ observed when eEF1B α or eEF1B δ are depleted, the crucial rescue experiment might be trying to rescue the phenotype of eEF1B α or eEF1B δ knockdown by adding eEF1B γ .

In addition to the need to repeat the study of overexpression of eEF1B subunits possibly with different controls, the mechanism by which knocking down eEF1B subunits knockdown induces apoptosis and by which overexpression induces proliferation is still unknown. The mechanism by which eEF1B γ is depleted by siRNA-induced knockdown of eEF1B α and eEF1B δ it also remains unknown. This might be due, at least in part, to increased protein degradation or reduced mRNA levels of GEF eEF1B α and eEF1B δ suppressing translation.

Further characterisation and studies are needed in order to confirm eEF1B subunits as truly having oncogenic properties. This would include investigating anchorage-independent growth in soft agar and *in vitro* invasion assays. Although extremely important to study cell culture systems, it might be more biologically significant to investigate tumour growth in nude mice, particularly due to the eEF1B complex expression of the subunits in animals. In addition, it would be of importance to identify the over expression mechanism of eEF1B subunits in tumours by determining whether there are any gene amplifications, rearrangements or point-mutations.

Protein synthesis is essential for the cell and misregulation of proteins involved in translation have been implicated in many different diseases including cancer. This study provides further insight into the possible involvement of eEF1B subunits in tumourigenesis.

6. General Discussion

The eEF1B complex is known to recycle GDP-bound eEF1A into its active GTP form during the elongation phase of protein synthesis. In mammals, the eEF1B complex is composed of the alpha and delta subunits which possess guanine exchange activity and a third subunit, gamma, with no known function. The complex has been extensively characterised biochemically, but little is known about the molecular biology. The purpose of this project was to characterise the eEF1B subunits and to begin to investigate their potential involvement in tumourigenesis.

eEF1B subunits were found to be regulated at multiple levels. They are all predicted to have 5' TOP sequences (Iadevaia et al., 2008) and CpG islands. DNA/RNA and protein-protein binding motifs have also been identified and several post-translational modifications have been predicted including phosphorylation sites for kinases involved in a variety of functions. Data from large-scale studies was also analysed and sites were mapped.

eEF1B δ was found to have a variety of previously unknown transcript variants and isoforms, including a tissue-restricted heavier isoform and a muscle specific isoform which were identified by *in silico* models and their presence confirmed *in vivo* (Chapters 3 and 4). An isoform that has previously been found in sea urchins (Le Sourd et al., 2006b), which is the product of exon skipping, was also present in human and mouse ESTs and seems to be expressed in all tested tissues and cell lines. Another transcript variant was also identified from mouse ESTs data which has a previously unknown exon. eEF1B α and eEF1B γ were also found to be expressed in all tissues, however eEF1B α appears to exist as a band double the expected size in a tissue-specific way. This band is likely to represent a dimer since there is no evidence for another transcript variant. Several pseudogenes were identified in both human and mouse sequence databases but none showed evidence of being expressed. eEF1B α was not expressed at an early-embryonic stage and

eEF1B δ was found to be highly expressed at embryonic and early post-natal stages compared with adult mice. Furthermore, tissue distribution of eEF1B subunits was not always consistent between the subunits in the same cell types and showed cytoplasmic and, surprisingly, nuclear expression. eEF1B subunits expression pattern seems to overlap, at least in part, with both eEF1A1 and eEF1A2 known expression patterns (Newbery et al., 2007). Moreover, the distribution of eEF1B subunits in cell lines was restricted to the cytoplasm and did not change in cell cycle arrested cells, although eEF1B δ was overexpressed in G2/M-arrested cells.

siRNA-induced knockdown of eEF1B subunits individually decreased proliferation, the proportion of cells in the G2/M- and S-phase and increased apoptosis via caspase 3/7 in cells with and without eEF1A2. Furthermore, cells with a strong eEF1B δ reduction showed an abnormal distribution of α -tubulin. Also, siRNA-induced reduction of either eEF1B α or eEF1B δ led to a decrease in protein levels of eEF1B γ which might account for the similar knockdown phenotype seen with each subunit. In contrast, overexpression of V5 tagged eEF1B subunits constructs in HeLa cells induced proliferation and the proportion of cells in the G0/G1 phase and reduced apoptosis. Overexpression of individual subunits appeared not to affect the protein levels of the other eEF1B subunits. This result is in agreement with the potential role of eEF1B in tumorigenesis and may indicate that the protein level of eEF1B subunits might be rate-limiting for translation.

As described above, reduced availability of eEF1B subunits with guanine exchange activity can lead to reduced eEF1B γ protein levels which indicates that eEF1B γ might be essential for the stability of the complex. Each eEF1B subunit also has a spatially and temporally restricted expression pattern and the subunits are not co-expressed in a large number of cell types, which questions the functionality of the complex and brings to light the differences between cell culture systems and *in vivo* study. Furthermore, although eEF1B α and eEF1B δ share a highly conserved C-terminal domain sequence, structure modelling of eEF1B δ predicted different

protein-binding clefts for the previously identified eEF1A binding clefts. This difference might give a slight advantage to one of the eEF1A variants or even a different efficiency rate for eEF1B α and eEF1B δ . Furthermore, there is the existence of several eEF1B δ isoforms in mammals that give an extra potential complexity to the quaternary structure of eEF1B. In addition, more proteins have been suggested to be part of a larger complex such as valyl-tRNA synthetase and eEF1E, both of which, possess a domain identical to eEF1B α , eEF1B γ and other multisynthetase complex subunits which are likely to form a multimer via a GST-like dimer fold domain (Quevillon and Mirande, 1996, Sang Lee et al., 2002, Bec et al., 1989).

6.1 Future studies

6.1.1 eEF1B subunits in cancer

None of the studies of eEF1B δ overexpression distinguish between isoforms. It is important to determine if a particular isoform is associated with overexpression in tumours. Before starting to investigate the mechanism of overexpression, it would be vital to determine in which tumour types eEF1B subunits are overexpressed at the mRNA level and protein level, where they are expressed and if the expression pattern of the subunits correlates, using immunohistochemistry. Analysis of tissue microarrays (TMAs), hundreds of samples on a single slide, can facilitate this task. Moreover, it would be important to determine if the overexpression correlates with different factors such as sex, age, tumour grade, tumour type, invasiveness, and survival. Correlation with eEF1A1, eEF1A2, TCTP and even eEF2 may be of interest to study since might give an insight into the possible link between tumourigenesis and increased translation.

Central to a better understanding of the involvement of eEF1B subunits in tumourigenesis would be to repeat the overexpression studies and investigate anchorage-independent growth in soft agar, *in vitro* invasion assays and tumour growth in nude mice. In addition, it would be important to attempt to rescue the knockdown lethal phenotype by overexpressing the eEF1B subunits and repeating the knockdown experiment in non-cancerous cell lines.

Once the types of tumour in which eEF1B subunits are overexpressed have been identified, and eEF1B subunits found to be truly oncogenic, it would be essential to determine the mechanism of overexpression. If the mRNA is overexpressed then factors like copy number changes, rearrangements, methylation status, mutations in the promoter region, exons and intron/exons boundaries (if a particular eEF1B δ isoform is overexpressed) should be investigated.

6.1.2 eEF1B subunits expression and regulation

Promoter regions for each eEF1B subunits and transcription factor binding sites were predicted by *in silico* analysis. However, in order to appreciate the regulation of the eEF1B subunits at the transcription level, the transcription start site should be determined and the 5'UTR studied by for instance RACE-PCR, thus functionally characterising the promoter and 5'UTR region by for example fusing it with a reporter gene such as Luciferase or GFP and determining gene expression. Furthermore mutations could be created and their affect on gene expression determined.

The presence of more transcript variants should be investigated by RACE-PCR and Northern blotting. Furthermore, it should be investigated as to whether the various transcript variants are due to mutations in the intro/exon boundaries or whether they are due to alternative promoters. In order to determine if all the transcripts are translated into protein, and to investigate possible tissue specificity, sub-cellular localisation, and expression pattern during development and cell cycle, antibodies against each of the isoforms should be produced. To build up the knowledge of potential isoform specific functions, siRNA mediated knockdown and overexpression by transfection with tagged constructs of each isoform should be carried out and the effects determined for of each isoform by a variety of assays in the same way as it was performed for this study. It would also be important to determine if eEF1B subunits exist in the cells at a limiting concentration or if there is some sort of threshold below which the cell dies. This can be achieved by performing RNAi at different knockdown efficiencies. Moreover, rescue experiments should be carried out to determine if the increased apoptosis phenotype of siRNA induced knockdown can be reversed by overexpression of eEF1B subunits. It is possible to establish stable cell lines to study differently expressed sub-populations of cells in which to measure the long term impact of different efficiencies of knockdown and overexpression on cells. Ultimately, the effect observed *in vitro* might not be the same as *in vivo* and it is essential to produce

a knockdown, by shRNA, or knockout, by mutagenesis or gene trap, to evaluate the phenotypic alterations upon down-regulation or complete absence of each subunit and each eEF1B δ isoform. Since knockdown in human cell lines led to increased apoptosis, and knockouts in other species leads to a lethal phenotype it is expected that knockout mice might have a lethal phenotype as well. For that reason it might be more useful to do an inducible system, such as cre-lox, so that expression can be controlled temporally and spatially. Exogenous expression of eEF1B subunits in mice could also provide some insight into possible functions.

Further investigations of the expression of eEF1B subunits during the cell cycle and in particular mitosis, under cellular stress conditions and their possible link to cytoskeleton should be carried out. Time-lapse microscopy would be able to determine the dynamic redistribution of cytoskeletal and regulatory proteins as well as the eEF1B subunits. The use of drugs that disrupt either cell cycle or the cytoskeletal proteins dynamics or even induce cellular stress could be used to consider the dependence of eEF1B subunit expression and function on cell cycle stage or cytoskeletal interaction and their involvement in stress response. Since eEF1B subunits protein levels do not change substantially during the cell cycle, and they are known to be phosphorylated by cell cycle specific kinases in other species, it would be interesting to determine the phosphorylation status during cell cycle and mitosis in human cells. Since it is known that there are several sites that are often phosphorylated in eEF1B subunits, phospho-antibodies could be produced. Alternatively, less specific but still useful serine, tyrosine and threonine phospho antibodies can be used to study the phosphorylation status of purified proteins. Potentially, the phosphorylation sites could be mutated to examine the effects in the expression or function of the proteins. However, eEF1B subunit expression levels, expression pattern or phosphorylation state have not been studied upon cellular stress. Investigating their response in relation to various cellular stresses, including formation of stress granules where other translation factors are known to be involved would be essential in better understanding this putative function.

6.1.3 eEF1B complex structure

It is clear from the expression studies *in vivo* and the knockdown effect in a cell culture system that the eEF1B complex most likely changes configuration and conformation *in vivo* and that this differs from *in vitro*. It is crucial to determine the interactions of the subunits between themselves and interactions with proteins such as eEF1A variants, tRNAs, other translation factors, cytoskeletal proteins, and proteolysis machinery proteins. With previous eEF1B complex models disagreeing about the molecular weight of the complex, molar ratios and even which terminus of the subunits interacts with other subunits, it is essential to determine the intrinsic interaction sites between the subunits within the complex as well as the factors or conditions that determine the complex composition to change.

Protein-protein interaction studies preferably *in vivo* such as bimolecular fluorescence complementation (BiFC) or fluorescence resonance energy transfer (FRET) would be of particular interest (*in vivo* protein-protein interaction systems reviewed in Ciruela, 2008). Also by mutating the GST, leucine-zipper, transmembrane, disordered as well as other conserved domains would be possible to identify the site of interactions and to validate the protein-protein interaction studies at the same time. In addition, *in vivo* protein-protein interaction would provide information about the sub-cellular localisation of the complex in a stable non-reversible way (eg. BiFC) or in a dynamic reversible system such as FRET. In addition, these methods can be used to study protein-protein interactions upon knockdown and overexpression, cell cycle and cytoskeleton disruption, under cellular stress conditions or even to study tRNA acetylation. These protein-protein interaction methods can be easily analysed by microscopy, flow cytometry and fluorometry.

6.1.4 Implications for protein synthesis

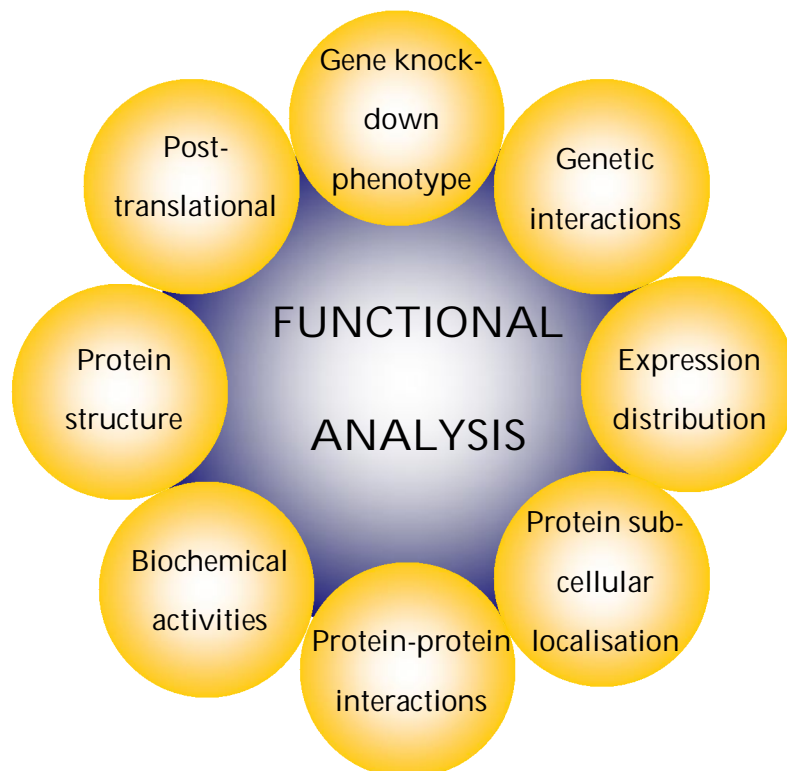
Compartmentalisation of translation can take place in membranes, cytoskeleton, cytosol or controversially in the nucleus (Dahlberg and Lund, 2004). Is the interaction with the cytoskeleton, the presence of transmembranes and the nuclear expression, besides the expected cytoplasmic expression, a reflection of translation compartmentalisation or non-canonical functions? There is no easy way of addressing this question. However, polysomal microarrays of sub-cellular fractions corresponding to membrane, cytoskeleton, nuclear and cytosolic, might give a good insight into differently synthesised proteins. Furthermore, since phosphorylation of eEF1B subunits alters protein synthesis in a membrane and cytosolic way, it might be interesting to study overexpressed and slight knockdown (non-lethal) of eEF1B subunits and perform polysomal microarray analysis as described above.

With a variety of complex structures, is the eEF1B complex always functional? Is there any particular protein region that alters translation? Is eEF1B rate-limiting rather than initiation which many believe to be the rate-limiting reaction in translation (Sonenberg et al., 2000)? Does overexpression or slight down-regulation of eEF1B subunits alter translation? Does the restricted expression of eEF1B subunits give an insight into temporal and local translation? Probably the best way to examine this problem is to establish stable cell lines with either overexpressed, knockdown constructs (at a non-lethal concentration) or even mutated eEF1B subunit proteins and measure a series of parameters, such as translation initiation rate (methionine synthesis), translation elongation rate (monitoring incorporation of several different labelled amino acids such as valine, at least one tRNA from the MSC, and at least one free tRNA), eEF1A bound to GDP, tRNA binding to the ribosome and polysome analysis to determine the translation phenotype, in addition to determining apoptosis, proliferation and cell cycle changes. It might also be of interest to investigate IRES gene expression, ability to

translate proteins from different sub-cellular fractions such as membrane, cytoplasm and cytosol, as well as the ability of tRNAs to become acetylated. Phosphorylation of eEF1B subunits clearly also has an impact on translation in other species, therefore it would be appealing to measure the same sort of translation parameters upon phosphorylation by different kinases.

6.2 Conclusion

This project sheds light into the considerably more intricate role of eEF1B in translation than previously understood, the potential vital importance of functional eEF1B subunits in tissue culture cells and the likely variation in composition of the eEF1B complex throughout development in different cell sub-populations *in vivo*. More work is needed to clarify the involvement of eEF1B subunits in translation and possible non-canonical functions such as tumourigenesis, cytoskeleton remodelling, cell cycle regulation, stress response, translation fidelity and tRNA acetylation.



References

- ABE, T., TAKAHASHI, S. & FUKUUCHI, Y. (2002) Reduction of Alamar Blue, a novel redox indicator, is dependent on both the glycolytic and oxidative metabolism of glucose in rat cultured neurons. *Neurosci Lett*, 326, 179-82.
- ABRAMOFF, M. D., MAGELHAES, P. J. & RAM, S. J. (2004) Image Processing with ImageJ. *Biophotonics International*, 11, 36-42.
- AHMED, K., GERBER, D. A. & COCHET, C. (2002) Joining the cell survival squad: an emerging role for protein kinase CK2. *Trends Cell Biol*, 12, 226-30.
- AHN, H. C., KIM, S. & LEE, B. J. (2003) Solution structure and p43 binding of the p38 leucine zipper motif: coiled-coil interactions mediate the association between p38 and p43. *FEBS Lett*, 542, 119-24.
- AKSENOVA, A., MUNOZ, I., VOLKOV, K., ARINO, J. & MIRONOVA, L. (2007) The HAL3-PPZ1 dependent regulation of nonsense suppression efficiency in yeast and its influence on manifestation of the yeast prion-like determinant [ISP(+)]. *Genes Cells*, 12, 435-45.
- AL-MAGHREBI, M., ANIM, J. T. & OLALU, A. A. (2005) Up-regulation of eukaryotic elongation factor-1 subunits in breast carcinoma. *Anticancer Res*, 25, 2573-7.
- ALTSCHUL, S. F., GISH, W., MILLER, W., MYERS, E. W. & LIPMAN, D. J. (1990) Basic local alignment search tool. *J Mol Biol*, 215, 403-10.
- AMIRI, A., NOEI, F., JEGANATHAN, S., KULKARNI, G., PINKE, D. E. & LEE, J. M. (2007) eEF1A2 activates Akt and stimulates Akt-dependent actin remodeling, invasion and migration. *Oncogene*, 26, 3027-40.
- ANAND, N., MURTHY, S., AMANN, G., WERNICK, M., PORTER, L. A., CUKIER, I. H., COLLINS, C., GRAY, J. W., DIEBOLD, J., DEMETRICK, D. J. & LEE, J. M. (2002) Protein elongation factor eEF1A2 is a putative oncogene in ovarian cancer. *Nat Genet*, 31, 301-5.
- ANDERSEN, G. R., PEDERSEN, L., VALENTE, L., CHATTERJEE, I., KINZY, T. G., KJELDGAARD, M. & NYBORG, J. (2000) Structural basis for nucleotide exchange and competition with tRNA in the yeast elongation factor complex eEF1A:eEF1B α . *Mol Cell*, 6, 1261-6.
- ANDERSEN, G. R., VALENTE, L., PEDERSEN, L., KINZY, T. G. & NYBORG, J. (2001) Crystal structures of nucleotide exchange intermediates in the eEF1A-eEF1B α complex. *Nat Struct Biol*, 8, 531-4.
- ASHBURNER, M., BALL, C. A., BLAKE, J. A., BOTSTEIN, D., BUTLER, H., CHERRY, J. M., DAVIS, A. P., DOLINSKI, K., DWIGHT, S. S., EPPIG, J. T., HARRIS, M. A., HILL, D. P., ISSEL-TARVER, L., KASARSKIS, A., LEWIS, S., MATESE, J. C., RICHARDSON, J. E., RINGWALD, M., RUBIN, G. M. & SHERLOCK, G. (2000) Gene ontology: tool for the unification of biology. The Gene Ontology Consortium. *Nat Genet*, 25, 25-9.

- ASSELIN, J., BELLE, R., BOYER, J., MULNER, O. & OZON, R. (1984) [A 45 kDa phosphorylated protein, resistant to alkaline treatment, appears at the time of rupture of the nuclear envelope during the 1st meiotic division of the *Xenopus* oocyte]. *C R Acad Sci III*, 299, 127-9.
- BEC, G., KERJAN, P. & WALLER, J. P. (1994) Reconstitution in vitro of the valyl-tRNA synthetase-elongation factor (EF) 1 beta gamma delta complex. Essential roles of the NH2-terminal extension of valyl-tRNA synthetase and of the EF-1 delta subunit in complex formation. *J Biol Chem*, 269, 2086-92.
- BEC, G., KERJAN, P., ZHA, X. D. & WALLER, J. P. (1989) Valyl-tRNA synthetase from rabbit liver. I. Purification as a heterotypic complex in association with elongation factor 1. *J Biol Chem*, 264, 21131-7.
- BELLE, R., DERANCOURT, J., POULHE, R., CAPONY, J. P., OZON, R. & MULNER-LORILLON, O. (1989) A purified complex from *Xenopus* oocytes contains a p47 protein, an in vivo substrate of MPF, and a p30 protein respectively homologous to elongation factors EF-1 gamma and EF-1 beta. *FEBS Lett*, 255, 101-4.
- BENKO, A. L., VADUVA, G., MARTIN, N. C. & HOPPER, A. K. (2000) Competition between a sterol biosynthetic enzyme and tRNA modification in addition to changes in the protein synthesis machinery causes altered nonsense suppression. *Proc Natl Acad Sci U S A*, 97, 61-6.
- BENSON, D. A., KARSCH-MIZRACHI, I., LIPMAN, D. J., OSTELL, J. & SAYERS, E. W. (2009) GenBank. *Nucleic Acids Res*, 37, D26-31.
- BERGER, N. A., KUROHARA, K. K., PETZOLD, S. J. & SIKORSKI, G. W. (1979) Aphidicolin inhibits eukaryotic DNA replication and repair --- implications for involvement of DNA polymerase alpha in both processes. *Biochem Biophys Res Commun*, 89, 218-25.
- BERMAN, H. M., WESTBROOK, J., FENG, Z., GILLILAND, G., BHAT, T. N., WEISSIG, H., SHINDYALOV, I. N. & BOURNE, P. E. (2000) The Protein Data Bank. *Nucleic Acids Res*, 28, 235-42.
- BERNHARD, O. K., CUNNINGHAM, A. L. & SHEIL, M. M. (2004) Analysis of proteins copurifying with the CD4/lck complex using one-dimensional polyacrylamide gel electrophoresis and mass spectrometry: comparison with affinity-tag based protein detection and evaluation of different solubilization methods. *J Am Soc Mass Spectrom*, 15, 558-67.
- BERNSTEIN, E., CAUDY, A. A., HAMMOND, S. M. & HANNON, G. J. (2001) Role for a bidentate ribonuclease in the initiation step of RNA interference. *Nature*, 409, 363-6.
- BILANGES, B., ARGONZA-BARRETT, R., KOLESNICHENKO, M., SKINNER, C., NAIR, M., CHEN, M. & STOKOE, D. (2007) Tuberous sclerosis complex proteins 1 and 2 control serum-dependent translation in a TOP-dependent and -independent manner. *Mol Cell Biol*, 27, 5746-64.

- BILLAUT-MULOT, O., FERNANDEZ-GOMEZ, R. & OUAISSI, A. (1997) Phenotype of recombinant *Trypanosoma cruzi* which overexpress elongation factor 1-gamma: possible involvement of EF-1gamma GST-like domain in the resistance to clomipramine. *Gene*, 198, 259-67.
- BIRMINGHAM, A., ANDERSON, E. M., REYNOLDS, A., ILSLEY-TYREE, D., LEAKE, D., FEDOROV, Y., BASKERVILLE, S., MAKSIMOVA, E., ROBINSON, K., KARPILOW, J., MARSHALL, W. S. & KHVOROVA, A. (2006) 3' UTR seed matches, but not overall identity, are associated with RNAi off-targets. *Nat Methods*, 3, 199-204.
- BLANC, J. F., LALANNE, C., PLOMION, C., SCHMITTER, J. M., BATHANY, K., GION, J. M., BIOULAC-SAGE, P., BALABAUD, C., BONNEU, M. & ROSENBAUM, J. (2005) Proteomic analysis of differentially expressed proteins in hepatocellular carcinoma developed in patients with chronic viral hepatitis C. *Proteomics*, 5, 3778-89.
- BLANCO, E. & ABRIL, J. F. (2009) Computational gene annotation in new genome assemblies using GeneID. *Methods Mol Biol*, 537, 243-61.
- BLOM, N., GAMMELTOFT, S. & BRUNAK, S. (1999) Sequence and structure-based prediction of eukaryotic protein phosphorylation sites. *J Mol Biol*, 294, 1351-62.
- BLOM, N., SICHERITZ-PONTEN, T., GUPTA, R., GAMMELTOFT, S. & BRUNAK, S. (2004) Prediction of post-translational glycosylation and phosphorylation of proteins from the amino acid sequence. *Proteomics*, 4, 1633-49.
- BOHNSACK, M. T., REGENER, K., SCHWAPPACH, B., SAFFRICH, R., PARASKEVA, E., HARTMANN, E. & GORLICH, D. (2002) Exp5 exports eEF1A via tRNA from nuclei and synergizes with other transport pathways to confine translation to the cytoplasm. *Embo J*, 21, 6205-15.
- BOON, K., CARON, H. N., VAN ASPEREN, R., VALENTIJN, L., HERMUS, M. C., VAN SLUIS, P., ROOBEEK, I., WEIS, I., VOUTE, P. A., SCHWAB, M. & VERSTEEG, R. (2001) N-myc enhances the expression of a large set of genes functioning in ribosome biogenesis and protein synthesis. *Embo J*, 20, 1383-93.
- BORRADAILE, N. M., BUHMAN, K. K., LISTENBERGER, L. L., MAGEE, C. J., MORIMOTO, E. T., ORY, D. S. & SCHAFFER, J. E. (2006) A critical role for eukaryotic elongation factor 1A-1 in lipotoxic cell death. *Mol Biol Cell*, 17, 770-8.
- BOULBEN, S., MONNIER, A., LE BRETON, M., MORALES, J., CORMIER, P., BELLE, R. & MULNER-LORILLON, O. (2003) Sea urchin elongation factor 1delta (EF1delta) and evidence for cell cycle-directed localization changes of a sub-fraction of the protein at M phase. *Cell Mol Life Sci*, 60, 2178-88.
- BOUTLA, A., DELIDAKIS, C., LIVADARAS, I., TSAGRIS, M. & TABLER, M. (2001) Short 5'-phosphorylated double-stranded RNAs induce RNA interference in *Drosophila*. *Curr Biol*, 11, 1776-80.

7. REFERENCES

- BOUWMEESTER, T., BAUCH, A., RUFFNER, H., ANGRAND, P. O., BERGAMINI, G., CROUGHTON, K., CRUCIAT, C., EBERHARD, D., GAGNEUR, J., GHIDELLI, S., HOPF, C., HUHSE, B., MANGANO, R., MICHON, A. M., SCHIRLE, M., SCHLEGL, J., SCHWAB, M., STEIN, M. A., BAUER, A., CASARI, G., DREWES, G., GAVIN, A. C., JACKSON, D. B., JOBERTY, G., NEUBAUER, G., RICK, J., KUSTER, B. & SUPERTI-FURGA, G. (2004) A physical and functional map of the human TNF-alpha/NF-kappa B signal transduction pathway. *Nat Cell Biol*, 6, 97-105.
- BRANDSMA, M., KERJAN, P., DIJK, J., JANSSEN, G. M. & MOLLER, W. (1995) Valyl-tRNA synthetase from *Artemia*. Purification and association with elongation factor 1. *Eur J Biochem*, 233, 277-82.
- BUCHOU, T., VERNET, M., BLOND, O., JENSEN, H. H., POINTU, H., OLSEN, B. B., COCHET, C., ISSINGER, O. G. & BOLDYREFF, B. (2003) Disruption of the regulatory beta subunit of protein kinase CK2 in mice leads to a cell-autonomous defect and early embryonic lethality. *Mol Cell Biol*, 23, 908-15.
- BURGE, C. B. & KARLIN, S. (1998) Finding the genes in genomic DNA. *Curr Opin Struct Biol*, 8, 346-54.
- BYRD, M. P., ZAMORA, M. & LLOYD, R. E. (2002) Generation of multiple isoforms of eukaryotic translation initiation factor 4G1 by use of alternate translation initiation codons. *Mol Cell Biol*, 22, 4499-511.
- CAMPUZANO, S. & MODOLELL, J. (1980) Hydrolysis of GTP on elongation factor Tu. ribosome complexes promoted by 2'(3')-O-L-phenylalanyladenosine. *Proc Natl Acad Sci U S A*, 77, 905-9.
- CANAANI, D. (2009) Methodological approaches in application of synthetic lethality screening towards anticancer therapy. *Br J Cancer*, 100, 1213-8.
- CANS, C., PASSER, B. J., SHALAK, V., NANCY-PORTEBOIS, V., CRIBLE, V., AMZALLAG, N., ALLANIC, D., TUFINO, R., ARGENTINI, M., MORAS, D., FIUCCI, G., GOUD, B., MIRANDE, M., AMSON, R. & TELERMAN, A. (2003) Translationally controlled tumor protein acts as a guanine nucleotide dissociation inhibitor on the translation elongation factor eEF1A. *Proc Natl Acad Sci U S A*, 100, 13892-7.
- CAO, H., ZHU, Q., HUANG, J., LI, B., ZHANG, S., YAO, W. & ZHANG, Y. (2009) Regulation and functional role of eEF1A2 in pancreatic carcinoma. *Biochem Biophys Res Commun*, 380, 11-6.
- CARR-SCHMID, A., DURKO, N., CAVALLIUS, J., MERRICK, W. C. & KINZY, T. G. (1999a) Mutations in a GTP-binding motif of eukaryotic elongation factor 1A reduce both translational fidelity and the requirement for nucleotide exchange. *J Biol Chem*, 274, 30297-302.

- CARR-SCHMID, A., VALENTE, L., LOIK, V. I., WILLIAMS, T., STARITA, L. M. & KINZY, T. G. (1999b) Mutations in elongation factor 1beta, a guanine nucleotide exchange factor, enhance translational fidelity. *Mol Cell Biol*, 19, 5257-66.
- CARTHARIUS, K., FRECH, K., GROTE, K., KLOCKE, B., HALTMEIER, M., KLINGENHOFF, A., FRISCH, M., BAYERLEIN, M. & WERNER, T. (2005) MatInspector and beyond: promoter analysis based on transcription factor binding sites. *Bioinformatics*, 21, 2933-42.
- CARVER, T. J. & MULLAN, L. J. (2005) JAE: Jemboss Alignment Editor. *Appl Bioinformatics*, 4, 151-4.
- CERONI, A., PASSERINI, A., VULLO, A. & FRASCONI, P. (2006) DISULFIND: a disulfide bonding state and cysteine connectivity prediction server. *Nucleic Acids Res*, 34, W177-81.
- CHAMBERS, D. M., PETERS, J. & ABBOTT, C. M. (1998) The lethal mutation of the mouse wasted (wst) is a deletion that abolishes expression of a tissue-specific isoform of translation elongation factor 1alpha, encoded by the Eef1a2 gene. *Proc Natl Acad Sci U S A*, 95, 4463-8.
- CHAMBERS, D. M., ROULEAU, G. A. & ABBOTT, C. M. (2001) Comparative genomic analysis of genes encoding translation elongation factor 1B(alpha) in human and mouse shows EEF1B1 to be a recent retrotransposition event. *Genomics*, 77, 145-8.
- CHANG, R. & WANG, E. (2007) Mouse translation elongation factor eEF1A-2 interacts with Prdx-I to protect cells against apoptotic death induced by oxidative stress. *J Cell Biochem*, 100, 267-78.
- CHANG, Y. W. & TRAUGH, J. A. (1997) Phosphorylation of elongation factor 1 and ribosomal protein S6 by multipotential S6 kinase and insulin stimulation of translational elongation. *J Biol Chem*, 272, 28252-7.
- CHANG, Y. W. & TRAUGH, J. A. (1998) Insulin stimulation of phosphorylation of elongation factor 1 (eEF-1) enhances elongation activity. *Eur J Biochem*, 251, 201-7.
- CHEKMENEV, D. S., HAID, C. & KEL, A. E. (2005) P-Match: transcription factor binding site search by combining patterns and weight matrices. *Nucleic Acids Res*, 33, W432-7.
- CHEN, C. J. & TRAUGH, J. A. (1995) Expression of recombinant elongation factor 1 beta from rabbit in Escherichia coli. Phosphorylation by casein kinase II. *Biochim Biophys Acta*, 1264, 303-11.
- CHI, K., JONES, D. V. & FRAZIER, M. L. (1992) Expression of an elongation factor 1 gamma-related sequence in adenocarcinomas of the colon. *Gastroenterology*, 103, 98-102.
- CHO, D. I., OAK, M. H., YANG, H. J., CHOI, H. K., JANSSEN, G. M. & KIM, K. M. (2003) Direct and biochemical interaction between dopamine D3 receptor and elongation factor-1Bbetagamma. *Life Sci*, 73, 2991-3004.

- CHUANG, C. C., TAN, S. K., TAI, L. K., HSIN, J. P. & WANG, F. F. (1998) Evidence for the involvement of protein kinase C in the inhibition of prolactin gene expression by transforming growth factor-beta2. *Mol Pharmacol*, 53, 1054-61.
- CIRUELA, F. (2008) Fluorescence-based methods in the study of protein-protein interactions in living cells. *Curr Opin Biotechnol*, 19, 338-43.
- CLEMENS, M. J. (2004) Targets and mechanisms for the regulation of translation in malignant transformation. *Oncogene*, 23, 3180-8.
- CLINE, M. S., SMOOT, M., CERAMI, E., KUCHINSKY, A., LANDYS, N., WORKMAN, C., CHRISTMAS, R., AVILA-CAMPILO, I., CREECH, M., GROSS, B., HANSPERS, K., ISSERLIN, R., KELLEY, R., KILLCOYNE, S., LOTIA, S., MAERE, S., MORRIS, J., ONO, K., PAVLOVIC, V., PICO, A. R., VAILAYA, A., WANG, P. L., ADLER, A., CONKLIN, B. R., HOOD, L., KUIPER, M., SANDER, C., SCHMULEVICH, I., SCHWIKOWSKI, B., WARNER, G. J., IDEKER, T. & BADER, G. D. (2007) Integration of biological networks and gene expression data using Cytoscape. *Nat Protoc*, 2, 2366-82.
- CORMIER, P., OSBORNE, H. B., MORALES, J., BASSEZ, T., MINELLA, O., POULHE, R., BELLE, R. & MULNER-LORILLON, O. (1993) Elongation factor 1 contains two homologous guanine-nucleotide exchange proteins as shown from the molecular cloning of beta and delta subunits. *Nucleic Acids Res*, 21, 743.
- CORMIER, P., PYRONNET, S., SALAUN, P., MULNER-LORILLON, O. & SONENBERG, N. (2003) Cap-dependent translation and control of the cell cycle. *Prog Cell Cycle Res*, 5, 469-75.
- CUFF, J. A., CLAMP, M. E., SIDDIQUI, A. S., FINLAY, M. & BARTON, G. J. (1998) JPred: a consensus secondary structure prediction server. *Bioinformatics*, 14, 892-3.
- DAHLBERG, J. E. & LUND, E. (2004) Does protein synthesis occur in the nucleus? *Curr Opin Cell Biol*, 16, 335-8.
- DAHLBERG, J. E., LUND, E. & GOODWIN, E. B. (2003) Nuclear translation: what is the evidence? *RNA*, 9, 1-8.
- DAVULURI, R. V. (2003) Application of FirstEF to find promoters and first exons in the human genome. *Curr Protoc Bioinformatics*, Chapter 4, Unit4 7.
- DE BORTOLI, M., CASTELLINO, R. C., LU, X. Y., DEYO, J., STURLA, L. M., ADESINA, A. M., PERLAKY, L., POMEROY, S. L., LAU, C. C., MAN, T. K., RAO, P. H. & KIM, J. Y. (2006) Medulloblastoma outcome is adversely associated with overexpression of EEF1D, RPL30, and RPS20 on the long arm of chromosome 8. *BMC Cancer*, 6, 223.
- DE NADAL, E., FADDEN, R. P., RUIZ, A., HAYSTEAD, T. & ARINO, J. (2001) A role for the Ppz Ser/Thr protein phosphatases in the regulation of translation elongation factor 1Balpha. *J Biol Chem*, 276, 14829-34.

- DELALANDE, C., MONNIER, A., CORMIER, P., MULNER-LORILLON, O. & BELLE, R. (1998) Changes in elongation factor-1[alpha] transcripts are uncoupled to changes in EF-1[delta] during sea urchin development. *Biology of the Cell*, 90, 661-663.
- DONG, K., WANG, R., WANG, X., LIN, F., SHEN, J. J., GAO, P. & ZHANG, H. Z. (2009) Tumor-specific RNAi targeting eIF4E suppresses tumor growth, induces apoptosis and enhances cisplatin cytotoxicity in human breast carcinoma cells. *Breast Cancer Res Treat*, 113, 443-56.
- DOREE, M. (1990) Control of M-phase by maturation-promoting factor. *Curr Opin Cell Biol*, 2, 269-73.
- EDGAR, R. C. (2004) MUSCLE: multiple sequence alignment with high accuracy and high throughput. *Nucleic Acids Res*, 32, 1792-7.
- EDMONDS, B. T., BELL, A., WYCKOFF, J., CONDEELIS, J. & LEYH, T. S. (1998) The effect of F-actin on the binding and hydrolysis of guanine nucleotide by Dictyostelium elongation factor 1A. *J Biol Chem*, 273, 10288-95.
- EMANUELSSON, O., BRUNAK, S., VON HEIJNE, G. & NIELSEN, H. (2007) Locating proteins in the cell using TargetP, SignalP and related tools. *Nat Protoc*, 2, 953-71.
- ENDER, B., LYNCH, P., KIM, Y. H., INAMDAR, N. V., CLEARY, K. R. & FRAZIER, M. L. (1993) Overexpression of an elongation factor-1 gamma-hybridizing RNA in colorectal adenomas. *Mol. Carcinog.*, 7, 18-20.
- ESWAR, N., ERAMIAN, D., WEBB, B., SHEN, M. Y. & SALI, A. (2008) Protein structure modeling with MODELLER. *Methods Mol Biol*, 426, 145-59.
- EVERLEY, P. A., KRIJGSVELD, J., ZETTER, B. R. & GYGI, S. P. (2004) Quantitative cancer proteomics: stable isotope labeling with amino acids in cell culture (SILAC) as a tool for prostate cancer research. *Mol Cell Proteomics*, 3, 729-35.
- EWING, R. M., CHU, P., ELISMA, F., LI, H., TAYLOR, P., CLIMIE, S., MCBROOM-CERAJEWSKI, L., ROBINSON, M. D., O'CONNOR, L., LI, M., TAYLOR, R., DHARSEE, M., HO, Y., HEILBUT, A., MOORE, L., ZHANG, S., ORNATSKY, O., BUKHMAN, Y. V., ETHIER, M., SHENG, Y., VASILESCU, J., ABU-FARHA, M., LAMBERT, J. P., DUEWEL, H. S., STEWART, II, KUEHL, B., HOGUE, K., COLWILL, K., GLADWISH, K., MUSKAT, B., KINACH, R., ADAMS, S. L., MORAN, M. F., MORIN, G. B., TOPALOGLOU, T. & FIGEYS, D. (2007) Large-scale mapping of human protein-protein interactions by mass spectrometry. *Mol Syst Biol*, 3, 89.
- FINN, R. D., TATE, J., MISTRY, J., COGGILL, P. C., SAMMUT, S. J., HOTZ, H. R., CERIC, G., FORSLUND, K., EDDY, S. R., SONNHAMMER, E. L. & BATEMAN, A. (2008) The Pfam protein families database. *Nucleic Acids Res*, 36, D281-8.

- FIRE, A., XU, S., MONTGOMERY, M. K., KOSTAS, S. A., DRIVER, S. E. & MELLO, C. C. (1998) Potent and specific genetic interference by double-stranded RNA in *Caenorhabditis elegans*. *Nature*, 391, 806-11.
- FRAZIER, M. L., INAMDAR, N., ALVULA, S., WU, E. & KIM, Y. H. (1998) Few point mutations in elongation factor-1 γ gene in gastrointestinal carcinoma. *Mol. Carcinog.*, 22, 9-15.
- FRED, R. G. & WELSH, N. (2009) The importance of RNA binding proteins in preproinsulin mRNA stability. *Mol Cell Endocrinol.*, 297, 28-33.
- FURUKAWA, R., JINKS, T. M., TISHGARTEN, T., MAZZAWI, M., MORRIS, D. R. & FECHHEIMER, M. (2001) Elongation factor 1 β is an actin-binding protein. *Biochim Biophys Acta*, 1527, 130-40.
- GANGWANI, L., MIKRUT, M., GALCHEVA-GARGOVA, Z. & DAVIS, R. J. (1998) Interaction of ZPR1 with translation elongation factor-1 α in proliferating cells. *J Cell Biol*, 143, 1471-84.
- GASTEIGER, E., GATTIKER, A., HOOGLAND, C., IVANYI, I., APPEL, R. D. & BAIROCH, A. (2003) ExpASY: The proteomics server for in-depth protein knowledge and analysis. *Nucleic Acids Res*, 31, 3784-8.
- GEBAUER, F. & HENTZE, M. W. (2004) Molecular mechanisms of translational control. *Nat Rev Mol Cell Biol*, 5, 827-35.
- GHOSH, H. P. & GHOSH, K. (1972) Specificity of the initiator methionine tRNA for terminal and internal recognition. *Biochem Biophys Res Commun*, 49, 550-7.
- GILLEN, C. M., GAO, Y., NIEHAUS-SAUTER, M. M., WYLDE, M. R. & WHEATLY, M. G. (2008) Elongation factor 1B γ (eEF1B γ) expression during the molting cycle and cold acclimation in the crayfish *Procambarus clarkii*. *Comp Biochem Physiol B Biochem Mol Biol*, 150, 170-6.
- GIRALDEZ, A. J., MISHIMA, Y., RIHEL, J., GROCOCK, R. J., VAN DONGEN, S., INOUE, K., ENRIGHT, A. J. & SCHIER, A. F. (2006) Zebrafish MiR-430 promotes deadenylation and clearance of maternal mRNAs. *Science*, 312, 75-9.
- GODAR, D. E. & YANG, D. C. (1988) Mammalian high molecular weight and monomeric forms of valyl-tRNA synthetase. *Biochemistry*, 27, 2181-6.
- GODON, C., LAGNIEL, G., LEE, J., BUHLER, J. M., KIEFFER, S., PERROT, M., BOUCHERIE, H., TOLEDANO, M. B. & LABARRE, J. (1998) The H₂O₂ stimulon in *Saccharomyces cerevisiae*. *J Biol Chem*, 273, 22480-9.
- GOPALKRISHNAN, R. V., SU, Z. Z., GOLDSTEIN, N. I. & FISHER, P. B. (1999) Translational infidelity and human cancer: role of the PTI-1 oncogene. *Int J Biochem Cell Biol*, 31, 151-62.

- GRIFFITHS-JONES, S., SAINI, H. K., VAN DONGEN, S. & ENRIGHT, A. J. (2008) miRBase: tools for microRNA genomics. *Nucleic Acids Res*, 36, D154-8.
- GROSS, S. R. & KINZY, T. G. (2005) Translation elongation factor 1A is essential for regulation of the actin cytoskeleton and cell morphology. *Nat Struct Mol Biol*, 12, 772-8.
- GROSS, S. R. & KINZY, T. G. (2007) Improper organization of the actin cytoskeleton affects protein synthesis at initiation. *Mol Cell Biol*, 27, 1974-89.
- GROSSHANS, H., HURT, E. & SIMOS, G. (2000) An aminoacylation-dependent nuclear tRNA export pathway in yeast. *Genes Dev*, 14, 830-40.
- GROVE, B. K. & JOHNSON, T. C. (1974) The role of ribosomal ribonucleic acid in the structure and function of mammalian brain ribosomes. *Biochem J*, 143, 419-26.
- GRUNWELLER, A., WYSZKO, E., BIEBER, B., JAHNEL, R., ERDMANN, V. A. & KURRECK, J. (2003) Comparison of different antisense strategies in mammalian cells using locked nucleic acids, 2'-O-methyl RNA, phosphorothioates and small interfering RNA. *Nucleic Acids Res*, 31, 3185-93.
- GUERRUCCI, M. A., MONNIER, A., DELALANDE, C. & BELLE, R. (1999) The elongation factor-1delta (EF-1delta) originates from gene duplication of an EF-1beta ancestor and fusion with a protein-binding domain. *Gene*, 233, 83-7.
- HAASNOOT, J. & BERKHOUT, B. (2009) Nucleic acids-based therapeutics in the battle against pathogenic viruses. *Handb Exp Pharmacol*, 243-63.
- HALL, T. A. (1999) BioEdit: a user-friendly biological sequence alignment editor and analysis program for Windows 95/98/NT. *Nucl. Acids. Symp. Ser.*, 41, 95-98.
- HAMID, R., ROTSHTEYN, Y., RABADI, L., PARIKH, R. & BULLOCK, P. (2004) Comparison of alamar blue and MTT assays for high through-put screening. *Toxicol In Vitro*, 18, 703-10.
- HAMILTON, T. L., STONELEY, M., SPRIGGS, K. A. & BUSHELL, M. (2006) TOPs and their regulation. *Biochem Soc Trans*, 34, 12-6.
- HANBAUER, I., BOJA, E. S. & MOSKOVITZ, J. (2003) A homologue of elongation factor 1 gamma regulates methionine sulfoxide reductase A gene expression in *Saccharomyces cerevisiae*. *Proc Natl Acad Sci U S A*, 100, 8199-204.
- HARRIS, M. N., OZPOLAT, B., ABDI, F., GU, S., LEGLER, A., MAWUENYEGA, K. G., TIRADO-GOMEZ, M., LOPEZ-BERESTEIN, G. & CHEN, X. (2004) Comparative proteomic analysis of all-trans-retinoic acid treatment reveals systematic posttranscriptional control mechanisms in acute promyelocytic leukemia. *Blood*, 104, 1314-23.
- HART, G. T., RAMANI, A. K. & MARCOTTE, E. M. (2006) How complete are current yeast and human protein-interaction networks? *Genome Biol*, 7, 120.

- HERNANDEZ-TORO, J., PRIETO, C. & DE LAS RIVAS, J. (2007) APID2NET: unified interactome graphic analyzer. *Bioinformatics*, 23, 2495-7.
- HESS, J. L. (2003) The Cancer Genome Anatomy Project: power tools for cancer biologists. *Cancer Invest*, 21, 325-6.
- HIRAGA, K., SUZUKI, K., TSUCHIYA, E. & MIYAKAWA, T. (1993) Cloning and characterization of the elongation factor EF-1 beta homologue of *Saccharomyces cerevisiae*. EF-1 beta is essential for growth. *FEBS Lett*, 316, 165-9.
- HOFMANN, K. & STOFFEL, W. (1993) TMbase - A database of membrane spanning proteins segments. *Biol. Chem. Hoppe-Seyler*, 374, 196.
- HOMMA, M. K. & HOMMA, Y. (2005) Regulatory role of CK2 during the progression of cell cycle. *Mol Cell Biochem*, 274, 47-52.
- HORNBECK, P. V., CHABRA, I., KORNHAUSER, J. M., SKRZYPEK, E. & ZHANG, B. (2004) PhosphoSite: A bioinformatics resource dedicated to physiological protein phosphorylation. *Proteomics*, 4, 1551-61.
- HUANG, H. Y., CHIEN, C. H., JEN, K. H. & HUANG, H. D. (2006) RegRNA: an integrated web server for identifying regulatory RNA motifs and elements. *Nucleic Acids Res*, 34, W429-34.
- HUBBARD, T. J., AKEN, B. L., AYLING, S., BALLESTER, B., BEAL, K., BRAGIN, E., BRENT, S., CHEN, Y., CLAPHAM, P., CLARKE, L., COATES, G., FAIRLEY, S., FITZGERALD, S., FERNANDEZ-BANET, J., GORDON, L., GRAF, S., HAIDER, S., HAMMOND, M., HOLLAND, R., HOWE, K., JENKINSON, A., JOHNSON, N., KAHARI, A., KEEFE, D., KEENAN, S., KINSELLA, R., KOKOCINSKI, F., KULESHA, E., LAWSON, D., LONGDEN, I., MEGY, K., MEIDL, P., OVERDUIN, B., PARKER, A., PRITCHARD, B., RIOS, D., SCHUSTER, M., SLATER, G., SMEDLEY, D., SPOONER, W., SPUDICH, G., TREVANION, S., VILELLA, A., VOGEL, J., WHITE, S., WILDER, S., ZADISSA, A., BIRNEY, E., CUNNINGHAM, F., CURWEN, V., DURBIN, R., FERNANDEZ-SUAREZ, X. M., HERRERO, J., KASPRZYK, A., PROCTOR, G., SMITH, J., SEARLE, S. & FLICEK, P. (2009) Ensembl 2009. *Nucleic Acids Res*, 37, D690-7.
- HULO, N., BAIROCH, A., BULLIARD, V., CERUTTI, L., DE CASTRO, E., LANGENDIJK-GENEVAUX, P. S., PAGNI, M. & SIGRIST, C. J. A. (2006) The PROSITE database. *Nucl. Acids Res.*, 34, D227-230.
- HUNTER, S., APWEILER, R., ATTWOOD, T. K., BAIROCH, A., BATEMAN, A., BINNS, D., BORK, P., DAS, U., DAUGHERTY, L., DUQUENNE, L., FINN, R. D., GOUGH, J., HAFT, D., HULO, N., KAHN, D., KELLY, E., LAUGRAUD, A., LETUNIC, I., LONSDALE, D., LOPEZ, R., MADERA, M., MASLEN, J., MCANULLA, C., MCDOWALL, J., MISTRY, J., MITCHELL, A., MULDER, N., NATALE, D., ORENGO, C., QUINN, A. F., SELENGUT, J. D., SIGRIST, C. J., THIMMA, M., THOMAS, P. D., VALENTIN, F., WILSON, D., WU, C. H. & YEATS, C. (2009) InterPro: the integrative protein signature database. *Nucleic Acids Res*, 37, D211-5.

- IADEVAIA, V., CALDAROLA, S., TINO, E., AMALDI, F. & LORENI, F. (2008) All translation elongation factors and the e, f, and h subunits of translation initiation factor 3 are encoded by 5'-terminal oligopyrimidine (TOP) mRNAs. *Rna*, 14, 1730-6.
- IAKOUCHEVA, L. M., RADIVOJAC, P., BROWN, C. J., O'CONNOR, T. R., SIKES, J. G., OBRADOVIC, Z. & DUNKER, A. K. (2004) The importance of intrinsic disorder for protein phosphorylation. *Nucleic Acids Res*, 32, 1037-49.
- IBORRA, F. J., JACKSON, D. A. & COOK, P. R. (2004) The case for nuclear translation. *J Cell Sci*, 117, 5713-20.
- JACOB, A. N., KANDPAL, G. & KANDPAL, R. P. (1996) Isolation of expressed sequences that include a gene for familial breast cancer (BRCA2) and other novel transcripts from a five megabase region on chromosome 13q12. *Oncogene*, 13, 213-21.
- JANSSEN, G. M., MAESSEN, G. D., AMONS, R. & MOLLER, W. (1988) Phosphorylation of elongation factor 1 beta by an endogenous kinase affects its catalytic nucleotide exchange activity. *J Biol Chem*, 263, 11063-6.
- JANSSEN, G. M. & MOLLER, W. (1988) Elongation factor 1 beta gamma from *Artemia*. Purification and properties of its subunits. *Eur J Biochem*, 171, 119-29.
- JANSSEN, G. M., VAN DAMME, H. T., KRIEK, J., AMONS, R. & MOLLER, W. (1994) The subunit structure of elongation factor 1 from *Artemia*. Why two alpha-chains in this complex? *J Biol Chem*, 269, 31410-7.
- JENKINS, C. & FUERST, J. A. (2001) Phylogenetic analysis of evolutionary relationships of the planctomycete division of the domain bacteria based on amino acid sequences of elongation factor Tu. *J Mol Evol*, 52, 405-18.
- JENSEN, L. J., GUPTA, R., STAERFELDT, H. H. & BRUNAK, S. (2003) Prediction of human protein function according to Gene Ontology categories. *Bioinformatics*, 19, 635-42.
- JEPPESEN, M. G., ORTIZ, P., SHEPARD, W., KINZY, T. G., NYBORG, J. & ANDERSEN, G. R. (2003) The crystal structure of the glutathione S-transferase-like domain of elongation factor 1Bgamma from *Saccharomyces cerevisiae*. *J Biol Chem*, 278, 47190-8.
- JIANG, S., WOLFE, C. L., WARRINGTON, J. A. & NORCUM, M. T. (2005) Three-dimensional reconstruction of the valyl-tRNA synthetase/elongation factor-1H complex and localization of the delta subunit. *FEBS Lett*, 579, 6049-54.
- JOHANSEN, M. B., KIEMER, L. & BRUNAK, S. (2006) Analysis and prediction of mammalian protein glycation. *Glycobiology*, 16, 844-53.
- JOSEPH, P., LEI, Y. X., WHONG, W. Z. & ONG, T. M. (2002) Oncogenic potential of mouse translation elongation factor-1 delta, a novel cadmium-responsive proto-oncogene. *J Biol Chem*, 277, 6131-6.

- JOSEPH, P., O'KERNICK, C. M., OTHUMPANGAT, S., LEI, Y. X., YUAN, B. Z. & ONG, T. M. (2004) Expression profile of eukaryotic translation factors in human cancer tissues and cell lines. *Mol Carcinog*, 40, 171-9.
- JULENIUS, K. (2007) NetCGlyc 1.0: prediction of mammalian C-mannosylation sites. *Glycobiology*, 17, 868-76.
- JULENIUS, K., MOLGAARD, A., GUPTA, R. & BRUNAK, S. (2005) Prediction, conservation analysis, and structural characterization of mammalian mucin-type O-glycosylation sites. *Glycobiology*, 15, 153-64.
- JUNG, M., KONDRATYEV, A. D. & DRITSCHILO, A. (1994a) Elongation factor 1 delta is enhanced following exposure to ionizing radiation. *Cancer Res*, 54, 2541-3.
- JUNG, M., KONDRATYEV, A. D. & DRITSCHILO, A. (1994b) Elongation factor 1 delta is enhanced following exposure to ionizing radiation. *Cancer Res.*, 54, 2541-2543.
- KAMATH, R. S., FRASER, A. G., DONG, Y., POULIN, G., DURBIN, R., GOTTA, M., KANAPIN, A., LE BOT, N., MORENO, S., SOHRMANN, M., WELCHMAN, D. P., ZIPPERLEN, P. & AHRINGER, J. (2003) Systematic functional analysis of the *Caenorhabditis elegans* genome using RNAi. *Nature*, 421, 231-7.
- KAMBOURIS, N. G., BURKE, D. J. & CREUTZ, C. E. (1993) Cloning and genetic characterization of a calcium- and phospholipid-binding protein from *Saccharomyces cerevisiae* that is homologous to translation elongation factor-1 gamma. *Yeast*, 9, 151-63.
- KAMIIE, K., NOMURA, Y., KOBAYASHI, S., TAIRA, H., KOBAYASHI, K., YAMASHITA, T., KIDOU, S. & EJIRI, S. (2002) Cloning and expression of *Bombyx mori* silk gland elongation factor 1gamma in *Escherichia coli*. *Biosci Biotechnol Biochem*, 66, 558-65.
- KATO, K., KAWAGUCHI, Y., TANAKA, M., IGARASHI, M., YOKOYAMA, A., MATSUDA, G., KANAMORI, M., NAKAJIMA, K., NISHIMURA, Y., SHIMOJIMA, M., PHUNG, H. T., TAKAHASHI, E. & HIRAI, K. (2001) Epstein-Barr virus-encoded protein kinase BGLF4 mediates hyperphosphorylation of cellular elongation factor 1delta (EF-1delta): EF-1delta is universally modified by conserved protein kinases of herpesviruses in mammalian cells. *J Gen Virol*, 82, 1457-63.
- KAWAGUCHI, Y., BRUNI, R. & ROIZMAN, B. (1997) Interaction of herpes simplex virus 1 alpha regulatory protein ICP0 with elongation factor 1delta: ICP0 affects translational machinery. *J Virol*, 71, 1019-24.
- KAWAGUCHI, Y., KATO, K., TANAKA, M., KANAMORI, M., NISHIYAMA, Y. & YAMANASHI, Y. (2003) Conserved protein kinases encoded by herpesviruses and cellular protein kinase cdc2 target the same phosphorylation site in eukaryotic elongation factor 1delta. *J Virol*, 77, 2359-68.

7. REFERENCES

- KAWAGUCHI, Y., MATSUMURA, T., ROIZMAN, B. & HIRAI, K. (1999) Cellular elongation factor 1delta is modified in cells infected with representative alpha-, beta-, or gammaherpesviruses. *J Virol*, 73, 4456-60.
- KAWAGUCHI, Y., VAN SANT, C. & ROIZMAN, B. (1998) Eukaryotic elongation factor 1delta is hyperphosphorylated by the protein kinase encoded by the U(L)13 gene of herpes simplex virus 1. *J Virol*, 72, 1731-6.
- KEENAN, J., MURPHY, L., HENRY, M., MELEADY, P. & CLYNES, M. (2009) Proteomic analysis of multidrug-resistance mechanisms in adriamycin-resistant variants of DLKP, a squamous lung cancer cell line. *Proteomics*, 9, 1556-66.
- KELLER, D. M., ZENG, X., WANG, Y., ZHANG, Q. H., KAPOOR, M., SHU, H., GOODMAN, R., LOZANO, G., ZHAO, Y. & LU, H. (2001) A DNA damage-induced p53 serine 392 kinase complex contains CK2, hSpt16, and SSRP1. *Mol Cell*, 7, 283-92.
- KERJAN, P., CERINI, C., SEMERIVA, M. & MIRANDE, M. (1994) The multienzyme complex containing nine aminoacyl-tRNA synthetases is ubiquitous from Drosophila to mammals. *Biochim Biophys Acta*, 1199, 293-7.
- KESHAVA PRASAD, T. S., GOEL, R., KANDASAMY, K., KEERTHIKUMAR, S., KUMAR, S., MATHIVANAN, S., TELIKICHERLA, D., RAJU, R., SHAFREEN, B., VENUGOPAL, A., BALAKRISHNAN, L., MARIMUTHU, A., BANERJEE, S., SOMANATHAN, D. S., SEBASTIAN, A., RANI, S., RAY, S., HARRYS KISHORE, C. J., KANTH, S., AHMED, M., KASHYAP, M. K., MOHMOOD, R., RAMACHANDRA, Y. L., KRISHNA, V., RAHIMAN, B. A., MOHAN, S., RANGANATHAN, P., RAMABADRAN, S., CHAERKADY, R. & PANDEY, A. (2009) Human Protein Reference Database--2009 update. *Nucleic Acids Res*, 37, D767-72.
- KIEMER, L., BENDTSEN, J. D. & BLOM, N. (2005) NetAcet: prediction of N-terminal acetylation sites. *Bioinformatics*, 21, 1269-70.
- KIM, S., KELLNER, J., LEE, C. H. & COULOMBE, P. A. (2007) Interaction between the keratin cytoskeleton and eEF1Bgamma affects protein synthesis in epithelial cells. *Nat Struct Mol Biol*, 14, 982-3.
- KINZY, T. G., RIPMASTER, T. L. & WOOLFORD, J. L., JR. (1994) Multiple genes encode the translation elongation factor EF-1 gamma in *Saccharomyces cerevisiae*. *Nucleic Acids Res*, 22, 2703-7.
- KINZY, T. G. & WOOLFORD, J. L., JR. (1995) Increased expression of *Saccharomyces cerevisiae* translation elongation factor 1 alpha bypasses the lethality of a TEF5 null allele encoding elongation factor 1 beta. *Genetics*, 141, 481-9.
- KNUDSEN, S. M., FRYDENBERG, J., CLARK, B. F. & LEFFERS, H. (1993) Tissue-dependent variation in the expression of elongation factor-1 alpha isoforms: isolation and characterisation of a cDNA encoding a novel variant of human elongation-factor 1 alpha. *Eur J Biochem*, 215, 549-54.

- KOBAYASHI, S., KIDOU, S. & EJIRI, S. (2001) Detection and characterization of glutathione S-transferase activity in rice EF-1 β EF-1 γ and EF-1 γ expressed in *Escherichia coli*. *Biochem Biophys Res Commun*, 288, 509-14.
- KOLETTAS, E., LYMBOURA, M., KHAZAIE, K. & LUQMANI, Y. (1998) Modulation of elongation factor-1 delta (EF-1 delta) expression by oncogenes in human epithelial cells. *Anticancer Res*, 18, 385-92.
- KOONIN, E. V., MUSHEGIAN, A. R., TATUSOV, R. L., ALTSCHUL, S. F., BRYANT, S. H., BORK, P. & VALENCIA, A. (1994) Eukaryotic translation elongation factor 1 gamma contains a glutathione transferase domain--study of a diverse, ancient protein superfamily using motif search and structural modeling. *Protein Sci*, 3, 2045-54.
- KOZAK, M. & SHATKIN, A. J. (1978) Identification of features in 5' terminal fragments from reovirus mRNA which are important for ribosome binding. *Cell*, 13, 201-12.
- KRIEGSHEIM, A., PREISINGER, C. & KOLCH, W. (2008) Mapping of signaling pathways by functional interaction proteomics. *Methods Mol Biol*, 484, 177-92.
- KRUSE, C., WILLKOMM, D. K., GRUNWELLER, A., VOLLBRANDT, T., SOMMER, S., BUSCH, S., PFEIFFER, T., BRINKMANN, J., HARTMANN, R. K. & MULLER, P. K. (2000) Export and transport of tRNA are coupled to a multi-protein complex. *Biochem J*, 346 Pt 1, 107-15.
- KUHN, R. M., KAROLCHIK, D., ZWEIG, A. S., WANG, T., SMITH, K. E., ROSENBLOOM, K. R., RHEAD, B., RANEY, B. J., POHL, A., PHEASANT, M., MEYER, L., HSU, F., HINRICHS, A. S., HARTE, R. A., GIARDINE, B., FUJITA, P., DIEKHANS, M., DRESZER, T., CLAWSON, H., BARBER, G. P., HAUSSLER, D. & KENT, W. J. (2009) The UCSC Genome Browser Database: update 2009. *Nucleic Acids Res*, 37, D755-61.
- KUMABE, T., SOHMA, Y. & YAMAMOTO, T. (1992) Human cDNAs encoding elongation factor 1 gamma and the ribosomal protein L19. *Nucleic Acids Res*, 20, 2598.
- LAGE, H. (2009) Therapeutic potential of RNA interference in drug-resistant cancers. *Future Oncol*, 5, 169-85.
- LAKHANI, S. A., MASUD, A., KUIDA, K., PORTER, G. A., JR., BOOTH, C. J., MEHAL, W. Z., INAYAT, I. & FLAVELL, R. A. (2006) Caspases 3 and 7: key mediators of mitochondrial events of apoptosis. *Science*, 311, 847-51.
- LAMBERTI, A., CARAGLIA, M., LONGO, O., MARRA, M., ABBRUZZESE, A. & ARCARI, P. (2004) The translation elongation factor 1A in tumorigenesis, signal transduction and apoptosis: review article. *Amino Acids*, 26, 443-8.
- LANGDON, J. M., VONAKIS, B. M. & MACDONALD, S. M. (2004) Identification of the interaction between the human recombinant histamine releasing factor/translationally controlled tumor protein and elongation factor-1 delta (also known as eElongation factor-1B beta). *Biochim Biophys Acta*, 1688, 232-6.

- LAZARIS-KARATZAS, A., MONTINE, K. S. & SONENBERG, N. (1990) Malignant transformation by a eukaryotic initiation factor subunit that binds to mRNA 5' cap. *Nature*, 345, 544-7.
- LE SOURD, F., BOULBEN, S., LE BOUFFANT, R., CORMIER, P., MORALES, J., BELLE, R. & MULNER-LORILLON, O. (2006a) eEF1B: At the dawn of the 21st century. *Biochim Biophys Acta*, 1759, 13-31.
- LE SOURD, F., CORMIER, P., BACH, S., BOULBEN, S., BELLE, R. & MULNER-LORILLON, O. (2006b) Cellular coexistence of two high molecular subsets of eEF1B complex. *FEBS Lett*, 580, 2755-60.
- LEE, C. C. & CHIANG, B. L. (2008) RNA interference: new therapeutics in allergic diseases. *Curr Gene Ther*, 8, 236-46.
- LEI, Y. X., CHEN, J. K. & WU, Z. L. (2002) Blocking the translation elongation factor-1 delta with its antisense mRNA results in a significant reversal of its oncogenic potential. *Teratog Carcinog Mutagen*, 22, 377-83.
- LEW, Y., JONES, D. V., MARS, W. M., EVANS, D., BYRD, D. & FRAZIER, M. L. (1992) Expression of elongation factor-1 gamma-related sequence in human pancreatic cancer. *Pancreas*, 7, 144-152.
- LI, R., WANG, H., BEKELE, B. N., YIN, Z., CARAWAY, N. P., KATZ, R. L., STASS, S. A. & JIANG, F. (2006) Identification of putative oncogenes in lung adenocarcinoma by a comprehensive functional genomic approach. *Oncogene*, 25, 2628-35.
- LIEBMAN, S. W., CHERNOFF, Y. O. & LIU, R. (1995) The accuracy center of a eukaryotic ribosome. *Biochem Cell Biol*, 73, 1141-9.
- LIN, S. K., CHANG, M. C., TSAI, Y. G. & LUR, H. S. (2005) Proteomic analysis of the expression of proteins related to rice quality during caryopsis development and the effect of high temperature on expression. *Proteomics*, 5, 2140-56.
- LINDING, R., JENSEN, L. J., DIELLA, F., BORK, P., GIBSON, T. J. & RUSSELL, R. B. (2003) Protein disorder prediction: implications for structural proteomics. *Structure*, 11, 1453-9.
- LIU, G., TANG, J., EDMONDS, B. T., MURRAY, J., LEVIN, S. & CONDEELIS, J. (1996) F-actin sequesters elongation factor 1alpha from interaction with aminoacyl-tRNA in a pH-dependent reaction. *J Cell Biol*, 135, 953-63.
- LIU, H., HAN, H., LI, J. & WONG, L. (2005) DNAFSMiner: a web-based software toolbox to recognize two types of functional sites in DNA sequences. *Bioinformatics*, 21, 671-3.
- LIU, Y., CHEN, Q. & ZHANG, J. T. (2004) Tumor suppressor gene 14-3-3sigma is down-regulated whereas the proto-oncogene translation elongation factor 1delta is up-regulated in non-small cell lung cancers as identified by proteomic profiling. *J Proteome Res*, 3, 728-35.

- LUPAS, A., VAN DYKE, M. & STOCK, J. (1991) Predicting coiled coils from protein sequences. *Science*, 252, 1162-1164.
- MAERE, S., HEYMANS, K. & KUIPER, M. (2005) BiNGO: a Cytoscape plugin to assess overrepresentation of gene ontology categories in biological networks. *Bioinformatics*, 21, 3448-9.
- MALONE, J. & ULLRICH, R. (2007) Novel radiation response genes identified in gene-trapped MCF10A mammary epithelial cells. *Radiat Res*, 167, 176-84.
- MANSILLA, F., FRIIS, I., JADIDI, M., NIELSEN, K. M., CLARK, B. F. & KNUDSEN, C. R. (2002) Mapping the human translation elongation factor eEF1H complex using the yeast two-hybrid system. *Biochem J*, 365, 669-76.
- MARTINEAU, Y., DERRY, M. C., WANG, X., YANAGIYA, A., BERLANGA, J. J., SHYU, A. B., IMATAKA, H., GEHRING, K. & SONENBERG, N. (2008) Poly(A)-binding protein-interacting protein 1 binds to eukaryotic translation initiation factor 3 to stimulate translation. *Mol Cell Biol*, 28, 6658-67.
- MARTINEZ, M. A. (2009) Progress in the therapeutic applications of siRNAs against HIV-1. *Methods Mol Biol*, 487, 343-68.
- MASUTANI, M., SONENBERG, N., YOKOYAMA, S. & IMATAKA, H. (2007) Reconstitution reveals the functional core of mammalian eIF3. *Embo J*, 26, 3373-83.
- MATHEWS, M. B., SONENBERG, N. & HERSHEY, J. W. (2007) *Translational Control in Biology and Medicine*, Cold Spring Harbor, NY, Cold Spring Harbor Laboratories Press.
- MATHUR, S., CLEARY, K. R., INAMDAR, N., KIM, Y. H., STECK, P. & FRAZIER, M. L. (1998) Overexpression of elongation factor-1gamma protein in colorectal carcinoma. *Cancer*, 82, 816-821.
- MATSUOKA, S., BALLIF, B. A., SMOGORZEWSKA, A., MCDONALD, E. R., 3RD, HUROV, K. E., LUO, J., BAKALARSKI, C. E., ZHAO, Z., SOLIMINI, N., LERENTHAL, Y., SHILOH, Y., GYGI, S. P. & ELLEDGE, S. J. (2007) ATM and ATR substrate analysis reveals extensive protein networks responsive to DNA damage. *Science*, 316, 1160-6.
- MATYS, V., KEL-MARGOULIS, O. V., FRICKE, E., LIEBICH, I., LAND, S., BARRE-DIRRIE, A., REUTER, I., CHEKMENEV, D., KRULL, M., HORNISCHER, K., VOSS, N., STEGMAIER, P., LEWICKI-POTAPOV, B., SAXEL, H., KEL, A. E. & WINGENDER, E. (2006) TRANSFAC and its module TRANSCompel: transcriptional gene regulation in eukaryotes. *Nucleic Acids Res*, 34, D108-10.
- MAZAN-MAMCZARZ, K., LAL, A., MARTINDALE, J. L., KAWAI, T. & GOROSPE, M. (2006) Translational repression by RNA-binding protein TIAR. *Mol Cell Biol*, 26, 2716-27.
- MCGUFFIN, L. J., BRYSON, K. & JONES, D. T. (2000) The PSIPRED protein structure prediction server. *Bioinformatics*, 16, 404-5.

7. REFERENCES

- MIGNONE, F., GRILLO, G., LICCIULLI, F., IACONO, M., LIUNI, S., KERSEY, P. J., DUARTE, J., SACCONI, C. & PESOLE, G. (2005) UTRdb and UTRsite: a collection of sequences and regulatory motifs of the untranslated regions of eukaryotic mRNAs. *Nucleic Acids Res*, 33, D141-6.
- MIMORI, K., MORI, M., INOUE, H., UEO, H., MAFUNE, K., AKIYOSHI, T. & SUGIMACHI, K. (1996) Elongation factor 1 gamma mRNA expression in oesophageal carcinoma. *Gut*, 38, 66-70.
- MIMORI, K., MORI, M., TANAKA, S., AKIYOSHI, T. & SUGIMACHI, K. (1995) The overexpression of elongation factor 1 gamma mRNA in gastric carcinoma. *Cancer*, 75, 1446-9.
- MINELLA, O., MULNER-LORILLON, O., BEC, G., CORMIER, P. & BELLE, R. (1998) Multiple phosphorylation sites and quaternary organization of guanine-nucleotide exchange complex of elongation factor-1 (EF-1beta/gamma/delta/VaIRS) control the various functions of EF-1alpha. *Biosci Rep*, 18, 119-27.
- MINELLA, O., MULNER-LORILLON, O., DE SMEDT, V., HOURDEZ, S., CORMIER, P. & BELLE, R. (1996a) Major intracellular localization of elongation factor-1. *Cell Mol Biol (Noisy-le-grand)*, 42, 805-10.
- MINELLA, O., MULNER-LORILLON, O., POULHE, R., BELLE, R. & CORMIER, P. (1996b) The guanine-nucleotide-exchange complex (EF-1 beta gamma delta) of elongation factor-1 contains two similar leucine-zipper proteins EF-1 delta, p34 encoded by EF-1 delta 1 and p36 encoded by EF-1 delta 2. *Eur J Biochem*, 237, 685-90.
- MIYAMOTO-SATO, E., ISHIZAKA, M., HORISAWA, K., TATEYAMA, S., TAKASHIMA, H., FUSE, S., SUE, K., HIRAI, N., MASUOKA, K. & YANAGAWA, H. (2005) Cell-free cotranslation and selection using in vitro virus for high-throughput analysis of protein-protein interactions and complexes. *Genome Res*, 15, 710-7.
- MONIGATTI, F., GASTEIGER, E., BAIROCH, A. & JUNG, E. (2002) The Sulfinator: predicting tyrosine sulfation sites in protein sequences. *Bioinformatics*, 18, 769-70.
- MONNIER, A., BELLE, R., MORALES, J., CORMIER, P., BOULBEN, S. & MULNER-LORILLON, O. (2001a) Evidence for regulation of protein synthesis at the elongation step by CDK1/cyclin B phosphorylation. *Nucleic Acids Res*, 29, 1453-7.
- MONNIER, A., MORALES, J., CORMIER, P., BOULBEN, S., BELLE, R. & MULNER-LORILLON, O. (2001b) Protein translation during early cell divisions of sea urchin embryos regulated at the level of polypeptide chain elongation and highly sensitive to natural polyamines. *Zygote*, 9, 229-36.
- MORGENSTERN, B. (2004) DIALIGN: multiple DNA and protein sequence alignment at BiBiServ. *Nucleic Acids Res*, 32, W33-6.
- MORRIS, K. V. (2008) RNA-mediated transcriptional gene silencing in human cells. *Curr Top Microbiol Immunol*, 320, 211-24.

- MOSCHOS, S. A., SPINKS, K., WILLIAMS, A. E. & LINDSAY, M. A. (2008) Targeting the lung using siRNA and antisense based oligonucleotides. *Curr Pharm Des*, 14, 3620-7.
- MOTORIN, Y. A., WOLFSON, A. D., LOHR, D., ORLOVSKY, A. F. & GLADILIN, K. L. (1991) Purification and properties of a high-molecular-mass complex between Val-tRNA synthetase and the heavy form of elongation factor 1 from mammalian cells. *Eur J Biochem*, 201, 325-31.
- MOTORIN YU, A., WOLFSON, A. D., ORLOVSKY, A. F. & GLADILIN, K. L. (1988) Mammalian valyl-tRNA synthetase forms a complex with the first elongation factor. *FEBS Lett*, 238, 262-4.
- MULNER-LORILLON, O., CORMIER, P., CAVADORE, J. C., MORALES, J., POULHE, R. & BELLE, R. (1992) Phosphorylation of Xenopus elongation factor-1 gamma by cdc2 protein kinase: identification of the phosphorylation site. *Exp Cell Res*, 202, 549-51.
- MULNER-LORILLON, O., MINELLA, O., CORMIER, P., CAPONY, J. P., CAVADORE, J. C., MORALES, J., POULHE, R. & BELLE, R. (1994) Elongation factor EF-1 delta, a new target for maturation-promoting factor in Xenopus oocytes. *J Biol Chem*, 269, 20201-7.
- MULNER-LORILLON, O., POULHE, R., CORMIER, P., LABBE, J. C., DOREE, M. & BELLE, R. (1989) Purification of a p47 phosphoprotein from Xenopus laevis oocytes and identification as an in vivo and in vitro p34cdc2 substrate. *FEBS Lett*, 251, 219-24.
- MUNSHI, R., KANDL, K. A., CARR-SCHMID, A., WHITACRE, J. L., ADAMS, A. E. & KINZY, T. G. (2001) Overexpression of translation elongation factor 1A affects the organization and function of the actin cytoskeleton in yeast. *Genetics*, 157, 1425-36.
- NEGRUTSKII, B. S., SHALAK, V. F., KERJAN, P., EL'SKAYA, A. V. & MIRANDE, M. (1999) Functional interaction of mammalian valyl-tRNA synthetase with elongation factor EF-1alpha in the complex with EF-1H. *J Biol Chem*, 274, 4545-50.
- NEIMAN, P. E., RUDDLELL, A., JASONI, C., LORING, G., THOMAS, S. J., BRANDVOLD, K. A., LEE, R., BURNSIDE, J. & DELROW, J. (2001) Analysis of gene expression during myc oncogene-induced lymphomagenesis in the bursa of Fabricius. *Proc Natl Acad Sci U S A*, 98, 6378-83.
- NEWBERY, H. J., LOH, D. H., O'DONOGHUE, J. E., TOMLINSON, V. A., CHAU, Y. Y., BOYD, J. A., BERGMANN, J. H., BROWNSTEIN, D. & ABBOTT, C. M. (2007) Translation elongation factor eEF1A2 is essential for post-weaning survival in mice. *J Biol Chem*, 282, 28951-9.
- NGUYEN, T. N. & GOODRICH, J. A. (2006) Protein-protein interaction assays: eliminating false positive interactions. *Nat Methods*, 3, 135-9.
- O'BRIEN, J., WILSON, I., ORTON, T. & POGNAN, F. (2000) Investigation of the Alamar Blue (resazurin) fluorescent dye for the assessment of mammalian cell cytotoxicity. *Eur J Biochem*, 267, 5421-6.

- OGAWA, K., UTSUNOMIYA, T., MIMORI, K., TANAKA, Y., TANAKA, F., INOUE, H., MURAYAMA, S. & MORI, M. (2004) Clinical significance of elongation factor-1 delta mRNA expression in oesophageal carcinoma. *Br J Cancer*, 91, 282-6.
- OLAREWAJU, O., ORTIZ, P. A., CHOWDHURY, W. Q., CHATTERJEE, I. & KINZY, T. G. (2004) The translation elongation factor eEF1B plays a role in the oxidative stress response pathway. *RNA Biol*, 1, 89-94.
- ONG, L. L., ER, C. P., HO, A., AUNG, M. T. & YU, H. (2003) Kinectin anchors the translation elongation factor-1 delta to the endoplasmic reticulum. *J Biol Chem*, 278, 32115-23.
- ONG, L. L., LIN, P. C., ZHANG, X., CHIA, S. M. & YU, H. (2006) Kinectin-dependent assembly of translation elongation factor-1 complex on endoplasmic reticulum regulates protein synthesis. *J Biol Chem*, 281, 33621-34.
- PALEN, E., VENEMA, R. C., CHANG, Y. W. & TRAUGH, J. A. (1994) GDP as a regulator of phosphorylation of elongation factor 1 by casein kinase II. *Biochemistry*, 33, 8515-20.
- PAVITT, G. D. (2005) eIF2B, a mediator of general and gene-specific translational control. *Biochem Soc Trans*, 33, 1487-92.
- PEARSON, W. R. (1990) Rapid and sensitive sequence comparison with FASTP and FASTA. *Methods Enzymol*, 183, 63-98.
- PEREZ, J. M., SIEGAL, G., KRIEK, J., HARD, K., DIJK, J., CANTERS, G. W. & MOLLER, W. (1999) The solution structure of the guanine nucleotide exchange domain of human elongation factor 1beta reveals a striking resemblance to that of EF-Ts from Escherichia coli. *Structure*, 7, 217-26.
- PERRON, M. P. & PROVOST, P. (2009) Protein components of the microRNA pathway and human diseases. *Methods Mol Biol*, 487, 369-85.
- PERTEA, M., LIN, X. & SALZBERG, S. L. (2001) GeneSplicer: a new computational method for splice site prediction. *Nucleic Acids Res*, 29, 1185-90.
- PETERS, H. I., CHANG, Y. W. & TRAUGH, J. A. (1995) Phosphorylation of elongation factor 1 (EF-1) by protein kinase C stimulates GDP/GTP-exchange activity. *Eur J Biochem*, 234, 550-6.
- PETRUSHENKO, Z. M., NEGRUTSKII, B. S., LADOKHIN, A. S., BUDKEVICH, T. V., SHALAK, V. F. & EL'SKAYA, A. V. (1997) Evidence for the formation of an unusual ternary complex of rabbit liver EF-1alpha with GDP and deacylated tRNA. *FEBS Lett*, 407, 13-7.
- PEYRL, A., KRAPPENBAUER, K., SLAVC, I., YANG, J. W., STROBEL, T. & LUBEC, G. (2003) Protein profiles of medulloblastoma cell lines DAOY and D283: identification of tumor-related proteins and principles. *Proteomics*, 3, 1781-800.
- PIDDUBNYAK, V., RIGOU, P., MICHEL, L., RAIN, J. C., GENESTE, O., WOLKENSTEIN, P., VIDAUD, D., HICKMAN, J. A., MAUVIEL, A. & POYET, J. L. (2007) Positive regulation of

- apoptosis by HCA66, a new Apaf-1 interacting protein, and its putative role in the physiopathology of NF1 microdeletion syndrome patients. *Cell Death Differ*, 14, 1222-33.
- PIZZUTI, A., GENNARELLI, M., NOVELLI, G., COLOSIMO, A., LO CICERO, S., CASKEY, C. T. & DALLAPICCOLA, B. (1993) Human elongation factor EF-1 beta: cloning and characterization of the EF1 beta 5a gene and assignment of EF-1 beta isoforms to chromosomes 2,5,15 and X. *Biochem Biophys Res Commun*, 197, 154-62.
- POMERENING, J. R., VALENTE, L., KINZY, T. G. & JACOBS, T. W. (2003) Mutation of a conserved CDK site converts a metazoan Elongation Factor 1Bbeta subunit into a replacement for yeast eEF1B α . *Mol Genet Genomics*, 269, 776-88.
- PRADO, M. A., CASADO, P., ZUAZUA-VILLAR, P., DEL VALLE, E., ARTIME, N., CABAL-HIERRO, L., MARTINEZ-CAMPA, C. M., LAZO, P. S. & RAMOS, S. (2007) Phosphorylation of human eukaryotic elongation factor 1Bgamma is regulated by paclitaxel. *Proteomics*, 7, 3299-304.
- PROUD, C. G. (2002) Regulation of mammalian translation factors by nutrients. *Eur J Biochem*, 269, 5338-49.
- PROUD, C. G. & DENTON, R. M. (1997) Molecular mechanisms for the control of translation by insulin. *Biochem J*, 328 (Pt 2), 329-41.
- PUNTERVOLL, P., LINDING, R., GEMUND, C., CHABANIS-DAVIDSON, S., MATTINGSDAL, M., CAMERON, S., MARTIN, D. M., AUSIELLO, G., BRANNETTI, B., COSTANTINI, A., FERRE, F., MASELLI, V., VIA, A., CESARENI, G., DIELLA, F., SUPERTIFURGA, G., WYRWICZ, L., RAMU, C., MCGUIGAN, C., GUDAVALLI, R., LETUNIC, I., BORK, P., RYCHLEWSKI, L., KUSTER, B., HELMER-CITTERICH, M., HUNTER, W. N., AASLAND, R. & GIBSON, T. J. (2003) ELM server: A new resource for investigating short functional sites in modular eukaryotic proteins. *Nucleic Acids Res*, 31, 3625-30.
- QIN, X. & SARNOW, P. (2004) Preferential translation of internal ribosome entry site-containing mRNAs during the mitotic cycle in mammalian cells. *J Biol Chem*, 279, 13721-8.
- QUEVILLON, S. & MIRANDE, M. (1996) The p18 component of the multisynthetase complex shares a protein motif with the beta and gamma subunits of eukaryotic elongation factor 1. *FEBS Lett*, 395, 63-7.
- RAJASEKARAN, S., BALLA, S., GRADIE, P., GRYK, M. R., KADAVERU, K., KUNDETI, V., MACIEJEWSKI, M. W., MI, T., RUBINO, N., VYAS, J. & SCHILLER, M. R. (2009) Minimotif miner 2nd release: a database and web system for motif search. *Nucleic Acids Res*, 37, D185-90.
- REN, J., GAO, X., JIN, C., ZHU, M., WANG, X., SHAW, A., WEN, L., YAO, X. & XUE, Y. (2009) Systematic study of protein sumoylation: Development of a site-specific predictor of SUMOsp 2.0. *Proteomics*.

- RICE, P., LONGDEN, I. & BLEASBY, A. (2000) EMBOSS: the European Molecular Biology Open Software Suite. *Trends Genet*, 16, 276-7.
- ROBLICK, U. J., HIRSCHBERG, D., HABERMANN, J. K., PALMBERG, C., BECKER, S., KRUGER, S., GUSTAFSSON, M., BRUCH, H. P., FRANZEN, B., RIED, T., BERGMANN, T., AUER, G. & JORNVALL, H. (2004) Sequential proteome alterations during genesis and progression of colon cancer. *Cell Mol Life Sci*, 61, 1246-55.
- ROSSJOHN, J., MCKINSTRY, W. J., OAKLEY, A. J., VERGER, D., FLANAGAN, J., CHELVANAYAGAM, G., TAN, K. L., BOARD, P. G. & PARKER, M. W. (1998) Human theta class glutathione transferase: the crystal structure reveals a sulfate-binding pocket within a buried active site. *Structure*, 6, 309-22.
- ROST, B., YACHDAV, G. & LIU, J. (2004) The PredictProtein server. *Nucleic Acids Res*, 32, W321-6.
- ROZEN, S. & SKALETSKY, H. (2000) Primer3 on the WWW for general users and for biologist programmers. *Methods Mol Biol*, 132, 365-86.
- RUSSEL, R. B. & GIBSON, T. J. (2008) A careful disorderliness in the proteome: sites for interaction and targets for future therapies. *FEBS Lett.*, 582, 1271-1275.
- RYDEN, L. G. & HUNT, L. T. (1993) Evolution of protein complexity: the blue copper-containing oxidases and related proteins. *J Mol Evol*, 36, 41-66.
- SAHIN, O., LOBKE, C., KORF, U., APPELHANS, H., SULTMANN, H., POUSTKA, A., WIEMANN, S. & ARLT, D. (2007) Combinatorial RNAi for quantitative protein network analysis. *Proc Natl Acad Sci U S A*, 104, 6579-84.
- SANDBAKEN, M. G. & CULBERTSON, M. R. (1988) Mutations in elongation factor EF-1 alpha affect the frequency of frameshifting and amino acid misincorporation in *Saccharomyces cerevisiae*. *Genetics*, 120, 923-34.
- SANDERS, J., BRANDSMA, M., JANSSEN, G. M., DIJK, J. & MOLLER, W. (1996) Immunofluorescence studies of human fibroblasts demonstrate the presence of the complex of elongation factor-1 beta gamma delta in the endoplasmic reticulum. *J Cell Sci*, 109 (Pt 5), 1113-7.
- SANDERS, J., MAASSEN, J. A., AMONS, R. & MOLLER, W. (1991) Nucleotide sequence of human elongation factor-1 beta cDNA. *Nucleic Acids Res*, 19, 4551.
- SANDERS, J., MAASSEN, J. A. & MOLLER, W. (1992) Elongation factor-1 messenger-RNA levels in cultured cells are high compared to tissue and are not drastically affected further by oncogenic transformation. *Nucleic Acids Res*, 20, 5907-10.
- SANDERS, J., RAGGIASCHI, R., MORALES, J. & MOLLER, W. (1993) The human leucine zipper-containing guanine-nucleotide exchange protein elongation factor-1 delta. *Biochim Biophys Acta*, 1174, 87-90.

- SANG LEE, J., GYU PARK, S., PARK, H., SEOL, W., LEE, S. & KIM, S. (2002) Interaction network of human aminoacyl-tRNA synthetases and subunits of elongation factor 1 complex. *Biochem Biophys Res Commun*, 291, 158-64.
- SAROV, M. & STEWART, A. F. (2005) The best control for the specificity of RNAi. *Trends Biotechnol*, 23, 446-8.
- SCANLAN, M. J., CHEN, Y. T., WILLIAMSON, B., GURE, A. O., STOCKERT, E., GORDAN, J. D., TURECI, O., SAHIN, U., PFREUNDSCHUH, M. & OLD, L. J. (1998) Characterization of human colon cancer antigens recognized by autologous antibodies. *Int J Cancer*, 76, 652-8.
- SCHIRMAIER, F. & PHILIPPSEN, P. (1984) Identification of two genes coding for the translation elongation factor EF-1 alpha of *S. cerevisiae*. *Embo J*, 3, 3311-5.
- SHAMOVSKY, I., IVANNIKOV, M., KANDEL, E. S., GERSHON, D. & NUDLER, E. (2006) RNA-mediated response to heat shock in mammalian cells. *Nature*, 440, 556-60.
- SHANNON, A. J., TYSON, T., DIX, I., BOYD, J. & BURNELL, A. M. (2008) Systemic RNAi mediated gene silencing in the anhydrobiotic nematode *Panagrolaimus superbus*. *BMC Mol Biol*, 9, 58.
- SHEN, R., SU, Z. Z., OLSSON, C. A. & FISHER, P. B. (1995) Identification of the human prostatic carcinoma oncogene PTI-1 by rapid expression cloning and differential RNA display. *Proc Natl Acad Sci U S A*, 92, 6778-82.
- SHENTON, D. & GRANT, C. M. (2003) Protein S-thiolation targets glycolysis and protein synthesis in response to oxidative stress in the yeast *Saccharomyces cerevisiae*. *Biochem J*, 374, 513-9.
- SHEU, G. T. & TRAUGH, J. A. (1997) Recombinant subunits of mammalian elongation factor 1 expressed in *Escherichia coli*. Subunit interactions, elongation activity, and phosphorylation by protein kinase CKII. *J Biol Chem*, 272, 33290-7.
- SHEU, G. T. & TRAUGH, J. A. (1999) A structural model for elongation factor 1 (EF-1) and phosphorylation by protein kinase CKII. *Mol Cell Biochem*, 191, 181-6.
- SHUDA, M., KONDOH, N., TANAKA, K., RYO, A., WAKATSUKI, T., HADA, A., GOSEKI, N., IGARI, T., HATSUSE, K., AIHARA, T., HORIUCHI, S., SHICHITA, M., YAMAMOTO, N. & YAMAMOTO, M. (2000) Enhanced expression of translation factor mRNAs in hepatocellular carcinoma. *Anticancer Res*, 20, 2489-94.
- SILVA, A. L. & ROMAIO, L. (2009) The mammalian nonsense-mediated mRNA decay pathway: to decay or not to decay! Which players make the decision? *FEBS Lett*, 583, 499-505.
- SIMMER, F., MOORMAN, C., VAN DER LINDEN, A. M., KUIJK, E., VAN DEN BERGHE, P. V., KAMATH, R. S., FRASER, A. G., AHRINGER, J. & PLASTERK, R. H. (2003) Genome-wide RNAi of *C. elegans* using the hypersensitive rrf-3 strain reveals novel gene functions. *PLoS Biol*, 1, E12.

- SINHA, P., KOHL, S., FISCHER, J., HUTTER, G., KERN, M., KOTTGEN, E., DIETEL, M., LAGE, H., SCHNOLZER, M. & SCHADENDORF, D. (2000) Identification of novel proteins associated with the development of chemoresistance in malignant melanoma using two-dimensional electrophoresis. *Electrophoresis*, 21, 3048-57.
- SONENBERG, N., HERSHEY, H. P. & MATHEWS, M. (2000) *Translational control of gene expression*, CSHL Press.
- SONENBERG, N. & MEEROVITCH, K. (1990) Translation of poliovirus mRNA. *Enzyme*, 44, 278-91.
- SONNICHSEN, B., KOSKI, L. B., WALSH, A., MARSCHALL, P., NEUMANN, B., BREHM, M., ALLEAUME, A. M., ARTELT, J., BETTENCOURT, P., CASSIN, E., HEWITSON, M., HOLZ, C., KHAN, M., LAZIK, S., MARTIN, C., NITZSCHE, B., RUER, M., STAMFORD, J., WINZI, M., HEINKEL, R., RODER, M., FINELL, J., HANTSCH, H., JONES, S. J., JONES, M., PIANO, F., GUNSALUS, K. C., OEGEMA, K., GONCZY, P., COULSON, A., HYMAN, A. A. & ECHEVERRI, C. J. (2005) Full-genome RNAi profiling of early embryogenesis in *Caenorhabditis elegans*. *Nature*, 434, 462-9.
- STUMPF, M. P., THORNE, T., DE SILVA, E., STEWART, R., AN, H. J., LAPPE, M. & WIUF, C. (2008) Estimating the size of the human interactome. *Proc Natl Acad Sci U S A*, 105, 6959-64.
- THEODORAKIS, N. G., BANERJI, S. S. & MORIMOTO, R. I. (1988) HSP70 mRNA translation in chicken reticulocytes is regulated at the level of elongation. *J Biol Chem*, 263, 14579-85.
- THOMPSON, J. D., HIGGINS, D. G. & GIBSON, T. J. (1994) CLUSTAL W: improving the sensitivity of progressive multiple sequence alignment through sequence weighting, position-specific gap penalties and weight matrix choice. *Nucleic Acids Res*, 22, 4673-80.
- TOKUMOTO, T., KONDO, A., MIWA, J., HORIGUCHI, R., TOKUMOTO, M., NAGAHAMA, Y., OKIDA, N. & ISHIKAWA, K. (2003) Regulated interaction between polypeptide chain elongation factor-1 complex with the 26S proteasome during *Xenopus* oocyte maturation. *BMC Biochem*, 4, 6.
- TOMLINSON, V. (2006) eEF1A2 in ovarian cancer. *Medical Genetics*. University of Edinburgh.
- TOMLINSON, V. A., NEWBERY, H. J., BERGMANN, J. H., BOYD, J., SCOTT, D., WRAY, N. R., SELLAR, G. C., GABRA, H., GRAHAM, A., WILLIAMS, A. R. & ABBOTT, C. M. (2007) Expression of eEF1A2 is associated with clear cell histology in ovarian carcinomas: overexpression of the gene is not dependent on modifications at the EEF1A2 locus. *Br J Cancer*, 96, 1613-20.
- TOMLINSON, V. A., NEWBERY, H. J., WRAY, N. R., JACKSON, J., LARIONOV, A., MILLER, W. R., DIXON, J. M. & ABBOTT, C. M. (2005) Translation elongation factor eEF1A2

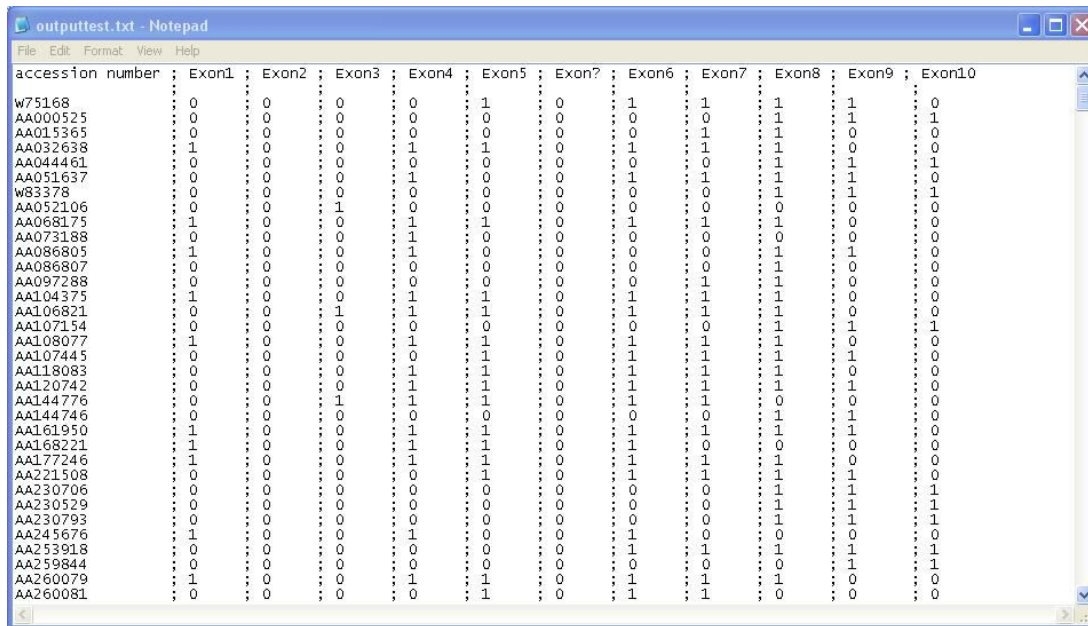
- is a potential oncoprotein that is overexpressed in two-thirds of breast tumours. *BMC Cancer*, 5, 113.
- TUSCHL, T., ZAMORE, P. D., LEHMANN, R., BARTEL, D. P. & SHARP, P. A. (1999) Targeted mRNA degradation by double-stranded RNA in vitro. *Genes Dev*, 13, 3191-7.
- UNIPROT CONSORTIUM, T. (2009) The Universal Protein Resource (UniProt). *Nucleic Acids Res*, 37, D169-74.
- VAN DAMME, H. T., AMONS, R., KARSSIES, R., TIMMERS, C. J., JANSSEN, G. M. & MOLLER, W. (1990) Elongation factor 1 beta of artemia: localization of functional sites and homology to elongation factor 1 delta. *Biochim Biophys Acta*, 1050, 241-7.
- VENEMA, R. C., PETERS, H. I. & TRAUGH, J. A. (1991a) Phosphorylation of elongation factor 1 (EF-1) and valyl-tRNA synthetase by protein kinase C and stimulation of EF-1 activity. *J Biol Chem*, 266, 12574-80.
- VENEMA, R. C., PETERS, H. I. & TRAUGH, J. A. (1991b) Phosphorylation of valyl-tRNA synthetase and elongation factor 1 in response to phorbol esters is associated with stimulation of both activities. *J Biol Chem*, 266, 11993-8.
- VERMES, I., HAANEN, C., STEFFENS-NAKKEN, H. & REUTELINGSPERGER, C. (1995) A novel assay for apoptosis. Flow cytometric detection of phosphatidylserine expression on early apoptotic cells using fluorescein labelled Annexin V. *J Immunol Methods*, 184, 39-51.
- VICKERS, T. J. & FAIRLAMB, A. H. (2004) Trypanothione S-transferase activity in a trypanosomatid ribosomal elongation factor 1B. *J Biol Chem*, 279, 27246-56.
- VICKERS, T. J., WYLLIE, S. & FAIRLAMB, A. H. (2004) Leishmania major elongation factor 1B complex has trypanothione S-transferase and peroxidase activity. *J Biol Chem*, 279, 49003-9.
- VIDO, K., SPECTOR, D., LAGNIEL, G., LOPEZ, S., TOLEDANO, M. B. & LABARRE, J. (2001) A proteome analysis of the cadmium response in *Saccharomyces cerevisiae*. *J Biol Chem*, 276, 8469-74.
- VON DER KAMMER, H., KLAUDINY, J., ZIMMER, M. & SCHEIT, K. H. (1991) Human elongation factor 1 beta: cDNA and derived amino acid sequence. *Biochem Biophys Res Commun*, 177, 312-7.
- WANG, J. F., ENGELSBERG, B. N., JOHNSON, S. W., WITMER, C., MERRICK, W. C., ROZMIAREK, H. & BILLINGS, P. C. (1997) DNA binding activity of the mammalian translation elongation complex: recognition of chromium- and transplatin-damaged DNA. *Arch Toxicol*, 71, 450-4.
- WANG, M. & MARIN, A. (2006) Characterization and prediction of alternative splice sites. *Gene*, 366, 219-27.

7. REFERENCES

- WANG, Y. H., LIU, S., ZHANG, G., ZHOU, C. Q., ZHU, H. X., ZHOU, X. B., QUAN, L. P., BAI, J. F. & XU, N. Z. (2005) Knockdown of c-Myc expression by RNAi inhibits MCF-7 breast tumor cells growth in vitro and in vivo. *Breast Cancer Res*, 7, R220-8.
- WATSON, J. D., OSTER, S. K., SHAGO, M., KHOSRAVI, F. & PENN, L. Z. (2002) Identifying genes regulated in a Myc-dependent manner. *J Biol Chem*, 277, 36921-30.
- WHEELAN, S. J., CHURCH, D. M. & OSTELL, J. M. (2001) Spidey: a tool for mRNA-to-genomic alignments. *Genome Res*, 11, 1952-7.
- WU, L., FAN, J. & BELASCO, J. G. (2006) MicroRNAs direct rapid deadenylation of mRNA. *Proc Natl Acad Sci U S A*, 103, 4034-9.
- XIAO, H., NEUVEUT, C., BENKIRANE, M. & JEANG, K. T. (1998) Interaction of the second coding exon of Tat with human EF-1 delta delineates a mechanism for HIV-1-mediated shut-off of host mRNA translation. *Biochem Biophys Res Commun*, 244, 384-9.
- ZAHER, H. S. & GREEN, R. (2009) Fidelity at the molecular level: lessons from protein synthesis. *Cell*, 136, 746-62.
- ZAMORE, P. D., TUSCHL, T., SHARP, P. A. & BARTEL, D. P. (2000) RNAi: double-stranded RNA directs the ATP-dependent cleavage of mRNA at 21 to 23 nucleotide intervals. *Cell*, 101, 25-33.
- ZENG, X., LIAO, A. J., TANG, H. L., YI, L., XIE, N. & SU, Q. (2007) [Screening human gastric carcinoma-associated antigens by serologic proteome analysis]. *Ai Zheng*, 26, 1080-4.
- ZHANG, L., PAN, X. & HERSHEY, J. W. (2007) Individual overexpression of five subunits of human translation initiation factor eIF3 promotes malignant transformation of immortal fibroblast cells. *J Biol Chem*, 282, 5790-800.
- ZHANG, L., SMIT-MCBRIDE, Z., PAN, X., RHEINHARDT, J. & HERSHEY, J. W. (2008) An oncogenic role for the phosphorylated h-subunit of human translation initiation factor eIF3. *J Biol Chem*, 283, 24047-60.
- ZISCHKA, H., OEHME, F., PINTSCH, T., OTT, A., KELLER, H., KELLERMANN, J. & SCHUSTER, S. C. (1999) Rearrangement of cortex proteins constitutes an osmoprotective mechanism in Dictyostelium. *Embo J*, 18, 4241-9.

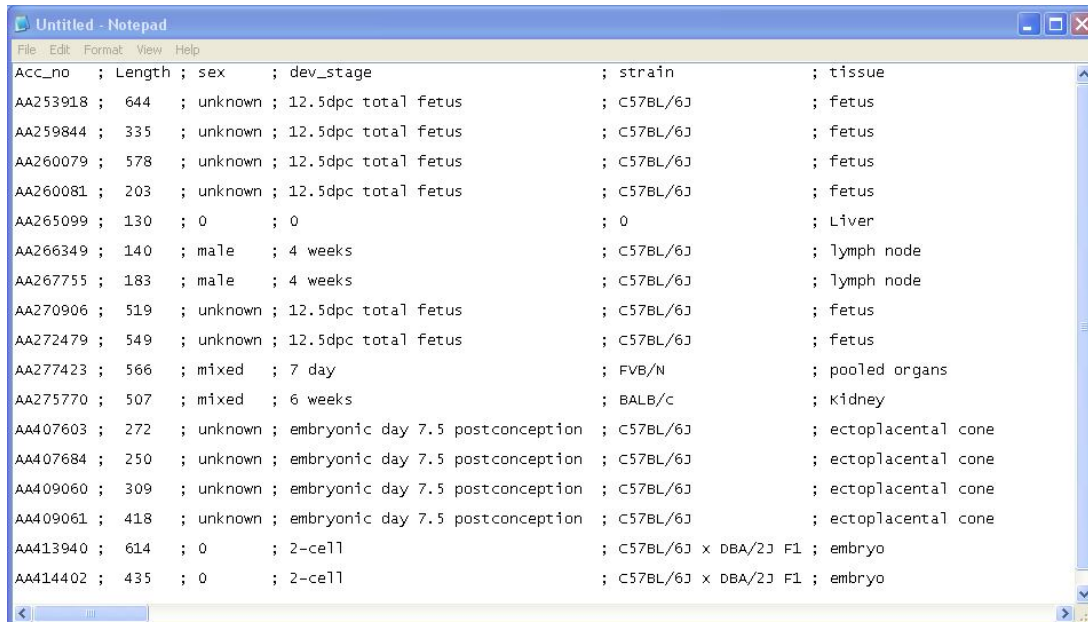
Appendix 1 – Perl tools

Appendix 1.1 – Gene structure tool



accession number	Exon1	Exon2	Exon3	Exon4	Exon5	Exon?	Exon6	Exon7	Exon8	Exon9	Exon10
w75168	0	0	0	0	1	0	1	1	1	1	0
AA000525	0	0	0	0	0	0	0	0	1	1	1
AA015365	0	0	0	0	0	0	0	1	1	0	0
AA032638	1	0	0	1	1	0	1	1	1	0	0
AA044461	0	0	0	0	0	0	0	0	1	1	1
AA051637	0	0	0	1	0	0	1	1	1	1	0
w83378	0	0	0	0	0	0	0	0	1	1	1
AA052106	0	0	1	0	0	0	0	0	0	0	0
AA068175	1	0	0	1	1	0	1	1	1	0	0
AA073188	0	0	0	1	0	0	0	0	0	0	0
AA086805	1	0	0	1	0	0	0	0	1	1	0
AA086807	0	0	0	0	0	0	0	0	1	0	0
AA097288	0	0	0	0	0	0	0	1	1	0	0
AA104375	1	0	0	1	1	0	1	1	1	0	0
AA106821	0	0	1	1	1	0	1	1	1	0	0
AA107154	0	0	0	0	0	0	0	0	1	1	1
AA108077	1	0	0	1	1	0	1	1	1	0	0
AA107445	0	0	0	0	1	0	1	1	1	1	0
AA118083	0	0	0	1	1	0	1	1	1	0	0
AA120742	0	0	0	1	1	0	1	1	1	1	0
AA144776	0	0	1	1	1	0	1	1	1	0	0
AA144746	0	0	0	0	0	0	0	0	1	1	0
AA161950	1	0	0	1	1	0	1	1	1	1	0
AA168221	1	0	0	1	1	0	1	0	0	0	0
AA177246	1	0	0	1	1	0	1	1	1	0	0
AA221508	0	0	0	0	1	0	1	1	1	1	1
AA230706	0	0	0	0	0	0	0	0	1	1	0
AA230529	0	0	0	0	0	0	0	0	1	1	1
AA230793	0	0	0	0	0	0	0	0	1	1	1
AA245676	1	0	0	1	0	0	1	0	0	0	0
AA253918	0	0	0	0	0	0	1	1	1	1	1
AA259844	0	0	0	0	0	0	0	0	0	1	1
AA260079	1	0	0	1	1	0	1	1	1	0	0
AA260081	0	0	0	0	1	0	1	1	1	0	0

Appendix 1.2 – GenBank file data extrapolation



Acc_no	Length	sex	dev_stage	strain	tissue
AA253918	644	unknown	12.5dpc total fetus	C57BL/6J	fetus
AA259844	335	unknown	12.5dpc total fetus	C57BL/6J	fetus
AA260079	578	unknown	12.5dpc total fetus	C57BL/6J	fetus
AA260081	203	unknown	12.5dpc total fetus	C57BL/6J	fetus
AA265099	130	0	0	0	Liver
AA266349	140	male	4 weeks	C57BL/6J	lymph node
AA267755	183	male	4 weeks	C57BL/6J	lymph node
AA270906	519	unknown	12.5dpc total fetus	C57BL/6J	fetus
AA272479	549	unknown	12.5dpc total fetus	C57BL/6J	fetus
AA277423	566	mixed	7 day	FVB/N	pooled organs
AA275770	507	mixed	6 weeks	BALB/c	kidney
AA407603	272	unknown	embryonic day 7.5 postconception	C57BL/6J	ectoplacental cone
AA407684	250	unknown	embryonic day 7.5 postconception	C57BL/6J	ectoplacental cone
AA409060	309	unknown	embryonic day 7.5 postconception	C57BL/6J	ectoplacental cone
AA409061	418	unknown	embryonic day 7.5 postconception	C57BL/6J	ectoplacental cone
AA413940	614	0	2-cell	C57BL/6J x DBA/2J F1	embryo
AA414402	435	0	2-cell	C57BL/6J x DBA/2J F1	embryo

Appendix 2

Supplier's name	Supplier's address
Abcam	Cambridge Science Park, Cambridge, CB4 0FL
Abnova	132 Siyuan Rd, Jhongli City, Taoyuan County, 320 Taiwan
Amaxa Biosystems	Lonza Cologne, Nattermannallee 1, 50829 Cologne, Germany
Ambion	Applied Biosystems, Lingley House, 120 Birchwood Boulevard, Warrington, WA3 7QH
Amersham	GE Healthcare Life Sciences, Amersham Place, Little Chalfont, Buckinghamshire, HP7 9NA
Appied Biosystems	Lingley House, 120 Birchwood Boulevard, Warrington, WA3 7QH
Beckman coulter	Kingsmead Business Park, High Wycombe, Buckinghamshire, HP11 1JU
Bethyl Laboratories	Universal Biologicals, Passhouse Farmhouse, Papworth St. Agnes, Cambridge, CB23 8QU
BioRad	Maxted Road, Hemel Hempstead, Hertfordshire, HP2 7DX
Chemicon	Millipore, Building 6, Croxley Green Business Park, Watford, WD18 8YH
Dako	Cambridge House, St Thomas Place, Ely, Cambridgeshire, CB7 4EX
Fisher Scientific	Bishop Meadow Road, Loughborough, Leicestershire, LE11 5RG
Weiss-Gallenkamp	Units 37 - 38, The Technology Centre, Epinal Way, Loughborough, LE11 3GE
Geneservice	Units 24 - 25, William James House, Cowley Road, Cambridge, CB4 0WU
Greiner Bio-One	Brunel Way, Stroudwater Business Park, Stonehouse, GL10 3 SX
Invitrogen	Fountain Drive, Inchinnan Business Park, Paisley, PA4 9RF
NEB	75 - 77 Knowl Piece, Wilbury Way, Hitchin, Hertfordshire, SG4 0TY
New Brunswick Scientific	17 Alban Park, Hatfield Road, St. Albans, Hertfordshire, AL4 0JJ
Olympus	KeyMed House, Stock Road, Southend-on-Sea, Essex, SS2 5QH
Pierce	Unit 9, Atley Way, North Nelson Industrial Estate, Cramlington, Northumberland, NE231WA
Promega	Southampton Science Park, Southampton, Hampshire, SO16 7NS
Qiagen	Fleming Way, Crawley, West Sussex, RH10 9NQ
Roche	Charles Avenue, Burgess Hill, RH15 9RY
Scientific Laboratory Supplies	Bishop Meadow Road, Loughborough, Leicestershire, LE11 5RG
Sigma	New road, Gillingham, Dorset, SP8 4XT
Proteintech group	Manchester Science Park, Manchester, M15 6SE
Santa cruz	2145 Delaware Avenue, Santa Cruz, CA. 95060, U.S.A.

Appendix 3 – Pseudogenes summary

eEF1B α	Chromosomal location	Number of introns	poly-A tail signal	Frame-shifts	Different N-terminus	In-frame stop codon	Percentage identity
Mouse	3F1	0	+	-	+	-	97
Human	2q37.1	1	+	+	+	+	92
	3q26.31	1	-	-	-	+	87
	5q13.1 (B3)	1	-	-	-	-	95
	6q12	1	-	-	+	+	84
	7q32.3	1	+	-	+	-	97
	12q23.3	1 (inversion)	+	+	+	+	90
	15q21.2	0	+	-	+	-	95
	Xp22.11	0	+	-	+	-	98

Appendix 3.1 - Summary table of eEF1B α mouse and human pseudogenes chromosomal location, number of introns, presence or absence of poly-A tail signal and frame-shifts, different start codon, in-frame stop codons and in silico protein percentage of identity compared with the reference protein sequence.

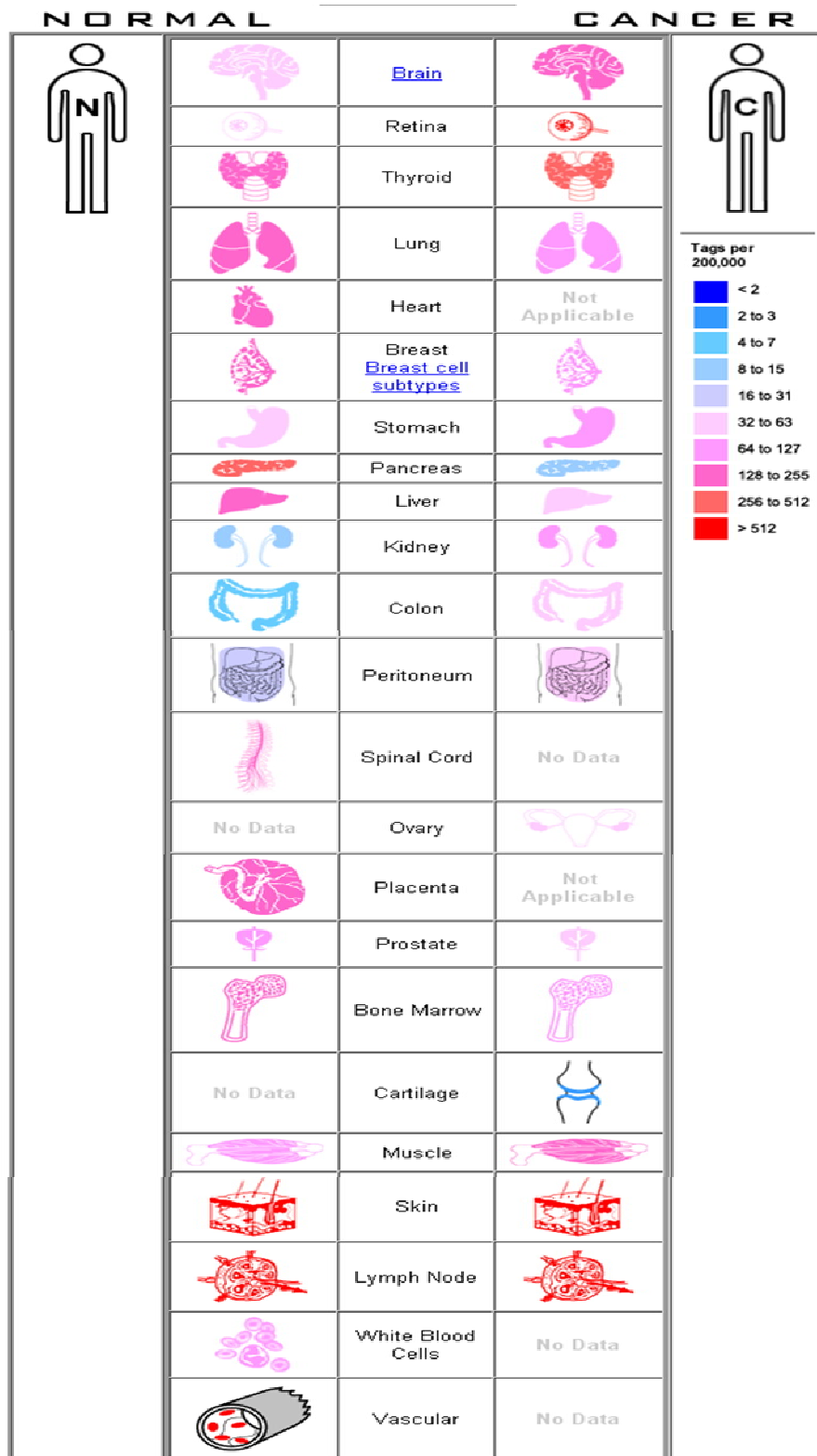
eEF1B δ	Chromosomal location	Number of introns	poly-A tail signal	Frame-shifts	Different N-terminus	In-frame stop codon	Percentage identity
Mouse	4D1	1	+	-	+	+	82
	11E2	0	+	+	-	+	74
Human	19p13.12	0	+	-	-	-	94
	9q22.31	0	+	-	-	-	94
	11q12.3	0	-	+	-	+	89
	17q23.3	0	+	+	Missing	-	84
	7q11.21	5	+	-	+	-	88
	13q13.1	0	+	+	-	+	90
	6q22.33	2	+	-	Missing	-	85
	1p36.32	0	+	-	Missing	-	89

Appendix 3.2 - Summary table of eEF1B δ mouse and human pseudogenes chromosomal location, number of introns, presence or absence of poly-A tail signal and frame-shifts, different start codon, in-frame stop codons and in silico protein percentage of identity compared with the reference protein sequence.

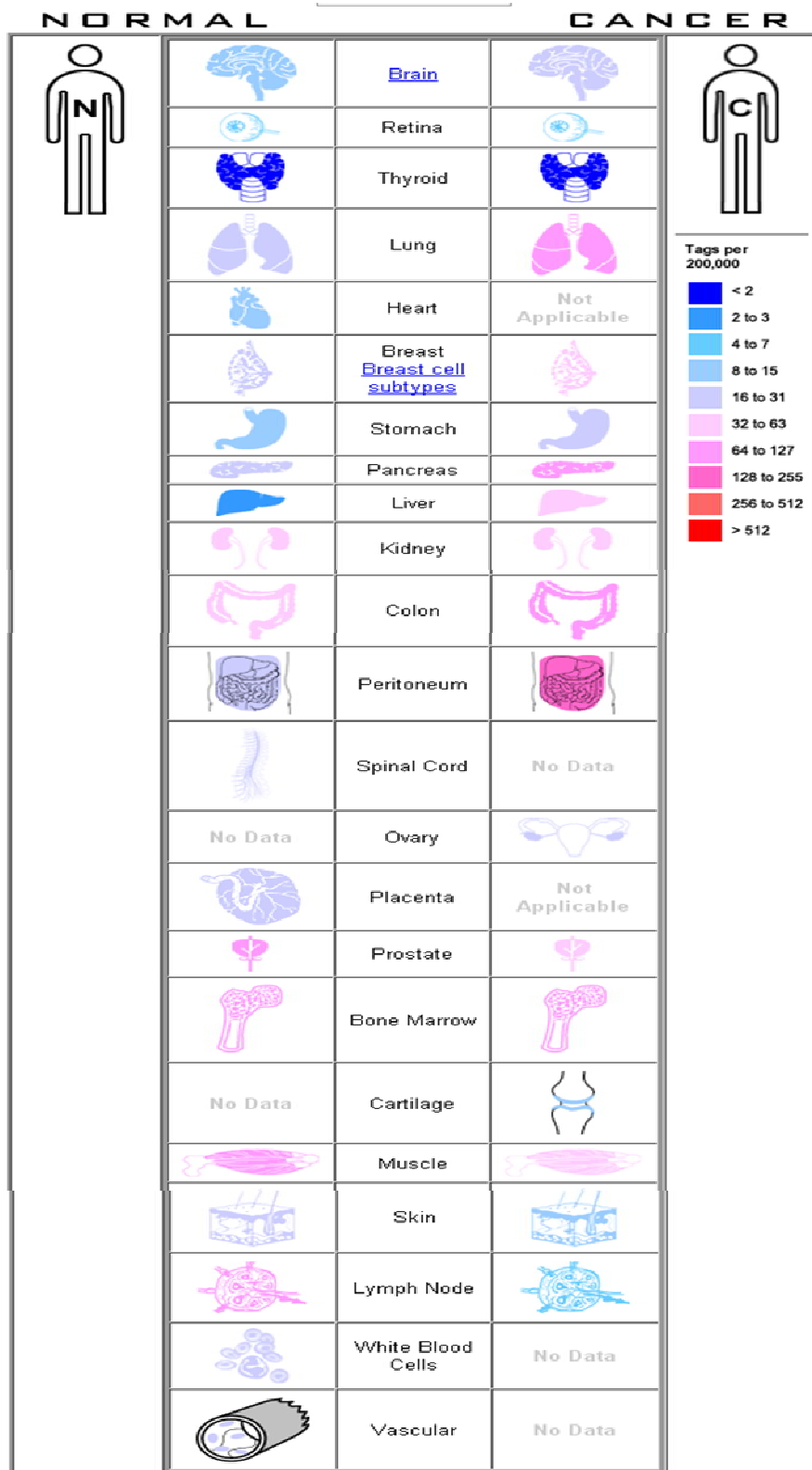
eEF1B γ	Chromosomal location	Number of introns	poly-A tail signal	Frame-shifts	Different N-terminus	In-frame stop codon	Percentage identity
Mouse	19D3	0	+	+	+	-?	84
	4B2	0	-	+	+	+	75
	15A1	1	+	+	Missing	+	88
	6D2	0	-	+	+	+	81
	16B1	0	+	+	+	+	87
	1A5	0	+	-	+	+	96
	7F1	0	-	-	+	-?	99
	14A3	0	-	+	Missing	+	77
	13A1	0	-	+	+	+	72
Human	3q26.1	0	+	+	+	+	81
	4q28.2	0	+	+	+	+	82
	Xq23	0	+	+	+	+	95
	7q32.3	0	-	-	+	-	97

Appendix 3.3 - Summary table of eEF1B γ mouse and human pseudogenes chromosomal location, number of introns, presence or absence of poly-A tail signal and frame-shifts, different start codon, in-frame stop codons and in silico protein percentage of identity compared with the reference protein sequence.

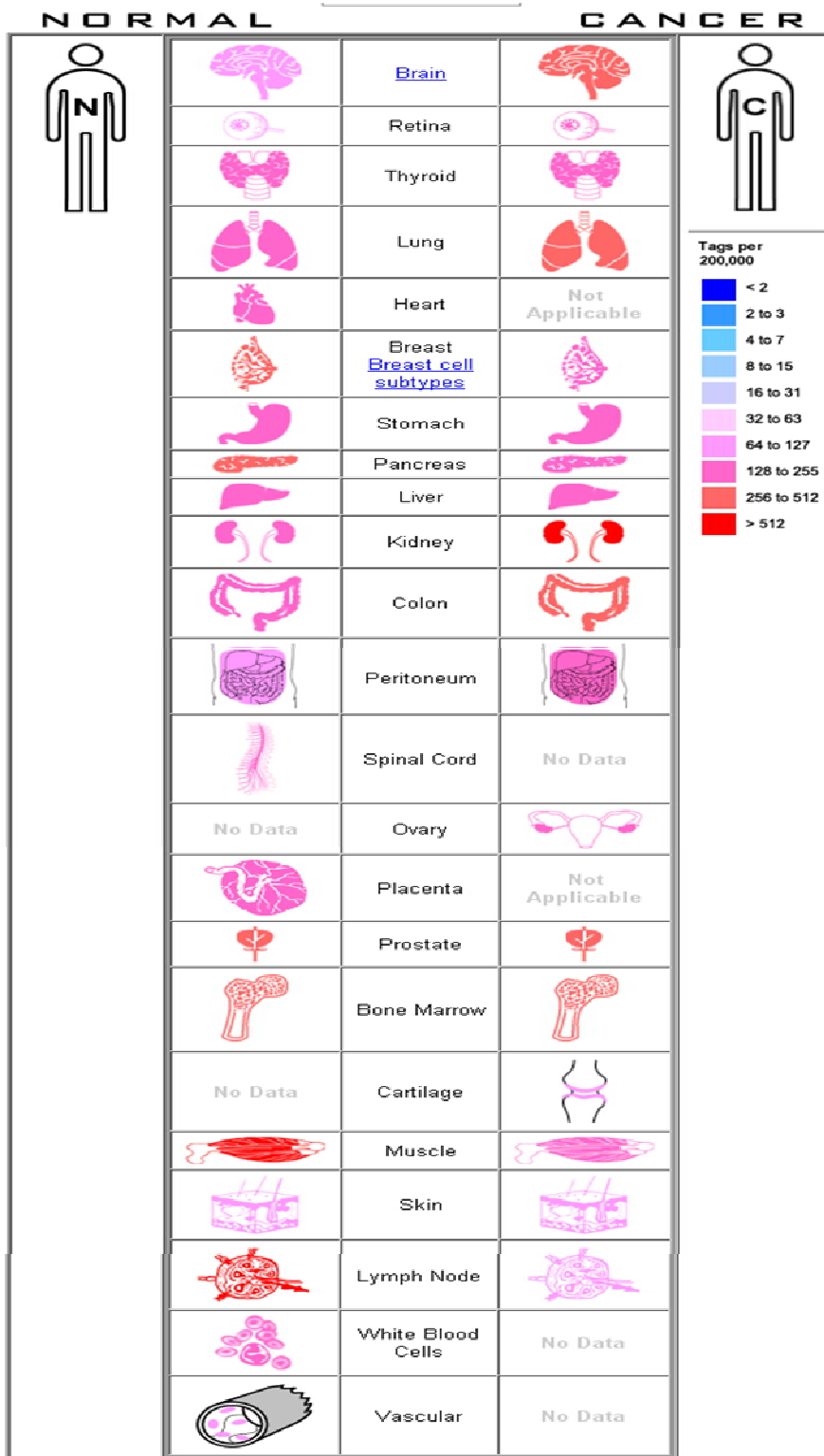
Appendix 4 – CGAP SAGE summary



Appendix 4.1 – eEF1B α



Appendix 4.2 – eEF1B δ



Appendix 4.3 – eEF1By

Appendix 5 – miRNA prediction

	Rfam ID	Score	Start	End
eEF1B α	hsa-miR-130b	17.2246	531	552
	hsa-miR-7-1*	17.1245	508	531
	hsa-miR-23b	17.104	694	714
	hsa-miR-16-1*	16.7239	863	884
	hsa-miR-379*	16.6238	50	71
	hsa-miR-23a	16.6009	694	714
	hsa-miR-301b	16.4504	528	552
	hsa-miR-23b	16.3997	505	525
	hsa-miR-23a	16.3997	505	525
	hsa-miR-337-3p	16.2232	734	755
	hsa-miR-556-3p	16.123	876	898
	hsa-miR-202*	16.123	53	75
	hsa-miR-640	16.0979	1	17
	hsa-miR-639	15.9519	384	406
	hsa-miR-411*	15.8226	50	71
eEF1B δ	hsa-miR-663	17.2829	22	43
	hsa-miR-297	16.8033	11	31
	hsa-miR-933	16.6007	4	26
	hsa-miR-603	16.487	1	14
	hsa-miR-574-3p	15.9185	1	12
	hsa-miR-550*	15.691	16	37
	hsa-miR-523	15.6121	7	29
	hsa-miR-560	15.5181	7	27
	hsa-miR-517b	15.2362	1	19
eEF1B γ	hsa-miR-339-5p	16.6303	31	53
	hsa-miR-337-3p	16.0322	43	65

Appendix 6 – eEF1B subunits homologues

Appendix 6.1 – eEF1B α homologues proteins

	Species	Genomic location	UniProt
Protozoa	<i>Plasmodium yoelii</i>	1.8Kb	XP_726756
	<i>Plasmodium falciparum</i>	9(515Kb)	NP_704672
	<i>Trypanosoma brucei</i>	4(1Mb)	XP_825370
	<i>Trypanosoma cruzi</i>	34Kb	EF1B_TRYCR
Fungi	<i>Candida albicans</i>	IV:126Kb	EF1B_CANAL
	<i>Schizosaccharomyces pombe</i>	III:1.7Mb	EF1B_SCHPO
	<i>Candida glabrata</i>	F:853Kb	XP_446340
	<i>Gibberella zeae</i>	3Mb	Q4IP50_GIBZE
	<i>Magnaporthe grisea</i>	IV:342Kb	Q5EN21_MAGGR
	<i>Chaetomium globosum</i>	n.a.	Q2GMD1_CHAGB
	<i>Podospora anserine</i>	n.a.	Q875E8_PODAN
	<i>Aspergillus fumigatus</i>	I:3Mb	XP_752484
	<i>Cryptococcus neoformans</i>	III:1Mb	XP_569674
	<i>Neurospora crassa</i>	VII:49Kb	Q7S4F0_NEUCR
	<i>Saccharomyces cerevisiae</i>	I:140Mb	EF1B_YEAST
Worms	<i>Caenorhabditis elegans</i>	n.a.	EF1B2_CAEEL
		8Mb	<u>EF1B1_CAEEL</u>
Sea urchin	<i>Strongylocentrotus purpuratus</i>	5Kb	<u>XP_780033</u>
Arachnidan	<i>Ixodes scapularis</i>	n.a.	Q4PMB1_IXOSC
Insects	<i>Apis mellifera</i>	n.a.	XP_625027
	<i>Plutella xylostella</i>	n.a.	Q6F447_PLUXY
	<i>Bombyx mori</i>	n.a.	EF1B2_BOMMO
	<i>Anopheles gambiae</i>	n.a.	Q7Q8Q6_ANOGA
	<i>Aedes aegypti</i>	n.a.	Q6Q9G8_AEDAE
	<i>Tribolium castaneum</i>	n.a.	XP_973769
	<i>Drosophila melanogaster</i>	2R53D	EF1B_DROME
Frogs	<i>Xenopus laevis</i>	n.a.	EF1B_XENLA
	<i>Xenopus tropicalis</i>	n.a.	EF1B_XENTR
Crustacean	<i>Artemia salina</i>	n.a.	EF1B_ARTSA
Fish	<i>Brachydanio rerio</i>	6(8.6Mb)	Q6IQE2_BRARE
	<i>Ictalurus punctatus</i>	n.a.	Q2I161_ICTPU
Birds	<i>Gallus gallus</i>	7 (13Mb)	EF1B_CHICK
	<i>Bos taurus</i>	2(55Mb)	EF1B_BOVIN
Mammals	<i>Oryctolagus cuniculus</i>	n.a.	EF1B_RABIT
	<i>Mus musculus</i>	1 C2	EF1B_MOUSE
	<i>Rattus norvegicus</i>	9q31	<u>XP_343581</u>
	<i>Canis familiaris</i>	37(17.7Mb)	XP_536040
	<i>Sus scrofa</i>	n.a.	EF1B_PIG
	<i>Pan troglodytes</i>	n.a.	<u>XP_516048</u>
	<i>Homo sapiens</i>	2q33.3	EF1B_HUMAN

Appendix 6.2 – eEF1B δ homologues proteins

	Species	Genomic location	UniProt/GenBank
Sea urchin	<i>Sphaerechinus granularis</i>	n.a.	O18681
		n.a.	Q4VY59
Insects	<i>Bombyx mori</i>	n.a.	Q9BPS1
	<i>Drosophila melanogaster</i>	2L-31B1	EF1D_DROME
Crustacean	<i>Artemia salina</i>	n.a.	EF1D_ARTSA
Frogs	<i>Xenopus laevis</i>	n.a.	EF1D_XENLA; Q91733
	<i>Xenopus tropicalis</i>	n.a.	Q28G98
Fish	<i>Brachydanio rerio</i>	n.a.	Q5SPC9; Q5SPD0
Birds	<i>taeniopygia guttata</i>	n.a.	gi:224046810
	<i>Gallus Gallus</i>	n.a.	gi:118087445
Mammals	<i>Bos taurus</i>	n.a.	gi:119906216
	<i>Oryctolagus cuniculus</i>	n.a.	EF1D_RABIT
	<i>Mus musculus</i>	15 E1	EF1D_MOUSE; Q91VK2; Q80T06; Q68FG5
	<i>Rattus norvegicus</i>	7q34	Q68FR9
	<i>Canis familiaris</i>	n.a.	gi:73974698
	<i>Pan troglodytes</i>	n.a.	
	<i>Macaca fascicularis</i>	n.a.	
	<i>Ovis aries</i>	n.a.	Q717R8
	<i>Homo sapiens</i>	8q24.3	EF1D_HUMAN; Q4VBZ6; Q96I38

Appendix 6.3 – eEF1B α or eEF1B δ homologues proteins in plants

Plants	<i>Triticum aestivum</i>	n.a.	EF1B2_WHEAT
	<i>Pimpinella brachycarpa</i>	n.a.	EF1B_PIMBR
	<i>Beta vulgaris</i>	n.a.	EF1B_BETVU
	<i>Arabidopsis thaliana</i>	n.a.	EF1B1_ARATH
		n.a.	EF1B2_ARATH
		n.a.	EF1D1_ARATH
		n.a.	EF1D2_ARATH
		n.a.	EF1B1_ORYSA
	<i>Oryza sativa</i>	n.a.	EF1B2_ORYSA
		n.a.	EF1D1_ORYSA
		n.a.	EF1D2_ORYSA

Appendix 6.4 – eEF1B γ homologues proteins

	Species	Genomic location	UniProt
protozoa	<i>Cryptosporidium parvum</i>	n.a.	Q5CXY4
	<i>Cryptosporidium hominis</i>	n.a.	Q5CM55
	<i>Plasmodium yoelii yoelii</i>	n.a.	Q7R8U9
	<i>Leishmania infantum</i>	n.a.	<u>9BHZ6</u>
	<i>Crithidia fasciculata</i>	n.a.	Q6QE10
	<i>Trypanosoma cruzi</i>	n.a.	EF1G_TRYCR
Fungi	<i>Schizosaccharomyces pombe</i>	n.a.	EF1G_SCHPO
	<i>Cryptococcus neoformans</i>	I:1Mb	XP_566751
	<i>Aspergillus fumigatus</i>	I:4Mb	Q4WDF5
	<i>Saccharomyces cerevisiae</i>	n.a.	EF1G1_YEAST
Plants	<i>Prunus avium</i>	n.a.	EF1G_PRUAV
	<i>Glycine max</i>	n.a.	Q6QE10
	<i>Arabidopsis thaliana</i>	n.a.	EF1G1_ARATH
		n.a.	EF1G2_ARATH
	<i>Oryza sativa</i>	n.a.	EF1G1_ORYSA
		n.a.	EF1G3_ORYSA
worms	<i>Caenorhabditis elegans</i>	n.a.	EF1G2_ORYSA
Sea urchin	<i>Strongylocentrotus purpuratus</i>	n.a.	EF1G_CAEEL
Insects	<i>Locusta migratoria</i>	n.a.	Q4VY61
	<i>Bombyx mori</i>	n.a.	Q8T8P6
	<i>Drosophila melanogaster</i>	n.a.	Q9BPS3
Frogs	<i>Xenopus laevis</i>	3R: 99A1	EF1G_DROME
crustacean	<i>Artemia salina</i>	n.a.	Q91733
Fish	<i>Brachydanio rerio</i>	n.a.	EF1G_ARTSA
	<i>Carassius auratus</i>	14: 3Mb	EF1G_BRARE
	<i>Oryctolagus cuniculus</i>	n.a.	EF1G_CARAU
	<i>Mus musculus</i>	n.a.	EF1G_RABIT
	<i>Rattus norvegicus</i>	19 A	EF1G_MOUSE
	<i>Homo sapiens</i>	1q43	EF1G_RAT
		11q12.3	EF1G_HUMAN

Appendix 7 – eEF1B Motifs

eEF1B subunit	domain	location	e-value	database
Human eEF1B α	EF1_beta_acid (PF10587)	103-130	1.3e-10	Pfam
	EF1_GNE (PF00736)	139-225	9.4e-53	Pfam
	GST_CTLD (IPR014038)	10-81	1.9-09	Interpro
Plant B α 1	GST_C	14-65	4.2e-05	Pfam
	EF1_GNE	139-228	6.7e-41	Pfam
Plant B α 2	GST_C	18-65	0.0015	Pfam
	EF1_GNE	135-224	5.9e-38	Pfam
Plant B β 1	EF1_GNE	142-231	4.6e-42	Pfam
	EF1_beta_acid***	112-138	0.05	Pfam
Plant B β 2	EF1_GNE	142-231	1.2e-42	Pfam
	EF1_beta_acid***	112-138	0.05	Pfam
Human eEF1B δ iso b	EF-1_beta_acid	159-186	5.8e-10	Pfam
	EF1_GNE	195-281	3.5e-51	Pfam
	DUF526	55-117	0.5***	Pfam
	bZIP_1	79-113	0.023***	Pfam
	Vsp51	84-111	0.38***	Pfam
	Vac_Fusion	103-118	0.31***	Pfam
	SPT2	127-171	0.83***	Pfam
Human eEF1B γ	EF1G (PF00647)	275-381	3.9e-80	Pfam
	GST_N (PF02798)	2-81	1.6e-23	Pfam
	GST_C (PF00043)	106-198	3.4e-27	Pfam
	DDRKG (PF09756)	211-372	0.42***	Pfam
	Calreticulin (PF00262)	308 - 322	0.23***	Pfam

EF1_GNE EF-1 guanine nucleotide exchange domain
 EF-1_beta_acid Eukaryotic elongation factor 1 beta central acidic region
 GST-CTLD Glutathione S-transferase (GST), C-terminal like domain
 EF1G Elongation factor 1 gamma, conserved domain
 GST_C Glutathione S-transferase, C-terminal domain
 GST_N Glutathione S-transferase, N-terminal domain
 *** insignificant

Appendix 8 – eEF1B subunits structural features

	Characteristics	loc	Predicted tool
eEF1B α	Disorder	1-11 63-71 77-100 107-118 125-149	DisEMBL
	Low complexity	86-124	SEG
eEF1B δ iso a	Disulphide	8-156 148-305	disulfind
	Repeats	11-41;375-405 4-29; 223-248 225-243;308-326	RPT
	Disorder	65-99 191-200 251-300 346-363 1-18	DisEMBL
	Low complexity	51-69 95-108 130-144 264-281	SEG
eEF1B δ iso b	Leucine zipper	80-101	prosite
	Disorder	1-16 30-41 60-75 121-155 165-172 183-204 264-273	DisEMBL
	Low complexity	63-75 140-155	SEG
	coils	82-120 162-189	Coils
eEF1B γ	Transmembranes	157-174	PhDhtm
	Disorder	217-262 427-437 150-159 274-282	DisEMBL
	Low complexity	238-262	SEG

Appendix 9 –predicted post-translational modifications

	PTM	Location	Prediction tool
eEF1B α	methylation	130-133	MnM
	acetylation	71, 89, 169	Prosit
	SUMOylation	156-159	ELM
	N-glycosylation	89-92	ELM;
	Glycation	22, 96, 116, 132, 139, 197	NetGlycate
eEF1B δ iso a	Sulfation	20, 28	Sulfinator
	Amidation	273	Prosit
	acetylation	95, 151, 162, 195, 223, 266, 285, 355	Prosit
	N-glycosylation	166	NetNGlyc, Prosit
	GalNAc	199	NetOGlyc
	ManNAc	161	NetCGlyc
	Glycation	5, 86, 89, 93, 128, 366	NetGlycate
	methylation	275-279	MnM
eEF1B δ iso b	acetylation	68, 225	prosit
	N-glycosylation	91	Prosit
	GalNAc	125, 129, 133, 147	NetOGlyc
	Glycation	10, 56, 144, 189, 195, 203	NetGlycate
	methylation		MnM
eEF1B γ	Sulfation	194-197	Sulfinator
	acetylation	4, 140, 364, 379, 405	prosit
	N-glycosylation	45, 367	ELM; NetNGlyc, prosit
	Glycation	125, 173, 208, 212, 220, 228, 235, 241, 253, 296, 351, 434, 437	NetGlycate
	SUMOylation	131-135	ELM, MnM
	methylation		MnM

Appendix 10 – eEF1B subunits phosphorylation prediction sites and *in vitro* and *in vivo* phosphorylation sites

eEF1B α	Likelihood of phosphorylation Disphos	Predicted phosphorylation sites by NetPhosK	NetPhos	Predicted phosphorylation sites			Known phosphorylation sites and reference	Species
				ELM	MnM	HPRD		
S8	0.126	p38MAPK	0.56	WW, MAPK	Erk	WW, CKI, GSK-3, ERK1, ERK2, CDK5, Growth associated histone H1	(Dephoure et al., 2008)	Human
Y18	0.038			STAT5	Cholesterol, APS, EGFR, TC-PTP, PLCgamma, STAT5	EGFR, TC-PTP		
S23	0.094	CKII, PKG	0.53, 0.59	CKII	Myt1 is phosphorylated by PLK1, CKII	CKII		
Y24	0.1	EGFR	0.54	Src, STAT5, USP7 NTD	PLCgamma, STAT5	ALK		
Y28	0.065			Src, STAT5	STAT5	SHP1		
S31	0.099	DNAPK, ATM	0.63, 0.52	PIKK	CKII, ATM	DNAPK, Pyruvate dehydrogenase, ATM, CKII		
S42	0.145					PIk1, CKI		
S43	0.203	p38MAPK, GSK3	0.56, 0.5	WW, MAPK	Erk	PIk1, WW, GSK-3, ERK1, ERK2, CDK5, MAPK		
Y56	0.066				Cholesterol, Syk, JAK2, Blnk,	JAK2		
S61	0.067	PKC, cdc2	0.51, 0.55			CKII		
Y62	0.131				Src	Src		
S68	0.227	PKA	0.51			PKA, PKC, CKI		
Y79	0.101				Src	Src	(Rikova et al., 2007, Dai et al., 2007)	Human and mouse
T87	0.11					b-Adrenergic Receptor	(Chen et al., 2009, Dephoure et al., 2008)	Human
T88	0.14	CKII	0.52		KAPP	CKI, MAPK	(Dephoure et al., 2008)	Human
S90	0.649			CKI	CK I	CKI, CKII, MAPK	(Oppermann et al., 2009, Li et al., 2009, Chen et al.,	Human and mouse

							2009, Dephoure et al., 2008)	
T93	0.196	CKII	0.51				CKI (Molina et al., 2007, Chen et al., 2009, Dephoure et al., 2008)	
S95	0.737	CKII	0.53	USP7 NTD, CKI	CamKII, CKII	b-Adrenergic Receptor, Pyruvate dehydrogenase, CKII	(Dephoure et al., 2008, Molina et al., 2007, Oppermann et al., 2009)	
S106	0.994	CKII	0.77	CKII	CamKII, CKII	BARD1, CKII	CKII and Ppz1 (Chen and Traugh, 1995, Palen et al., 1994, Janssen et al., 1988, Belle et al., 1989, Aksenova et al., 2007, Oppermann et al., 2009, Li et al., 2009, Chen et al., 2009, Zanivan et al., 2008a, Tsai et al., 2008, Daub et al., 2008, Dephoure et al., 2008, Sui et al., 2008, Trinidad et al., 2008, Han et al., 2008, Huang et al., 2007, Molina et al., 2007, Villen et al., 2007, Dai et al., 2007, Ballif et al., 2006, Beausoleil et al., 2004, Shu et al., 2004)	Frog, rabbit, mouse, rat, yeast and human
S112	1	CKII	0.67	CKII		CKI, CKII, MAPK, b-Adrenergic Receptor	CKII (Chen and Traugh, 1995, Palen et al., 1994, Janssen et al., 1988, Belle et al., 1989, Dephoure et al., 2008, Dai et al., 2007)	Xenopus, rabbit, mouse and human
Y126	0.052	INSR	0.52		Src	Src	(Molina et al., 2007)	Human
S128	0.443	PKC, cdc2	0.92, 0.51		PKCalpha	WW, CKI, SK-3, ERK1, ERK2, CDK5, Growth associated histone H1	(Molina et al., 2007)	Human
S140	0.376	PKA	0.54			b-Adrenergic Receptor, PKA, PKC	(Huang et al., 2007)	Rat
S141	0.303			USP7 NTD		PIK1	(Huang et al., 2007, Molina	Human

							et al., 2007)	
T153	0.048	CKII	0.56		KAPP	PIK1		
S164	0.098							
S174	0.057	PKC	0.62		PKCalpha			
S175	0.043					PIK1		
Y182	0.018				Src	PIK1, PKA, PKC and MAPK		
T200	0.051	CKII	0.67		Rad53, RSK	Src		
T208	0.009	CKII	0.56			PKA and PKC		
Y213	0			STAT5	STAT5, TC-PTP	CKI and CKII		
S216	0	CKII	0.57		EGFR, CamKII, CKII	SHP1, PTP1B, TC-PTP and EGFR		

eEF1Bδ	Likelihood of phosphorylation Disphos	Predicted phosphorylation sites by NetPhosK	NetPhos	Predicted phosphorylation sites			Known phosphorylation sites and reference	Species
				ELM	MnM	HPRD		
T3	0.008				Rad53	PKA, PKC and G protein-coupled receptor 1		
Y18	0.061			Src	Src	Src		
Y26	0.083				Fyn, PI3K, Shc1, SHB, Src, Shc, Blnk	PI3K, Src and ALK		
T34	0.154	PKC	0.66	USP7 NTD	Ime1, KAPP			
S35	0.199							
S37	0.23	cdc2	0.53	CKII	CKII	CKII		
Isoform b	S44	0.096	PKA,cdc2	0.52, 0.56				
	S60	0.106	PKA	0.56		G protein-coupled receptor 1, MAPKAPK2 and GSK3	(Molina et al., 2007)	Human

Isoform c	S71	0.351	p38MAPK, GSK3, cdk5	0.5, 0.52, 0.56	WW, MAPK	ERK, Ime1	GSK-3, ERK1, ERK2, CDK5, CK II ,WW		
	T79	0.077	cdk5	0.51	WW, GSK3, MAPK	ERK, GSK3	GSK-3, ERK1, ERK2, CDK5 ,CK I ,WW		
	T82	0.141	cdc2	0.54	USP7 NTD	Ime1			
S64	0.556					Skp1	PIK1, G protein-coupled receptor 1, MAPKAPK2, GSK3	(Dephoure et al., 2008)	Human
S65	0.569	PKC	0.52				and Plk1		
S70	0.727				USP7 NTD		PIK1, CKI, CKII and GSK3		
S71	0.667	cdc2	0.61				PIK1 and CKII		
T73	0						CKII		
S74	0						CKII		
S78	0.266								
T85	0.004	CKII	0.54		CKII	CKII			
S86	0.279	DNAPK, PKA	0.52, 0.58		PKA	PKA, RSK, CamKII	14-3-3 and Chk1, CamIV and CamII, CKII, PKA and PKC		
S93	0						CK I ,PKA		
S106	0.172	CKII, cdc2	0.53, 0.6		CKII	CKII	CKI and CKII		
S118	0.586	cdc2	0.51		GSK3		PIK1	(Molina et al., 2007)	Human
S119	0.529				WW, MAPK	ERK	PIK1, WW, GSK-3, ERK1, ERK2, CDK5, PKA and PKC	(Molina et al., 2007)	Human
T125	0.491	PKG	0.5		GSK3, PKA	PKA	PKA, PKC and G protein-coupled receptor 1		
T129	0.339	PKC	0.74		GSK3, PIKK	Ime1, GSK3, ATM		(Oppermann et al., 2009, Zanivan et al., 2008a, Daub et al., 2008, Molina et al., 2007)	Human and mouse
S133	0.403	p38MAPK	0.53		WW , CDK, GSK3, MAPK	CDK2, Skp1, ERK	WW and GSK-3, ERK1, ERK2, CDK5, CDK1, 2, 4, 6, Growth associated histone	Viral kinases and p38 cdc2 (Dephoure et al., 2008, Mulner-Lorillon et al.,	Human, mouse, rat and rabbit

						HI, and Cdc2	1994, Monnier et al., 2001b, Kawaguchi et al., 1997, Kawaguchi et al., 1998, Kawaguchi et al., 1999, Kato et al., 2001, Kawaguchi et al., 2003, Daub et al., 2008, Oppermann et al., 2009, Zanivan et al., 2008b, Zanivan et al., 2008a, Tsai et al., 2008, Trinidad et al., 2008, Villen et al., 2007, Molina et al., 2007, Chen et al., 2009)	
T147	0.61	CKII	0.55	WW , CKII, MAPK	CKII, ERK, RSK	WW, PKA, PKC, GSK3, Erk1, Erk2, CDK5 and CKII	CKII and X (Minella et al., 1998, Chen et al., 2009, Zanivan et al., 2008b, Daub et al., 2008, Dephoure et al., 2008, Molina et al., 2007, Villen et al., 2007, Olsen et al., 2006)	Human and mouse
S162	0.969	CKII	0.77	CKII	BARD1, CKII	CKII	CKII (Chen and Traugh, 1995, Palen et al., 1994, Janssen et al., 1988, Belle et al., 1989, Daub et al., 2008, Oppermann et al., 2009, Li et al., 2009, Zanivan et al., 2008a, Chen et al., 2009, Dephoure et al., 2008, Han et al., 2008, Molina et al., 2007, Sui et al., 2008, Villen et al., 2007, Olsen et al., 2006, Dai et al., 2007, Huang et al., 2007)	Human, mouse, rat and rabbit
Y182	0.052				Src	Src	(Rikova et al., 2007)	Human
T190	0.211	PKC	0.64	PKA	PKG, KAPP, RSK	b-Adrenergic Receptor, PKA,		

						PKC		
S196	0.256	PKA	0.63	USP7 NTD		PIK1		
S197	0.247				Rad9	PIK1, PKA and PKC		
T209	0.03	CKII	0.56		KAPP	CKI and b-Adrenergic Receptor		
T216	0.043				GSK3			
S220	0.035			GSK3	Skp1			
S231	0.025	cdc2	0.5			G protein-coupled receptor 1		
Y238	0.023				Src	Src		
T256	0.069	CKII	0.72		RSK, Rad53	PKA and PKC		
T264	0.014	CKII	0.65	CKII	CKII, Skp2	CKI and CKII		
S272	0.141	CKII	0.54		CamKII	G protein-coupled receptor 1		

eEF1B δ isoform a N-termina I	Likelihood of phosphorylation Disphos	Predicted phosphorylation sites by NetPhosK	NetPhos	Predicted phosphorylation sites			Known phosphorylation sites and reference	Species
				ELM	MnM	HPRD		
S3	0.522	PKC	0.79		PKCalpha, GSK3	G protein-coupled receptor 1, PKA, PKC, MAPK, GSK3		
S7	0.255	PKA	0.77			PKA, PKC		
T9		CKI	0.58					
T12	0.133	CKII,	0.54, 0.7	CKII	CKII	b-Adrenergic Receptor , CKII		

		PKC						
Y20	0.07	EGFR	0.63		Src	Src		
T33	0.054	DNAPK	0.61	PIKK	Skp2, ATM	G protein-coupled receptor 1		
S38	0.152			USP7 NTD				
S53	0.394			GSK3, PIKK	ATM, CKII, GSK3	G protein-coupled receptor 1, b-Adrenergic Receptor , DNAPK , Pyruvate dehydrogenase , ATM, CKII, MAPK		
T57	0.289				Skp2	G protein-coupled receptor 1, b-Adrenergic Receptor , CKI		
T60	0.412				Skp2, KAPP			
T68	0.5			USP7 NTD, GSK3	Ime1, Skp1, GSK3	G protein-coupled receptor 1		
S69	0.707			CKI	PKCalpha, CKI	PKA, PKC, CKI, CKII		
S70	0.649	PKC	0.63		CKII	Pyruvate dehydrogenase , CKII, , Pik1		
S72	0.81	RSK, DNAPK	0.54, 0.61					
S77	0.568	RSK, PKG, PKA	0.51, 0.68, 0.83	USP7 NTD		CKII		
S91	0.87	cdc2	0.5	WW, CKI, PKA, MAPK	MLCK, p70s6k, PKA, PKCalpha, PKG, Erk, CamKII, CKI, RSK	GSK-3, ERK1, ERK2, CDK5, MAPK, ZIP, PKA, PKC, Pim1, CamKII, CKI, CKII, 14-3-3, WW	(Dephoure et al., 2008)	Human
S94	0.219				Ime1		(Dephoure et al., 2008)	Human
S107	0.082				CamKII			
S123	0.174	PKC	0.65			b-Adrenergic Receptor		
S124	0.117	PKC	0.88	USP7 NTD	PKCalpha	ALK, PKA, PKC, , Pik1		
Y125	0.045							
T149	0.019				KAPP, Ime1	CKI, CKII		

S152	0.026							
T160	0.002				Chk2, Rad53			
S168	0.005				CKII	Pyruvate dehydrogenase , CKII		
S181	0.065	DNAPK, PKA, ATM	0.63, 0.61, 0.55	PIKK	ATM	DNAPK , ATM, CKII		
S183	0.073				Rad9	G protein-coupled receptor 1		
S191	0.223			USP7 NTD	PKCalpha	PKA, PKC		
T196	0.176	p38MAP K	0.5	WW, MAPK	Erk, CamKII ,	GSK-3, ERK1, ERK2, CDK5, CamKII, PKC, CKI, WW		
T199	0.134	cdc2	0.51		Ime1	G protein-coupled receptor 1, b-Adrenergic Receptor		
S224	0.071	PKA	0.61	USP7 NTD				
Y239	0.091	SRC, EGFR	0.53, 0.64		Src	Src		
Y247	0.257				Shc1, SHB, Src, Syk, Shc, JAK2, Blnk	Src, JAK2, ALK		
S266	0.629			CKII, PIKK, PKA	Skp2, ATM, CKII, PKA	CKI, PKA, PKC, DNAPK , ATM, CKII		
T271	0.285					PKA, PKC		
S280	0.265					CKI		
S291	0.574	cdc2	0.54	14-3-3	CamKII, RSK	CamKII , PKA, PKC, 14-3-3		
Y304	0.049				SHP-1			
Y306	0.056			STAT5	STAT5			
S318	0.101			CKI	CKI	CKI, CKII		
T321	0.041				KAPP	G protein-coupled receptor 1, PKA, PKC, DNAPK , CKII		
Y322	0.155	EGFR	0.51		Src	Src		
S324	0.032					b-Adrenergic Receptor , CKII		
S345	0.166					CKI		
T351	0.693	cdc2	0.52	WW, PKA, MAPK	KAPP, Erk, PKA	GSK-3, ERK1, ERK2, CDK5,		

						PKA, PKC, DNAPK , Growth associated histone HI , CKI, CKII, WW		
S354	0.798	cdc2	0.51	CKI	lme1, CKI			
S357	0.624	CaM-II, PKA, cdc2	0.5, 0.55, 0.51	CKI		DNA dependent Protein, CKII, CKI		
S359	0.818	cdc2	0.59	USP7 NTD		G protein-coupled receptor 1		
S360	0.796					PKA, PKC, PIk1		

eEF1B γ	Likelihood of phosphoryl ation Disphos	Predicted phosphor ylation sites by NetPhosK	NetPhos	Predicted phosphorylation sites			Known phosphorylation sites and reference	Species
				ELM	MnM	HPRD		
T5	0.021	CKI, PKC	0.58, 0.55			PP2C delta, CKI and Dual specificity protein 6		
Y7	0.089			STAT5	Mek, Blnk	Crk SH2 and RasGAP C- terminal SH2 and Src, PP2C delta and Dual specificity protein 6		
T8	0.018	PKC	0.68	CKII	CKII	CK II		
Y9	0.005				Abl, Src			
Y24	0.029				Src	Src		
S25	0.042							
S33	0.123	PKG	0.69		RSK, CKII, CamKII	CamKII, PKA and PKC		
T43	0.025	PKC	0.78		PKCalpha	G protein-coupled receptor 1, PKA, PKC and CKI		

T46	0.262	p38MAPK, cdk5	0.57, 0.54	WW, MAPK	Erk	WW and GSK-3, ERK1, ERK2, CDK5 and Growth associated histone H1	(Dephoure et al., 2008)	Human
S72	0.048					b-Adrenergic Receptor and G protein-coupled receptor 1		
Y77	0.011				SHP-1			
Y78	0.064			STAT5	TC-PTP	TC-PTP		
S80	0.151	CKII	0.59	CKII	CKII	CK II		
s87	0.272	CKII, PKA, cdc2	0.51, 0.67, 0.53	CKII, PKA	PKA	PIK1		
T88	0.185			MAPK	Erk, CKII, RSK, CamKII	PIK1, WW, CamKII, PKA, PKC, G protein-coupled receptor 1, GSK-3, ERK1, ERK2, CDK5 and CKII		
S100	0.056			GSK3	CKII, GSK3	G protein-coupled receptor 1, Pyruvate dehydrogenase, CKII, MAPKAPK2 and GSK3		
S104	0.037	cdc2	0.5		GSK3	MAPKAPK2, GSK3 and b-Adrenergic Receptor		
S111	0.057				Ime1	PIK1		
T112	0.028					PIK1 and G protein-coupled receptor 1		
T117	0.008					DNAPK		
T128	0.021				RSK	G protein-coupled receptor 1, PKA and PKC		
Y148	0.022			STAT5	PLCgamma1	SHP1		
T150	0.01	cdc2	0.5		RSK			
T158	0.037			PKA	CKII, PKA	AMP-activated protein, CKI, CKII, PKA and PKC		
T163	0.011			GSK3	GSK3	G protein-coupled receptor 1 and CKI		

T167	0.001							
Y172	0.005				Abl, JAK2	JAK2		
S179	0.05					DNAPK, G protein-coupled receptor 1, PKA and PKC		
T187	0.037				Ime1, PKCalpha			
T193	0.004	PKC	0.58					
T224	0.412	DNAPK, PKC	0.57, 0.79	PIKK	ATM	b-Adrenergic Receptor and PKA		
T230	0.872	p38MAPK	0.54	WW, CDK, PKA, MAPK	PKG, CDK2, Erk, RSK, PKCalpha	WW, GSK-3, ERK1, ERK2, CDK1, 2, 4, 5, 6, Cdc2, b-Adrenergic Receptor, Growth associated histone HI, PKA and PKC	P38 cdc2 (Monnier et al., 2001a, Asselin et al., 1984, Olsen et al., 2006)	Frogs, sea urchin and human
S237	0.975	CKII	0.56	CKII	CKII	CKI, CKII, PKA and PKC		
S286	0.167				Ime1	PIK1		
T287	0.075					PIK1, PKA and PKC		
Y297	0.078	INSR	0.52	GRB2	Grb2, Src	Grb2 and Src		
S298	0.329	RSK, PKA, PKG	0.52, 0.79, 0.52	GSK3, PKA	PKG, PKA, RSK, CamKII	CamKIV, CamKII, PKA, Pim1, PKC, PKCepsilon, CKII, CKI, G protein-coupled receptor 1, MAPKAPK2 and Pyruvate dehydrogenase	(Huang et al., 2007)	Human
T302	0.062					MAPKAPK2 and CKI		
S304	0.061					b-Adrenergic Receptor and CKI		
Y309	0.026			STAT5		ALK		
S320	0.144			GSK3	CKII, GSK3	PKA, CKI, CKII, MAPKAPK2, GSK3, and G protein-coupled receptor 1		
Y323	0.013				Src	Src and ALK and CKII		
S324	0.11				GSK3	MAPKAPK2, GSK3 and G protein-coupled receptor 1		

Y326	0.037	EGFR	0.57		TC-PTP, EGFR, Blnk	Crk, RasGAP, EGFR and TC-PTP		
T333	0.011	DNAPK	0.56	PIKK	ATM	CKI		
T335	0.003					CKI and CKII		
S338	0.016				CKII	CKII		
T343	0.007							
S359	0.044	PKC, PKA	0.76, 0.68	USP7 NTD				
T365	0.011				CKII	G protein-coupled receptor 1, CKI and CKII		
S368	0.046			GSK3	GSK3	Plk1, CKII, MAPKAPK2 and GSK3		
S369	0.053	cdc2	0.53			Plk1 and CKI,		
S370	0.06	CKI	0.5	CKI	CKI			
S372	0.058			GSK3	CKII, GSK3	CKI, CKII, MAPKAPK2 and GSK3		
S387	0.067	p38MAPK, GSK3	0.53, 0.52	WW, MAPK	Erk, Ime1, CamKII	WW, GSK-3, ERK1, ERK2, CDK5		
Y394	0.2	INSR	0.51		TC-PTP, EGFR	EGFR, TC-PTP and Src		
S396	0.053	PKC	0.64		CKII	b-Adrenergic Receptor, CKI and CKII		
Y397	0.053			STAT5	Src	SHP1 and Src		
T398	0.097	PKC	0.52		PKCalpha	CKII, PKA and PKC		
S406	0.159	CKII, CKI	0.51, 0.51	CKI	Ime1, CKI	G protein-coupled receptor 1, CKI and CKII		
T409	0.027	CKI, DNAPK	0.59	PIKK	ATM, CKII	CKI and CKII		
T411	0.189					CKI and b-Adrenergic Receptor		
Y416	0.022			STAT5	TC-PTP, EGFR	EGFR and TC-PTP		
S418	0.038				CKII	G protein-coupled receptor 1, CKI and CKII		

Appendix 11 – eEF1B other motifs

eEF1B	Motifs	Details	Location	Prediction tool
eEF1B α	Targeting signals	Nuclear trafficking	116-119	MnM
		Endocytosis trafficking	24-28 56-59	MnM
		Lysosomes trafficking	1-11	MnM
		Golgi trafficking	202-205	MnM
	Protein binding motifs	GADS	129-133	MnM
		Calmodulin	53-72	Calmodulin target database
			12-24	MnM
			136-148	MnM
			158-170	MnM
			184-196	MnM
	207-219	MnM		
eEF1B δ iso b	Targeting signals	Nuclear trafficking (via CRM1 exportin protein)	98-109	ELM
		Golgi-lysosome trafficking	95-100	ELM
		Peroxisome trafficking	12-16	ELM
		Nuclear trafficking	204-207	MnM
		Lysosome trafficking	154-168	MnM
		Peroxisome trafficking	298-300	MnM
		Endocytosis trafficking	26-29	MnM
	Protein binding motifs	TRAF6	167-172	ELM, MnM
		TRAF2	37-40	MnM
			181-184	MnM
		Calmodulin	46-55	Calmodulin target database
			57-67	MnM
			99-109	MnM
			211-221	MnM
			233-243	MnM
			255-265	MnM
			273-283	MnM
285-295	MnM			
14-3-3e	269-273	MnM		
GADS	204-207	MnM		
eEF1B δ iso a	Targeting signals	Peroxisome trafficking	139-144	MnM
			273-278	MnM
		Mitochondrial trafficking	223-226	MnM
		ER export trafficking	188-196	MnM
	Protein binding motifs	Nuclear trafficking	97-100	MnM
		Zinc	164-167	MnM
		TRAF2	63-66	MnM
		Cortactin	362-369	MnM
		CIN85	151-156	MnM
		Shp-1	150-156	MnM
		GADS	89-92	MnM
97-100	MnM			

			2-5	MnM		
			101-104	MnM		
		Calmodulin	232-251	ELM		
			115-125	MnM		
			140-150	MnM		
			269-273	MnM		
		Grb2	269-273	MnM		
		eEF1By	Targeting signals	Peroxisome trafficking	390-394	ELM
					419-423	ELM
					319-323	ELM
					322-326	ELM
Nuclear trafficking (via CRM1 exportin protein)	161-174			ELM		
Golgi-lysosome trafficking	137-142			ELM		
	408-413			ELM		
Endocytosis trafficking	172-175			MnM		
	323-326			MnM		
	394-397			MnM		
	416-419	MnM				
		TRAF2	237-240	ELM, MnM		
			258-261	ELM, MnM		
			259-262	ELM		
			80-83	ELM, MnM		
			131-134	ELM, MnM		
		TRAF6	257-265	ELM, MnM		
		TRF1 and TRF2	384-388	ELM		
		GADS	122-125	MnM		
			282-285	MnM		
			313-316	MnM		
425-428	MnM					
CtBP	329-333	ELM				
Grb2	10-14	MnM				
	47-51	MnM				
	185-189	MnM				
	244-248	MnM				
Calmodulin	351-361	Calmodulin target database				
	49-59	MnM				
	75-85	MnM				
	142-152	MnM				
	153-163	MnM				
	171-181	MnM				
	191-201	MnM				
	310-320	MnM				
	332-342	MnM				
426-436	MnM					

Appendix 12 – Protein interaction network

eEF1B α

Biological Processes

GO-ID	p-value	Description
6446	3.50E-09	regulation of translational initiation
44419	2.78E-08	interspecies interaction between organisms
6445	3.71E-08	regulation of translation
32268	1.76E-07	regulation of cellular protein metabolic process
10608	2.45E-07	posttranscriptional regulation of gene expression
31326	2.96E-07	regulation of cellular biosynthetic process
51246	1.07E-06	regulation of protein metabolic process
51706	1.58E-05	multi-organism process
6913	2.38E-05	nucleocytoplasmic transport
51169	2.59E-05	nuclear transport
6416	7.89E-05	translation
51128	1.84E-04	regulation of cellular component organization and biogenesis
30097	4.92E-04	hemopoiesis
48534	7.48E-04	hemopoietic or lymphoid organ development
44267	7.98E-04	cellular protein metabolic process
6886	8.23E-04	intracellular protein transport
2520	8.59E-04	immune system development
19538	9.12E-04	protein metabolic process
2521	9.25E-04	leukocyte differentiation
6606	9.69E-04	protein import into nucleus
51170	1.06E-03	nuclear import
22618	1.11E-03	ribonucleoprotein complex assembly
44260	1.13E-03	cellular macromolecule metabolic process
59	1.24E-03	protein import into nucleus, docking
6605	1.63E-03	protein targeting
60	1.90E-03	protein import into nucleus, translocation
6454	2.28E-03	translational initiation
17038	2.46E-03	protein import
42112	2.48E-03	T cell differentiation
30461	3.10E-03	conjugation with cellular fusion
15853	3.10E-03	adenine transport
51045	3.10E-03	negative regulation of membrane protein ectodomain proteolysis
746	3.10E-03	conjugation
65003	3.48E-03	macromolecular complex assembly
46907	3.55E-03	intracellular transport
6455	3.85E-03	translational elongation
43933	4.04E-03	macromolecular complex subunit organization

Molecular Functions

GO-ID	p-value	Description
8135	1.06E-16	translation factor activity, nucleic acid binding
45182	2.43E-16	translation regulator activity
3745	9.96E-14	translation initiation factor activity
5515	4.81E-08	protein binding
5488	5.51E-06	binding
8182	2.65E-05	translation elongation factor activity
22844	4.09E-05	voltage-gated anion channel activity
5544	4.67E-05	calcium-dependent phospholipid binding
8139	1.77E-04	nuclear localization sequence binding
1948	2.36E-04	glycoprotein binding
4859	3.03E-04	phospholipase inhibitor activity
55102	3.78E-04	lipase inhibitor activity
3676	6.91E-04	nucleic acid binding
5253	8.45E-04	anion channel activity
3723	8.54E-04	RNA binding
17111	1.25E-03	nucleoside-triphosphatase activity
8249	1.27E-03	signal sequence binding
16462	1.60E-03	pyrophosphatase activity
16818	1.65E-03	hydrolase activity, acting on acid anhydrides, in phosphorus-containing anhydrides
16817	1.68E-03	hydrolase activity, acting on acid anhydrides
42610	2.95E-03	CD8 receptor binding
3724	3.07E-03	RNA helicase activity
8026	3.10E-03	ATP-dependent helicase activity
42609	5.89E-03	CD4 receptor binding
30957	5.89E-03	Tat protein binding
8509	6.08E-03	anion transmembrane transporter activity
42623	6.58E-03	ATPase activity, coupled
166	7.69E-03	nucleotide binding
5543	7.82E-03	phospholipid binding
4386	8.78E-03	helicase activity
42289	8.83E-03	MHC class II protein binding
19834	8.83E-03	phospholipase A2 inhibitor activity
8384	8.83E-03	IkappaB kinase activity

eEF1B δ **Biological Processes**

GO-ID	p-value	Description
42981	1.25E-05	regulation of apoptosis
43067	1.36E-05	regulation of programmed cell death
43687	1.62E-05	post-translational protein modification
50793	2.25E-05	regulation of developmental process
43412	3.08E-05	biopolymer modification
6468	4.03E-05	protein amino acid phosphorylation
44267	1.15E-04	cellular protein metabolic process
16310	1.17E-04	phosphorylation
19538	1.29E-04	protein metabolic process
6464	1.47E-04	protein modification process
44260	1.56E-04	cellular macromolecule metabolic process
51094	2.55E-04	positive regulation of developmental process
2699	2.71E-04	positive regulation of immune effector process
19079	3.09E-04	viral genome replication
50851	3.09E-04	antigen receptor-mediated signaling pathway
6796	4.07E-04	phosphate metabolic process
6793	4.07E-04	phosphorus metabolic process
43283	4.90E-04	biopolymer metabolic process
2429	5.39E-04	immune response-activating cell surface receptor signaling pathway
2768	5.92E-04	immune response-regulating cell surface receptor signaling pathway
6455	6.11E-04	translational elongation
2757	7.06E-04	immune response-activating signal transduction
2764	7.67E-04	immune response-regulating signal transduction
51242	9.76E-04	positive regulation of cellular process
46645	1.65E-03	positive regulation of gamma-delta T cell activation
46643	1.65E-03	regulation of gamma-delta T cell activation
45588	1.65E-03	positive regulation of gamma-delta T cell differentiation
45586	1.65E-03	regulation of gamma-delta T cell differentiation
43366	1.65E-03	beta selection
2697	1.68E-03	regulation of immune effector process
48518	1.75E-03	positive regulation of biological process
6916	1.79E-03	anti-apoptosis
44238	1.86E-03	primary metabolic process
19058	1.87E-03	viral infectious cycle
8624	1.87E-03	induction of apoptosis by extracellular signals
8152	2.43E-03	metabolic process
43170	2.44E-03	macromolecule metabolic process
50870	2.59E-03	positive regulation of T cell activation
22415	2.82E-03	viral reproductive process
9967	2.93E-03	positive regulation of signal transduction
60056	3.30E-03	mammary gland involution

45401	3.30E-03	positive regulation of interleukin-3 biosynthetic process
45399	3.30E-03	regulation of interleukin-3 biosynthetic process
1820	3.30E-03	serotonin secretion
51251	3.81E-03	positive regulation of lymphocyte activation
16032	3.95E-03	viral reproduction
2696	4.37E-03	positive regulation of leukocyte activation
50867	4.37E-03	positive regulation of cell activation
2253	4.51E-03	activation of immune response
46640	4.95E-03	regulation of alpha-beta T cell proliferation
46641	4.95E-03	positive regulation of alpha-beta T cell proliferation
45921	4.95E-03	positive regulation of exocytosis
33005	4.95E-03	positive regulation of mast cell activation
43306	4.95E-03	positive regulation of mast cell degranulation
43302	4.95E-03	positive regulation of leukocyte degranulation
45425	4.95E-03	positive regulation of granulocyte macrophage colony-stimulating factor biosynthetic process
43066	5.01E-03	negative regulation of apoptosis
43069	5.21E-03	negative regulation of programmed cell death
16567	5.26E-03	protein ubiquitination
50863	5.57E-03	regulation of T cell activation
32446	6.06E-03	protein modification by small protein conjugation
45597	6.23E-03	positive regulation of cell differentiation
45579	6.59E-03	positive regulation of B cell differentiation
32743	6.59E-03	positive regulation of interleukin-2 production
33003	6.59E-03	regulation of mast cell activation
2726	6.59E-03	positive regulation of T cell cytokine production
43304	6.59E-03	regulation of mast cell degranulation
45423	6.59E-03	regulation of granulocyte macrophage colony-stimulating factor biosynthetic process
50884	6.59E-03	neuromuscular process controlling posture
6689	6.59E-03	ganglioside catabolic process
6416	6.62E-03	translation
8285	6.81E-03	negative regulation of cell proliferation
50778	7.28E-03	positive regulation of immune response
42127	7.50E-03	regulation of cell proliferation
43065	7.80E-03	positive regulation of apoptosis
43068	8.06E-03	positive regulation of programmed cell death
2724	8.23E-03	regulation of T cell cytokine production
2711	8.23E-03	positive regulation of T cell mediated immunity
43300	8.23E-03	regulation of leukocyte degranulation
46479	8.23E-03	glycosphingolipid catabolic process
51249	8.59E-03	regulation of lymphocyte activation
44249	8.66E-03	cellular biosynthetic process
65007	8.67E-03	biological regulation
44237	8.74E-03	cellular metabolic process

Molecular Functions

GO-ID	p-value	Description
8182	3.37E-06	translation elongation factor activity
8135	1.53E-05	translation factor activity, nucleic acid binding
45182	1.98E-05	translation regulator activity
4713	1.47E-04	protein tyrosine kinase activity
50222	1.76E-04	protein kinase activity
8134	2.79E-04	transcription factor binding
4674	3.31E-04	protein serine/threonine kinase activity
16773	4.66E-04	phosphotransferase activity, alcohol group as acceptor
5515	5.06E-04	protein binding
16301	9.05E-04	kinase activity
51287	1.40E-03	NAD binding
16772	2.09E-03	transferase activity, transferring phosphorus-containing groups
3713	2.15E-03	transcription coactivator activity
8384	4.51E-03	IkappaB kinase activity
4704	6.01E-03	NF-kappaB-inducing kinase activity
4563	6.01E-03	beta-N-acetylhexosaminidase activity
8353	7.51E-03	RNA polymerase subunit kinase activity
3712	8.77E-03	transcription cofactor activity
16563	8.94E-03	transcription activator activity
16616	1.02E-02	oxidoreductase activity, acting on the CH-OH group of donors, NAD or NADP as acceptor

eEF1By**Biological Processes**

GO-ID	p-value	Description
16071	6.25E-10	mRNA metabolic process
6397	4.98E-08	mRNA processing
16070	5.61E-08	RNA metabolic process
6395	1.26E-07	RNA splicing
43283	4.38E-07	biopolymer metabolic process
6139	9.39E-07	nucleobase, nucleoside, nucleotide and nucleic acid metabolic process
6394	3.67E-06	RNA processing
43170	6.01E-06	macromolecule metabolic process
33036	7.02E-06	macromolecule localization
6606	7.87E-06	protein import into nucleus
51170	9.45E-06	nuclear import
15031	1.26E-05	protein transport
45184	1.29E-05	establishment of protein localization
51649	1.48E-05	establishment of localization in cell
6913	2.22E-05	nucleocytoplasmic transport
51169	2.49E-05	nuclear transport
51641	3.29E-05	cellular localization
8104	4.65E-05	protein localization
17038	5.05E-05	protein import
8152	7.81E-05	metabolic process
6886	9.54E-05	intracellular protein transport
46907	1.11E-04	intracellular transport
6374	1.31E-04	nuclear mRNA splicing, via spliceosome
375	1.31E-04	RNA splicing, via transesterification reactions
377	1.31E-04	RNA splicing, via transesterification reactions with bulged adenosine as nucleophile
6901	1.45E-04	vesicle coating
51656	1.70E-04	establishment of organelle localization
6900	1.80E-04	membrane budding
44238	2.00E-04	primary metabolic process
44237	2.18E-04	cellular metabolic process
65003	2.76E-04	macromolecular complex assembly
10467	3.59E-04	gene expression
43933	3.65E-04	macromolecular complex subunit organization
51640	4.69E-04	organelle localization
6461	4.76E-04	protein complex assembly
60	5.09E-04	protein import into nucleus, translocation
184	5.09E-04	nuclear-transcribed mRNA catabolic process, nonsense-mediated decay
6259	6.62E-04	DNA metabolic process
956	7.62E-04	nuclear-transcribed mRNA catabolic process

6402	1.34E-03	mRNA catabolic process
43623	1.48E-03	cellular protein complex assembly
6605	1.54E-03	protein targeting
43285	1.98E-03	biopolymer catabolic process
48220	2.46E-03	cis-Golgi to rough ER vesicle-mediated transport
48219	2.46E-03	inter-Golgi cisterna vesicle-mediated transport
48206	2.46E-03	vesicle targeting, cis-Golgi to rough ER
48205	2.46E-03	COPI coating of Golgi vesicle
48204	2.46E-03	vesicle targeting, inter-Golgi cisterna
48200	2.46E-03	Golgi transport vesicle coating
16050	2.72E-03	vesicle organization and biogenesis
51028	2.76E-03	mRNA transport
48194	2.99E-03	Golgi vesicle budding
44248	3.21E-03	cellular catabolic process
6974	3.21E-03	response to DNA damage stimulus

Molecular Functions

GO-ID	p-value	Description
5515	4.87E-13	protein binding
5488	4.52E-06	binding
3720	1.39E-04	telomerase activity
166	1.97E-04	nucleotide binding
3723	2.64E-04	RNA binding
4386	4.65E-04	helicase activity
3676	5.64E-04	nucleic acid binding